



Australia's National
Science Agency



Australian Government



National
Water Grid®

Climate data characterisation for hydrological and agricultural scenario modelling across the Victoria, Roper and Southern Gulf catchments

A technical report from the CSIRO Victoria and Southern Gulf
Water Resource Assessments for the National Water Grid

David McJannet, Ang Yang, Lynn Seo



ISBN 978-1-4863-2067-7 (print)

ISBN 978-1-4863-2068-4 (online)

Citation

McJannet D, Yang A and Seo L (2023) Climate data characterisation for hydrological and agricultural scenario modelling across the Victoria, Roper and Southern Gulf catchments. A technical report from the CSIRO Victoria and Southern Gulf Water Resource Assessments for the National Water Grid. CSIRO, Australia.

Copyright

© Commonwealth Scientific and Industrial Research Organisation 2024. To the extent permitted by law, all rights are reserved and no part of this publication covered by copyright may be reproduced or copied in any form or by any means except with the written permission of CSIRO.

Important disclaimer

CSIRO advises that the information contained in this publication comprises general statements based on scientific research. The reader is advised and needs to be aware that such information may be incomplete or unable to be used in any specific situation. No reliance or actions must therefore be made on that information without seeking prior expert professional, scientific and technical advice. To the extent permitted by law, CSIRO (including its employees and consultants) excludes all liability to any person for any consequences, including but not limited to all losses, damages, costs, expenses and any other compensation, arising directly or indirectly from using this publication (in part or in whole) and any information or material contained in it.

CSIRO is committed to providing web accessible content wherever possible. If you are having difficulties with accessing this document please contact csiroenquiries@csiro.au.

CSIRO Victoria and Southern Gulf Water Resource Assessments acknowledgements

This report was funded through the National Water Grid's Science Program, which sits within the Australian Government's Department of Climate Change, Energy, the Environment and Water.

Aspects of the Assessments have been undertaken in conjunction with the Northern Territory and Queensland governments.

The Assessments were guided by three committees:

- i. The Governance Committee: CRC for Northern Australia/James Cook University; CSIRO; National Water Grid (Department of Climate Change, Energy, the Environment and Water); Northern Land Council; NT Department of Environment, Parks and Water Security; NT Department of Industry, Tourism and Trade; Office of Northern Australia; Queensland Department of Agriculture and Fisheries; Queensland Department of Regional Development, Manufacturing and Water
- ii. The joint Roper and Victoria River catchments Steering Committee: Amateur Fishermen's Association of the NT; Austrade; Centrefarm; CSIRO; National Water Grid (Department of Climate Change, Energy, the Environment and Water); Northern Land Council; NT Cattlemen's Association; NT Department of Environment, Parks and Water Security; NT Department of Industry, Tourism and Trade; NT Farmers; NT Seafood Council; Office of Northern Australia; Parks Australia; Regional Development Australia; Roper Gulf Regional Council Shire; Watertrust
- iii. The Southern Gulf catchments Steering Committee: Amateur Fishermen's Association of the NT; Austral Fisheries; Burketown Shire; Carpentaria Land Council Aboriginal Corporation; Health and Wellbeing Queensland; National Water Grid (Department of Climate Change, Energy, the Environment and Water); Northern Prawn Fisheries; Queensland Department of Agriculture and Fisheries; NT Department of Environment, Parks and Water Security; NT Department of Industry, Tourism and Trade; Office of Northern Australia; Queensland Department of Regional Development, Manufacturing and Water; Southern Gulf NRM

Responsibility for the Assessments' content lies with CSIRO. The Assessments' committees did not have an opportunity to review the Assessments' results or outputs prior to their release.

This report was reviewed by Dr Andrew Schepen (CSIRO) and Dr Samantha Munroe (CSIRO). Dr Francis Chiew (CSIRO) reviewed the future climate analysis.

The authors acknowledge advice and contributions provided by Ms C. Bruce (CSIRO). Jannatun Nahar (BOM) provided climatic descriptions of each of the catchments.

Acknowledgement of Country

CSIRO acknowledges the Traditional Owners of the lands, seas and waters, of the area that we live and work on across Australia. We acknowledge their continuing connection to their culture and pay our respects to their elders past and present.

Photo

Roper River, NT. Source: CSIRO

Director's foreword

Sustainable development and regional economic prosperity are priorities for the Australian, Queensland and Northern Territory (NT) governments. However, more comprehensive information on land and water resources across northern Australia is required to complement local information held by Indigenous Peoples and other landholders.

Knowledge of the scale, nature, location and distribution of likely environmental, social, cultural and economic opportunities and the risks of any proposed developments is critical to sustainable development. Especially where resource use is contested, this knowledge informs the consultation and planning that underpin the resource security required to unlock investment, while at the same time protecting the environment and cultural values.

In 2021, the Australian Government commissioned CSIRO to complete the Victoria River Water Resource Assessment and the Southern Gulf Water Resource Assessment. In response, CSIRO accessed expertise and collaborations from across Australia to generate data and provide insight to support consideration of the use of land and water resources in the Victoria and Southern Gulf catchments. The Assessments focus mainly on the potential for agricultural development, and the opportunities and constraints that development could experience. They also consider climate change impacts and a range of future development pathways without being prescriptive of what they might be. The detailed information provided on land and water resources, their potential uses and the consequences of those uses are carefully designed to be relevant to a wide range of regional-scale planning considerations by Indigenous Peoples, landholders, citizens, investors, local government, and the Australian, Queensland and NT governments. By fostering shared understanding of the opportunities and the risks among this wide array of stakeholders and decision makers, better informed conversations about future options will be possible.

Importantly, the Assessments do not recommend one development over another, nor assume any particular development pathway, nor even assume that water resource development will occur. They provide a range of possibilities and the information required to interpret them (including risks that may attend any opportunities), consistent with regional values and aspirations.

All data and reports produced by the Assessments will be publicly available.



Chris Chilcott

Project Director

The Victoria and Southern Gulf Water Resource Assessment Team

Project Director	Chris Chilcott
Project Leaders	Cuan Petheram, Ian Watson
Project Support	Caroline Bruce, Seonaid Philip
Communications	Emily Brown, Chanel Koeleman, Jo Ashley, Nathan Dyer

Activities

Agriculture and socio-economics	<u>Tony Webster</u> , Caroline Bruce, Kaylene Camuti ¹ , Matt Curnock, Jenny Hayward, Simon Irvin, Shokhrukh Jalilov, Diane Jarvis ¹ , Adam Liedloff, Stephen McFallan, Yvette Oliver, Di Prestwidge ² , Tiemen Rhebergen, Robert Speed ³ , Chris Stokes, Thomas Vanderbyl ³ , John Virtue ⁴
Climate	<u>David McJannet</u> , Lynn Seo
Ecology	<u>Danial Stratford</u> , Rik Buckworth, Pascal Castellazzi, Bayley Costin, Roy Aijun Deng, Ruan Gannon, Steve Gao, Sophie Gilbey, Rob Kenyon, Shelly Lachish, Simon Linke, Heather McGinness, Linda Merrin, Katie Motson ⁵ , Rocio Ponce Reyes, Nathan Waltham ⁵
Groundwater hydrology	<u>Andrew R. Taylor</u> , Karen Barry, Russell Crosbie, Margaux Dupuy, Geoff Hodgson, Anthony Knapton ⁶ , Shane Mule, Stacey Priestley, Jodie Pritchard, Matthias Raiber, Steven Tickell ⁷ , Axel Suckow
Indigenous water values, rights, interests and development goals	<u>Marcus Barber/Kirsty Wissing</u> , <u>Pethie Lyons</u> , Peta Braedon, Kristina Fisher, Petina Pert
Land suitability	<u>Ian Watson</u> , Jenet Austin, Bart Edmeades ⁷ , Linda Gregory, Ben Harms ¹⁰ , Jason Hill ⁷ , Jeremy Manders ¹⁰ , Gordon McLachlan, Seonaid Philip, Ross Searle, Uta Stockmann, Evan Thomas ¹⁰ , Mark Thomas, Francis Wait ⁷ , Peter L. Wilson, Peter R. Wilson, Peter Zund
Surface water hydrology	<u>Justin Hughes</u> , Matt Gibbs, Fazlul Karim, Julien Lerat, Steve Marvanek, Cherry Mateo, Catherine Ticehurst, Biao Wang
Surface water storage	<u>Cuan Petheram</u> , Giulio Altamura ⁸ , Fred Baynes ⁹ , Jamie Campbell ¹¹ , Lachlan Cherry ¹¹ , Kev Devlin ⁴ , Nick Hombsch ⁸ , Peter Hyde ⁸ , Lee Rogers, Ang Yang

Note: Assessment team as at September, 2024. All contributors are affiliated with CSIRO unless indicated otherwise. Activity Leaders are underlined. For the Indigenous water values, rights, interests and development goals activity (Victoria catchment), Marcus Barber was Activity Leader for the project duration except August 2022 – July 2023 when Kirsty Wissing (a CSIRO employee at the time) undertook this role.

¹James Cook University; ²DBP Consulting; ³Badu Advisory Pty Ltd; ⁴Independent contractor; ⁵Centre for Tropical Water and Aquatic Ecosystem Research. James Cook University; ⁶CloudGMS; ⁷NT Department of Environment, Parks and Water Security; ⁸Rider Levett Bucknall; ⁹Baynes Geologic; ¹⁰QG Department of Environment, Science and Innovation; ¹¹Entura

Shortened forms

SHORT FORM	FULL FORM
ABARES	Australian Bureau of Agricultural and Resource Economics and Sciences
APE	areal potential evaporation
APSIM	Agricultural Production Systems sIMulator
AWRA-L	Australian Water Resource Assessment Landscape
AWRC	Australian Water Resources Council
CCAM	conformal-cubic atmospheric model
CMIP	Coupled Model Intercomparison Project
CV	coefficient of variation
DMI	dipole mode index
DOI	digital object identifier
ENSO	El Niño–Southern Oscillation
GCM	global climate model (IPCC refers to this as general circulation model)
GCM-PS	global climate model – pattern scaling
IOD	Indian Ocean dipole
IPCC	Intergovernmental Panel on Climate Change
IPO	Interdecadal Pacific Oscillation
MJO	Madden–Julian Oscillation
NOAA	National Oceanic and Atmospheric Administration
NSW	New South Wales
NT	Northern Territory
PE	potential evaporation
RAMS	regional atmospheric modelling system
RCP	Representative Concentration Pathway
RoA	rest of Australia
RoNA	rest of northern Australia
RoW	rest of the world
SA	southern Australia
SDF	seven-day streamflow forecast
SILO	scientific information for land owners
SOI	Southern Oscillation Index
SSF	seasonal streamflow forecast
SSP	Shared Socioeconomic Pathway
SST	sea surface temperature
TC	tropical cyclone
UNEP	United Nations Environment Programme
VPD	vapour pressure deficit

Units

UNIT	DESCRIPTION
h	hour
ha	hectare
hPa	hectopascal
km	kilometre
km²	square kilometre
m	metre
m³	cubic metres
MJ	megajoule
ML	megalitre
mm	millimetre
s	second
t	tonne
y	year

Preface

Sustainable development and regional economic prosperity are priorities for the Australian, NT and Queensland governments. In the Queensland Water Strategy, for example, the Queensland Government (2023) looks to enable regional economic prosperity through a vision which states ‘Sustainable and secure water resources are central to Queensland’s economic transformation and the legacy we pass on to future generations.’ Acknowledging the need for continued research, the NT Government (2023) announced a Territory Water Plan priority action to accelerate the existing water science program ‘to support best practice water resource management and sustainable development.’

Governments are actively seeking to diversify regional economies, considering a range of factors, including Australia’s energy transformation. The Queensland Government’s economic diversification strategy for north west Queensland (Department of State Development, Manufacturing, Infrastructure and Planning, 2019) includes mining and mineral processing; beef cattle production, cropping and commercial fishing; tourism with an outback focus; and small business, supply chains and emerging industry sectors. In its 2024–25 Budget, the Australian Government announced large investment in renewable hydrogen, low-carbon liquid fuels, critical minerals processing and clean energy processing (Budget Strategy and Outlook, 2024). This includes investing in regions that have ‘traditionally powered Australia’ – as the North West Minerals Province, situated mostly within the Southern Gulf catchments, has done.

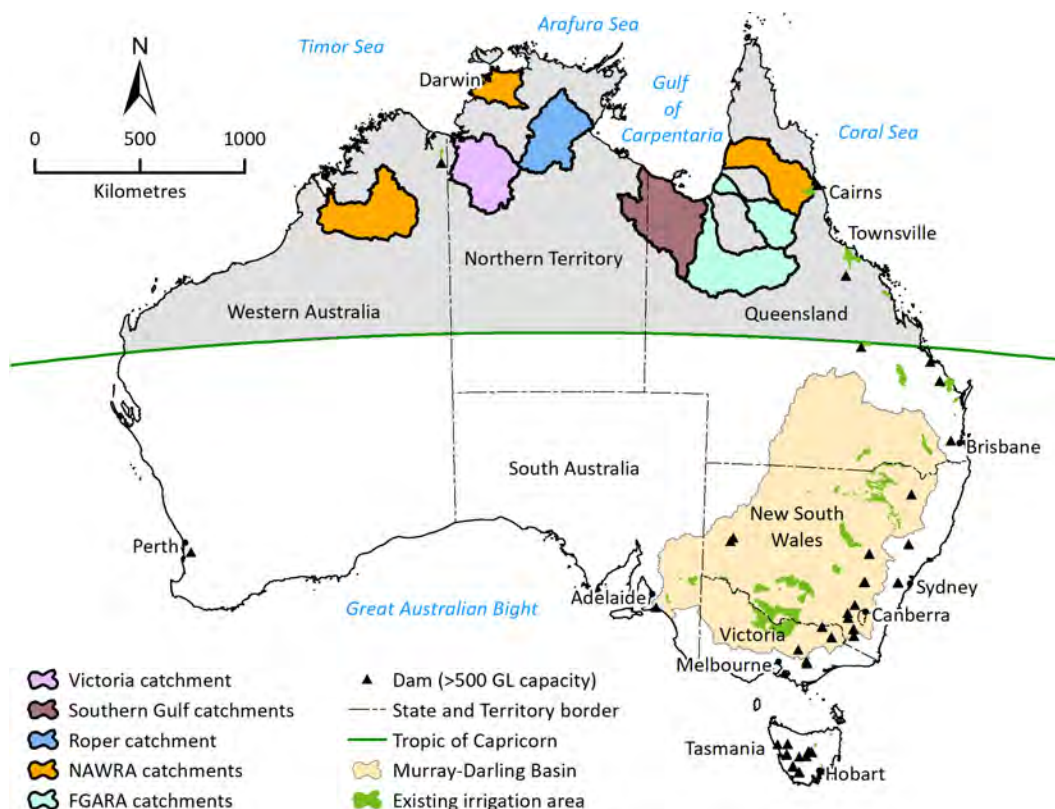
For very remote areas like the Victoria and Southern Gulf catchments, the land (Preface Figure 1-1), water and other environmental resources or assets will be key in determining how sustainable regional development might occur. Primary questions in any consideration of sustainable regional development relate to the nature and the scale of opportunities, and their risks.

How people perceive those risks is critical, especially in the context of areas such as the Victoria and Southern Gulf catchments, where approximately 75% and 27% of the population (respectively) is Indigenous (compared to 3.2% for Australia as a whole) and where many Indigenous Peoples still live on the same lands they have inhabited for tens of thousands of years. About 31% of the Victoria catchment and 12% of the Southern Gulf catchments are owned by Indigenous Peoples as inalienable freehold.

Access to reliable information about resources enables informed discussion and good decision making. Such information includes the amount and type of a resource or asset, where it is found (including in relation to complementary resources), what commercial uses it might have, how the resource changes within a year and across years, the underlying socio-economic context and the possible impacts of development.

Most of northern Australia’s land and water resources have not been mapped in sufficient detail to provide the level of information required for reliable resource allocation, to mitigate investment or environmental risks, or to build policy settings that can support good judgments. The Victoria and Southern Gulf Water Resource Assessments aim to partly address this gap by

providing data to better inform decisions on private investment and government expenditure, to account for intersections between existing and potential resource users, and to ensure that net development benefits are maximised.



Preface Figure 1-1 Map of Australia showing Assessment areas (Victoria and Southern Gulf catchments) and other recent CSIRO Assessments

FGARA = Flinders and Gilbert Agricultural Resource Assessment; NAWRA = Northern Australia Water Resource Assessment.

The Assessments differ somewhat from many resource assessments in that they consider a wide range of resources or assets, rather than being single mapping exercises of, say, soils. They provide a lot of contextual information about the socio-economic profile of the catchments, and the economic possibilities and environmental impacts of development. Further, they consider many of the different resource and asset types in an integrated way, rather than separately.

The Assessments have agricultural developments as their primary focus, but they also consider opportunities for and intersections between other types of water-dependent development. For example, the Assessments explore the nature, scale, location and impacts of developments relating to industrial, urban and aquaculture development, in relevant locations. The outcome of no change in land use or water resource development is also valid.

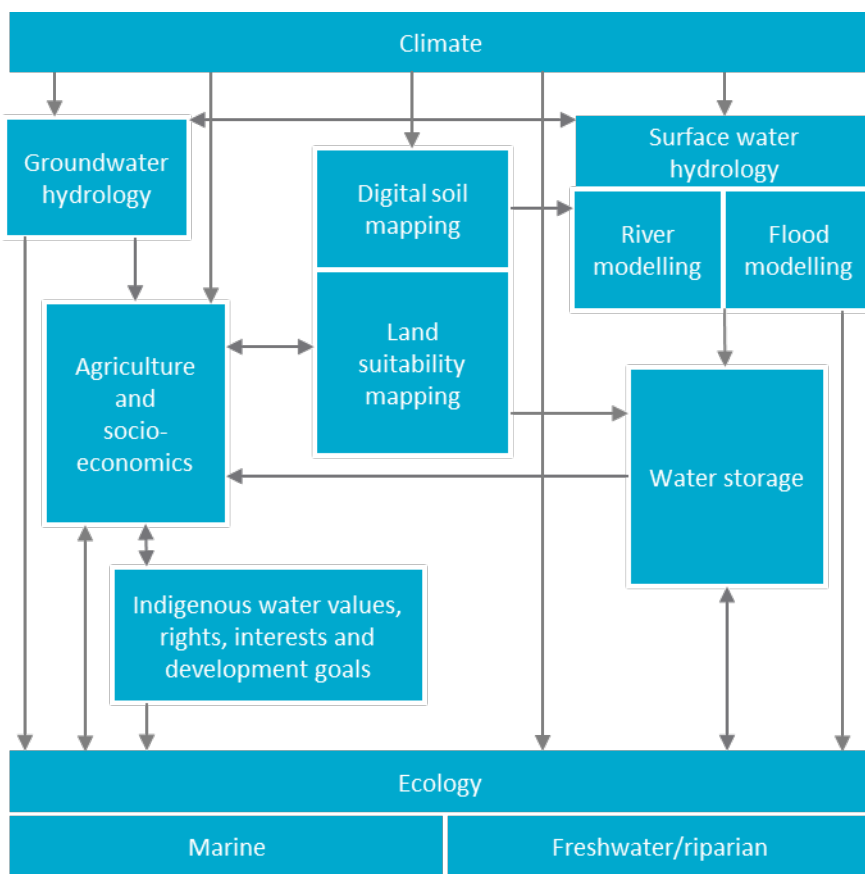
The Assessments were designed to inform consideration of development, not to enable any particular development to occur. As such, the Assessments inform – but do not seek to replace – existing planning, regulatory or approval processes. Importantly, the Assessments do not assume a given policy or regulatory environment. Policy and regulations can change, so this flexibility enables the results to be applied to the widest range of uses for the longest possible time frame.

It was not the intention of – and nor was it possible for – the Assessments to generate new information on all topics related to water and irrigation development in northern Australia. Topics

not directly examined in the Assessments are discussed with reference to and in the context of the existing literature.

CSIRO has strong organisational commitments to Indigenous reconciliation and to conducting ethical research with the free, prior and informed consent of human participants. The Assessments allocated significant time to consulting with Indigenous representative organisations and Traditional Owner groups from the catchments to aid their understanding and potential engagement with their requirements. The Assessments did not conduct significant fieldwork without the consent of Traditional Owners.

Functionally, the Assessments adopted an activities-based approach (reflected in the content and structure of the outputs and products), comprising activity groups, each contributing its part to create a cohesive picture of regional development opportunities, costs and benefits, but also risks. Preface Figure 1-2 illustrates the high-level links between the activities and the general flow of information in the Assessments.



Preface Figure 1-2 Schematic of the high-level linkages between the eight activity groups and the general flow of information in the Assessments

Assessment reporting structure

Development opportunities and their impacts are frequently highly interdependent and, consequently, so is the research undertaken through these Assessments. While each report may be read as a stand-alone document, the suite of reports for each Assessment most reliably informs discussion and decisions concerning regional development when read as a whole.

The Assessments have produced a series of cascading reports and information products:

- Technical reports present scientific work with sufficient detail for technical and scientific experts to reproduce the work. Each of the activities (Preface Figure 1-2) has one or more corresponding technical reports.
- Catchment reports, one for each of the Victoria and Southern Gulf catchments, synthesise key material from the technical reports, providing well-informed (but not necessarily scientifically trained) users with the information required to inform decisions about the opportunities, costs and benefits associated with irrigated agriculture and other development options.
- Summary reports, one for each of the Victoria and Southern Gulf catchments, provide a shorter summary and narrative for a general public audience in plain English.
- Summary fact sheets, one for each of the Victoria and Southern Gulf catchments, provide key findings for a general public audience in the shortest possible format.

The Assessments have also developed online information products to enable users to better access information that is not readily available in print format. All of these reports, information tools and data products are available online at <https://www.csiro.au/victoriariver> and <https://www.csiro.au/southerngulf>. The webpages give users access to a communications suite including fact sheets, multimedia content, FAQs, reports and links to related sites, particularly about other research in northern Australia.

Executive summary

Climate variables, water availability and soil data are generally considered to be the most important environmental information for determining the agricultural suitability of particular locations. Equivalent-sized catchments in south-eastern Australia have about ten times more climate stations than those of northern Australia's Victoria, Roper and Southern Gulf catchments. While this reduces the certainty of hydrological modelling, the density of rainfall stations in the three study areas is considered adequate for the purpose of water resource planning.

A consistent set of historical climate data for the Assessment was assembled from daily gridded climate data. After consideration of palaeoclimate studies, rainfall trends and future global climate model – pattern scaled (GCM-PS) rainfall projections, a climate baseline from 1 September 1890 to 31 August 2022 was adopted for the Victoria and Southern Gulf catchments and a climate baseline of 1 September 1910 to 31 August 2019 is used for the Roper catchment. This follows the general principle that hydrological planning should use as long a hydroclimate sequence as possible to encapsulate the range of likely/plausible conditions and variability at different time scales. In collating and analysing the climate data for use by the Assessment's numerical models, climate statistics and maps were prepared for the Victoria, Roper and Southern Gulf catchments and are presented herein.

The mean annual rainfall, averaged over the 132-year historical period (1 September 1890 to 31 August 2022) for the Victoria and Southern Gulf catchments was 681 mm and 602 mm respectively. The mean annual rainfall, averaged over the 109-year historical period (1 September 1910 to 31 August 2019) for the Roper catchment was 792 mm. Of this rainfall 93, 95 and 97% was calculated as falling during the wet season (1 November to 30 April) in the Victoria, Roper and Southern Gulf catchments respectively. The highest median monthly rainfall in all three study areas occurred during the months of January and February, and the months with the lowest median rainfalls were July and August.

Particularly distinctive characteristics of northern Australia's climate are the high seasonality and high inter-annual variability of rainfall. The seasonality of rainfall in the three study areas is considerably higher than the seasonality of rainfall in southern Australia. The inter-annual variability of rainfall in all three catchments is moderately high compared to other rainfall stations in northern Australia and high compared to other rainfall stations around Australia with the same mean annual rainfall. The seasonality and inter-annual variability of rainfall have implications for dryland agriculture, grazing and the storage of water.

The rainfall-generating systems in northern Australia and their modes of variability combine to produce irregular runs of dry and wet years. The length and magnitude (intensity) of dry spells, in particular, strongly influences the scale, profitability and risk of water resource related investments. The duration of dry spells (i.e. consecutive years of annual rainfall below the median annual rainfall) in the Victoria, Roper and Southern Gulf catchments is comparable to other areas of eastern Australia and does not appear unusual. The run magnitude (intensity) of dry years at rainfall stations in the Victoria, Roper and Southern Gulf catchments is slightly larger than that of stations in the Murray–Darling Basin and the east coast of Australia.

Areal potential evaporation in the Victoria, Roper and Southern Gulf catchments exceeds 1900, 1800 and 1900 mm respectively in most years. All catchments exhibit a strong seasonal pattern in potential evaporation, ranging from 200 mm per month during the build-up (October to December) to about 100 mm per month during the middle of the dry season (June). Annual rainfall deficits (i.e. difference between annual rainfall and annual potential evaporation) are large in the Victoria and Southern Gulf catchments (~1250 to 1500 mm) and moderate in the Roper catchment (~1000 to 1250 mm). High rainfall deficits adversely affect surface water storages. As a consequence of the high potential evaporation and seasonality of rainfall, about 95% of the Victoria and Southern Gulf catchments and about 80% of the Roper catchment is classified as being semi-arid.

A brief review of palaeoclimate studies in northern Australia indicated that circulation patterns approximating the present climate conditions in northern Australia (e.g. Pacific circulation responsible for the El Niño–Southern Oscillation (ENSO)) are thought to have been in place since about 3 to 2.5 million years ago, though past climates have been both wetter and drier than the instrument record.

GCM projections were used to produce climate data reflecting the Intergovernmental Panel on Climate Change a Shared Socioeconomic Pathway SSP2-4.5, which is considered a likely future emissions scenario. SSP2-4.5 represents a global warming of 1.4 °C (range 1.0 to 1.9 °C) for approximately the year 2060. For the Victoria catchment, 25% of GCM-PS results indicated an increase in future mean annual rainfall, 28% indicated a decrease and 47% indicated 'little change' (i.e. a change sufficiently small ($\pm 5\%$) that it is within the bounds of GCM internal variability). For the Roper catchment, 16% of GCM-PS indicated an increase in future mean annual rainfall and 28% indicated a decrease and 56% 'little change', while for the Southern Gulf catchments, 16% of GCM-PS indicated an increase in future mean annual rainfall, 44% indicated a decrease and 40% indicated 'little change'.

Based on the weight of current understanding, the global frequency of TCs will either decrease or remain essentially unchanged owing to greenhouse warming, though there is very low confidence in projected changes in cyclone frequency for individual catchments. The current consensus is that some increase in the mean maximum wind speed of TCs is likely (+2 to +11% globally), although increases may not occur in all tropical regions. For the period 2081 to 2100 relative to 1986 to 2005, the IPCC AR5 reports that global sea levels will most likely rise between 0.38 to 0.81 m under Representative Concentration Pathway (RCP) 8.5. There is high confidence that sea levels will continue to rise for centuries even if the global mean temperature is stabilised in the short to medium term.

Page deliberately left blank

Contents

Director’s foreword.....	i
The Victoria and Southern Gulf Water Resource Assessment Team	ii
Shortened forms	iii
Units	iv
Preface	v
Executive summary.....	ix

Part I Introduction and overview **1**

1	Introduction	2
1.1	Climate variable characteristics across northern Australia and their importance to agriculture	2
1.2	Assessment area.....	5
1.3	Climate data availability across northern Australia	7
1.4	Key concepts and terminology	11
2	Large-scale processes controlling northern Australia’s climate.....	13
2.1	Key rainfall-generating mechanisms across northern Australia	14
2.2	Rainfall variability and long-term trends.....	18
2.3	Evaporation	31
2.4	Sea surface temperature	34
2.5	Palaeoclimates of northern Australia.....	35

Part II Local-scale processes **37**

3	Victoria catchment.....	38
3.1	Data availability	38
3.2	Local-scale climate in the Victoria catchment.....	42
4	Roper catchment	56
4.1	Data availability	56
4.2	Local-scale climate in the Roper catchment	60
5	Southern Gulf catchments.....	74
5.1	Data availability	74
5.2	Local-scale climate in the Southern Gulf catchments.....	78

Part III Future climate projections		93
6	Future climate projections.....	94
6.1	Methods	94
6.2	Results	96
Part IV Discussion and Summary		109
7	Discussion	110
7.1	Establishment of an appropriate hydroclimate baseline	110
8	Summary remarks.....	113
References	117
Part V Appendices		131
Appendix A	Annual future climate variations under global warming scenario SSP5-8.5.....	132
Appendix B	Seasonal future climate variations under global warming scenario SSP5-8.5..	134

Figures

Preface Figure 1-1 Map of Australia showing Assessment areas (Victoria and Southern Gulf catchments) and other recent CSIRO Assessments.....vi	vi
Preface Figure 1-2 Schematic of the high-level linkages between the eight activity groups and the general flow of information in the Assessments.....vii	vii
Figure 1-1 Crop yield under dryland and irrigated agriculture..... 3	3
Figure 1-2 Evapotranspiration (mm) in response to changes in temperature of -2°C to $+2^{\circ}\text{C}$ for a sorghum crop sown on 15 March at Fitzroy Crossing..... 4	4
Figure 1-3 Comparison of mean monthly radiation (MJ/m^2) at selected locations in northern Australia (Chillagoe, Darwin and Fitzroy Crossing) and northern NSW (Moree) 4	4
Figure 1-4 Location map of the northerly draining catchments in Northern Australia and the Victoria, Roper and Southern Gulf catchments 7	7
Figure 1-5 Decadal analysis of the location and completeness of Bureau of Meteorology stations measuring daily rainfall used in the SILO database 8	8
Figure 1-6 Decadal analysis of the location and completeness of Bureau of Meteorology stations measuring daily maximum temperature used in the SILO database 9	9
Figure 2-1 Pressure systems and circulation cells influencing Australia 14	14
Figure 2-2 Mean annual number of TCs in the Australian region in (a) El Niño years, (b) La Niña years..... 16	16
Figure 2-3 Mean annual lightning ground flash density 17	17
Figure 2-4 Mean weekly rainfall probabilities and expected 850 hPa (approximately 1.5 km above sea level) wind anomalies for each of the 8 MJO phases 20	20
Figure 2-5 Seasonality of rainfall for 96 high-quality stations across Australia..... 21	21
Figure 2-6 Annual variation in rainfall in northern Australia..... 22	22
Figure 2-7 (a) Coefficient of variation of annual rainfall; and (b) the coefficient of variation of annual rainfall plotted against mean annual rainfall for 96 rainfall stations from around Australia 23	23
Figure 2-8 Mean northern rainfall onset dates for (a) all, (b) SOI neutral, (c) SOI negative (El Niño) and (d) SOI positive (La Niña) years 25	25
Figure 2-9 Runs of wet (blue columns) and dry (red columns) years at Yarralin in the Victoria catchment 28	28
Figure 2-10 Runs of wet (blue columns) and dry (red columns) years at Mataranka in the Roper catchment 28	28
Figure 2-11 Runs of wet (blue columns) and dry (red columns) years at Burketown in the Southern Gulf catchments 28	28
Figure 2-12 Run length skewness of dry and wet years for 96 rainfall stations around Australia.....30	30

Figure 2-13 Run length of dry (a) and wet (b) years plotted against lag-one serial correlation coefficient for 96 high-quality rainfall stations around Australia.....	30
Figure 2-14 Run magnitude of dry spells (a) and run magnitude of dry spells plotted against the coefficient of variation of annual rainfall (b), for 96 rainfall stations around Australia.....	31
Figure 2-15 Mean annual and seasonal rainfall, PE and rainfall deficit (1930 to 2007).....	32
Figure 2-16 Köppen-Geiger climate classification of northern Australia	33
Figure 2-17 UNEP aridity index across Australia.....	34
Figure 2-18 Linear trend in annual averaged SST (°C per decade) from 1982 to 2015	35
Figure 3-1 A shaded relief map of the Victoria catchment.....	39
Figure 3-2 Decadal analysis of the location and completeness of Bureau of Meteorology stations measuring daily rainfall used in the SILO database	40
Figure 3-3 Decadal analysis of the location and completeness of Bureau of Meteorology stations in the Victoria catchment measuring daily maximum air temperature used in the SILO database	41
Figure 3-4 Historical (a) mean annual rainfall and (b) median annual rainfall across the Victoria catchment	42
Figure 3-5 Historical median rainfall during the (a) wet and (b) dry season in the Victoria catchment	43
Figure 3-6 Historical monthly rainfall in the Victoria catchment at Auvergne, Yarralin, Kalkarindji (Wave Hill) and Top Springs	44
Figure 3-7 Historical annual rainfall that was exceeded in (a) 1%, (b) 10%, (c) 90% and (d) 99% of years in the Victoria catchment.....	46
Figure 3-8 Historical daily rainfall that is exceeded in (a) 0.01%, (b) 0.1%, (c) 1% and (d) 10% of days in the Victoria catchment	47
Figure 3-9 Historical potential evaporation in the Victoria catchment at Auvergne, Yarralin, Kalkarindji (Wave Hill) and Top Springs	48
Figure 3-10 Historical median (a) annual, (b) wet-season, (c) dry-season rainfall; (d) annual, (e) wet-season, (f) dry-season potential evaporation; and (g) annual, (h) wet-season and (i) dry-season rainfall deficit in the Victoria catchment	49
Figure 3-11 Historical maximum and minimum air temperature in the Victoria catchment at Auvergne, Yarralin, Kalkarindji (Wave Hill) and Top Springs	50
Figure 3-12 Historical annual maximum air temperature that is exceeded in (a) 10%, (b) 50% and (c) 90% of years in the Victoria catchment.....	51
Figure 3-13 Historical annual minimum air temperature that is exceeded in (a) 10%, (b) 50% and (c) 90% of years in the Victoria catchment.....	51
Figure 3-14 Historical minimum temperature thresholds in the Victoria catchment.....	52

Figure 3-15 Historical annual radiation that is exceeded in (a) 10%, (b) 50% and (c) 90% of years in the Victoria catchment.....	52
Figure 3-16 Historical monthly radiation in the Victoria catchment at Auvergne, Yarralin, Kalkarindji (Wave Hill) and Top Springs	53
Figure 3-17 Historical annual relative humidity that is exceeded in (a) 10%, (b) 50% and (c) 90% of years in the Victoria catchment.....	54
Figure 3-18 Historical monthly relative humidity in the Victoria catchment at Auvergne, Yarralin, Kalkarindji (Wave Hill) and Top Springs	54
Figure 3-19 Historical monthly SST offshore Victoria catchment.....	55
Figure 4-1 A shaded relief map of the Roper catchment	57
Figure 4-2 Decadal analysis of the location and completeness of Bureau of Meteorology stations measuring daily rainfall used in the SILO database	58
Figure 4-3 Decadal analysis of the location and completeness of Bureau of Meteorology stations in the Roper catchment measuring daily maximum air temperature used in the SILO database.....	59
Figure 4-4 Historical (a) mean annual rainfall and (b) median annual rainfall across the Roper catchment	60
Figure 4-5 Historical median rainfall during the (a) wet and (b) dry season in the Roper catchment	61
Figure 4-6 Historical monthly rainfall in the Roper catchment at Ngukurr, Mataranka, Larrimah and Bulman	62
Figure 4-7 Historical annual rainfall that was exceeded in (a) 1%, (b) 10%, (c) 90% and (d) 99% of years in the Roper catchment.....	64
Figure 4-8 Historical daily rainfall that is exceeded in (a) 0.01%, (b) 0.1%, (c) 1% and (d) 10% of days in the Roper catchment.....	65
Figure 4-9 Historical potential evaporation in the Roper catchment at Ngukurr, Mataranka, Larrimah and Bulman.....	66
Figure 4-10 Historical median (a) annual, (b) wet-season, (c) dry-season rainfall; (d) annual, (e) wet-season, (f) dry-season potential evaporation; and (g) annual, (h) wet-season and (i) dry-season rainfall deficit in the Roper catchment.....	67
Figure 4-11 Historical maximum and minimum air temperature in the Roper catchment at Ngukurr, Mataranka, Larrimah and Bulman.....	68
Figure 4-12 Historical maximum air temperature that is exceeded in (a) 10%, (b) 50% and (c) 90% of years in the Roper catchment.....	69
Figure 4-13 Historical minimum air temperature that is exceeded in (a) 10%, (b) 50% and (c) 90% of years in the Roper catchment.....	69
Figure 4-14 Historical minimum temperature thresholds in the Roper catchment.....	70
Figure 4-15 Historical annual radiation that is exceeded in (a) 10%, (b) 50% and (c) 90% of years in the Roper catchment	70

Figure 4-16 Historical monthly radiation in the Roper catchment at Ngukurr, Mataranka, Larrimah and Bulman.....	71
Figure 4-17 Historical annual relative humidity that is exceeded in (a) 10%, (b) 50% and (c) 90% of years in the Roper catchment.....	72
Figure 4-18 Historical monthly relative humidity in the Roper catchment at Ngukurr, Mataranka, Larrimah and Bulman.....	72
Figure 4-19 Historical monthly SST offshore Roper catchment.....	73
Figure 5-1 A shaded relief map of the Southern Gulf catchments.....	75
Figure 5-2 Decadal analysis of the location and completeness of Bureau of Meteorology stations in the Southern Gulf catchments measuring daily rainfall used in the SILO database	76
Figure 5-3 Decadal analysis of the location and completeness of Bureau of Meteorology stations in the Southern Gulf catchments measuring daily maximum air temperature used in the SILO database.....	77
Figure 5-4 Historical (a) mean annual rainfall and (b) median annual rainfall in the Southern Gulf catchments.....	78
Figure 5-5 Historical median rainfall during the (a) wet and (b) dry season in the Southern Gulf catchments.....	79
Figure 5-6 Historical rainfall in the Southern Gulf catchments at Mount Isa, Doomadgee, Gregory and Burketown.....	81
Figure 5-7 Historical annual rainfall that was exceeded in (a) 1%, (b) 10%, (c) 90% and (d) 99% of years in the Southern Gulf catchments	82
Figure 5-8 Historical daily rainfall that is exceeded in (a) 0.01%, (b) 0.1%, (c) 1% and (d) 10% of days in the Southern Gulf catchments.....	83
Figure 5-9 Historical potential evaporation in the Southern Gulf catchments at Mount Isa, Doomadgee, Gregory and Burketown	84
Figure 5-10 Historical median (a) annual, (b) wet-season, (c) dry-season rainfall; (d) annual, (e) wet-season, (f) dry-season potential evaporation; and (g) annual, (h) wet-season and (i) dry-season rainfall deficit in the Southern Gulf catchments	85
Figure 5-11 Historical maximum and minimum monthly air temperature in the Southern Gulf catchments at Mount Isa, Doomadgee, Gregory and Burketown.....	86
Figure 5-12 Historical maximum air temperature that is exceeded in (a) 10%, (b) 50% and (c) 90% of years in the Southern Gulf catchments	87
Figure 5-13 Historical minimum air temperature that is exceeded in (a) 10%, (b) 50% and (c) 90% of years in the Southern Gulf catchments	87
Figure 5-14 Historical minimum temperature thresholds in the Southern Gulf catchments	88
Figure 5-15 Historical annual radiation that is exceeded in (a) 10%, (b) 50% and (c) 90% of years	88

Figure 5-16 Historical monthly radiation in the Southern Gulf catchments at Mount Isa, Doomadgee, Gregory and Burketown	89
Figure 5-17 Historical annual relative humidity that is exceeded in (a) 10%, (b) 50% and (c) 90% of years in the Southern Gulf catchments	90
Figure 5-18 Historical monthly relative humidity in the Southern Gulf catchments at Mount Isa, Doomadgee, Gregory and Burketown	90
Figure 5-19 Historical monthly SST offshore Southern Gulf catchments	91
Figure 6-1 Percentage change in rainfall and potential evaporation per degree of global warming for the 32 Scenario C simulations relative to Scenario A values for the Victoria catchment. GCM-PS ranked by increasing rainfall for SSP2-4.5	97
Figure 6-2 Percentage change in rainfall and potential evaporation per degree of global warming for the 32 Scenario C simulations relative to Scenario A values for the Roper catchment. GCM-PS ranked by increasing rainfall for SSP2-4.5	97
Figure 6-3 Percentage change in rainfall and potential evaporation per degree of global warming for the 32 Scenario C simulations relative to Scenario A values for the Southern Gulf catchments. GCM-PS ranked by increasing rainfall for SSP2-4.5	98
Figure 6-4 Spatial distribution of mean annual rainfall across the Victoria catchment under scenarios Cwet, Cmid and Cdry.....	100
Figure 6-5 Spatial distribution of percentage change in mean annual rainfall relative to Scenario A across the Victoria catchment under scenarios Cwet, Cmid and Cdry.....	100
Figure 6-6 Spatial distribution of mean annual rainfall across the Roper catchment under scenarios Cwet, Cmid and Cdry.....	100
Figure 6-7 Spatial distribution of percentage change in mean annual rainfall relative to Scenario A across the Roper catchment under scenarios Cwet, Cmid and Cdry	101
Figure 6-8 Spatial distribution of mean annual rainfall across the Southern Gulf catchments under scenarios Cwet, Cmid and Cdry	101
Figure 6-9 Spatial distribution of percentage change in mean annual rainfall relative to Scenario A across the Southern Gulf catchments under scenarios Cwet, Cmid and Cdry.....	101
Figure 6-10 Mean monthly rainfall (left column) and potential evaporation (right column) for the Victoria, Roper and Southern Gulf catchments under scenarios A and C.....	103
Figure 7-1 Wet and dry spells of catchment average runoff across the Flinders catchment over a 60-year period.....	111

Tables

Table 6-1 Changes in global surface temperature for selected 20-year time periods across the five emissions scenarios presented by the IPCC Sixth Assessment Report.....	94
Table 6-2 Percentage change in mean annual rainfall and potential evaporation per degree warming under scenarios Cwet, Cmid and Cdry for SSP2-4.5 and SSP5-8.5 emissions scenarios for the Victoria catchment.....	98
Table 6-3 Percentage change in mean annual rainfall and potential evaporation per degree warming under scenarios Cwet, Cmid and Cdry for SSP2-4.5 and SSP5-8.5 emissions scenarios for the Roper catchment.....	98
Table 6-4 Percentage change in mean annual rainfall and potential evaporation per degree warming under scenarios Cwet, Cmid and Cdry for SSP2-4.5 and SSP5-8.5 emissions scenarios for the Southern Gulf catchments	99
Table 6-5 Projected sea-level rise for the coast of the Victoria catchment	105
Table 6-6 Projected sea-level rise for the coast of the Roper catchment	105
Table 6-7 Projected sea-level rise for the coast of the Southern Gulf catchments.....	105

Page deliberately left blank

Part I Introduction and overview



1 Introduction

Climate variables, water availability and soil data are generally considered to be the most important environmental information for determining the suitability of particular locations for agriculture. Given climate is so closely linked to hydrology and water availability, understanding of climate and its variability is especially important in assessments of water resource development and irrigation in northern Australia.

The Northern Australia Water Resource Assessment (the Assessment) is primarily focused on assessing the opportunity for water resource development, including agriculture and irrigation, with currently available environmental resources. Given the changes in temperature and rainfall projected in the coming decades, and the sensitivity to that change of Australian agriculture and the natural resource base on which it depends (Reisinger et al., 2014), the effects of climate change on specific development options form part of this Assessment.

The primary purpose of this report is to: (i) provide a general overview of the current climate of the Victoria (Northern Territory, NT), Roper (NT) and Southern Gulf (Queensland) catchments within the context of suitability for agriculture; (ii) describe the method of scaling the historical climate series to represent projected climate change; and (iii) present the results of empirical scaling for an ensemble of 32 of the latest global climate models (GCMs) from the sixth Coupled Model Intercomparison Project (CMIP6) as used in the Intergovernmental Panel on Climate Change (IPCC) Sixth Assessment Report. This CSIRO report forms part of the Assessment and provides a consistent set of current and future climate data for use by other activities (Preface Figure 1-2).

This report is broken into four parts. Part I provides introductory and contextual information, including a brief description of the importance of climate to agriculture and aquaculture, a description of the three study areas and the availability of climate data in each. Key concepts and terminology are then described and an overview of the climate of northern Australia is provided. Part II discusses local-scale climate processes in each of the three study areas. Part III describes climate and streamflow forecasting and the methods by which the historical climate data were scaled to reflect projected climate change, as informed by CMIP6 GCMs used in the IPCC Sixth Assessment Report (IPCC, 2022). Discussions and summary remarks are captured in Part IV. The report contains two appendices. Appendix A provides mean annual future climate variations under global warming scenario SSP5-8.5 and Appendix B provides mean seasonal future climate variations under global warming scenario SSP5-8.5.

1.1 Climate variable characteristics across northern Australia and their importance to agriculture

Weather is the key source of uncertainty affecting crop yield. It influences the rate and vigour of crop growth, while catastrophic weather events can result in extensive crop losses. Key climate parameters controlling plant growth and crop productivity are discussed in turn below, although it should be noted that they never act in isolation but are interrelated so impact synergistically.

Of all the climate parameters affecting hydrology and agriculture in water-limited environments, rainfall is usually the most important. Rainfall is the main determinant of runoff and recharge and is a fundamental requirement for plant growth. For this reason, reporting of climate parameters is heavily biased towards rainfall data.

1.1.1 Rainfall

Water is essential for the maintenance of physiological and chemical processes within the plant, acting as an energy exchanger and carrier of nutrient food supply in solution. Across northern Australia the seasonality of rainfall is a key limitation to the growth of many dryland crops. In irrigated systems rainfall can supplement irrigation water, meaning larger areas can potentially be irrigated (e.g. Figure 1-1). However, where a plentiful supply of irrigation water is available, higher rainfall is associated with a reduction in radiation (due to cloud cover) and reduced trafficability on heavier soils, potentially resulting in reduced yields. Intense rainfall events (over 40 mm/hour) and associated winds can also damage broadacre and horticultural crops, and cause soil erosion and leaching of organics and nutrients. Excessive rainfall can also complicate the management of agricultural land, for example in managing runoff and on higher clay soils excess rainfall can contribute to waterlogging with subsequent loss of soil nitrogen through denitrification.

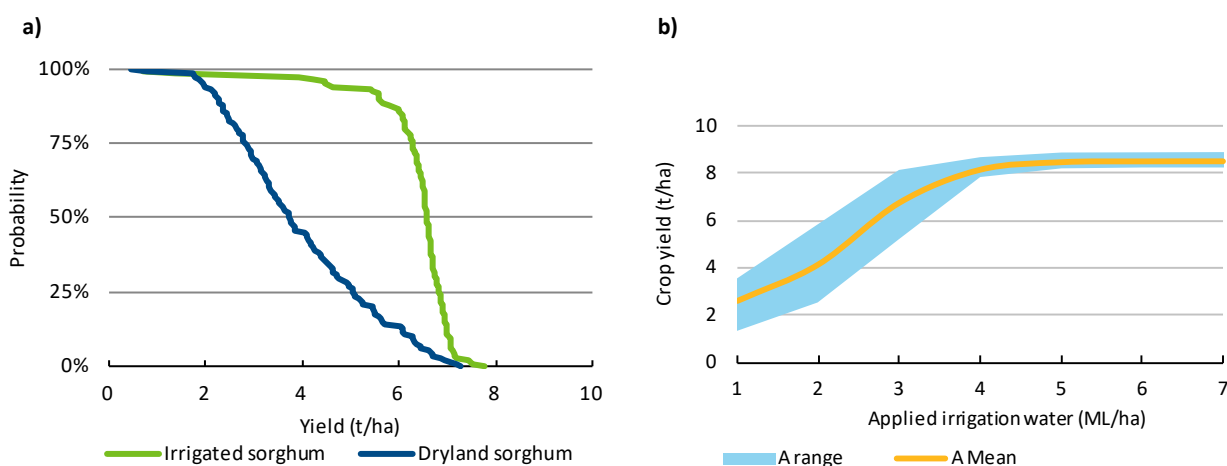


Figure 1-1 Crop yield under dryland and irrigated agriculture

(a) Probability of crop yield potential for dryland and fully irrigated sorghum (grain) sown in Georgetown (Gilbert catchment, northern Australia) climate on 15 January (Webster et al., 2013). (b) Crop yield plotted against applied irrigation water in Georgetown climate. A range is the 20th to 80th percentile exceedance and A mean crop yields for sorghum (grain). Assumes perfect timing of irrigation (i.e. no losses) (Webster et al., 2013).

1.1.2 Temperature

Temperature influences all plant physiological processes and is a particularly important factor controlling the length of the growing cycle of crops, where the optimal temperature for plant growth and maximising crop productivity varies between crop species. Temperature extremes at sensitive phenological stages can adversely impact on crop productivity, for example if extreme temperatures occur during flowering and pollination, cotton boll development or grain filling. Plant species have differing temperature thresholds for optimum growth and response during periods of extreme high or low temperature. For northern Australia, high temperatures generally occur during the early wet-season months of October to December. When high temperatures

coincide with little water in the soil, plants are unable to cool their leaves, photosynthesis is reduced and plant tissue damage can occur. Prior to the start of the wet-season rains, low soil water, higher air temperatures and solar radiation combine to heat soils low in vegetative cover. High soil temperatures can affect seedling emergence and crop establishment. For an irrigated crop higher temperatures induce higher evaporative demand with increased evapotranspiration (e.g. Figure 1-2) and thus a higher irrigation requirement. The occurrence of low temperatures at certain times of the year is also important in helping to manage soil disease and pests.

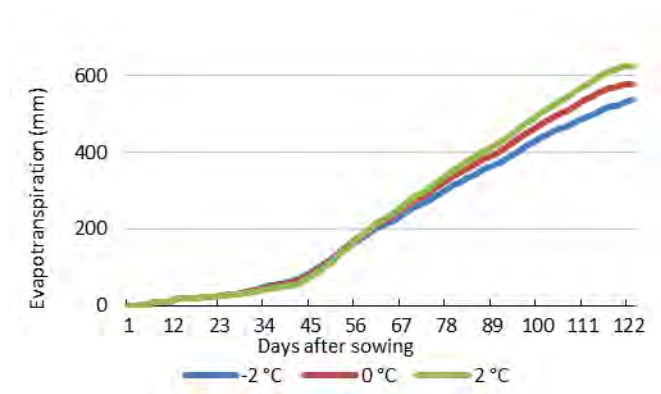


Figure 1-2 Evapotranspiration (mm) in response to changes in temperature of -2 °C to +2 °C for a sorghum crop sown on 15 March at Fitzroy Crossing

1.1.3 Radiation

Radiation is an important factor controlling plant growth through its effect on photosynthesis, and a basic principle for increasing crop yield is to maximise radiation interception. Radiation also influences the daily opening and closing of stomata and the formation of chlorophyll. Air temperature, another control on plant growth discussed above, is also indirectly dependent upon solar radiation. Although low latitudes have the most favourable sun angle, in northern Australia the amount of annual radiation is similar to mid-latitudes (e.g. Moree in NSW), but the timing is different (Figure 1-3). This is because radiation is generally reduced during the wet-season months over northern Australia due to cloud cover.

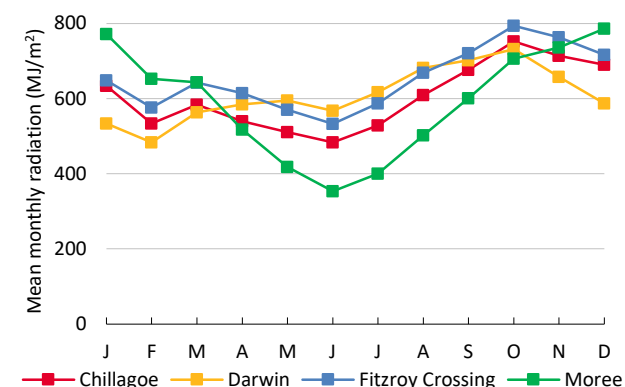


Figure 1-3 Comparison of mean monthly radiation (MJ/m²) at selected locations in northern Australia (Chillagoe, Darwin and Fitzroy Crossing) and northern NSW (Moree)

Low radiation in northern Australia is associated with increased cloud cover during the wet season (January to February) whereas low radiation at Moree is a result of the sun having a lower maximum elevation during winter in the southern hemisphere.

1.1.4 Humidity

Humidity is a measure of the amount of water vapour in the air, with the water holding capacity of the air dependent upon temperature. Humidity affects the opening and closing of the stomata, which regulates loss of water from the plant through transpiration as well as photosynthesis. Plants transpire or release water vapour to the atmosphere to regulate their internal temperature and to grow. Generally, water vapour moves from a higher concentration in the leaf to a lower concentration in the atmosphere. The more water in the atmosphere, the greater the vapour pressure exerted on the leaves and therefore transpiration is reduced. From a plant perspective the difference between the vapour pressure in their leaves and that of the air (for a particular temperature) can be described as vapour pressure deficit (VPD). A higher VPD is associated with greater atmospheric demand for moisture and therefore higher transpiration by the plant. While high VPD can contribute to water stress in a plant, periods of high humidity (low VPD) also influence the development of many plant diseases (Paul and Munkvold, 2005).

1.1.5 Wind speed

Wind can be both beneficial and harmful to crop and tree productivity. It can aid the process of pollination, and so is particularly important in the development of fruit and seed from wind-pollinated flowers (e.g. grasses). Wind also facilitates the exchange of gases. Strong winds, however, can cause excessive water loss through transpiration and can cause plants and trees to lodge and topple (Cleugh et al., 1998; Negrón-Juárez et al., 2014). Winds can be particularly harmful in combination with other factors. For example, windblown sand particles can damage vegetative surfaces. In conditions of low humidity, dry winds can result in particularly excessive plant water loss, which can cause plants to wilt. This can result in a decreased rate of photosynthesis, growth, yield and potentially death.

1.2 Assessment area

The Assessment comprises three study areas: the Victoria (NT), Roper (NT) and Southern Gulf (Queensland) catchments (Figure 1-4). These are discussed in turn below. In this report northern Australia is defined as the area north of the Tropic of Capricorn. The northerly draining basins are those Australian Water Resources Council (AWRC) catchments within the Timor Sea and the Gulf of Carpentaria drainage divisions. Population statistics in the following sections come from the Australia Bureau of Statistics (Australian Bureau of Statistics, 2021) and land use information comes from the Australian Bureau of Agricultural and Resource Economics (Australian Bureau of Agricultural and Resource Economics, 2022).

1.2.1 Victoria catchment

The Victoria catchment covers an area of 82,400 km² with the Victoria River extending about 720 km from Riveren Station at its source in the south, to the Joseph Bonaparte Gulf and ultimately Timor Sea in the north. The catchment population is distributed across the towns of Timber Creek (population 278) and a number of Aboriginal communities and outstations – the largest communities being Yarralin (283 people), Nitjpurru (Pigeon Hole) (106 people) and Daguragu–

Kalkarindji (575 people). The nearest major population centres are Katherine to the north-east and Kununurra to the west. The Victoria River is the longest singularly named permanent river in the NT and has one of the largest discharge of any river in Australia north of the Tropic of Capricorn, with a river mouth of more than 10 km. The main land use is pastoralism (60%), with large grazing leases carrying beef cattle. Nature conservation (17%, including Judbarra National Park), other protected areas including Indigenous uses (14%) and other minimal uses (9%, including for Defence) comprise the catchment's other main land uses. The catchment is characterised by grassy plains, rolling savannas, rocky spinifex country, mesas and plateaux.

1.2.2 Roper catchment

The Roper catchment covers an area of 77,400 km² and extends from just east of Katherine and south of Daly Waters to the Gulf of Carpentaria. Much of the catchment is low relief, consisting of open woodlands with escarpments, grassy alluvial plains, gorges and plateaux. The catchment is sparsely populated with a population at the 2016 Census of 2,512 people. This includes the regional centre of Mataranka (350 people), towns of Larrimah (47 people) and Daly Waters (55 people), as well as the Aboriginal communities of Ngukurr (largest population centre in the catchment with 1,149 people), Beswick, Barunga and Bamyili. There are also some smaller Indigenous communities, outstations and roadhouses. Katherine (population 6303 in 2016) is the closest urban service centre and is located about 100 km north-west of Mataranka, just outside the catchment. The nearest major city and population centre is the NT capital of Darwin (population of Greater Darwin area was 136,828 in 2016), approximately 420 km from Mataranka.

The Roper River is a large perennial flowing river with headwaters in the Mataranka Springs Complex and draining one of the largest catchment areas flowing into the western Gulf of Carpentaria. The main land uses are extensive grazing of beef cattle on native rangelands (46%), other protected areas including Indigenous freehold tenure (45%) and nature conservation (6%). Protected areas in the catchment include two national parks (Esey National Park (140 km²) and Limmen National Park 9300 km² (much of this extending beyond the Roper catchment) and the South East Arnhem Land Indigenous Protected Area. About 2040 ha of irrigated agriculture exists in the Roper catchment including 850 ha of sandalwood, 803 ha of melons and 320 ha of mangoes and 64 ha of sorghum forage. Adjacent to the Roper catchment are two contiguous marine parks, Limmen Bight (870 km²) in Territory waters and the Limmen Marine Park (1400 km²) in Commonwealth waters.

1.2.3 Southern Gulf catchment

The Southern Gulf catchments comprise four northerly draining catchments defined by the AWRC river basin boundaries: Settlement Creek (17,600 km²), Nicholson River (52,200 km²), Leichhardt River (33,400 km²), Morning Inlet (3700 km²) and the islands within the AWRC Mornington Island Basin (total 1200 km²). The total area of the mainland catchments is 106,900 km². Limited stream gauge data indicates that both the Gregory and Nicholson Rivers, at least in the upper portions of their catchments, are perennial. Flows in the upper Gregory River and Lawn Hill Creek are associated with limestone and dolostone aquifers. Mount Isa (population 17,936) is the region's commercial, administrative and industrial centre. Elsewhere across the catchments, the population is generally sparse, with Doomadgee (1,387 people), Gununa (on Mornington Island -

1,136 people) and Burketown (167 people) being the largest towns. A substantial proportion of the population is Indigenous, particularly in Doomadgee (more than 90%) and throughout the Mornington and Wellesley Islands (80%). The main commercial land use is extensive grazing of beef cattle (84%) including on productive black soil plains, with nature conservation through national parks including Boodjamulla (formerly Lawn Hill) National Park and Indigenous Protected Areas comprising 13% of the catchments' area. Century Zinc Mine – formerly one of the world's largest zinc mines – is located near Lawn Hill and there are large mining operations in and near Mount Isa. The catchment incorporates the edge of the Barkly Tablelands and is characterised by extensive alluvial grassy plains, distinctive marine plains, dissected hilly regions and erosional plains.

1.3 Climate data availability across northern Australia

An exploratory evaluation of the spatial and temporal extent of the available climate data across northern Australia reveals that the Gulf region has the best historical coverage of rainfall (Figure 1-5) and temperature (Figure 1-6) stations across northern Australia. Because rainfall has lower spatial and temporal correlation than other climate variables, the Bureau of Meteorology has established a higher spatial density of observation stations for rainfall than other climate variables; all have generally increased in density over time, although there has been a slight reduction since the 1990s (Figure 1-5 and Figure 1-6). Nevertheless, the lack of stations measuring non-rainfall parameters across northern Australia is a limitation for agronomists trying to assess local-scale conditions for growth and yield potential of crops, pastures and trees.

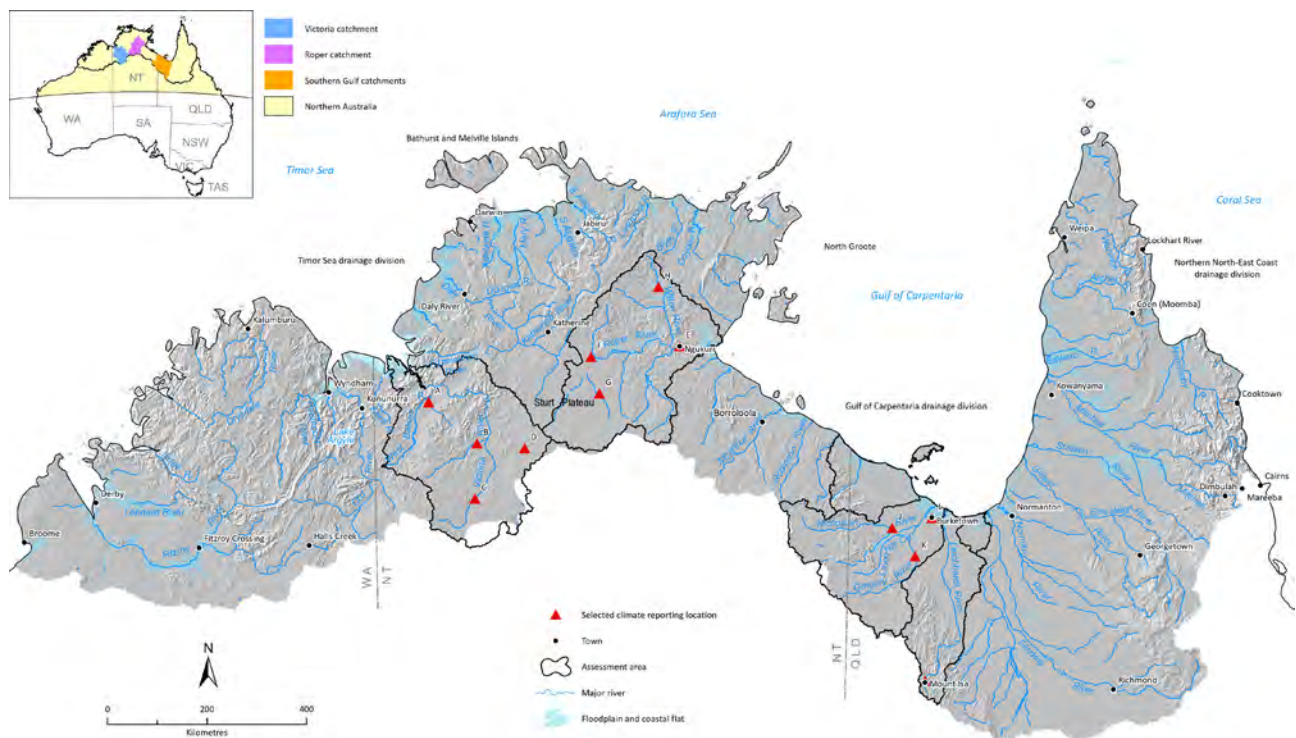


Figure 1-4 Location map of the northerly draining catchments in Northern Australia and the Victoria, Roper and Southern Gulf catchments

Climate stations: A – Auvergne, B – Yarralin, C – Kalkarindji, D – Top Springs, E – Ngukurr, F – Mataranka, G – Larrimah, H – Bulman, I – Mount Isa, J – Doomadgee, K – Gregory, L – Burketown. Inset shows Northern Australia and Timor Sea and Gulf of Carpentaria drainage divisions.

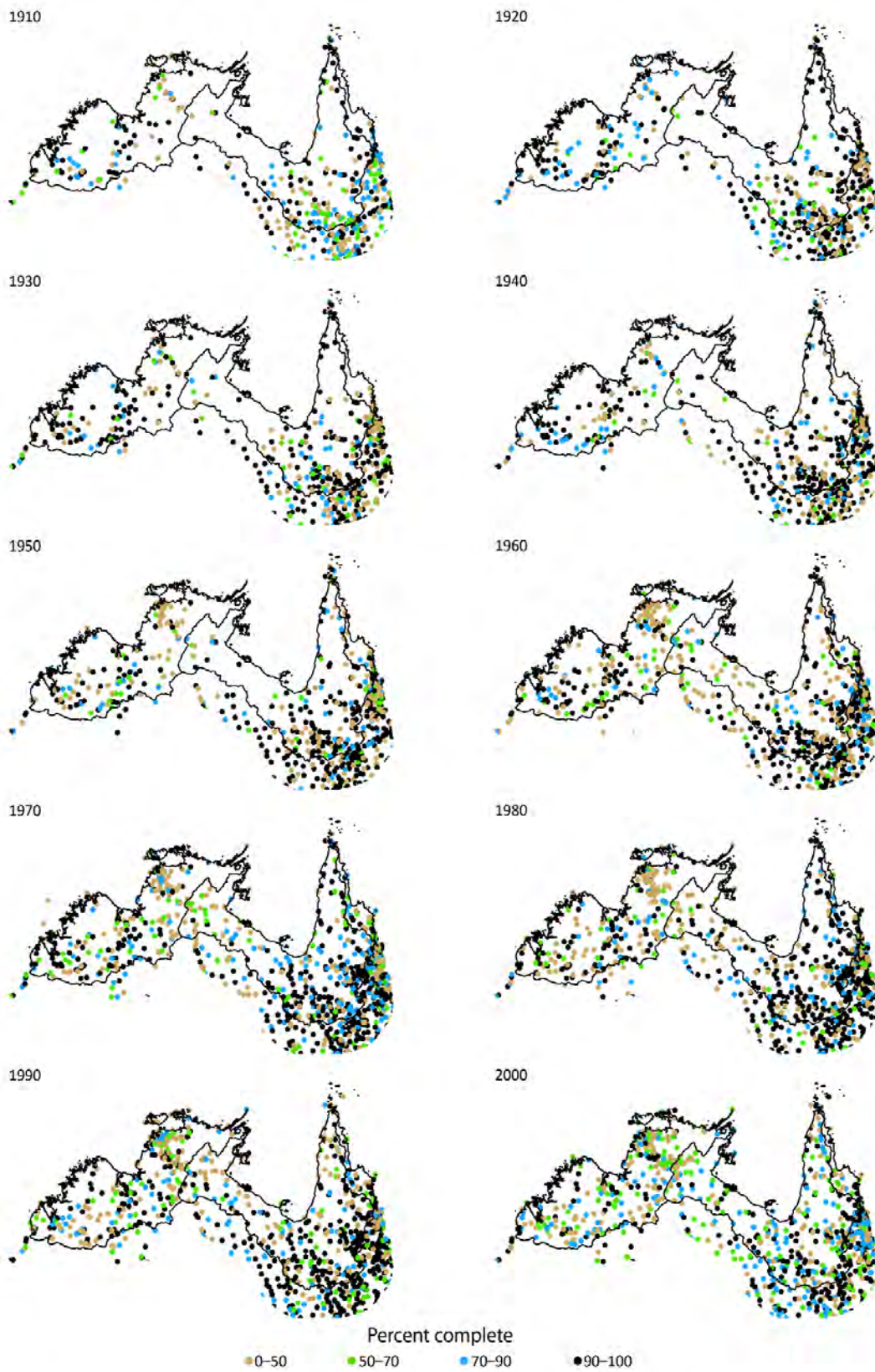


Figure 1-5 Decadal analysis of the location and completeness of Bureau of Meteorology stations measuring daily rainfall used in the SILO database

The decade labelled '1910' is defined from 1 January 1910 to 31 December 1919, and so on. At a station, a decade is 100% complete if there are observations for every day in that decade (Li et al., 2009).

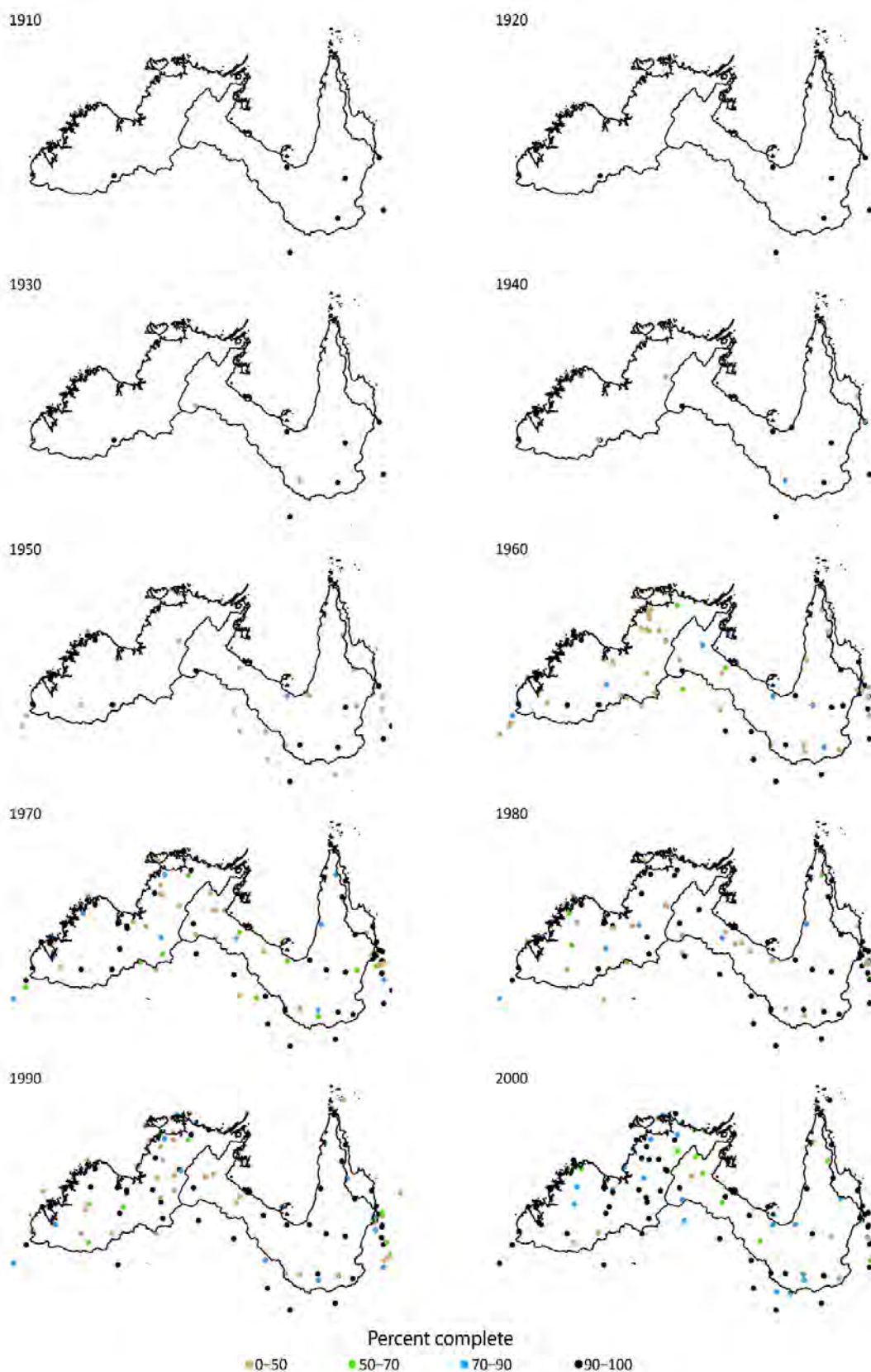


Figure 1-6 Decadal analysis of the location and completeness of Bureau of Meteorology stations measuring daily maximum temperature used in the SILO database

The decade labelled '1910' is defined from 1 January 1910 to 31 December 1919, and so on. At a station, a decade is 100% complete if there are observations for every day in that decade (Li et al., 2009).

1.3.1 Source of climate data

Spatially continuous climate datasets

This report, and the reports dependent upon it, is based on historical daily climate data derived from 0.05×0.05 degree ($\sim 5 \text{ km} \times 5 \text{ km}$) resolution grids. For the Roper catchment the 109-year period spanning 1 September 1910 to 31 August 2019 is used, while for the Victoria and Southern Gulf catchments the 132-year period spanning 1 September 1890 to 31 August 2022 is used. Data were sourced from the scientific information for land owners (SILO) data drill database, <http://www.longpaddock.qld.gov.au/silo/> (Jeffrey et al., 2001). SILO provides surfaces of daily climate data interpolated and infilled from point measurements made by the observation network developed and maintained by the Bureau of Meteorology.

The variables used were rainfall, incoming shortwave solar radiation, vapour pressure, maximum air temperature, minimum air temperature and relative humidity. These data were used to produce the spatially continuous maps of climate surfaces presented later. Prior to 1957 the SILO climate dataset used a variety of algorithms to synthetically generate non-rainfall parameter values based on the observed climate statistics between 1957 and current time (Jeffrey et al., 2001). For this reason, historical plots and maps for non-rainfall parameter values were calculated over the time period 1965 to 2015 (unless specified otherwise).

It is important to note that the gridded climate data are a modelled dataset (i.e. they are derived from observed data but do not contain the original observed data). Observations have been quality checked by the Bureau of Meteorology and the interpolation routines used have been subjected to additional error checking by the Queensland Government (Jeffrey et al., 2001). Data accuracy is expected to be lowest in areas where the observation density is low relative to the climate gradients and where observations are only available for shorter time periods.

In addition to daily rainfall data, the surface water and groundwater models used in the Assessment require estimates of potential evaporation (PE). This represents the atmospheric demand for water under given meteorological conditions and provides an upper limit to the actual evaporation in the hydrological modelling. Morton's wet environment areal potential evaporation (APE) (Morton, 1983) was calculated for the daily 0.05×0.05 degree grids using the following SILO data: (i) maximum and minimum air temperature, (ii) incoming solar radiation, and (iii) atmospheric vapour pressure (converted to relative humidity using the SILO actual vapour pressure divided by the saturation vapour pressure at the daily air temperature extremes). This method is outlined in Li et al. (2009).

APE represents the evaporation that would take place from a continually saturated surface that is large enough to render the effects of any upwind boundary transitions negligible, thus integrating local variations to an areal mean. In water-limited environments, daily hydrological modelling, when parameterised or calibrated against streamflow observations, is much less sensitive to errors in the PE data than it is to errors in the rainfall data (e.g. Andréassian et al. (2004)). It is also easier to provide reliable PE data for the hydrological modelling, as PE has lower spatial variance with smaller day-to-day variation compared to rainfall.

Point climate datasets

SILO patch point datasets were acquired for 96 rainfall stations around Australia. Unlike the SILO gridded data drill product referred to above, these data contain real observations, gap filled where necessary using interpolation from nearby stations. The 96 rainfall stations were selected for all of Australia on the basis that they and close neighbouring stations had near continuous rainfall data from 1 September 1890 to 31 August 2022 (three stations were located within or in close proximity to the three study areas). The SILO point patch datasets were acquired from <http://www.longpaddock.qld.gov.au/silo/>.

Sea surface temperature datasets

Mean monthly sea surface temperature (SST) data were sourced from the National Oceanic and Atmospheric Administration (NOAA) optimum interpolation sea surface temperature analysis (Reynolds et al., 2002; Smith et al., 2008b), a large-scale satellite dataset (i.e. with a horizontal resolution of one degree). The time period for which data are available is 1982 to 2015, unless stated otherwise. The period used to calculate the baseline climatology is 1981 to 2010. All ocean grid points north of 30° south and within 370 km of the Australian coastline were included in the northern Australia analysis. A representative grid point was also selected adjacent to the coastline of each of the study areas.

1.4 Key concepts and terminology

1.4.1 Definition of water year and seasons

Northern Australia experiences a highly seasonal climate, with most of rain falling during December to March. Unless specified otherwise, this Assessment defines the wet season as the 6-month period from 1 November to 30 April, and the dry season as the 6-month period from 1 May to 31 October. This wet season was chosen as it is the wettest 6-month period for all three study areas, however it should be noted that the transition from the dry to the wet season typically occurs in October or November and so an alternative northern wet season definition commonly used by meteorologists is 1 October to 30 April.

All results in the Assessment will be reported over the water year, defined as the period 1 September to 31 August, unless specified otherwise. This allows each individual wet season to be counted in a single 12-month period, rather than being split over two calendar years (i.e. counted as two separate seasons). This is more realistic for reporting climate statistics from a hydrological and agricultural assessment viewpoint.

1.4.2 Scenario definitions

Four scenarios will be evaluated in the Assessment, reflecting a combination of different levels of development and historical and future climates, much like those used in the Northern Australia Sustainable Yields Project (CSIRO, 2009a; 2009b; 2009c) and the Flinders and Gilbert Agriculture Resource Assessment (Petheram and Yang, 2013).

Scenario A

Scenario A is historical climate and current development. The historical climate series is defined as the observed climate (rainfall, temperature and PE) for water years from 1 September 1910 to 31 August 2019 for the Roper catchment and 1 September 1890 to 31 August 2022 for the Victoria and Southern Gulf catchments. All results presented in this report are calculated over these periods unless specified otherwise. The current level of surface water, groundwater and economic development will be assumed as at 31 August 2021. Scenario A will be used as the baseline against which assessments of relative change will be made. Historical tidal data will be used to specify downstream boundary conditions for the flood modelling.

Scenario B

Scenario B is historical climate and future development, as generated in the Assessment. Scenario B will use the same historical climate series as Scenario A. River inflow, groundwater recharge and flow, and agricultural productivity will be modified to reflect potential future development. The impacts of changes in flow due to this future development will be assessed, including impacts on:

- instream, riparian and near-shore ecology
- Indigenous water values
- economic costs and benefits
- opportunity costs of expanding irrigation
- institutional, economic and social considerations that may impede or enable adoption of irrigated agriculture.

Scenario C

Scenario C is future climate and current development. It will be based on the 109- or 132-year climate series (as in Scenario A) derived from GCM projections for an approximate 1.6 °C global temperature rise (~2060) relative to the 1990 scenario, representing Shared Socioeconomic Pathway, SSP2-4.5 The GCM projections will be used to modify the observed historical daily climate sequences. The current level of surface water, groundwater and economic development will be assumed.

Scenario D

Scenario D is future climate and future development. It will use the same future climate series as Scenario C. River inflow, groundwater recharge and flow, and agricultural productivity will be modified to reflect potential future development, as in Scenario B. Therefore, in this report, the climate data for Scenarios A and B are the same and the climate data for Scenarios C and D are the same.

2 Large-scale processes controlling northern Australia's climate

The primary characteristics of Australia's climate are a consequence of four major interrelated factors (Hobbs, 1998):

1. Its location within the subtropical latitudinal zone. Australia's landmass is centrally located within the dry descending air of the Hadley cell circulation. This results in much of the continent being affected by large eastward-travelling anticyclones (Figure 2-1). These high-pressure systems, which may extend up to 4000 km along their west–east axis, are responsible for the high temperatures and dryness that characterise much of the continent. Systems generating moisture occur either between individual anticyclones or to the north or south of them (Warner, 1986).
2. The size, shape and latitudinal range of the Australian continent. This has resulted in a broad range of climates, with 15 of the 30 Köppen–Geiger climate types spanning tropical, arid, temperate and cold (Crosbie et al., 2012; Peel et al., 2007).
3. The subdued relief (flatness) of the continent provides little obstruction to the prevailing atmospheric systems. The exception is the Great Dividing Range along the east coast of Australia.
4. Australia's long coastlines and vast expanses of ocean to the east, west and south ensure that much of the continent is subject to maritime influences.

Additionally, there are hemispherical-scale phenomena that drive seasonal to inter-annual variability, the predominant ones being the annual north–south cycle of the monsoon and the subtropical ridge and the multi-year variations of El Niño–Southern Oscillation (ENSO).

The net effect of these factors is the large semi-arid/arid zone and moderate to high seasonal variation with high inter-annual variability for which Australia is renowned (Hobbs, 1998). To the south of the arid centre (Köppen class B) the climate is predominantly Mediterranean (Köppen class Cs); to the north the climate is tropical (Köppen class A) and is characterised by highly seasonal, summer-dominated rainfall and year-round high temperatures and potential evaporation (PE) rates (Peel et al., 2007). Köppen zonation across northern Australia is shown in Section 2.3.1.

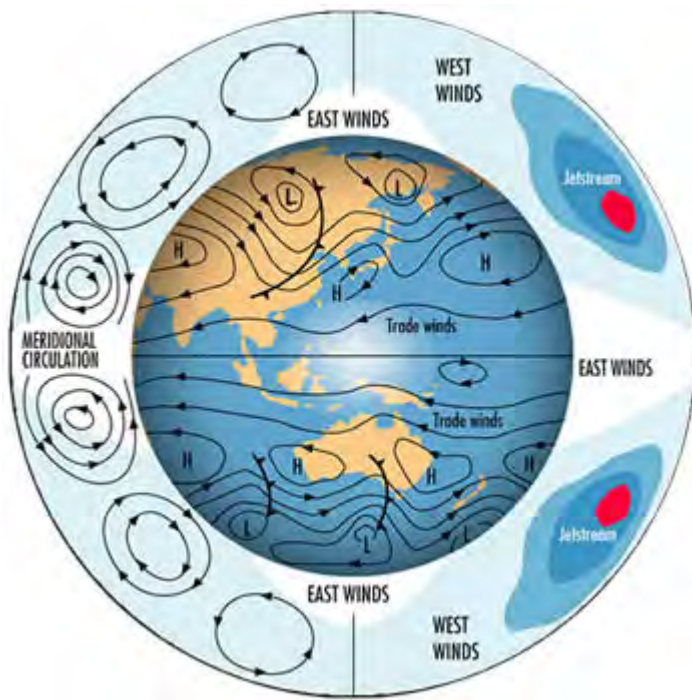


Figure 2-1 Pressure systems and circulation cells influencing Australia

Source: <http://www.bom.gov.au/climate/about/?bookmark=stridge>

2.1 Key rainfall-generating mechanisms across northern Australia

2.1.1 Monsoon

The annual northern Australian wet season is closely related to the Australian summer monsoon, the predominant large-scale circulation process that influences the southern hemisphere tropics in late spring, summer and autumn (McBride, 1998; Wheeler and McBride, 2012). The monsoon is driven by the summer heating of the Australian continent and the resulting change in land–sea temperature gradients (CSIRO and Bureau of Meteorology, 2015). Almost a month prior to the monsoon onset the surface temperature over northern Australia increases, resulting in anomalous cyclonic (i.e. low pressure) circulation. The wind direction changes from the south-easterly trade winds of the dry season to a north-westerly flow that draws high humidity into northern Australia, resulting in increased lower-level moisture convergence. This increases the amount of precipitation over the region and eventually starts the monsoon (Kullgren and Kim, 2006).

The monsoon season is most commonly observed from December to March, with high variability in the timing, extent and intensity of rain due to oscillations between ‘active’ and ‘break’ monsoon phases. Tropical low-pressure systems, ‘monsoon depressions’, are frequently generated along the monsoon trough line and are the dominant rainfall-producing systems, commonly associated with heavy rain. The monsoon season is modulated by ENSO and the Madden–Julian Oscillation (MJO, described later), as well as influencing tropical cyclone (TC) genesis (Wheeler and McBride, 2005). A stronger monsoon circulation is associated with an increased frequency of monsoon depressions and TCs. Rainfall variability is strongly tied to monsoon active/break cycles on intra-seasonal scales (MJO modulated) and large-scale influences, such as ENSO, on inter-annual time scales. Cook and Heerdegen (2001) note rainfall in the transitional periods, pre- and post-monsoon, is critical for

many ecological processes and conclude ecosystem function is determined by the temporal patterning of isolated rainfall events both before and after the monsoon season.

2.1.2 Tropical cyclones and depressions

The southern hemisphere TC season generally runs from November to April. Tropical depressions and TCs (intense tropical depressions) can be a major contributor to large-scale rainfall across northern Australia (CSIRO and Bureau of Meteorology, 2015). Lavender and Abbs (2013) determined that north-western Australia is the region with the greatest TC contribution to total annual rainfall (greater than 30%) as opposed to 10% over most of northern Australia. For coastal north-west stations TC contribution can be greater than 40% to annual rainfall and up to 70% of October to December rainfall (Ng et al., 2015). Dare (2013) found that the two measures with greatest correlation to TC rain volume contribution are total time spent over land and total land area covered by TCs during a season (correlation coefficients of 0.79 and 0.84, respectively). In an analysis over 41 seasons (1969–70 to 2009–10), Dare et al. (2012) found that on average two TCs cross or come within 500 km of the coastline of the Victoria, Roper and Southern Gulf catchments' coastlines, however those TC that do not cross the coast contribute little rainfall. A more detailed analysis of the frequency of TCs influencing each of the three study areas is included in Part II. Additionally, many localised intense events are not directly TC related, for example Rouillard et al. (2015) found that about 50% of flooding events in the north-west of northern Australia could be attributed to non-TC events.

Many authors have found a strong correlation between TC frequency and the phases of ENSO (Chand et al., 2013; Ramsay et al., 2008). In the Indian Ocean region adjacent to north-west Australia a double peak in TC activity is seen during La Niña, in December and March, with the number of days with TC activity 50 to 100% higher than in El Niño or neutral phases (Figure 2-2) (Liu and Chan, 2012). North-west TC frequency peaks in March for all three ENSO phases (Dowdy and Kuleshov, 2012; Kuleshov, 2012). Positive sea surface temperature (SST) and relative humidity and negative (cyclonic) vorticity anomalies during La Niña drive the enhanced TC activity, with opposite anomalies leading to suppressed TC activity during El Niño phases. It should be noted, however, that TC formation in the Australian region is not solely influenced by ENSO but also the interplay between ENSO phase and other modes of variability including MJO (Hall et al., 2001) and with the Interdecadal Pacific Oscillation (IPO) along the north-eastern coast of Australia (Grant and Walsh, 2001). The decadal-scale variation caused by the IPO was found to influence TC formation through its influence on ENSO, as during El Niño the region of highest SSTs and TC genesis shifts eastward away from Australia, reducing the propensity for Queensland land-falling TC formation. The influence of active MJO phases on enhanced TC activity is strengthened during El Niño events (Hall et al., 2001).

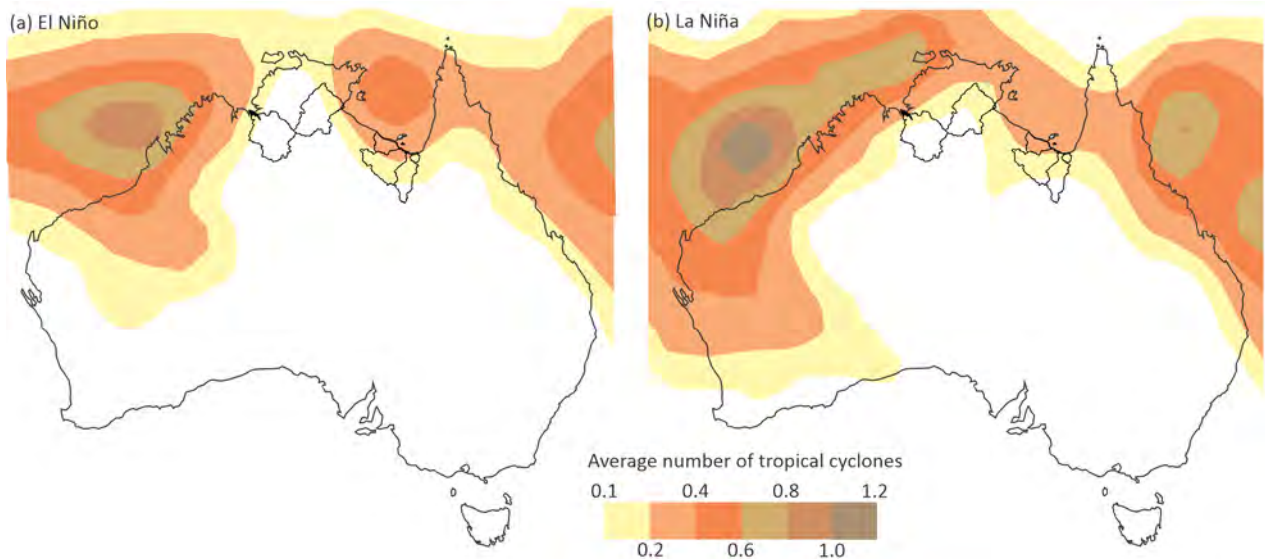


Figure 2-2 Mean annual number of TCs in the Australian region in (a) El Niño years, (b) La Niña years

Source: Bureau of Meteorology <http://www.bom.gov.au/climate/maps/averages/tropical-cyclones/>.

Trends in tropical cyclones in the Australian region

Although TC records can be considered complete and reliable since the introduction of meteorological satellites in the late 1960s, trend analysis is problematic due to this limited record and changes in observation technologies and analysis techniques (Kuleshov, 2012). Harper et al. (2008) reanalysed the TC dataset for the north-western region and concluded that earlier north-west Australian records (circa 1970s) contain underestimation biases in central pressure deficit of the order of 20%, leading to false trends. They concluded that there is no evidence of a trend in TC intensity over the last 30 years for north-west Australia. Kuleshov et al. (2010) applied nonparametric Monte Carlo techniques to determine whether there were trends in TC occurrence and intensity for the 1981–82 to 2006–07 seasons, in addition to those attributable to inter-annual variability or changes in observing practice, and also concluded that there were no significant trends in TC numbers in the Australian region. More recently, Dowdy (2014) investigated trends in Australian region TC numbers from 1981–82 to 2012–13, while accounting for the influence of ENSO. The study concluded that there was a significant decreasing trend in TC numbers (at a 0.93 to 0.98 confidence level) and a reduced influence of ENSO in recent decades, with ENSO accounting for about 35 to 50% of the variance in TC numbers during the first half of the study period, but only 10% during the second half.

2.1.3 Heat lows and thunderstorms

A heat low is caused by localised, often intense, heating of the Earth’s surface. The air in direct contact with the heated surface warms and rises, causing atmospheric pressure at the surface to decrease thus creating a region of low pressure (Trapasso, 2005). Lavender (2016) presents the first detailed assessment of heat-low climatology across northern Australia, finding that the Victoria catchment experiences up to two per year, whereas there is minimal heat-low presence over the Roper and Southern Gulf catchments. Heat lows in the Victoria and south of the Roper and Southern Gulf catchments impact the rainfall climate by modifying air flows, thus bringing moist air from the warm tropical oceans onshore. The thermal uplift associated with heat lows, in

combination with increased moisture, influences the formation of convective thunderstorms of varying size and intensity that are a frequent feature during the afternoon and evening through spring, summer and autumn. These can occasionally result in heavy rainfall and localised flooding. Thunderstorm development depends on sufficient moisture, which can also be brought over land by the afternoon sea breeze, to produce sufficient depth of moisture in a conditionally unstable atmosphere (Charles et al., 2015).

North-western Australia, which encompasses the Victoria catchment, has a high propensity for thunderstorms peaking during the December to March period. The north-west has stronger activity than the north-east based on satellite observations of lightning occurrence, as shown in Figure 2-3 (Dowdy and Kuleshov, 2014). Thunderstorm activity is generally not strongly influenced by ENSO in northern Australia, with only a very small region of far northern Australia having some indication of less activity for El Niño and more activity for La Niña during spring (September to November) (Dowdy, 2016). There are no published studies quantifying the relative contributions of thunderstorms to rainfall totals, however, the contributions could be significant, particularly in years with lower than average monsoon activity (Rouillard et al., 2015). Although climate models do not resolve small-scale processes such as thunderstorms, projected changes in climatology indicate the potential for an increased propensity for thunderstorm formation (Allen and Karoly, 2013; Allen et al., 2014a; 2014b). A recent international study has observed an increase in convective rainfall with increasing temperature (Berg et al., 2013).

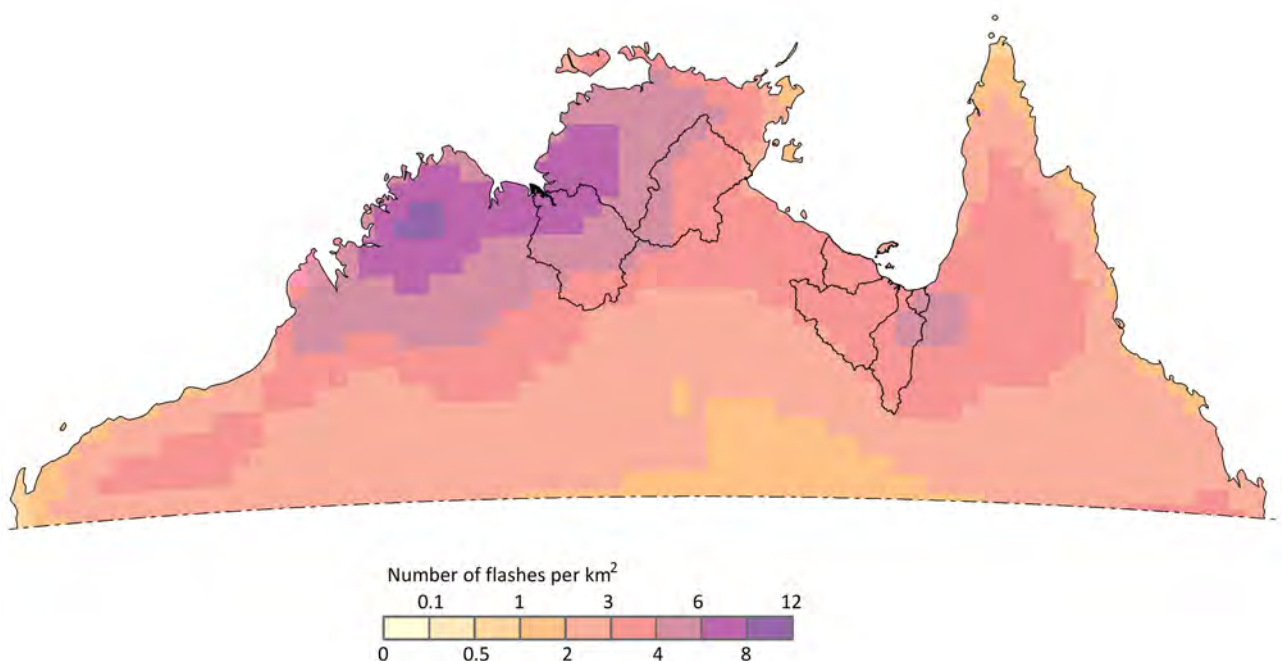


Figure 2-3 Mean annual lightning ground flash density

Bureau of Meteorology analysis based on NASA optical transient detector and lightning imaging sensor averaged over the 18-year period 1995–2012.

2.2 Rainfall variability and long-term trends

Climate variability is a natural phenomenon occurring across a range of time scales, from hourly (e.g. diurnal variation in the weather) to seasonal (e.g. wet/dry and hot/cold seasonal variation), and even to many millennia (e.g. Milankovitch cycles caused by variations in the Earth's orbit). A climate trend or change is a long-term shift or change in climate after variability mechanisms operating at shorter time scales have been accounted for. They may be due to natural processes that operate over long time scales, or they may be the result of an anthropogenic-forced 'changing' climate (e.g. enhanced greenhouse effect).

2.2.1 Diurnal variability

The diurnal cycle in temperature is evident due to the daily cycle of the sun's energy (radiation) input. Rainfall's diurnal properties are evident in the timing of convection, also predominantly driven by the daily solar cycle. A study of convection processes in the Victoria and Roper catchments found that during monsoon active periods convection peaks in the late morning. During monsoon break phases, in contrast, convection peaks in the early afternoon as it is linked closely to daytime surface heating and convergence associated with the sea breeze (Pope et al., 2008).

2.2.2 Intra-seasonal variability

Intra-seasonal variability gives rise to differences in climate from week to week, or fortnight to fortnight.

Madden–Julian Oscillation

The Madden–Julian Oscillation (MJO) (Madden and Julian, 1972) is a dominant feature of rainfall variability in the tropics. The MJO can be characterised as an eastward moving 'pulse' of cloud and rainfall near the equator that typically recurs every 30 to 60 days (Zhang, 2005). The MJO is the strongest driver of intra-seasonal variability in northern Australia, but also interacts over longer time scales to influence ENSO, the monsoon circulation, and TC generation.

MJO's strongest impact on northern Australian rainfall is during the extended summer months of November to April (Wheeler et al., 2009), causing many of the 'bursts' and 'breaks' of the Australian monsoon (Wheeler and McBride, 2012), which respectively enhance or suppress rainfall. Wheeler and Hendon (2004) have produced an MJO phase index defined as the covariability of the two leading principal components of empirical orthogonal functions of the combined fields of near-equatorially averaged 850-hPa zonal wind, 200-hPa zonal wind and satellite-observed outgoing longwave radiation. The enhanced convection of the MJO index active phase increases the probability of extreme weekly rainfall (i.e. upper 20th percentile) by a factor of three compared to non-active phases for far northern Australia in summer (Wheeler and Hendon, 2004), including the three study areas (Wheeler et al., 2009).

In the far north, such as around the Roper catchment, the MJO causes rainfall to be, on average, about 6 mm per day higher during the MJO wet phases (i.e. Phases 5 and 6 of the MJO index) than during the MJO dry phases (i.e. Phases 1 and 2). However, given the MJO's period of more than 30

days, its impact is best expressed as changes in weekly rainfall than daily rainfall, as shown for the chance of exceeding the normal weekly rainfall in Figure 2-4. This figure shows that in the Roper catchment the probability of greater than normal weekly rainfall is over 65% in MJO Phase 5, but less than 30% in MJO Phase 1. Similarly, for the Victoria catchment the probability is over 65% in Phase 5 for western parts of the catchment, but less than 30% across the catchment in Phase 1. For the Southern Gulf catchments, however, the phases of greatest probability change are shifted, being in phases 6 and 2 rather than phases 5 and 1. This shifted phase between western and eastern parts of northern Australia, which represents a difference in timing of about one week, is due to the eastward propagation of the MJO itself. Figure 2-4 also shows the wind changes that are experienced through the MJO cycle. Changes in temperature with the MJO cycle in northern Australia are linked with the changes in rainfall and cloudiness: lower maximum temperatures, of up to 1.5 °C below average, are experienced over northern Australia during phases 5 and 6 when it is wet and cloudy. Importantly, the MJO is predictable out to about 20 days with current technology (Rashid et al., 2011), enabling the MJO-associated impacts to be predicted a couple of weeks in advance.

Convectively coupled equatorial waves

Other intra-seasonal drivers of northern Australia's climate include the convectively coupled equatorial waves (Kiladis et al., 2009). Like the MJO, they cause oscillations in winds, pressure, rainfall and cloudiness that propagate in the tropics parallel to the equator. However, compared to the MJO, they have shorter periodicities and a shorter predictability horizon (Wheeler and Weickmann, 2001). That is, although they are useful tools for diagnosing what may be currently affecting the weather on any particular day, it is very difficult to use them to predict their weather impacts more than a few days in advance. However, it remains very important for dynamical prediction models to be able to accurately represent them.

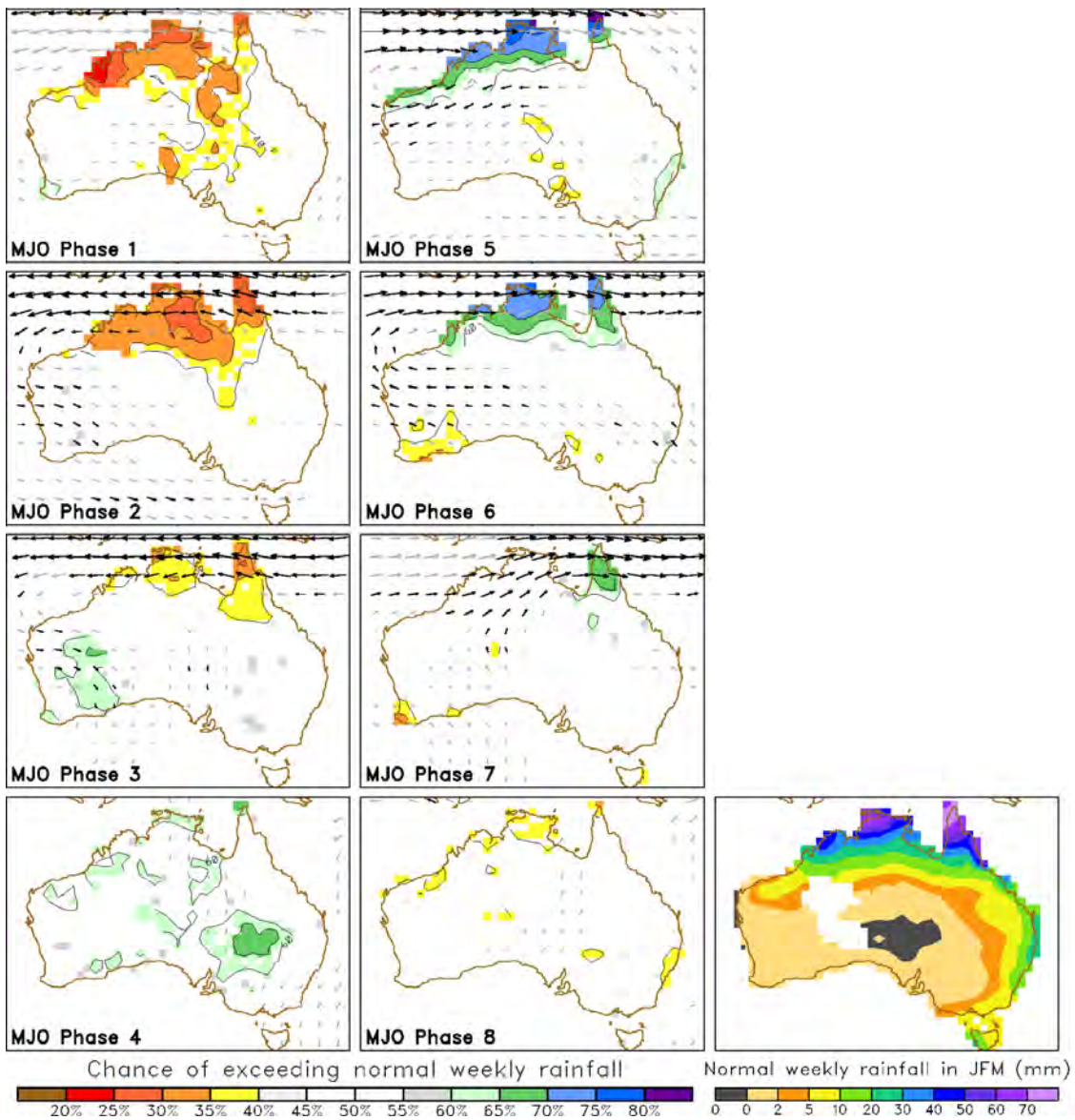


Figure 2-4 Mean weekly rainfall probabilities and expected 850 hPa (approximately 1.5 km above sea level) wind anomalies for each of the 8 MJO phases

Green and blue shading indicates higher than normal rainfall would be expected, while red and orange shading indicates lower than normal rainfall would be expected. The direction and length of the arrows indicate the direction and strength of the wind anomaly. The darker the arrow, the more reliable the information. The relationship of the MJO with Australian rainfall and winds changes with the season, and this figure is for January–February–March, when the impact of the MJO on rainfall in northern Australia is at its peak. Mean conditions for all seasons can be found at <http://www.bom.gov.au/climate/mjo/> - tabs=Average-conditions. Follows method of Wheeler et al. (2009).

2.2.3 Seasonal variability

A highly distinctive feature of northern Australia's climate is its strong seasonality of rainfall; this is driven by the annual solar cycle, which determines the position of the high pressure belt (subtropical ridge, STR), and the main tropical rainfall-generating mechanisms (monsoon, TCs, heat lows and thunderstorms) as discussed in Section 2.1. Figure 2-5 shows a measure of the seasonality of rainfall across Australia. Seasonality is the percentage of rain that occurs during the peak 3-month period. The figure shows that the seasonality of rainfall in Australia corresponds to latitude and that the seasonality of rainfall is considerably higher in northern Australia than southern Australia (i.e. below -23.44°). This has implications for dryland agriculture and water storage requirements.

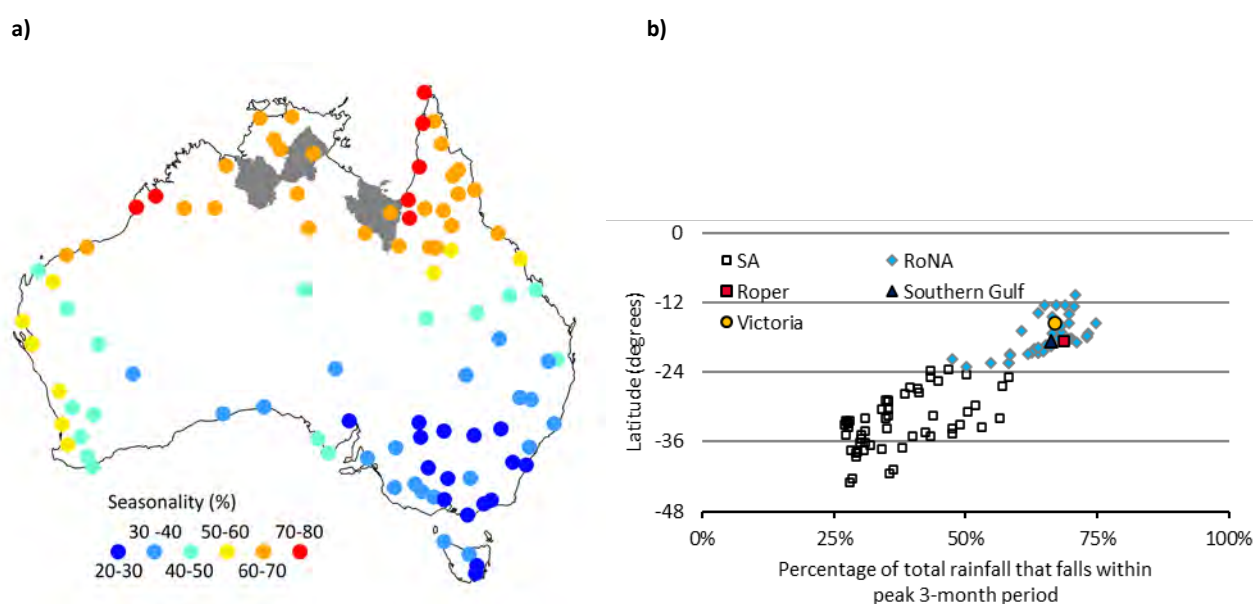


Figure 2-5 Seasonality of rainfall for 96 high-quality stations across Australia

(a) Seasonality of rainfall across Australia; (b) latitude plotted against seasonality of rainfall. Seasonality of rainfall is defined as the percentage of the total rainfall that occurs during the peak 3-month period. The grey polygons indicate the extent of the Victoria, Roper and Southern Gulf catchments. Rainfall stations in the Victoria, Roper and Southern Gulf catchments are given by yellow, red and blue symbols respectively. The light blue diamonds indicate rainfall stations from the rest of northern Australia (RoNA) and hollow squares indicate rainfall stations from southern Australia (SA).

There is growing scientific awareness of the value of understanding Indigenous seasonal calendars, given their insights and appropriateness for natural resource management (Woodward et al., 2012). Indigenous season calendars for northern Australia are available for specific regions at: <http://www.csiro.au/en/Research/Environment/Land-management/Indigenous/Indigenous-calendars>.

2.2.4 Inter-annual variability

Northern Australia experiences relatively strong year-to-year variations in rainfall. Nicholls et al. (1997), Peel et al. (2004) and Petheram et al. (2008) observed that for a given mean annual rainfall total, the inter-annual variability of rainfall in northern Australia is higher than that observed at rainfall stations from the rest of the world (RoW) for the same Köppen–Geiger climate types.

A commonly used measure of variability in hydrological and climate sciences is the coefficient of variation (CV) of annual rainfall (i.e. the standard deviation of annual rainfall divided by the mean annual rainfall) which provides a measure of the temporal variability of annual rainfall. The larger the CV value, the larger the relative variation in annual rainfall. In Figure 2-6 the CV of annual precipitation in northern Australia is compared to (a) the RoW and (b) the RoW of the same Köppen climate zones (Peel et al., 2007) as northern Australia. Stations from the RoW of the same Köppen climate type and mean annual rainfall typically exhibit a CV of annual rainfall between about 0.2 and 0.35 (Petheram et al., 2008).

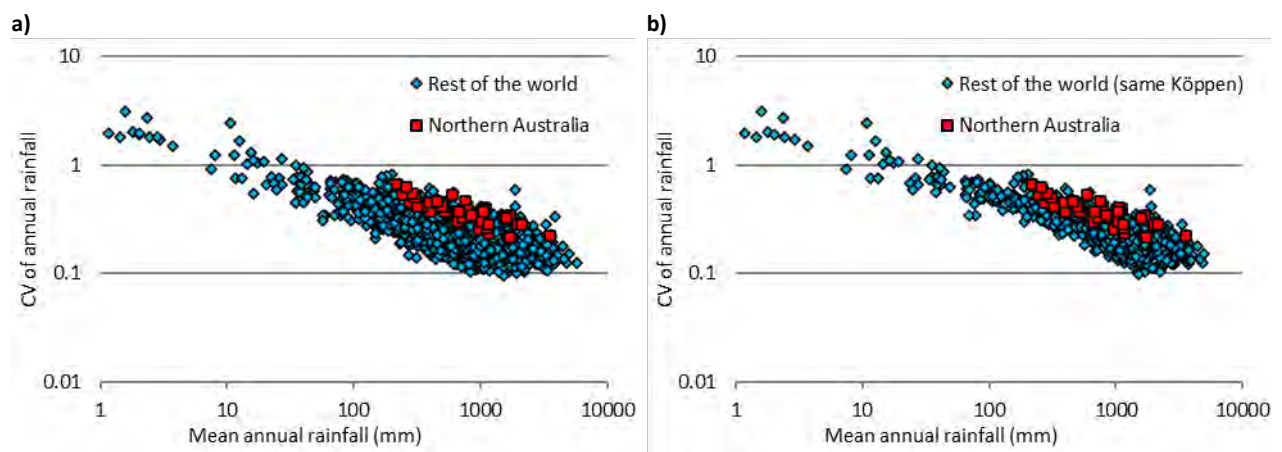


Figure 2-6 Annual variation in rainfall in northern Australia

(a) Coefficient of variation of annual rainfall in northern Australia compared to RoW; and (b) coefficient of variation of annual rainfall in northern Australia compared to stations of the same Köppen climate zone in the RoW.

The generally higher northern Australian variability is mostly attributed to the large impact of the ENSO (see further below). This has both positive and negative implications for agriculture and aquaculture in northern Australia: it is positive in the sense that seasonal predictions of rainfall have the potential to be more skilful in northern Australia than elsewhere in the globe, due to the high predictability and relatively large impact of ENSO; but negative in the sense that industry needs to be able to cope with larger year-to-year variations, and therefore have more to lose if skilful forecasts are unavailable or not used to manage the high variability in water availability.

In the Victoria, Roper and Southern Gulf catchments the CV of annual rainfall is typically between 0.2 and 0.4. Figure 2-7 shows that for a given mean annual rainfall the CV of annual rainfall in the Southern Gulf catchments is moderately high compared to other rainfall stations in northern Australia and high compared to other rainfall stations around Australia with the same mean annual rainfall. Rainfall stations in the Roper and Victoria catchments exhibit a moderately high variation in annual rainfall compared to other stations around Australia.

It should be noted that the inter-annual variability of the non-rainfall parameters is considerably less than that of rainfall. Non-rainfall parameters have higher spatial and temporal auto-correlation than rainfall. Annual areal potential evaporation (APE), for example, varied by approximately 10% between 1965 and 2015. The CV of annual PE for the Victoria, Roper and Southern Gulf catchments is about three to four times lower than that for rainfall.

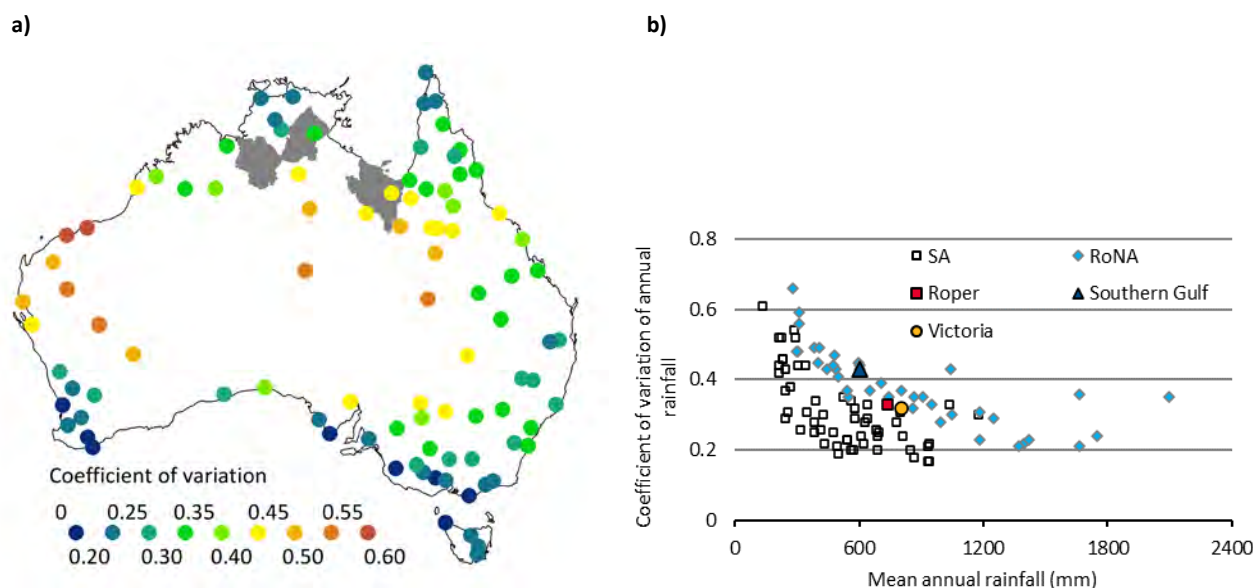


Figure 2-7 (a) Coefficient of variation of annual rainfall; and (b) the coefficient of variation of annual rainfall plotted against mean annual rainfall for 96 rainfall stations from around Australia

The grey polygons indicate the extent of the Victoria, Roper and Southern Gulf catchments. Rainfall stations in the Victoria, Roper and Southern Gulf catchments are given by yellow, red and blue symbols respectively. The light blue diamonds indicate rainfall stations from the rest of northern Australia (RoNA) and hollow squares indicate rainfall stations from southern Australia (SA).

El Niño–Southern Oscillation

ENSO is a coupled oceanic-atmospheric process originating in the equatorial Pacific producing SST and wind anomalies that influence climate variability globally on multi-year (sub-decadal) time scales (Trenberth, 1997). ENSO is commonly quantified as the strength of atmospheric pressure gradients across the Pacific (e.g. Southern Oscillation Index, SOI, defined as the standardised anomaly of the mean sea-level pressure difference between Tahiti and Darwin) or by SST anomalies in certain regions of the equatorial or near-equatorial Pacific. Its three dominant phases are the warm El Niño phase, cold La Niña phase and a neutral phase, with recent research identifying other variations of El Niño such as El Niño Modoki.

Although ENSO is the most important climate driver for inter-annual variations of northern Australian rainfall, the impact of ENSO on rainfall varies both seasonally and decadal. Correlations of the SOI, with seasonal-mean rainfall (McBride and Nicholls, 1983; Risbey et al., 2009) show the strongest historical relationship in northern Australia in austral spring (i.e. September–October–November), with statistically significant correlations of between 0.2 and 0.4 in the Victoria catchment, between 0.4 and 0.7 in the Roper catchment (among the highest in Australia) and 0.3 to 0.5 in the Southern Gulf catchments. The sign of the correlations confirm the well-known tendency for drier than normal conditions in El Niño and wetter than normal in La Niña. The relationship is weaker in austral summer (December–January–February) and autumn (March–April–May), and very weak in winter (June–July–August). During La Niña, northern and eastern Australian positive rainfall anomalies are proportionate to the strength of the La Niña, due to increases in the convection centre situated over Australia. For El Niño, in contrast, negative rainfall anomalies are not proportionate to El Niño strength as the convection centre has moved eastwards and so is remote from Australia (Cai et al., 2010).

Taschetto and England (2009b) note that the 'Modoki' El Niño, which is associated with anomalous warming in the central tropical Pacific together with cooling in the eastern and western tropical Pacific (Ashok et al., 2007), produces a different Australian rainfall response than the traditional El Niño. The Modoki events produce a large-scale reduction in autumn (March–April–May) rainfall across north-western Australia (i.e. which is of relevance to Victoria and Roper catchments) and across to the northern Murray–Darling Basin (Cai and Cowan, 2009). Climate model simulations suggest that El Niño Modoki SST warming in the central Pacific is associated with a shortening and intensification of the Australian monsoon season (Taschetto et al., 2009).

Another known impact of ENSO in northern Australia is the tendency for the onset of useful rains after the dry season to be earlier than normal in La Niña years and later than normal in El Niño years. Lo et al. (2007) and Drosowsky and Wheeler (2014) showed that the difference in onset date for an accumulation of 50 mm of rain (i.e. about the amount of rainfall required to provide new grass growth) between El Niño and La Niña years is about 3 weeks in the regions to the north of 20°S. The mean onset maps for all years, and for ENSO neutral, La Niña and El Niño years, are shown in Figure 2-8. This research is the basis of the Bureau of Meteorology's Northern Rainfall Onset outlook available at <http://www.bom.gov.au/climate/rainfall-onset/> - tabs=Rainfall-onset. Temperatures are also affected; for northern Australia the greatest impact is felt on minimum temperatures, which tend to be higher during La Niña compared to El Niño in winter/spring but lower during La Niña in summer. For maximum temperature, the greatest differences between El Niño and La Niña are seen over Cape York with higher temperatures during El Niño in summer (see <http://www.bom.gov.au/climate/enso/history/In-2010-12/ENSO-temperature.shtml>). The Bureau of Meteorology monitors and predicts the phase and strength of ENSO at <http://www.bom.gov.au/climate/enso/>.

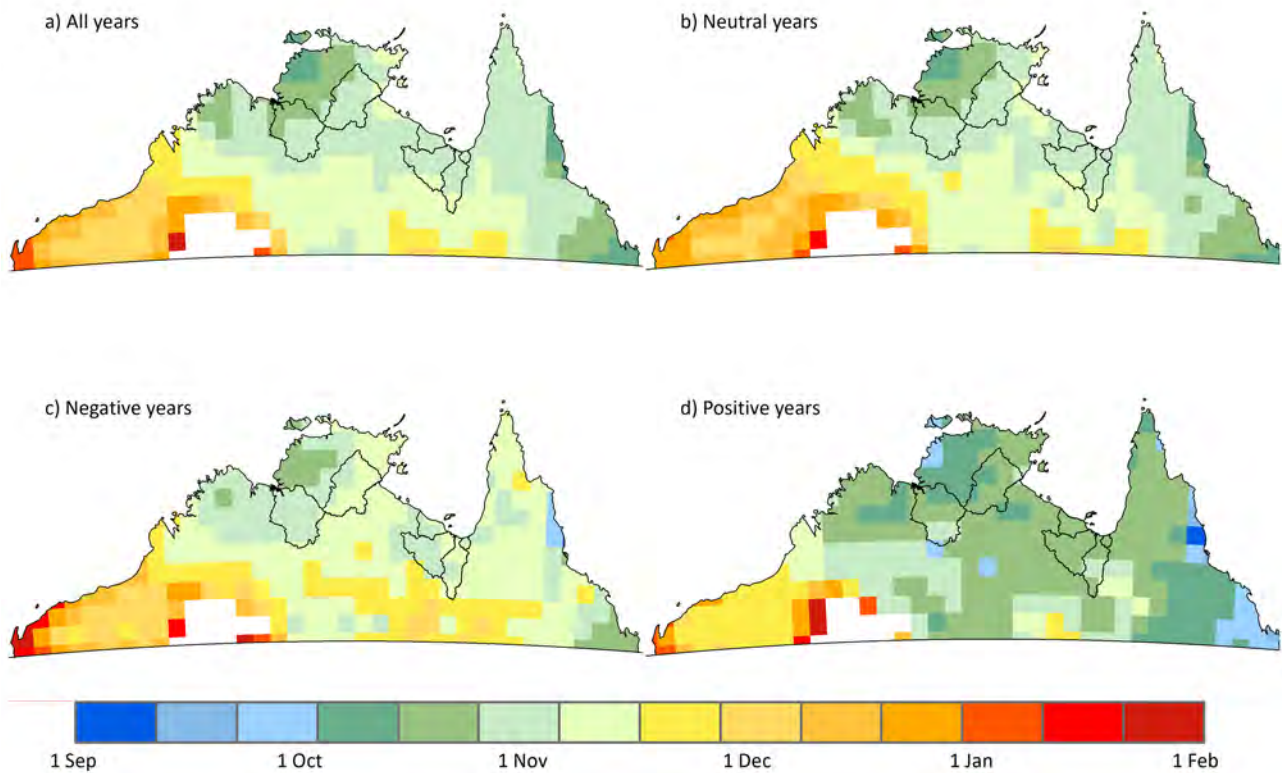


Figure 2-8 Mean northern rainfall onset dates for (a) all, (b) SOI neutral, (c) SOI negative (El Niño) and (d) SOI positive (La Niña) years

Onset dates defined as being an accumulation of 50 mm of rain. Classes defined as years where the July–August mean of the SOI has been below -8 (El Niño), above $+8$ (La Niña), or in between (neutral), calculated for all years between 1960 and 2009. White space indicates missing data.

Source: <http://www.bom.gov.au/climate/rainfall-onset/> - tabs=ENSO-influences.

Indian Ocean dipole

The IOD is a major pattern of Indian Ocean SST variability that impacts on Australia’s rainfall, consisting of contrasting SST anomalies between the western and eastern equatorial Indian Ocean (Saji et al., 1999). The phase and strength of the IOD can be determined using the dipole mode index (DMI), the difference between SSTs in a western box (50 to 70°E and 10°N to 10°S) and an eastern box (90 to 110°E and 0 to 10°S). A positive DMI occurs when the eastern SSTs are anomalously cool and western SSTs are anomalously warm. This contributes to drier conditions (during the winter–spring period) over central and southern Australia. In contrast, a negative DMI occurs when the eastern SSTs are anomalously warm and western SSTs are anomalously cool, contributing to wetter conditions over parts of northern, central and southern Australia. There have been nine positive IOD events since reliable records commenced in 1960 (1961, 1963, 1972, 1982, 1983, 1994, 1997, 2006 and 2012) and ten negative IOD events (1960, 1964, 1974, 1981, 1989, 1992, 1996, 1998, 2010 and 2016) (<http://www.bom.gov.au/climate/iod/>).

Risbey et al. (2009) show that there is a weak but significant negative correlation between the IOD (as measured by the DMI) and June–October rainfall for most of northern Australia. That is, years in which the DMI is positive, corresponding to warmer than normal SSTs in the western equatorial Indian Ocean and cooler than normal SSTs in the eastern equatorial Indian Ocean, tend to be drier than normal in northern Australia. But the correlations are weaker than those related to ENSO,

indicating that the IOD is less important overall than ENSO. The IOD interacts with ENSO to further enhance or suppress rainfall but the relationship is complicated and the key dependencies have not yet been fully resolved. Behera and Yamagata (2003) find there has been a statistically significant correlation between the DMI and Darwin pressure since the 1950s, with the exception of the 1980–89 decade when the relationship was non-significant. IOD events typically develop through winter (June–July–August) and peak in spring (September–October–November) and have some correlation with ‘build-up’ rainfall in the Victoria and Roper catchments (Cai et al., 2009a; Cai et al., 2011b). The correlation to build-up rainfall is important as agribusiness is sensitive to these early wet-season rains (Garnett and Williamson, 2010).

2.2.5 Inter-decadal variability

Interdecadal Pacific Oscillation

Correlations of northern Australia rainfall with other indices of ENSO, such as the Niño3, Niño3.4, and Niño4 indices of SSTs in the equatorial Pacific Ocean, are of similar magnitude as those with the SOI (Risbey et al., 2009). However, if the correlations are computed for different multi-decadal subsets of the historical data, substantial differences are found (Cai et al., 2001; Suppiah, 2004). For example, Risbey et al. (2009) found no significant correlation between the SOI and northern Australian spring rainfall during the years 1919–1947 and comparatively much higher correlations (up to 0.8) during the years 1948–1976.

Power et al. (1999) introduced the term Interdecadal Pacific Oscillation (IPO) to describe the phenomenon of inter-decadal SST variability in the Pacific Ocean. They found the IPO modulates inter-decadal variability in the influence of ENSO on the climate of Australia, with no robust relationship between ENSO and inter-annual Australian climate variations when the IPO positive phase has raised tropical Pacific SSTs. In contrast, the correlation between ENSO and Australian climate is strong when the IPO negative phase reduces tropical Pacific SSTs. These periods are generally wetter with enhanced flood risk, as rainfall anomalies associated with La Niña are enhanced.

Micevski et al. (2006) examined streamflow data along the east coast of Australia and found that the IPO modulated the flood risk in NSW and southern Queensland, with flood quantiles increasing by a factor of approximately 1.7 during IPO negative periods. However, they did not find an association between the IPO and ENSO in streamflow data north of the Tropic of Capricorn. The influence of IPO-modulated ENSO variation was found to relate to periods of increased or reduced drought risk for a NSW catchment on multi-decadal scales (Kiem and Franks, 2004). Although the IPO positive phase is associated with less severe ENSO impacts in Australia, there is a much larger drought risk in IPO positive than IPO negative phases because of the reduced frequency and intensity of La Niña events.

Whether these multi-decadal variations in ENSO’s impact are predictable remains uncertain (Power et al., 1999; Power et al., 2006), but importantly it means that it would be unwise to rely solely on the statistical relationship with ENSO for future seasonal predictions of rainfall: one either needs to incorporate other predictable drivers of climate variability and/or include predictable knowledge, if it exists, of the multi-decadal component. Using dynamical prediction models of the coupled ocean–atmosphere system is one way to incorporate predictability from multiple sources.

2.2.6 Trends

Numerous authors have looked at trends in rainfall and temperature across northern Australia. Over the north-west (CSIRO, 2009a; Lavender and Abbs, 2013) and north (CSIRO, 2009c) of northern Australia the literature consistently reports an increasing trend in annual and summer rainfall over recent decades. This has largely been attributed to an increase in the mean intensity of rainfall events (Smith et al., 2008a; Taschetto and England, 2009a), and the positive trend in annual and summer rainfall over north-west Australia could be related to more intense deep convection caused by changes in the monsoon trough (Taschetto et al., 2009). Lavender and Abbs (2013) attribute most of the increasing trend in annual and summer rainfall over north-western Australia (~60%) over the past four decades to rainfall contributions from closed lows rather than TC. It should be noted, however, that positive (or negative) trends in annual or summer rainfall do not necessarily mean rainfall trends during other seasons will be similar. For example Taschetto and England (2009b) reported a negative rainfall trend over north-west Australia during autumn (March–April–May), and speculated that this may be due to an earlier northward shift of the monsoon trough.

Evans et al. (2014) found a strong relationship between monsoon active periods and the MJO, and that the increasing rainfall trend observed at Darwin Airport was related to increased frequency of active monsoon days rather than increased intensity during active periods. They concluded periods of moderate active monsoon have been increasing in frequency at the expense of the weakest periods of the monsoon.

Over the north-east of northern Australia the literature is less conclusive, though most studies do not report a statistically significant trend in annual or summer rainfall over the Gulf of Carpentaria and Cape York Peninsula (CSIRO, 2009b; 2009c; Klingaman et al., 2013; Lavender and Abbs, 2013; Li et al., 2012). A decrease in rainfall over north-east Australia has been attributed to a weakening in the tropical Australian summer monsoon, possibly related to increased SST trends experienced across the north-east Indian Ocean (Li et al., 2012).

2.2.7 Dry and wet spells

The rainfall-generating systems in northern Australia and their modes of variability combine to produce irregular periods of runs of dry and wet years. The length and magnitude of dry spells in particular strongly influences the scale, profitability and risk of water resource related investments. A spell of consistently dry years may be associated with drought (though an agreed definition of drought continues to be elusive). It is also during dry years that existing water-dependent ecosystems will be most adversely impacted by water extraction. Thus the length and magnitude of dry spells is one of the most important considerations to investors in water resource related developments and water resource planners, and so for this reason an analysis of dry and wet spells in the three study areas was undertaken.

Runs of wet and dry years, referred to here as wet and dry spells, are shown as annual differences from the median rainfall for Yarralin in the Victoria catchment (Figure 2-9), Mataranka in the Roper catchment (Figure 2-10) and Burketown in the Southern Gulf catchments (Figure 2-11).

To enable the characteristics of wet and dry spells in the three study areas to be compared to other parts of the country, the following sections examine the length, magnitude and severity of

wet and dry spells for 96 high-quality rainfall stations across Australia (including three stations in or nearby to the Victoria, Roper and Southern Gulf catchments). Rainfall stations were selected because each had near continuous data between 1890 and 2011 or had very close neighbouring stations providing a complementary record. The run length and run magnitude of each rainfall station were summarised into a single number, to allow a simple comparison among stations.

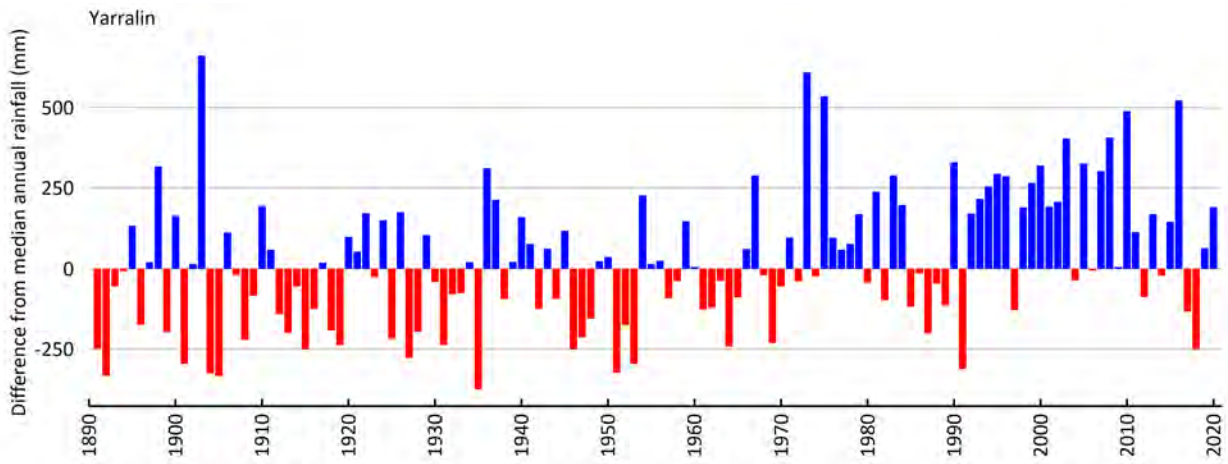


Figure 2-9 Runs of wet (blue columns) and dry (red columns) years at Yarralin in the Victoria catchment

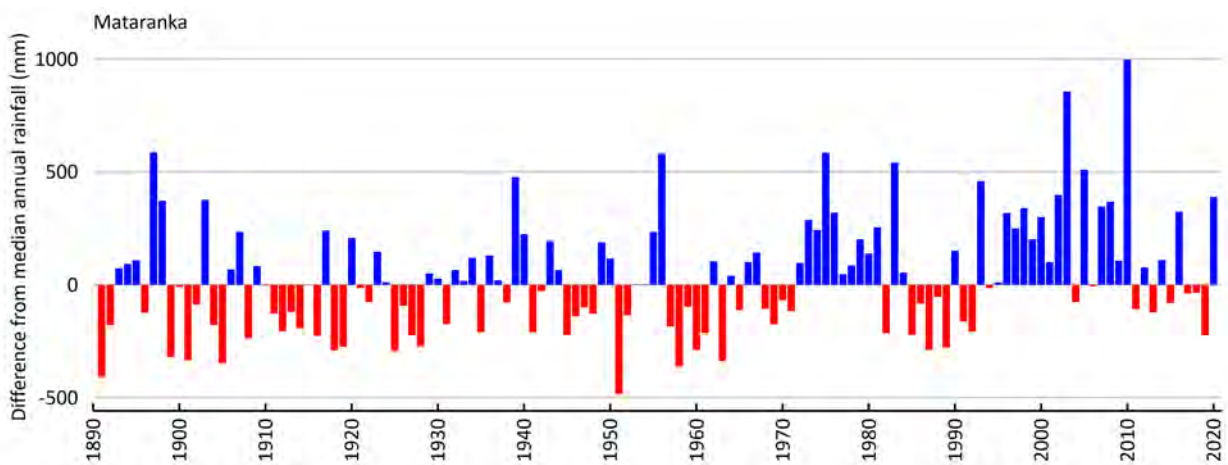


Figure 2-10 Runs of wet (blue columns) and dry (red columns) years at Mataranka in the Roper catchment

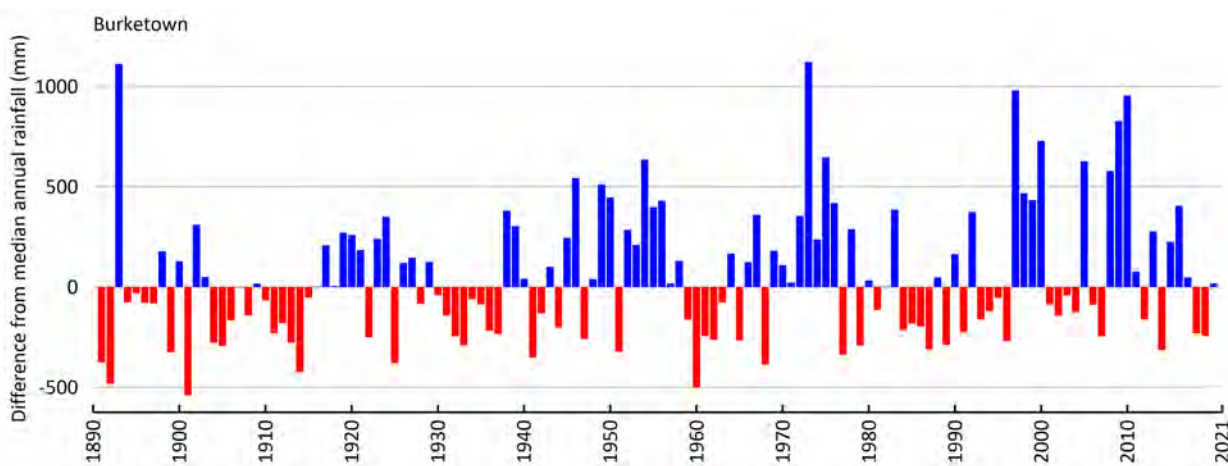


Figure 2-11 Runs of wet (blue columns) and dry (red columns) years at Burketown in the Southern Gulf catchments

Run length

Runs analysis, following the approach of Peel et al. (2004), is applied to annual rainfall data to describe and compare the length of wet and dry spells of rainfall stations in the three study areas to stations elsewhere across Australia. In this analysis, values that are equal to or below the median are defined as a dry year and values greater than the median are defined as a wet year. Run length is defined as a period of consecutive years of wet or dry.

Although the lag-one serial correlation (i.e. the correlation between consecutive values) is indicative of the run length behaviour of a time series, it does not completely determine run length behaviour. Peel et al. (2004) developed a metric (run length skewness, g) that summarises the run length behaviour of a time series (Equation 1). This metric was calculated for each annual rainfall station for both wet (g_{wet}) and dry (g_{dry}) run lengths and provides a simple way of comparing rainfall stations in the Victoria, Roper and Southern Gulf catchments to rainfall stations elsewhere around Australia.

$$g = \frac{\sum_i^j a_i b_i^3}{N - 1} \quad (1)$$

where a_i is the frequency of run length b_i , j is the longest observed run length and N is the number of years. The spatial distribution of run lengths for 96 long-term rainfall stations around Australia is plotted in Figure 2-12. In Figure 2-13 the run length behaviour is plotted against the lag-one serial correlation coefficient, with rainfall stations within or nearby to the Victoria, Roper and Southern Gulf catchments shown in red, black and yellow respectively. The black lines in this figure indicate the 90% confidence interval, developed using a lag-one autoregressive (AR(1)) model as described by Peel et al. (2004). These confidence intervals provide an indication as to whether the run length skewness metric of a station is unusual given that station's lag-one serial correlation coefficient.

Based on the raw g_{wet} and g_{dry} values, the annual rainfall for stations in the Victoria, Roper and Southern Gulf catchments tend to have equally long runs of dry and wet years and there is nothing unusual about their run length behaviour (i.e. the run lengths of rainfall stations in the Victoria, Roper and Southern Gulf catchments are well described by an AR(1) model (Figure 2-12)). Figure 2-13 indicates that the run length of wet and dry years of rainfall stations in the Victoria, Roper and Southern Gulf catchments are comparable to rainfall stations along the east coast of Australia. Peel et al. (2004) observed that for the two continents most affected by ENSO (Australia and South America), the ENSO-influenced rainfall stations displayed less bias towards longer runs than the non-ENSO-influenced stations. They concluded that stations influenced by ENSO are less likely to develop long runs equal to or below the median because ENSO variance is concentrated in the 2–6-year frequency band.

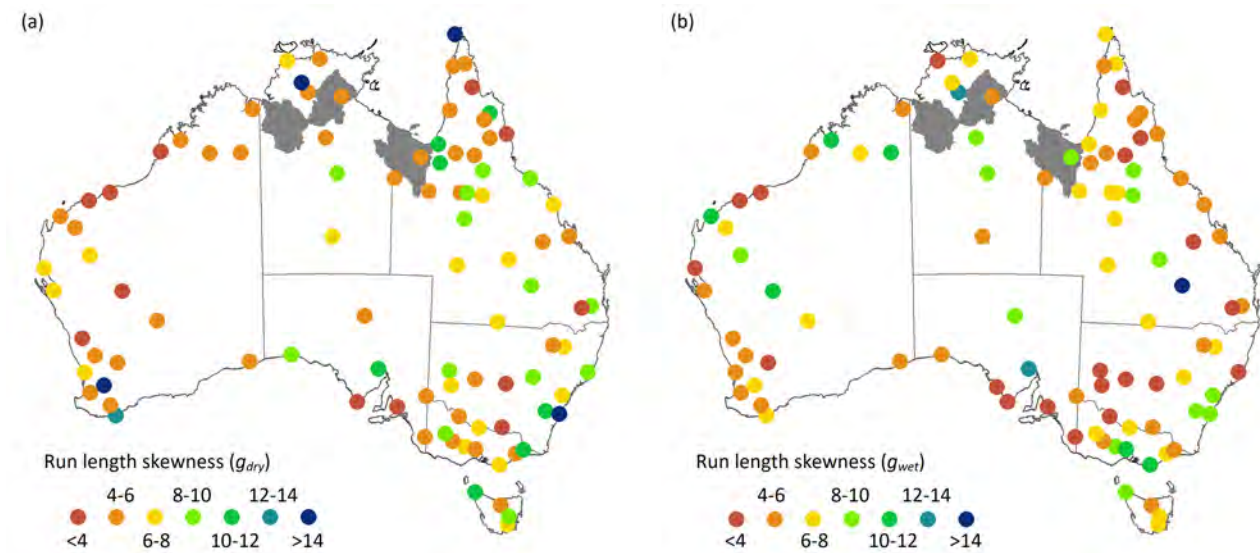


Figure 2-12 Run length skewness of dry and wet years for 96 rainfall stations around Australia
 The grey polygons indicate the extent of the Victoria, Roper and Southern Gulf catchments.

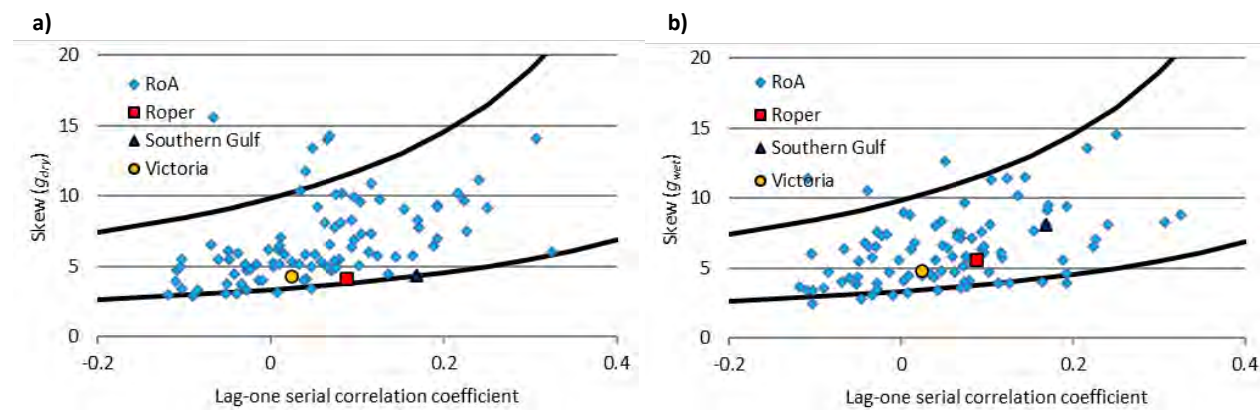


Figure 2-13 Run length of dry (a) and wet (b) years plotted against lag-one serial correlation coefficient for 96 high-quality rainfall stations around Australia
 The black lines indicate the 90% confidence limits developed by Peel et al. (2004). Rainfall stations in the Victoria, Roper and Southern Gulf catchments are given by yellow, red and blue symbols respectively. The light blue diamonds indicate rainfall stations from the rest of Australia (RoA).

Run magnitude

Run magnitude was assessed using the method of Peel et al. (2005), which utilises a measure of reservoir system vulnerability developed by Hashimoto et al. (1982), as a metric of run magnitude at each rainfall station. This metric is effectively the mean of the largest negative deviation from the median in each run length event divided by the median annual rainfall. This metric has the useful feature of summarising the run magnitude behaviour of all dry run lengths at a station into a single number ranging from 0 to 1, allowing simple comparison among stations.

The run magnitude of dry years at rainfall stations in the Victoria, Roper and Southern Gulf catchments is slightly larger than that of stations in the Murray–Darling Basin and the east coast of Australia (Figure 2-14a).

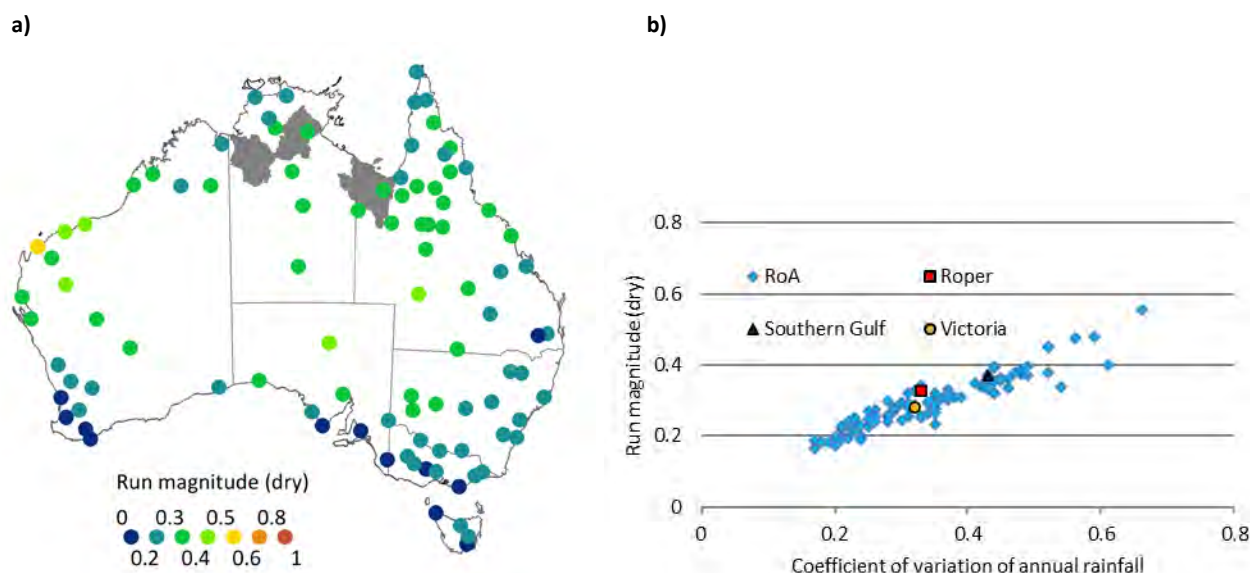


Figure 2-14 Run magnitude of dry spells (a) and run magnitude of dry spells plotted against the coefficient of variation of annual rainfall (b), for 96 rainfall stations around Australia

Grey-shaded polygons illustrate the extent of the Victoria, Roper and Southern Gulf catchments. Yellow, red and blue symbols indicate rainfall stations in the Victoria, Roper and Southern Gulf catchments, respectively. Light blue diamonds indicate rainfall stations from the rest of Australia (RoA).

Run severity has been defined by Yevjevich (1967) and Dracup et al. (1980) as the sum of the negative deviations from a threshold (the median in this analysis) for a given length of negative deviations. They also noted that drought severity is the product of drought length (the period of negative deviations) and drought magnitude (the mean of the negative deviations). Because the Victoria, Roper and Southern Gulf catchments had normal dry run lengths (comparable to stations in the Murray–Darling Basin and east coast of Australia) and moderate to high dry run magnitudes (slightly higher than stations in the Murray–Darling Basin and east coast of Australia), the run severity of dry periods was also found to be moderate, and comparable to stations in the Murray–Darling Basin and east coast of Australia.

Trends in ‘drought’ characteristics

There has been little literature looking at trends in drought across northern Australia. In one recent study, which used a different metric for assessing drought to that described above, Gallant et al. (2013b) looked at Australian drought variability between 1911 and 2009 and found general trends for tropical Australia to have less frequent, shorter duration and reduced intensity droughts, with the strongest of these trends for north-west Australia.

2.3 Evaporation

Evaporation is ‘the rate of liquid water transformation to vapour from open water, bare soil, or vegetation with soil beneath’, while transpiration is ‘that part of the total evaporation that enters the atmosphere from the soil through the plants’ (Shuttleworth, 1993).

There are three major ways in which evaporation (E_a) affects a region’s potential for irrigation. The first is through the catchment-wide losses by evaporation that determine runoff (R) and

drainage (D) or the ‘excess water’ ($R + D$), which forms the basis of the potentially exploitable resource, where P in Equation 2 is precipitation.

$$R + D = P - Ea \tag{2}$$

This is evaluated in the companion technical reports about river modelling calibration (Hughes et al., 2023) and groundwater hydrology (Knapton et al., 2023). The second major way in which evaporation affects irrigation potential is through evaporative losses from water storages. This is examined in the companion technical report about water storage (Petheram et al., 2022). The third way in which evaporation affects irrigation potential is via its influence on the crop water requirement. This is discussed in the companion technical report about agricultural productivity and socio-economics (Stokes et al., 2023).

The spatial distribution of annual, wet-season and dry-season rainfall, APE and rainfall deficit are shown in Figure 2-15. Mean annual (seasonal) rainfall minus mean annual (seasonal) APE is referred to as the mean annual (seasonal) rainfall deficit, a general measure of water availability. This metric is sometimes used as a first-cut assessment of the mean annual irrigation demand and net evaporation from water storages. To refine this estimate the water balance needs to be calculated at shorter time intervals to account for the intra-annual variability in precipitation and evaporation. This process is detailed in the companion technical report about agricultural productivity and socio-economics (Stokes et al., 2023).

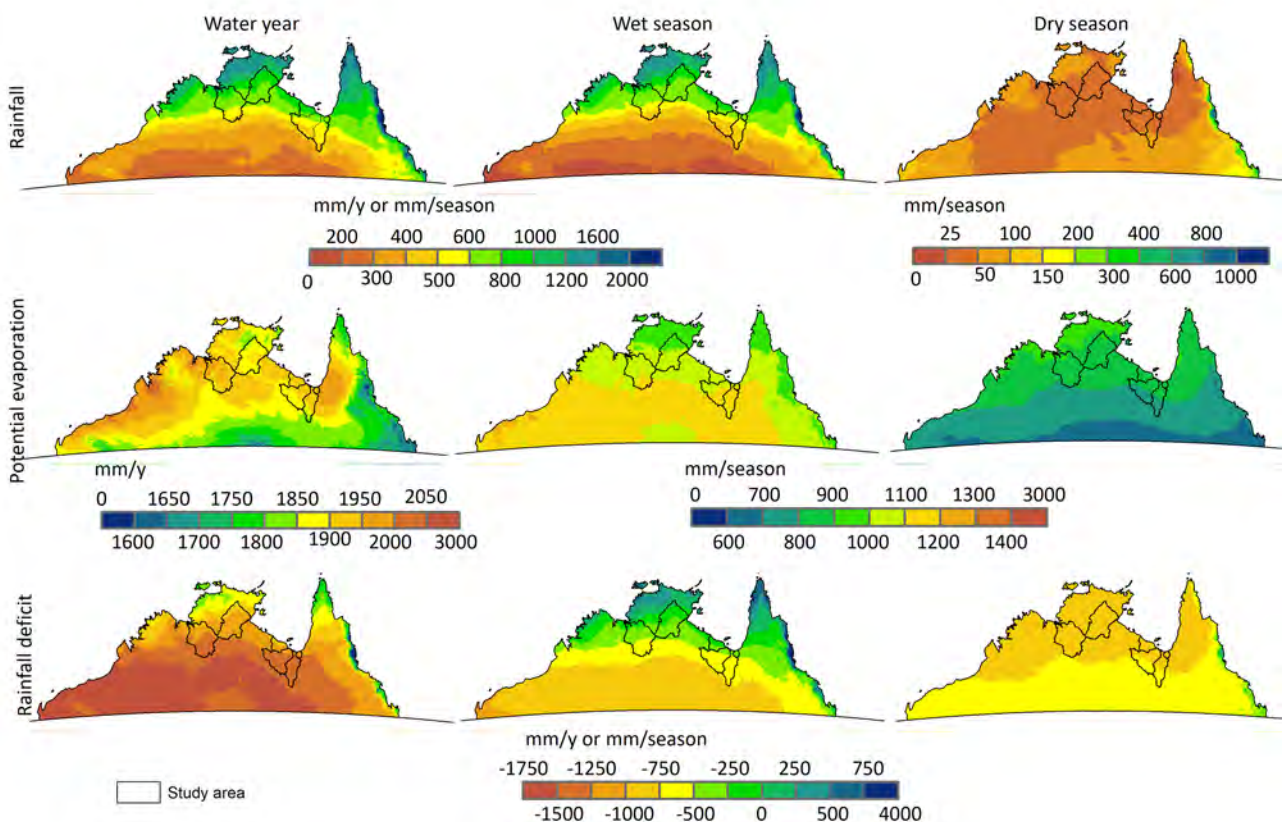


Figure 2-15 Mean annual and seasonal rainfall, PE and rainfall deficit (1930 to 2007)

PE calculated using Morton’s areal potential (Morton, 1983). Rainfall deficit is the rainfall minus PE.

2.3.1 Köppen classification and aridity index

The amount and temporal distribution of precipitation, temperature and PE do much to characterise climates. Two common methods for characterising climates are presented: the Köppen-Geiger classification (Köppen, 1936) and the United Nations Environment Programme (UNEP) aridity index.

The Köppen-Geiger classification as redefined by Peel et al. (2007) classifies the world into 30 climate types, of which seven are represented across northern Australia (Figure 2-16). These are the tropical rainforest Af; tropical monsoon Am; tropical savannah Aw; arid hot desert BWh; arid hot steppe BSh; temperate dry winter, hot summer Cwa; and temperate without dry season, hot summer Cfa. In southern Australia, where PE rates are typically lower, semi-arid landscapes occur around the 400 mm rainfall isohyet. In the NT, where PE rates are typically higher and there is a higher seasonality of rainfall, semi-arid landscapes typically occur around the 800 mm rainfall isohyet (Petheram and Bristow, 2008). Under the Köppen-Geiger classification most of the Victoria catchment is classified as arid hot steppe. In the Roper catchment the Köppen-Geiger classification is about 60% tropical savannah (northern sections) and about 40% arid hot steppe (southern part). The Southern Gulf catchments are predominantly arid hot steppe with a band of tropical savannah for locations with 75 km from the coast.

The UNEP aridity index is calculated by dividing rainfall by PE. Under this classification, the vast majority of the Victoria and Southern Gulf catchments is categorised as semi-arid. In the Roper catchment, approximately half of the catchment is classified as semi-arid and half as humid (Figure 2-17).

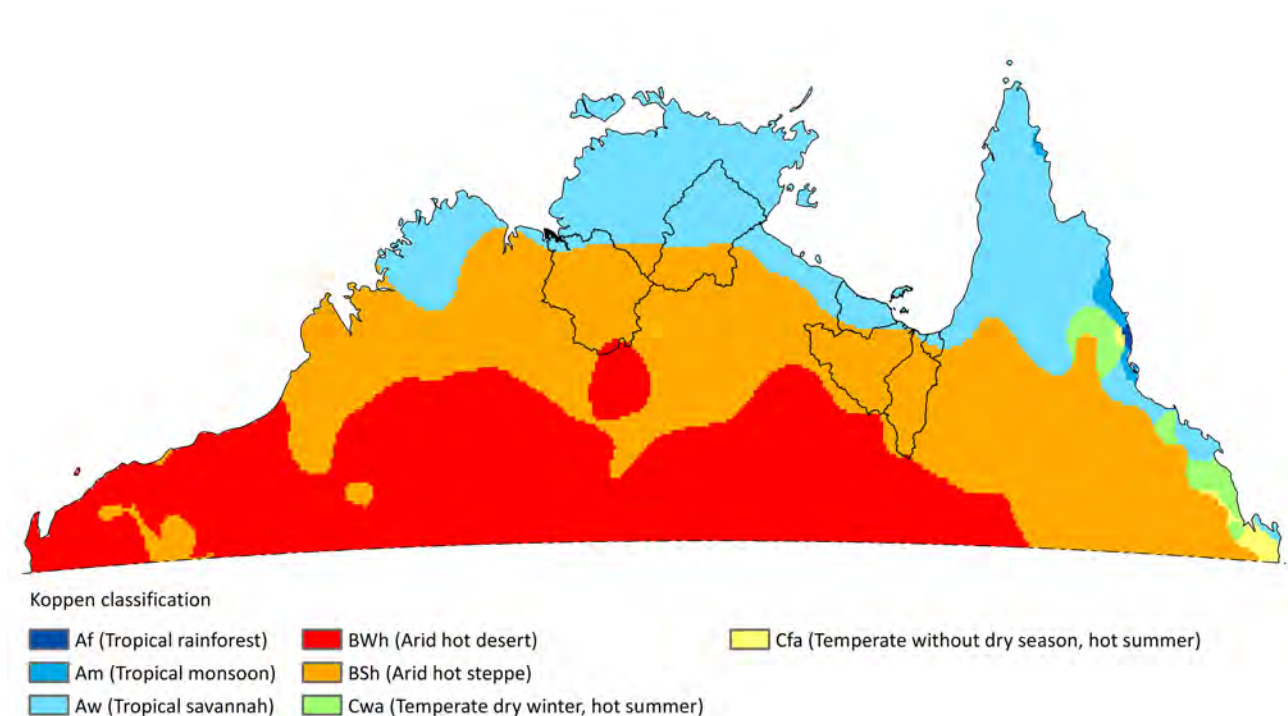


Figure 2-16 Köppen-Geiger climate classification of northern Australia

Source: Peel et al. (2007)

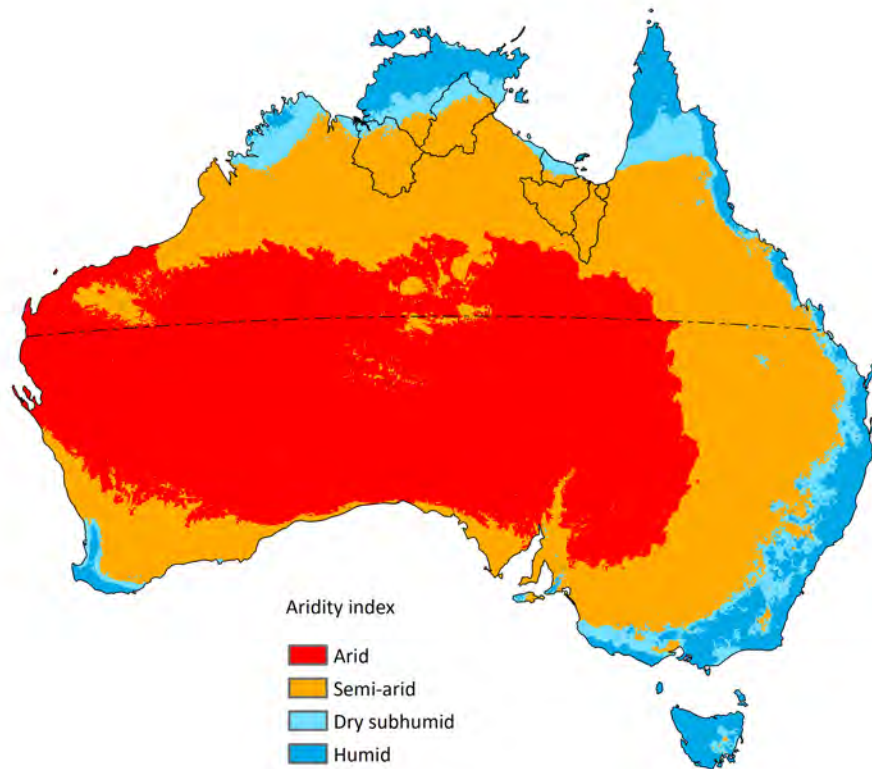


Figure 2-17 UNEP aridity index across Australia

2.4 Sea surface temperature

Warming and more intense and frequent climate extremes predicted for Australia (Hughes, 2003) can alter oceanic primary production, regional currents and water quality, which may cause a change in fish migration, abundance, growth and survival. SSTs and rainfall have been found to be positively correlated with the catch of seven coastal commercial fisheries species for regions along the Queensland coast (Meynecke and Lee, 2011). A regression model that included a measure of rainfall, SST and SOI explained between 30 and 70% of the variance in catch adjusted for effort for the same year for barramundi (*Lates calcarifer*), mud crabs (*Scylla serrata*), mullet (e.g. *Mugil cephalus*), flathead (e.g. *Platycephalus fuscus*), whiting (*Sillago spp.*), tiger prawns (*Penaeus monodon*, *P. semisulcatus*) and endeavour prawns (*Metapenaeus endeavouri*, *M. ensis*).

2.4.1 Trends in sea surface temperature

Recent (1982–2015) observations show a warming trend in annual SST around much of Australia (Figure 2-18). There are regional and seasonal differences in SST trends around northern Australia, with predominantly warming in all months with the exception of the winter months where northern and north-western coastlines are cooling. Of particular note is the high warming trend of greater than 0.4 °C per decade in the north-west for November and December. There has been an increase in the extent of record high values, and a decrease of low SSTs.

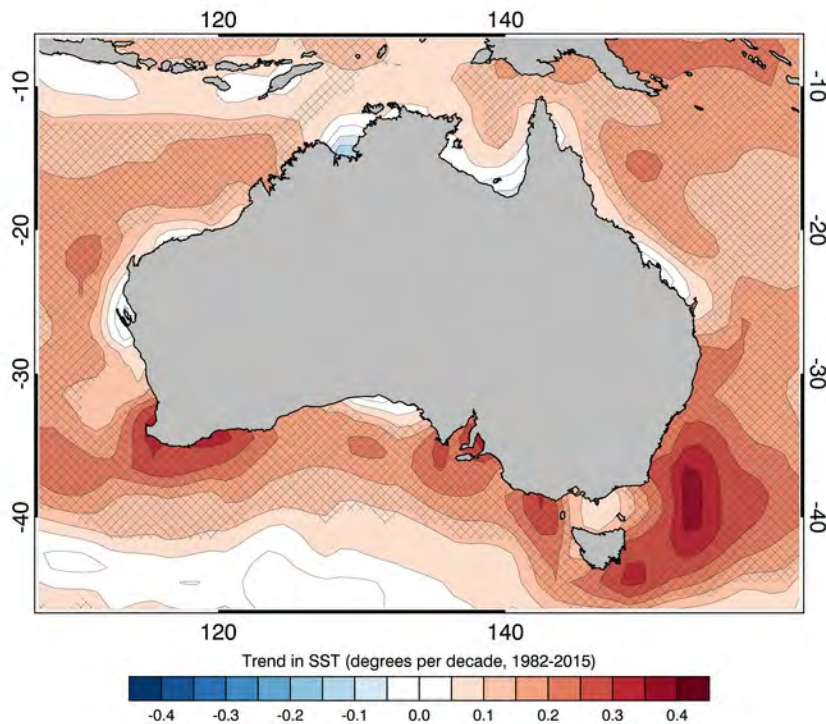


Figure 2-18 Linear trend in annual averaged SST (°C per decade) from 1982 to 2015

Hatched areas are where the trend is significant at the 95% level.

Correlations of sea surface temperature patterns with El Niño–Southern Oscillation

The timing of significant SST patterns displays some correlation to ENSO events. Over the period 1982 to 2016 the following observations can be made for northern Australian SSTs:

- Record low SSTs were observed for during the 1982–83 and 1992–93 El Niño events. However, this was not the case for the 1997–98 and 2015–16 El Niño events. From April to October 1998 much of the north to north-east coast experienced record temperatures. From February to July 2016 the north-western and northern coast were at record temperatures.
- Large regions of record high SSTs were observed in the months following El Niño events, such as the 1997–98 and 2015–16 events, but not the 1982–83 event. The record warming of 2015–16 has contributed to coral bleaching on the Great Barrier Reef and possibly to TC intensification (<https://theconversation.com/this-summer's-sea-temperatures-were-the-hottest-on-record-for-australia-heres-why-56906>).
- Large regions of record high SSTs were observed leading into La Niña events, as evident during 1989–1990 and 2010–11.
- Large regions of record low SSTs were observed directly after the 2010–11 and 2011–12 La Niña events.

2.5 Palaeoclimates of northern Australia

The instrumental record, particularly in Australia, is climatologically very short and so palaeoclimate knowledge is useful for placing the instrumental record, as well as climate change projections of possible future climate, into a broader context. Such information is useful for agricultural and water resource planning as well as understanding the extent to which northern

'natural' ecosystems may be dependent on current climate and hence their ability to adapt to changes in climate and flow.

The main driver of northern Australian climate, the monsoon, is thought to have originated up to 40 million years ago, while the circulation patterns in the Pacific responsible for ENSO are likely to have originated about 3 to 2.5 million years ago (Bowman et al., 2010). The ENSO–monsoon–rainfall relationships have varied throughout this time with wetter and drier periods of enhanced or reduced monsoonal activity (Bowler et al., 2001; Burrows et al., 2014; De Deckker et al., 2014; Gagan et al., 2004; Lewis and LeGrande, 2015; McGregor et al., 2013). Hence the ecosystems in northern Australia have experienced varying monsoonal and flow conditions on evolutionary time scales.

There are many sources of evidence of variable monsoon and ENSO strength over the past several thousand years, including stalagmites (Denniston et al., 2013; Griffiths et al., 2009), corals (Gagan et al., 2004; Lough et al., 2014), pollen (Shulmeister and Lees, 1995), peat (Burrows et al., 2014) and Indigenous art (McGowan et al., 2012). While several studies infer past ENSO variability from palaeo-rainfall, the relationships between rainfall, the monsoon and ENSO are themselves non-stationary and so relationships derived using current climate may not apply to the past (Denniston et al., 2013; Gallant et al., 2013a; Lewis and LeGrande, 2015).

Several studies have inferred variations in TC activity, with some linking TC variability to ENSO activity, over the last several thousand to several hundred years. The majority of such studies suggest higher frequency of high-intensity TCs (up to ten times more) before the instrumental period (Denniston et al., 2015; Forsyth et al., 2010; Haig et al., 2014; Nott et al., 2007; Nott and Jagger, 2013). Haig et al. (2014), for example, derived a record of TC activity over the past 1500 years for Cape Range, Western Australia, and Chillagoe, Queensland, and concluded the present low levels of TC activity are unprecedented over the past 550 to 1500 years.

A few studies have looked at palaeohydrology, such as Wohl et al. (1994) who reconstructed the past 4000-year flooding history for the Fitzroy and Margaret rivers. Their reconstruction indicated Geikie Gorge on the Fitzroy River experienced six floods of between 5000 to 30,000 m³/second discharge over the last 2000 years and the upper Margaret River experienced 13 floods ranging between 2000 to 20,000 m³/second during the last 4000 years. The magnitudes of these events suggest the relatively short-term observational gauge records in these basins may not adequately represent extreme discharges. For comparison, the highest 24-hour flow in the instrumental record at Diamond Gorge upstream of Geikie Gorge is 10,532 m³/second from a 52-year record, and for Margaret River at Mount Krause is 9570 m³/second from a 32-year record.

On balance, studies of northern Australian palaeoclimate suggest that the instrumental record does not account for the full range of possible climate and that the relationship between, and hence relative influence of, key drivers of climate variability can change over centennial time scales. Extreme events that occur rarely are thus potentially underestimated in the instrumental record and, therefore, projections of future conditions should be assessed with this in mind.

Part II Local-scale processes



3 Victoria catchment

3.1 Data availability

The Victoria (NT) catchment's (~82,400 km²) location, major features and relief are shown in Figure 3-1. The distributions of stations recording rainfall and maximum temperature are shown in Figure 3-2 and Figure 3-3, respectively. There are considerably fewer stations measuring rainfall and maximum temperature in the Victoria catchment, compared to the comparably sized Murrumbidgee catchment in south-eastern Australia (~84,000 km²).

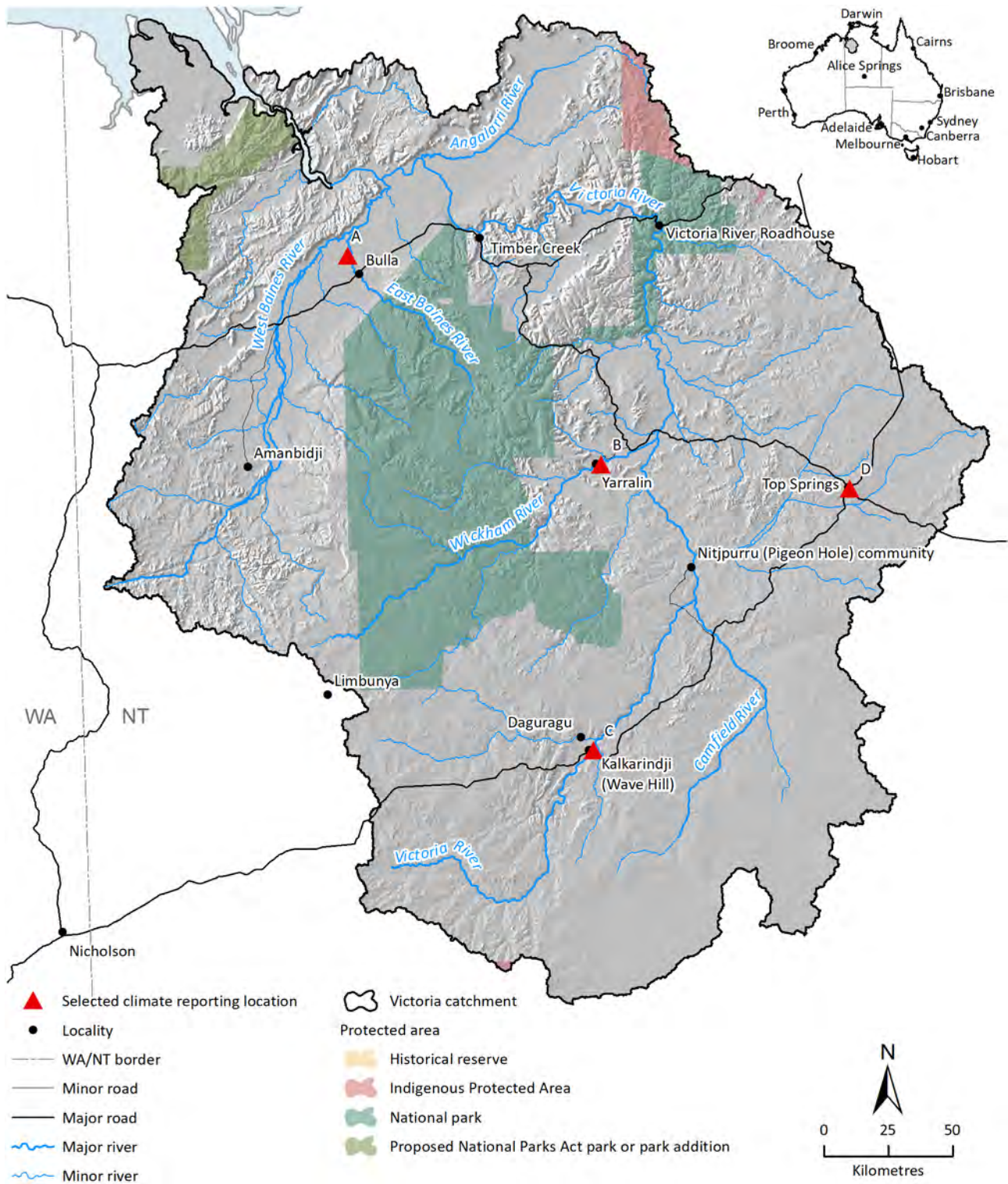


Figure 3-1 A shaded relief map of the Victoria catchment

Results are shown later for Auvergne (A), Yarralin (B), Kalkarindji (Wave Hill) (C) and Top Springs (D) climate reporting locations.

Source: (Department of Agriculture, Water and the Environment, 2020)

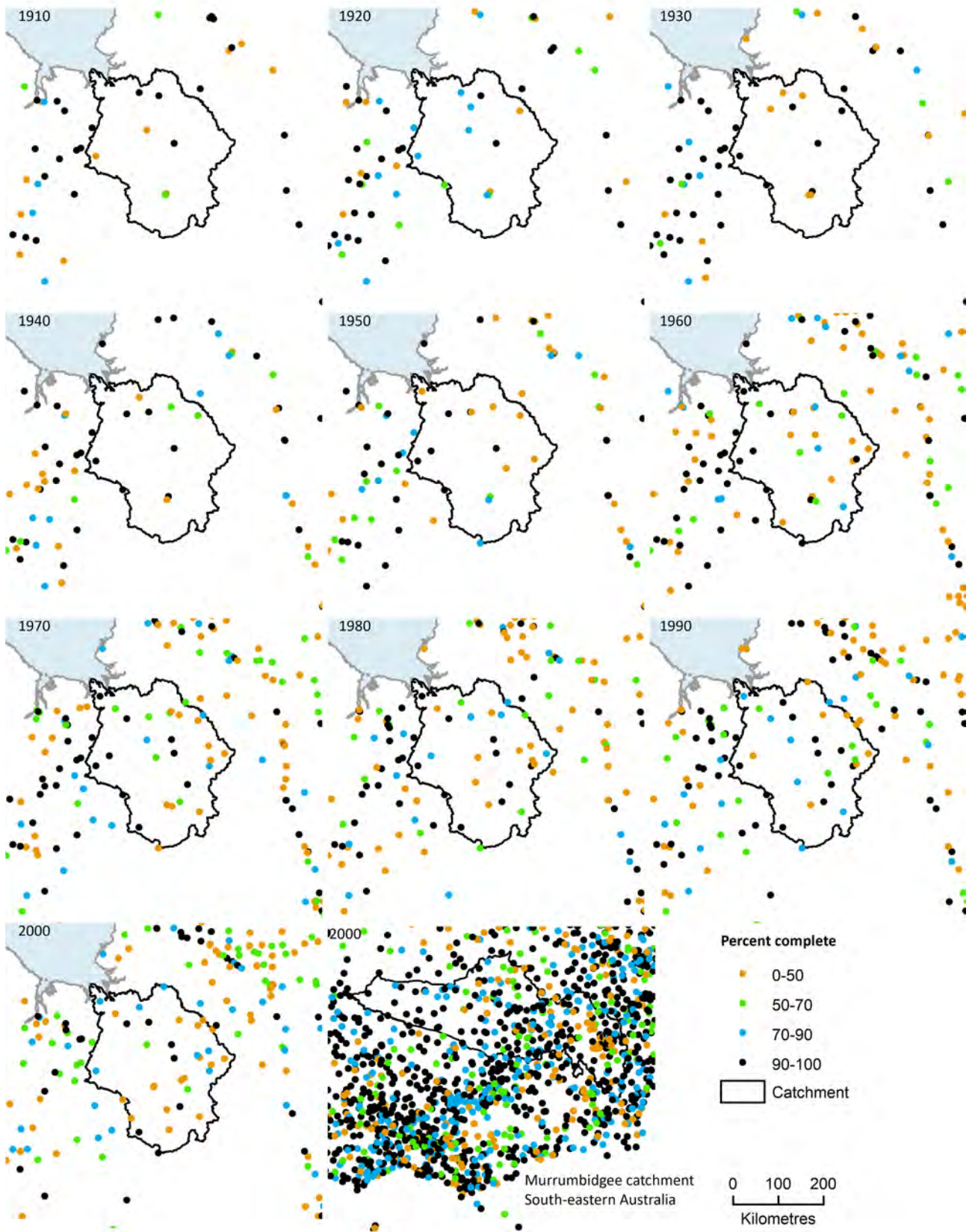


Figure 3-2 Decadal analysis of the location and completeness of Bureau of Meteorology stations measuring daily rainfall used in the SILO database

The decade labelled '1910' is defined from 1 January 1910 to 31 December 1919, and so on. At a station, a decade is 100% complete if there are observations for every day in that decade. The last panel shows the availability of rainfall data in the vicinity of the Murrumbidgee catchment in south-eastern Australia for comparison.

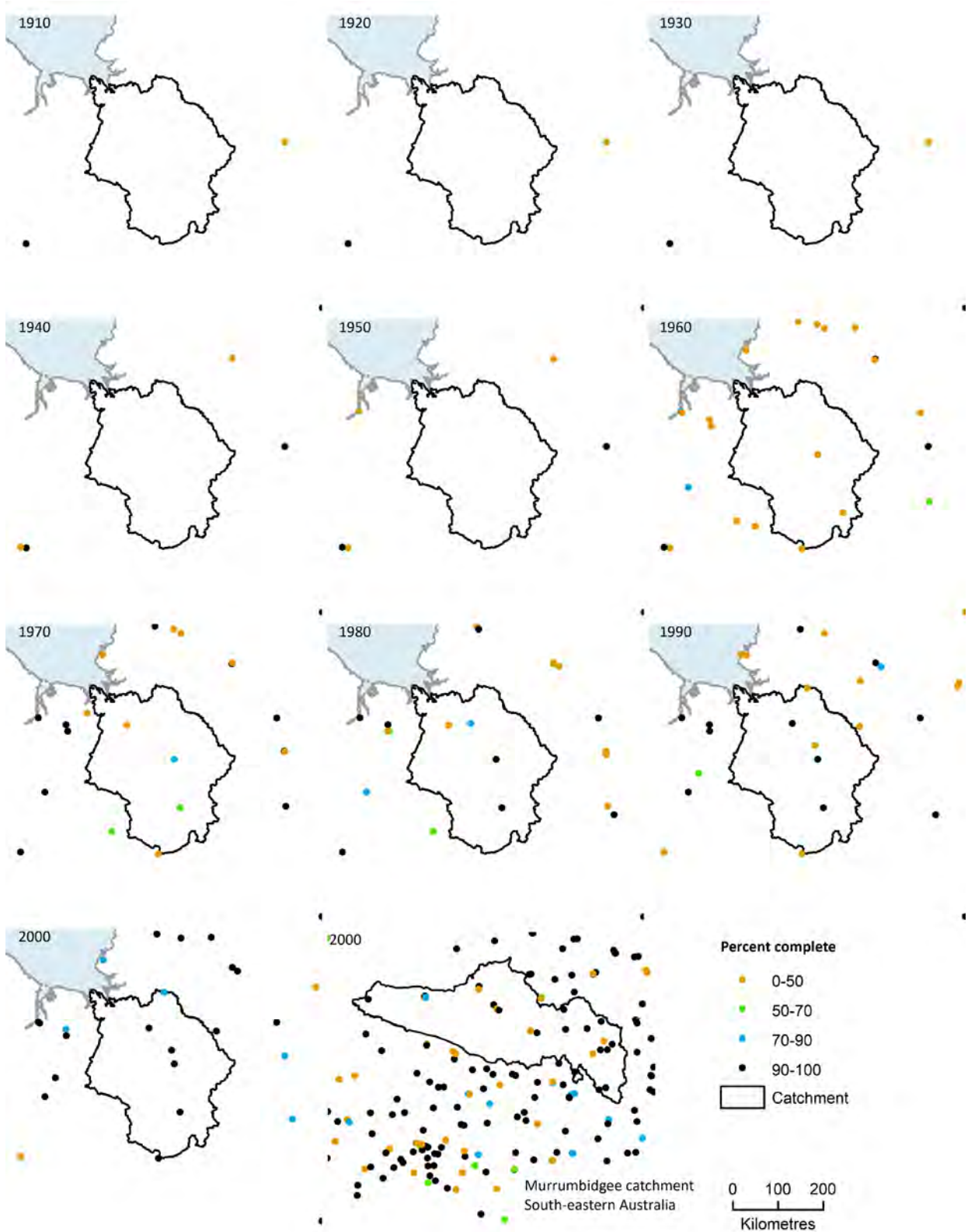


Figure 3-3 Decadal analysis of the location and completeness of Bureau of Meteorology stations in the Victoria catchment measuring daily maximum air temperature used in the SILO database

The decade labelled '1910' is defined from 1 January 1910 to 31 December 1919, and so on. At a station, a decade is 100% complete if there are observations for every day in that decade. The last panel shows the availability of maximum temperature data in the vicinity of the Murrumbidgee catchment in south-eastern Australia for comparison.

3.2 Local-scale climate in the Victoria catchment

3.2.1 Rainfall

The Victoria catchment lies near the typical southernmost extent of the deep westerly wind regime associated with the Australian summer monsoon, with a climate characterised by a highly distinctive wet and dry season. The mean annual rainfall, averaged over the Victoria catchment for the 132-year historical period (1 September 1890 to 31 August 2022), is 681 mm. Rainfall is highest in the northern parts of the catchment (Figure 3-4) that are more frequently affected by monsoon westerly winds. The trough, a primary trigger for diurnal thunderstorm activity over the catchment, separates moist maritime winds to its north and much drier continental air to its south.

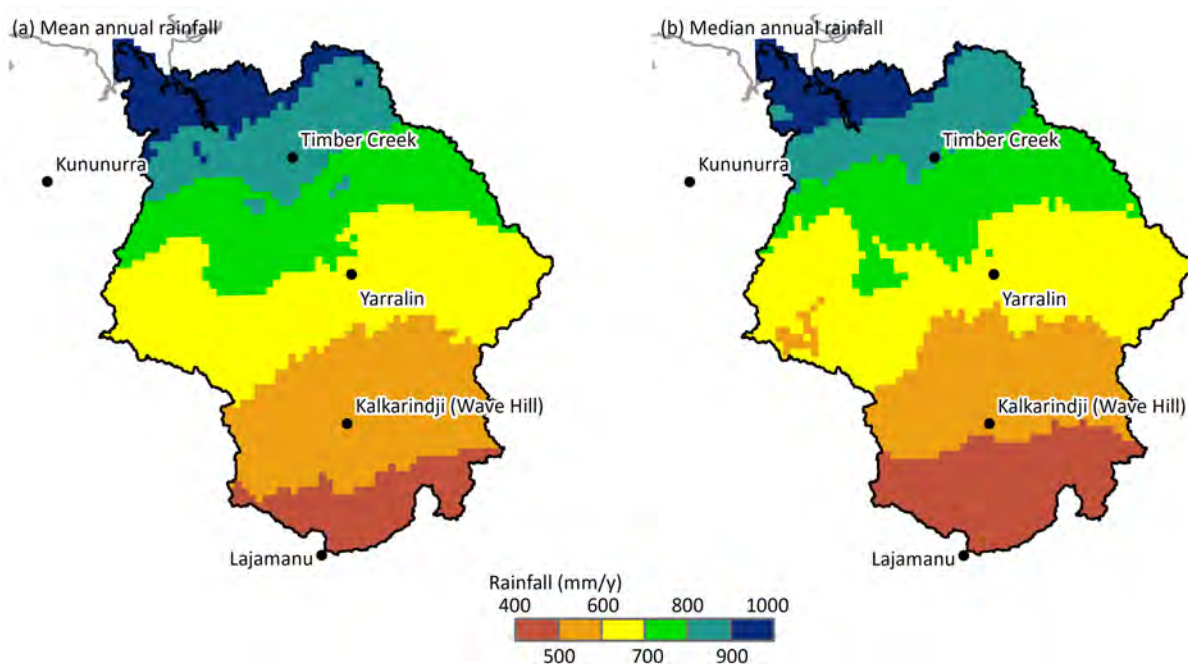


Figure 3-4 Historical (a) mean annual rainfall and (b) median annual rainfall across the Victoria catchment

For the historical period, 95% of annual rain falls during wet-season months (1 November to 30 April). The spatial distribution of rainfall during the wet and dry seasons is shown in Figure 3-5. Median wet-season rainfall shows a decrease from north to south but a distinct pattern is not observed during the dry season. The highest monthly rainfall totals typically occur during January, February and March (Figure 3-6). Note that, for all time series plots in this chapter, the data used is from the scientific information for land owners (SILO) data drill point closest to the indicated location of interest.

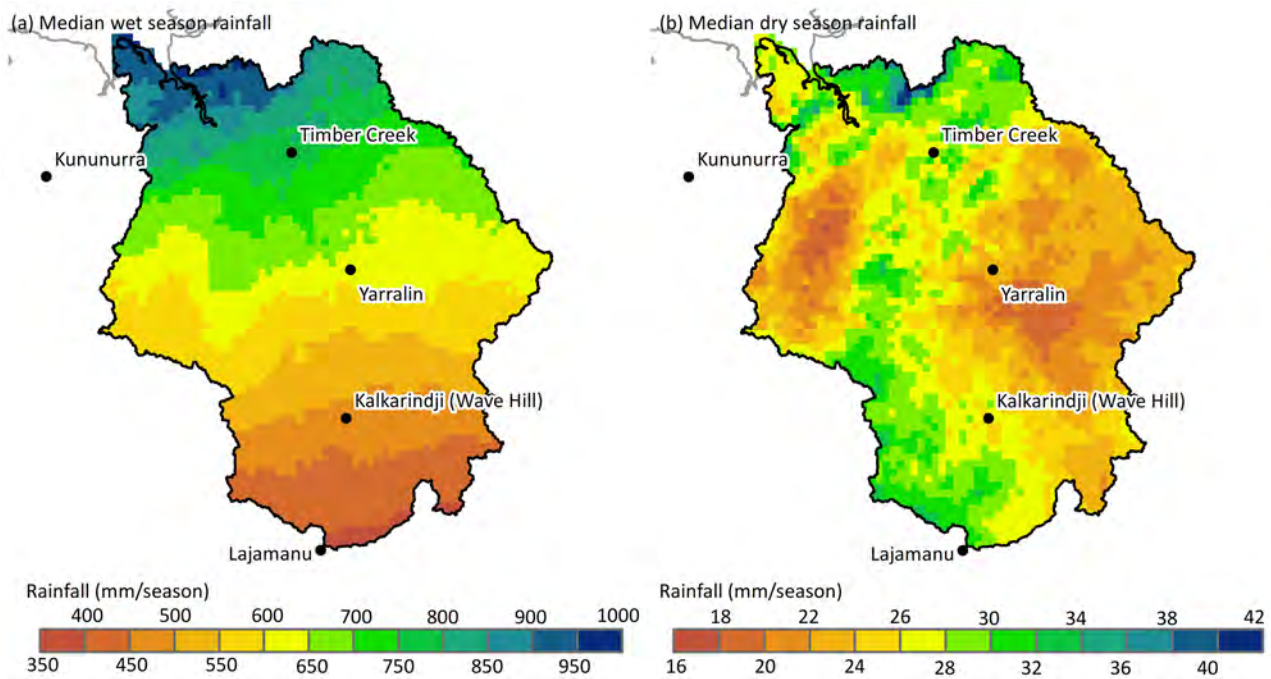


Figure 3-5 Historical median rainfall during the (a) wet and (b) dry season in the Victoria catchment

Tropical cyclones and the monsoon trough (westerly low-level winds)

Tropical cyclones (TCs) do not affect the Victoria catchment every year and so their contribution to total annual rainfall is highly variable from one year to the next. Correspondingly, therefore, infrequent extreme annual rainfall totals have strong north–south gradients (Figure 3-7). For the 53 TC seasons from the 1969–70 to 2021–22 period, 72% of seasons experienced no TCs, 21% one TC, and 6% two. When a TC or low does cross the catchment, typically 200 to 500 mm of rain falls over a 2–5-day period, and daily rainfall totals have exceeded 200 mm in the estuary area of the catchment (Figure 3-8).

One mechanism by which the catchment can experience active monsoonal conditions is for a tropical low or cyclone to form in the monsoon trough north of the region and subsequently be steered to the south to drag the monsoon over the catchment area. Locations to the north of the catchment area are more frequently affected by monsoonal westerly winds. This is one factor that contributes to the fairly large rainfall differential between the north and south of the catchment (Figure 3-4).

When affected by monsoonal westerly winds, coastal locations will typically experience the majority of the rainfall and thunderstorm activity, with a peak in activity from midnight to the early hours of the morning. Locations further inland may also see an increase in diurnal activity, with the westerly winds advecting more moisture, leading to an environment more conducive to shower and thunderstorm development. Counteracting this tendency, increased cloud cover, lower than normal temperatures and a potential lack of a trigger to initiate convection can also act to suppress afternoon activity inland.

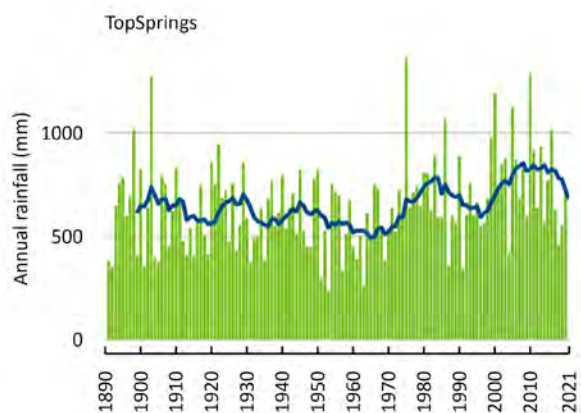
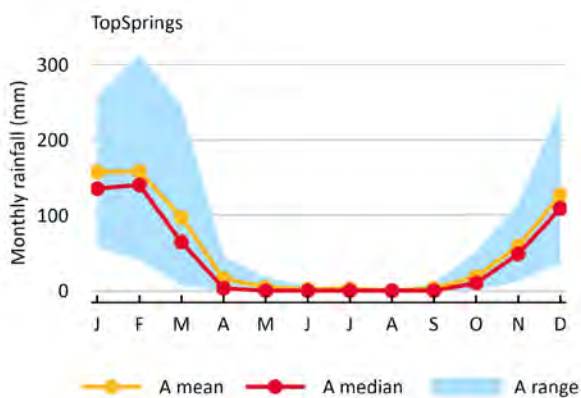
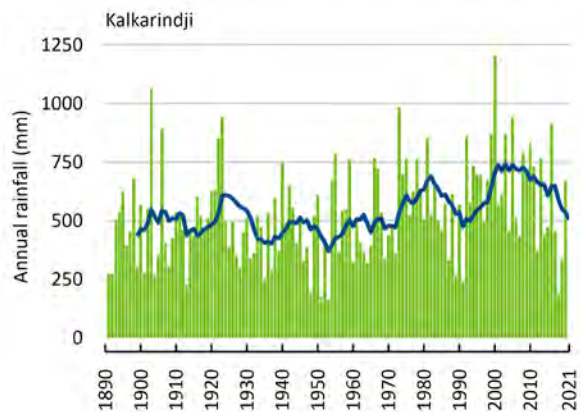
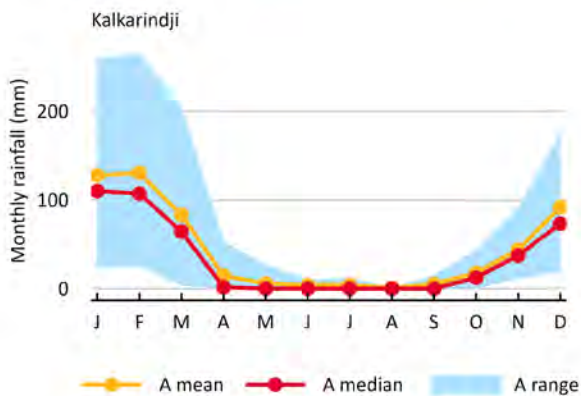
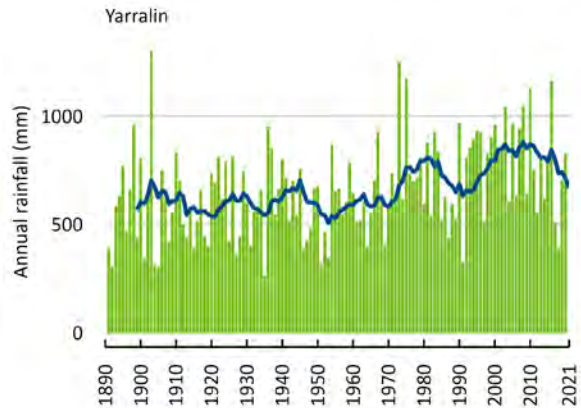
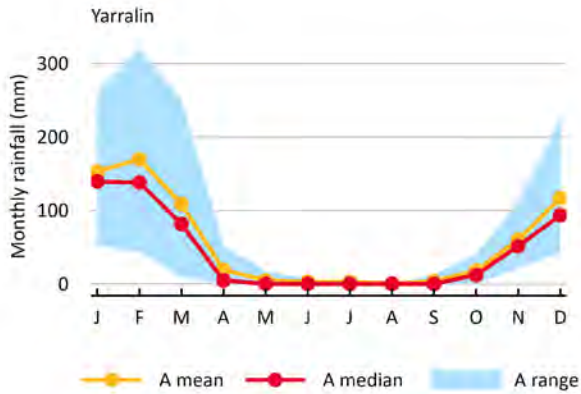
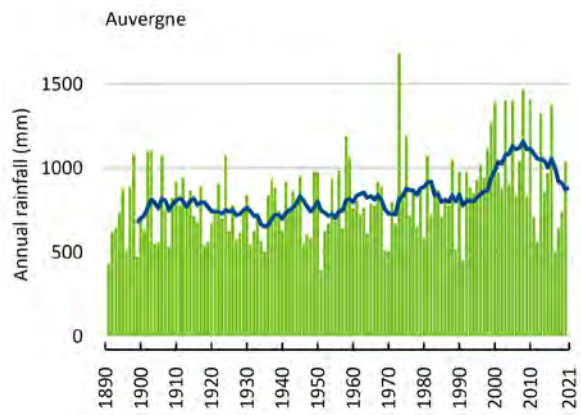
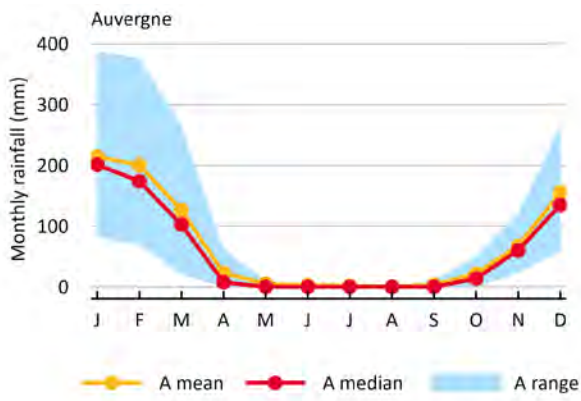


Figure 3-6 Historical monthly rainfall in the Victoria catchment at Auvergne, Yarralin, Kalkarindji (Wave Hill) and Top Springs

Left column shows monthly rainfall, right column shows time series of annual rainfall (A range is the 10th to 90th percentile monthly rainfall).

Diurnal storm activity (easterly low-level winds)

Spatial-temporal variability of the diurnal precipitation cycle in coastal regions in the Victoria catchment is mainly associated with insolation, the land-sea breeze circulation, and topography. Diurnal storm activity is related to the prominent land-sea breeze circulations, which are driven by the diurnally oscillating thermal contrast between land and adjacent ocean. These circulations can also affect other synoptic and mesoscale weather phenomena. Tropical deep convection generally peaks over land in the late afternoon, and over the ocean in the early morning.

The Kimberley heat trough, which is a persistent feature in northern Western Australia in the late spring and summer months, is the primary trigger for diurnal storm activity in the catchment area, particularly inland. The heat trough often coincides with a dry line; north of the trough typically sees moister maritime air, whereas to the south of the trough much drier continental air typically prevails, usually resulting in an unsuitable environment for thunderstorm development. The location of the trough shifts from 20°S in summer to well equatorward of Australia in winter (Arnup and Reeder, 2007). The dryline is most intense in spring, rather than in summer when the heat trough is stronger but located farther poleward.

The heat trough drives a sea-breeze circulation from the coastal side of the trough and a weak solenoidal circulation in the dry air inland of the trough. The coincidence of the heat trough with a dryline may cause diurnal storm activity, especially inland. This may produce more rain in the north side (near coast) of the catchment than in the southern side.

Sea breeze

Closer to the coast, sea breeze convergence is another potential trigger for diurnal shower and thunderstorm activity. The sea-breeze circulation is a regular feature around the northern coastline, which is strongest through spring and summer when the surface heating is most intense. The sea breeze advects tropical maritime air inland, producing a diffuse strip of moist air around the coastline. The boundary where the onshore sea breeze converges with the easterly synoptic flow can help to initiate shower or thunderstorm activity before these cells are then steered back towards the coast by easterly steering winds. The outflow boundaries from these cells can in turn help to initiate more convection. These cells often collapse as they are approaching the coast and interact destructively with the sea breeze (Noonan and Smith, 1986).

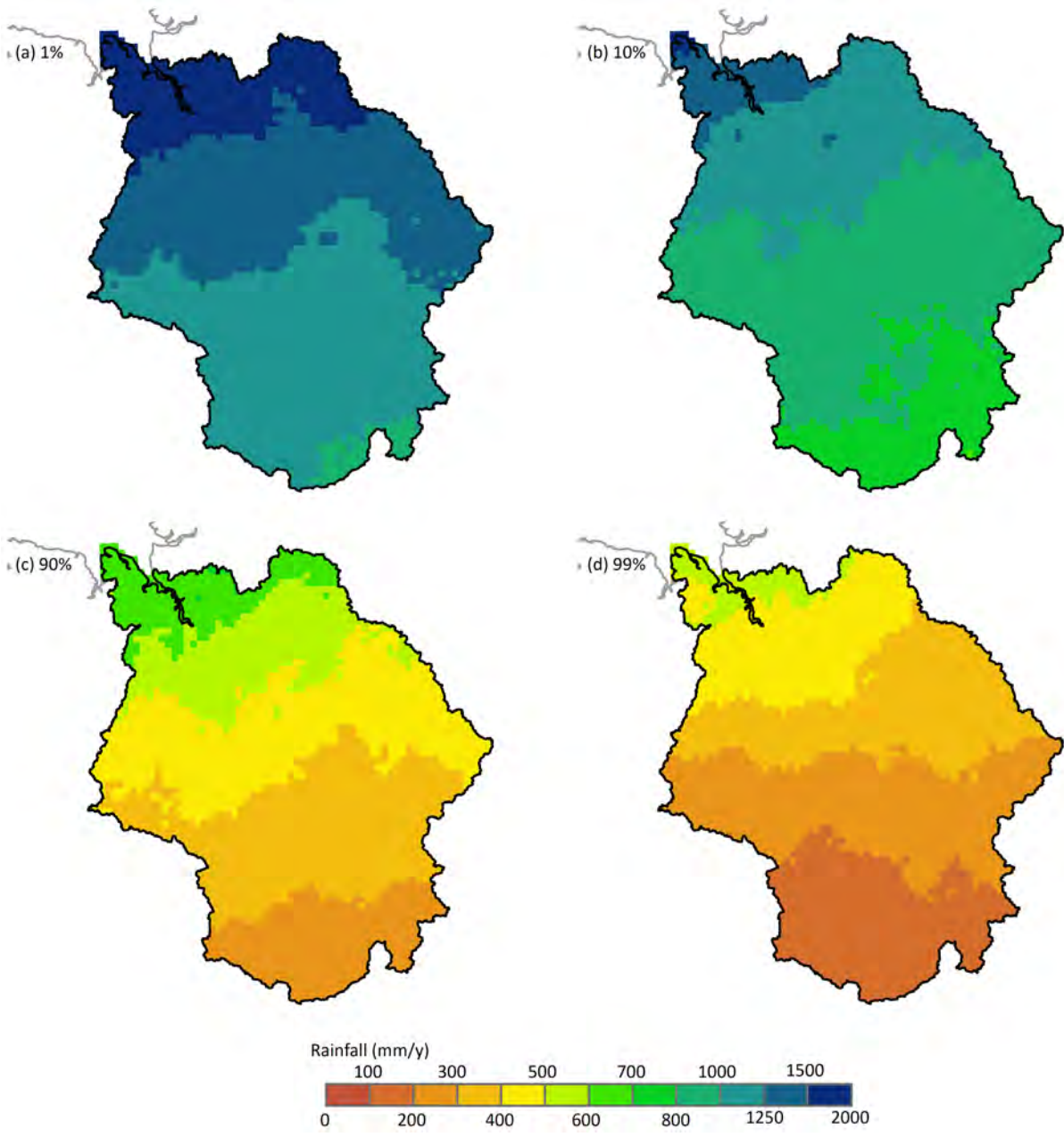


Figure 3-7 Historical annual rainfall that was exceeded in (a) 1%, (b) 10%, (c) 90% and (d) 99% of years in the Victoria catchment

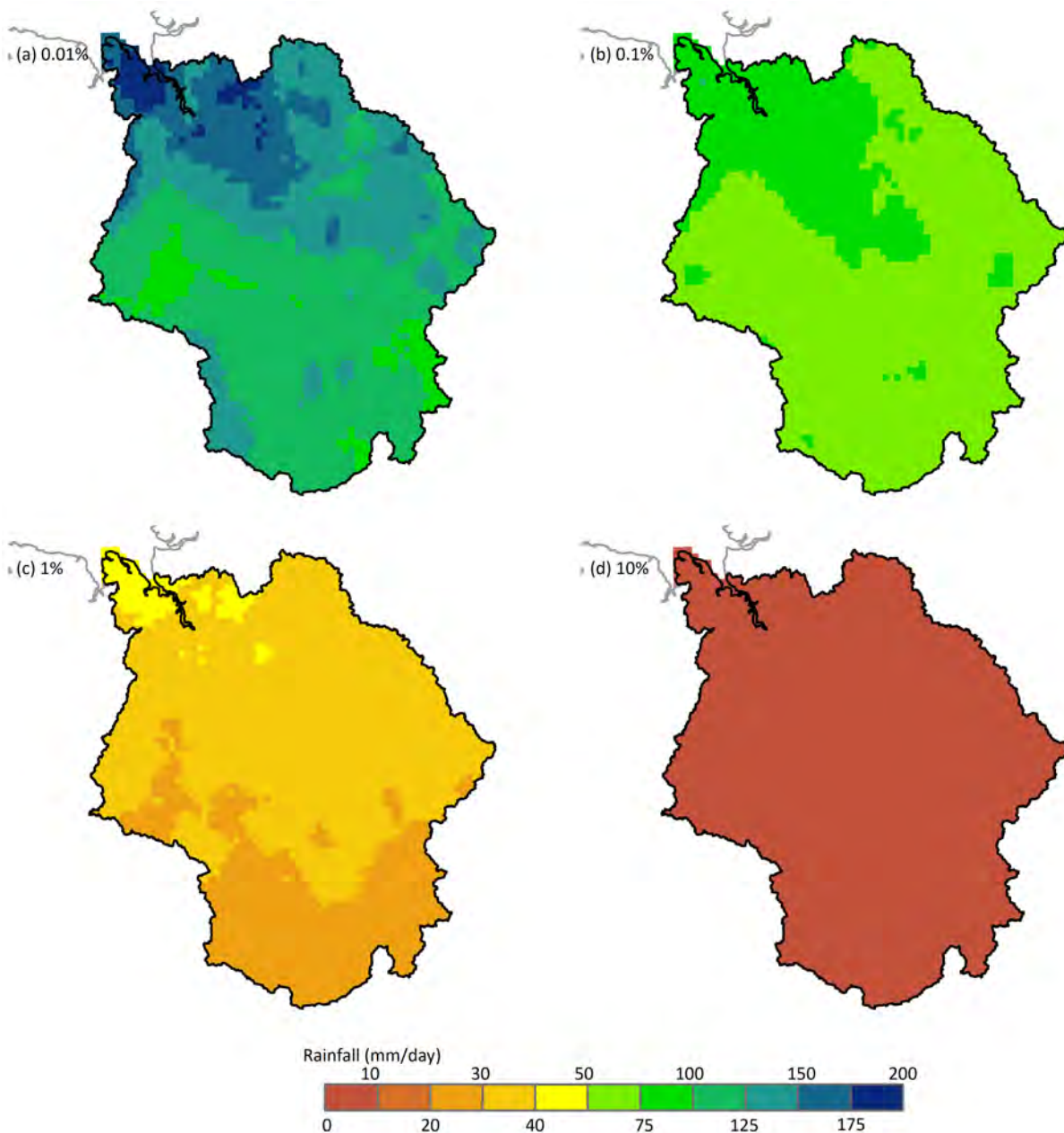


Figure 3-8 Historical daily rainfall that is exceeded in (a) 0.01%, (b) 0.1%, (c) 1% and (d) 10% of days in the Victoria catchment

3.2.2 Other climate parameters

Potential evaporation

Areal potential evaporation (APE) (as calculated using Morton's areal wet potential) in the Victoria catchment exceeds 1900 mm in most years (Figure 3-9). Evaporation is high all year round, but exhibits a strong seasonal pattern, ranging from over 200 mm per month during the build-up (October through December), which is typically the hottest time of year, to about 100 mm per month during the middle of the dry season (June) (Figure 3-9). The high mean annual potential evaporation (PE) and moderate mean annual rainfall result in a large mean annual rainfall deficit across most of the catchment (Figure 3-10). Consequently, a large proportion of the catchment is semi-arid.

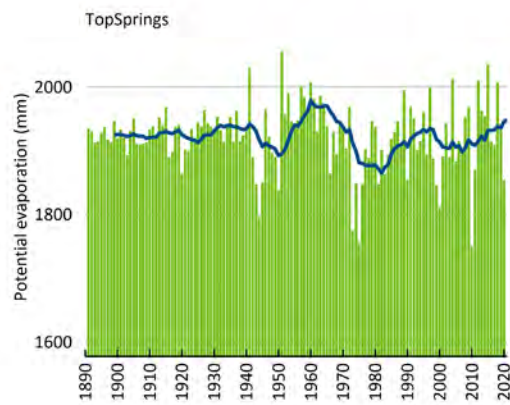
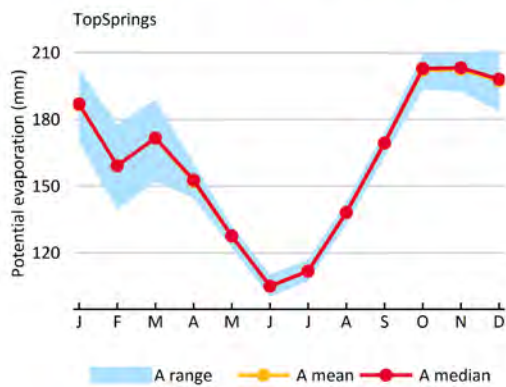
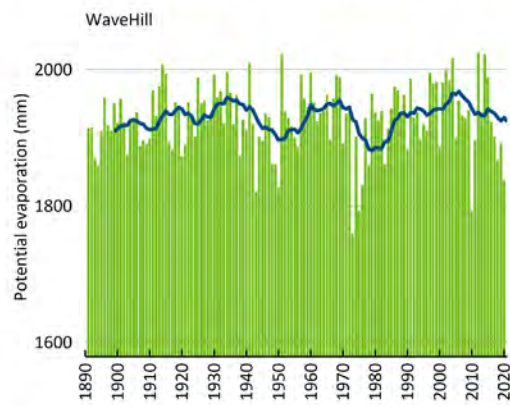
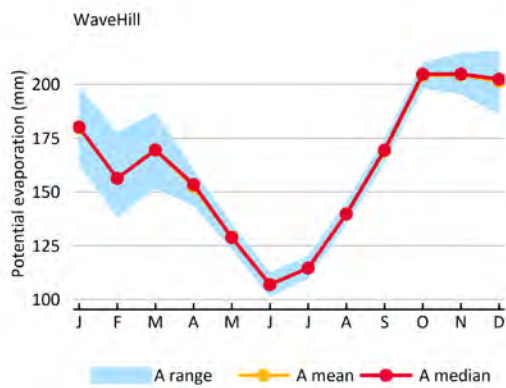
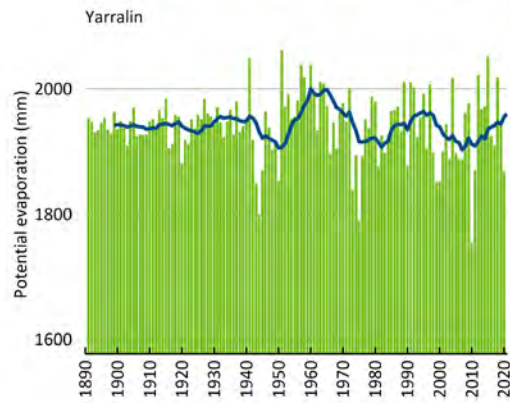
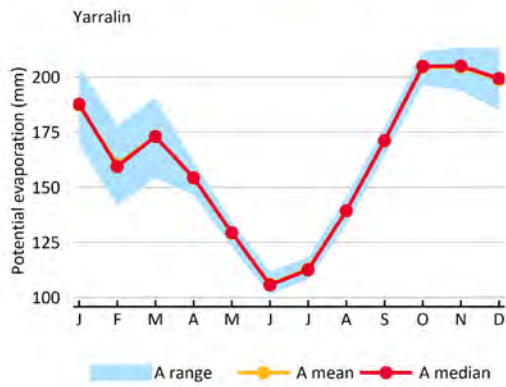
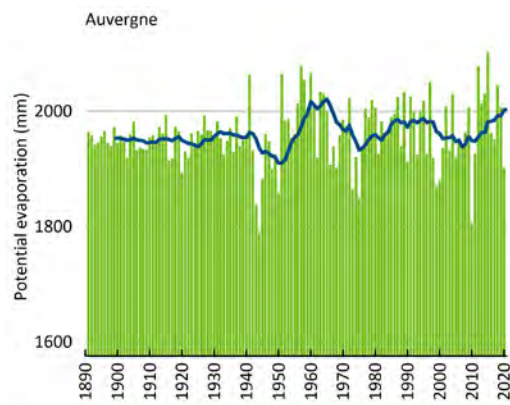
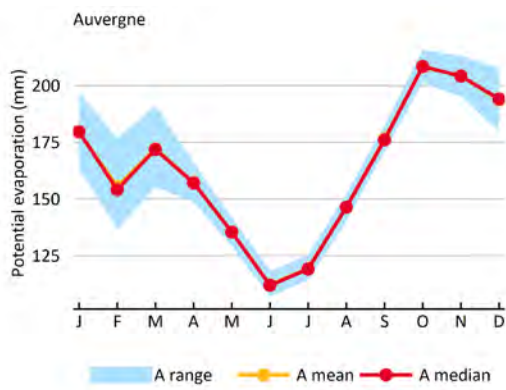


Figure 3-9 Historical potential evaporation in the Victoria catchment at Auvergne, Yarralin, Kalkarindji (Wave Hill) and Top Springs

Left column shows monthly PE, right column shows time series of annual PE (A range is the 10th to 90th percentile monthly rainfall). Note: A mean line is directly under the A median line in these figures.

Maximum and minimum temperatures

Monthly mean maximum temperature and monthly mean minimum temperature at Auvergne, Yarralin, Kalkarindji (Wave Hill) and Top Springs are shown in Figure 3-11. The highest mean monthly maximum temperatures occur in October to December and the lowest mean monthly minimum temperatures occur in June and July.

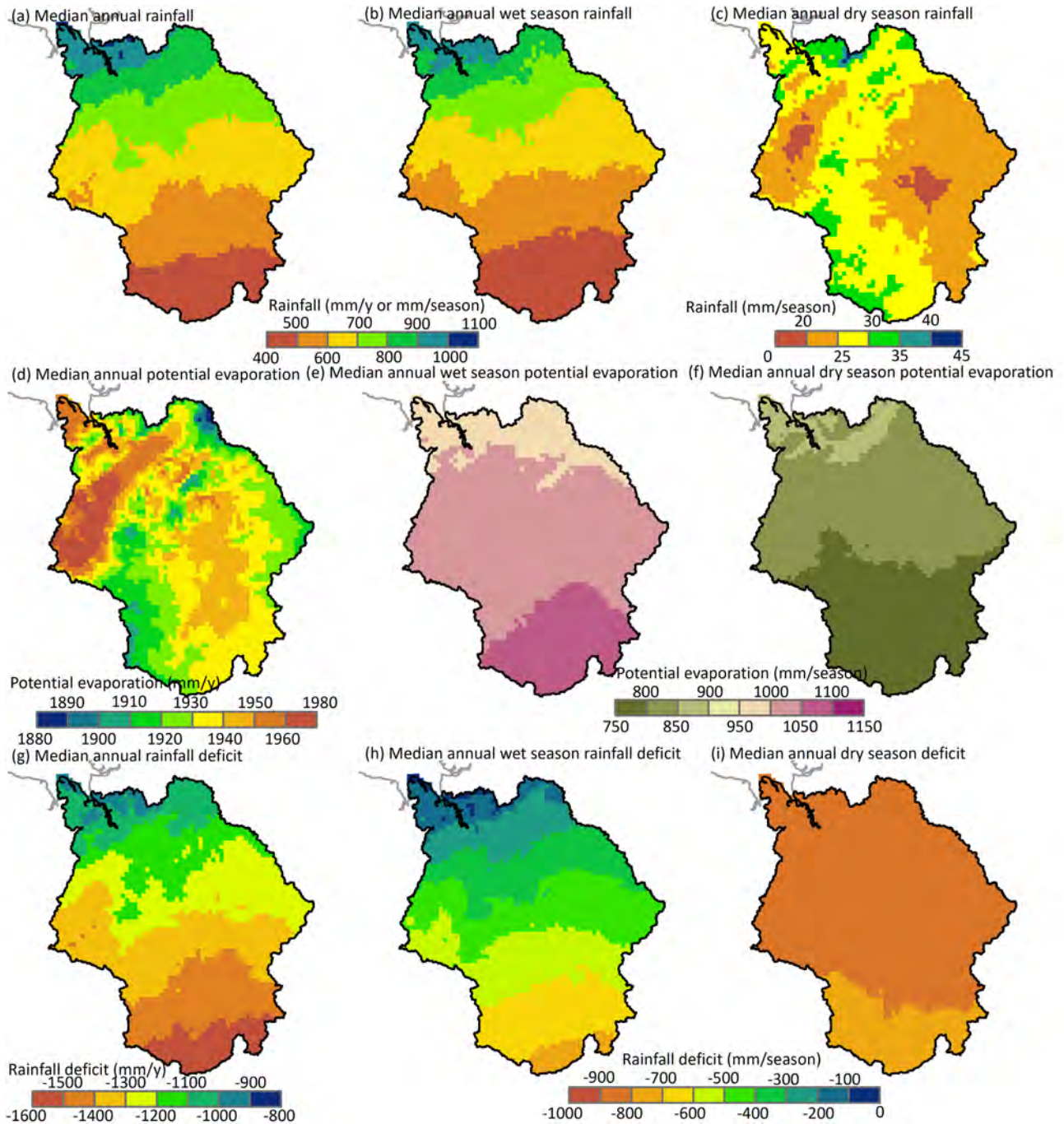


Figure 3-10 Historical median (a) annual, (b) wet-season, (c) dry-season rainfall; (d) annual, (e) wet-season, (f) dry-season potential evaporation; and (g) annual, (h) wet-season and (i) dry-season rainfall deficit in the Victoria catchment

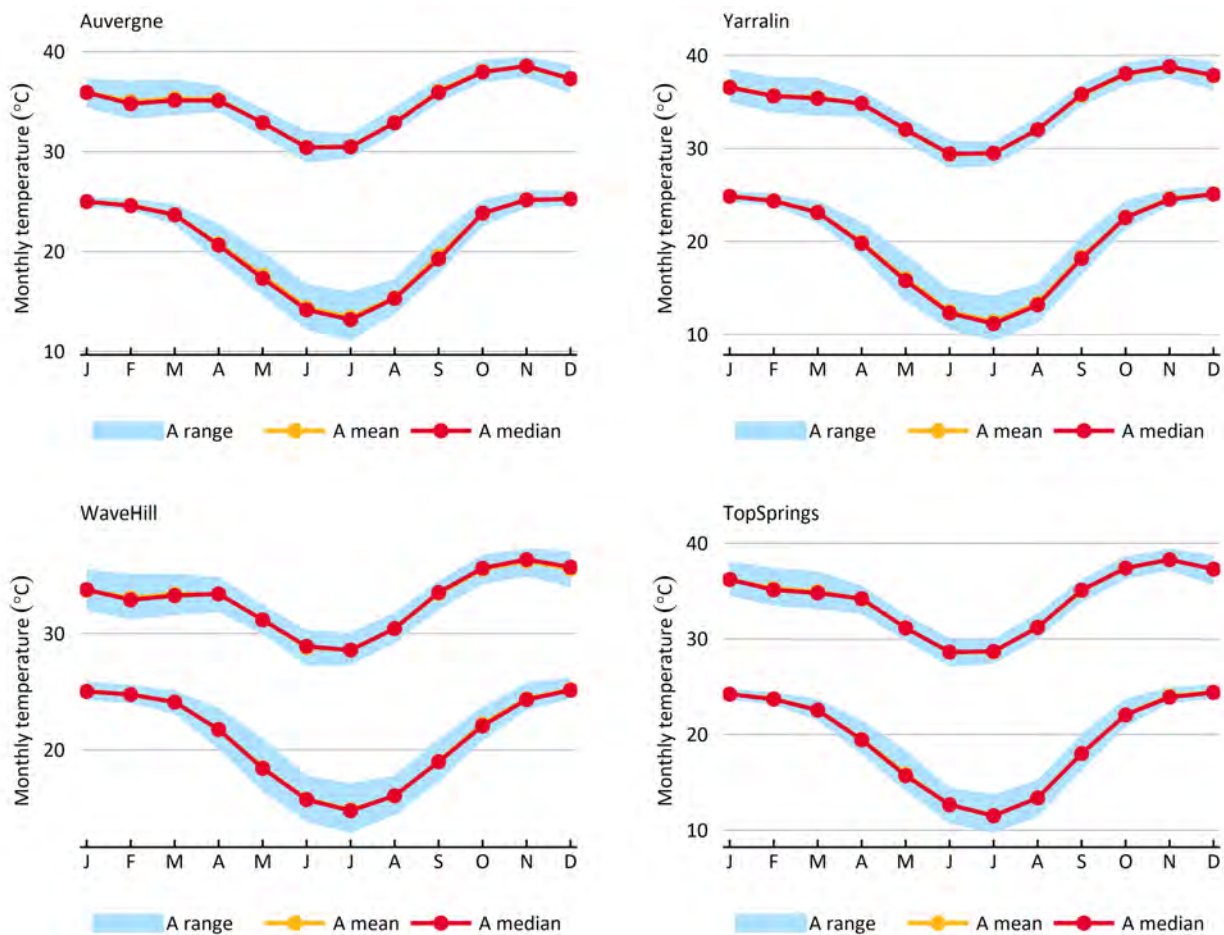


Figure 3-11 Historical maximum and minimum air temperature in the Victoria catchment at Auvergne, Yarralin, Kalkarindji (Wave Hill) and Top Springs

A range is the 10th to 90th percentile monthly temperature. Note: A mean line is directly under the A median line in these figures.

When considering the effect of temperature on crop yield, it is also important to take extreme conditions into account, particularly at sensitive stages of growth. Figure 3-12 shows the maximum annual temperature that is exceeded in 10, 50 and 90% of years, and Figure 3-13 shows the minimum annual temperature that is exceeded in 10, 50 and 90% of years. The highest maximum annual temperatures occur in the southern part of the catchment around Kalkarindji (Wave Hill) and lowest minimum annual temperatures occur in the southern-most limits of the catchment. Inland areas also experience greater variability in minimum monthly temperatures.

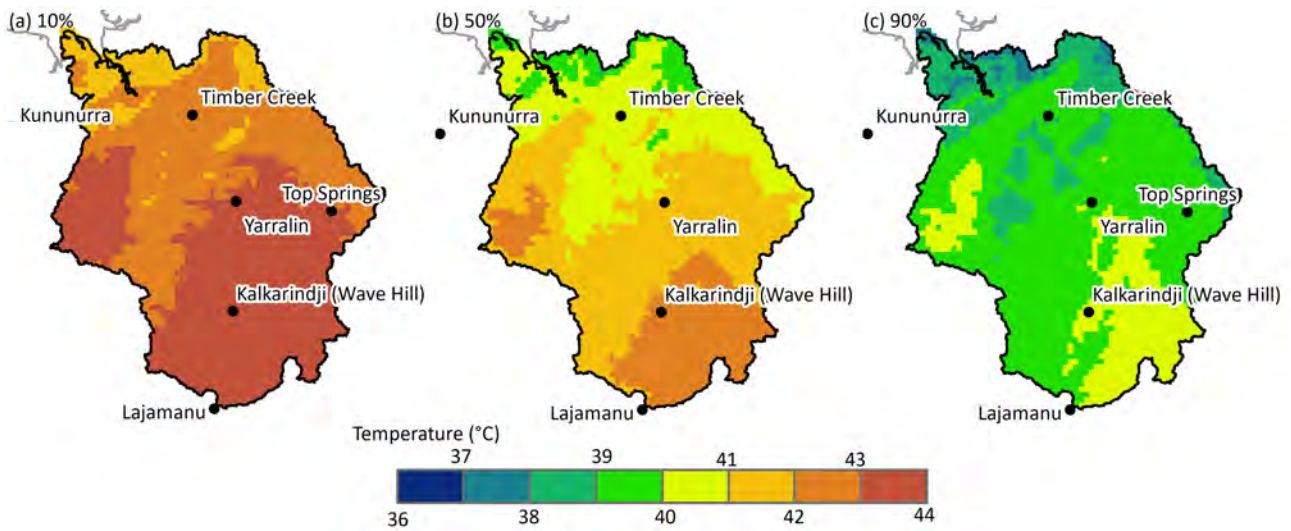


Figure 3-12 Historical annual maximum air temperature that is exceeded in (a) 10%, (b) 50% and (c) 90% of years in the Victoria catchment

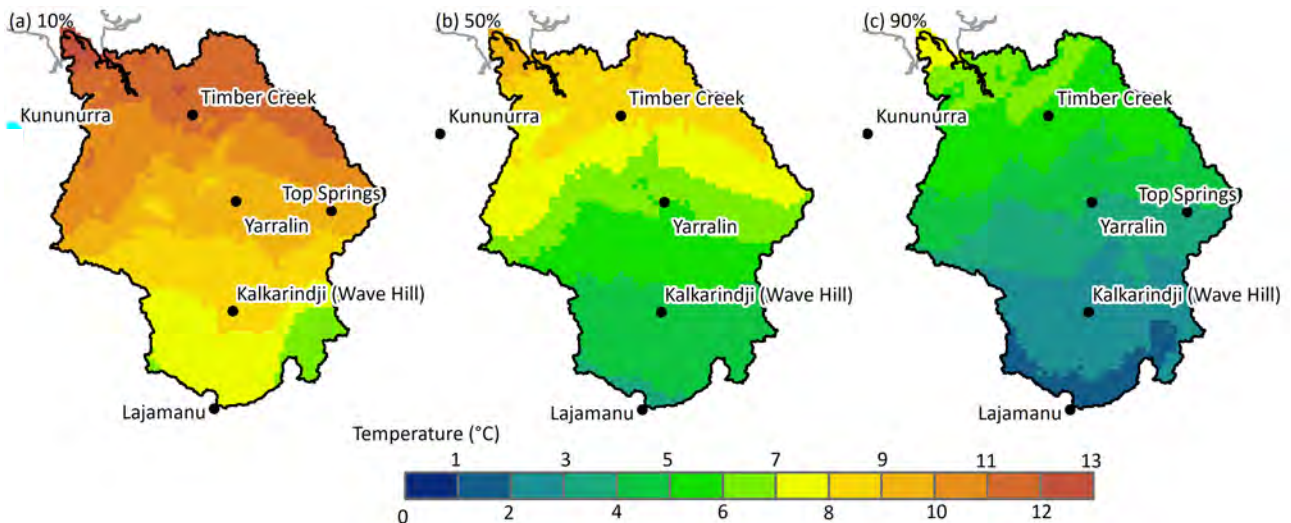


Figure 3-13 Historical annual minimum air temperature that is exceeded in (a) 10%, (b) 50% and (c) 90% of years in the Victoria catchment

Mean minimum temperatures are similar across most of the basin, except for coastal areas where minimum temperatures are consistently higher. Although mean minimum temperatures are similar, inland areas experience greater variability in minimum temperatures (i.e. temperatures often fall lower in these areas when conditions are favourable).

Frost hollows are virtually non-existent in the Fitzroy catchment, with minimum temperatures rarely going below 10 °C (Figure 3-14). If a rare frost event were to occur, it would most likely be in the most southern parts of the catchment during July.

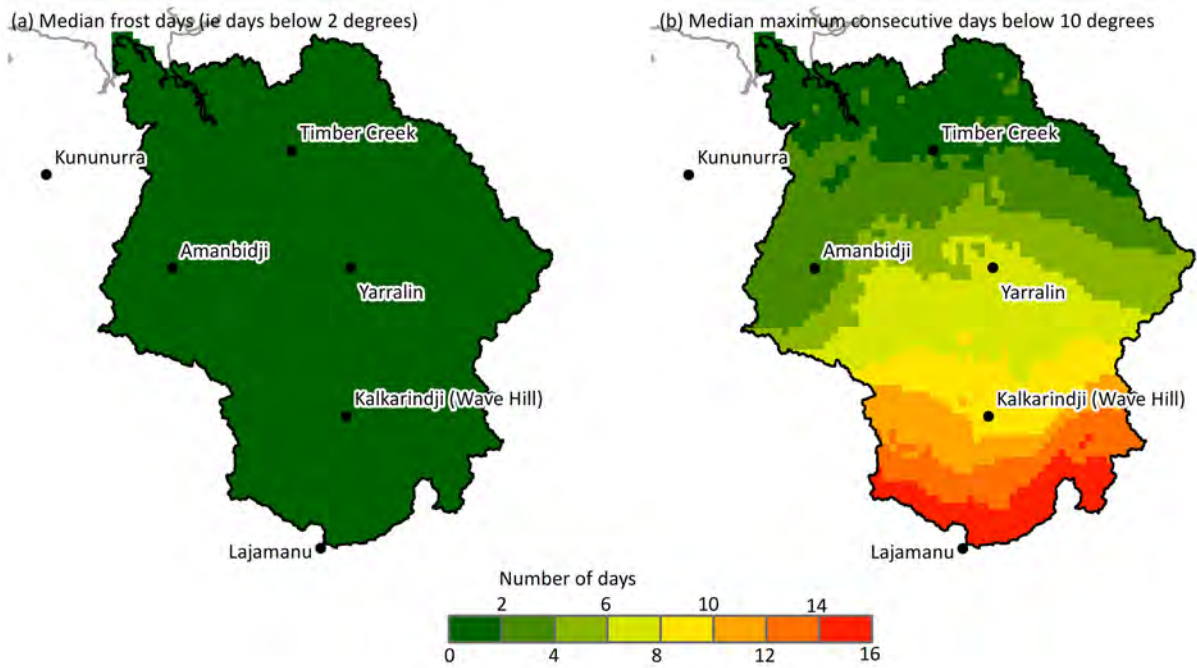


Figure 3-14 Historical minimum temperature thresholds in the Victoria catchment

(a) Median annual frost days (i.e. days below 2 °C); and (b) median annual maximum consecutive days below 10 °C.

Solar radiation

Mean annual radiation exceeded in 10, 50 and 90% of years in the Victoria catchment is shown in Figure 3-15. Higher cloud cover in the north of the catchment contributes to the pronounced north–south gradient. Monthly mean radiation at Auvergne, Yarralin, Kalkarindji (Wave Hill) and Top Springs is shown in Figure 3-16. The maximum values in October are due to the wet-season cloudiness decreasing radiation in the November to February period, and minimum values are due to the low sun angle in the middle of the dry season.

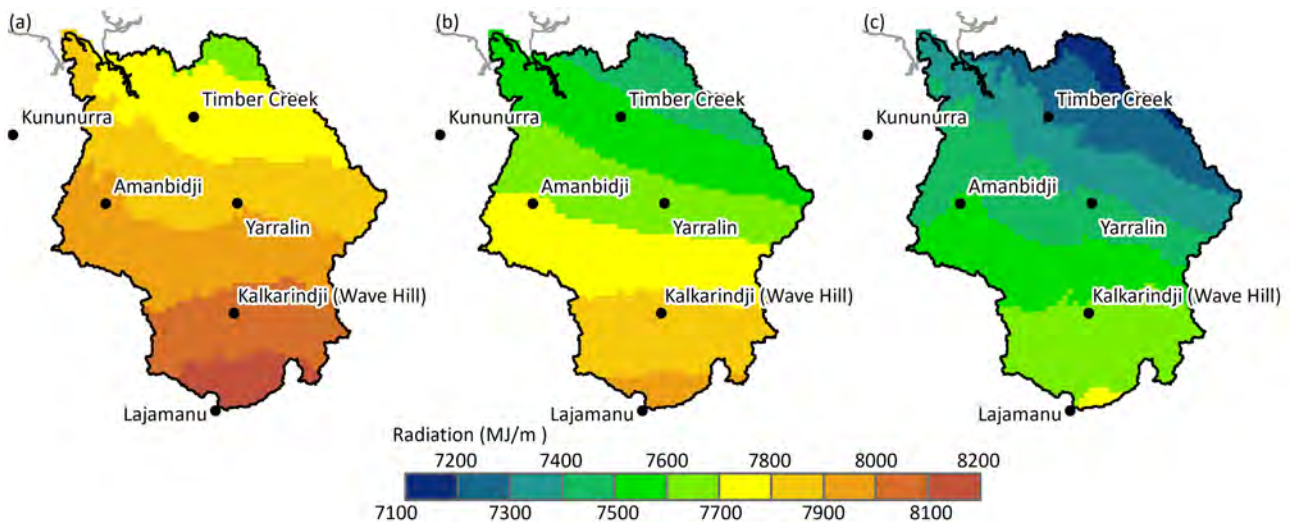


Figure 3-15 Historical annual radiation that is exceeded in (a) 10%, (b) 50% and (c) 90% of years in the Victoria catchment

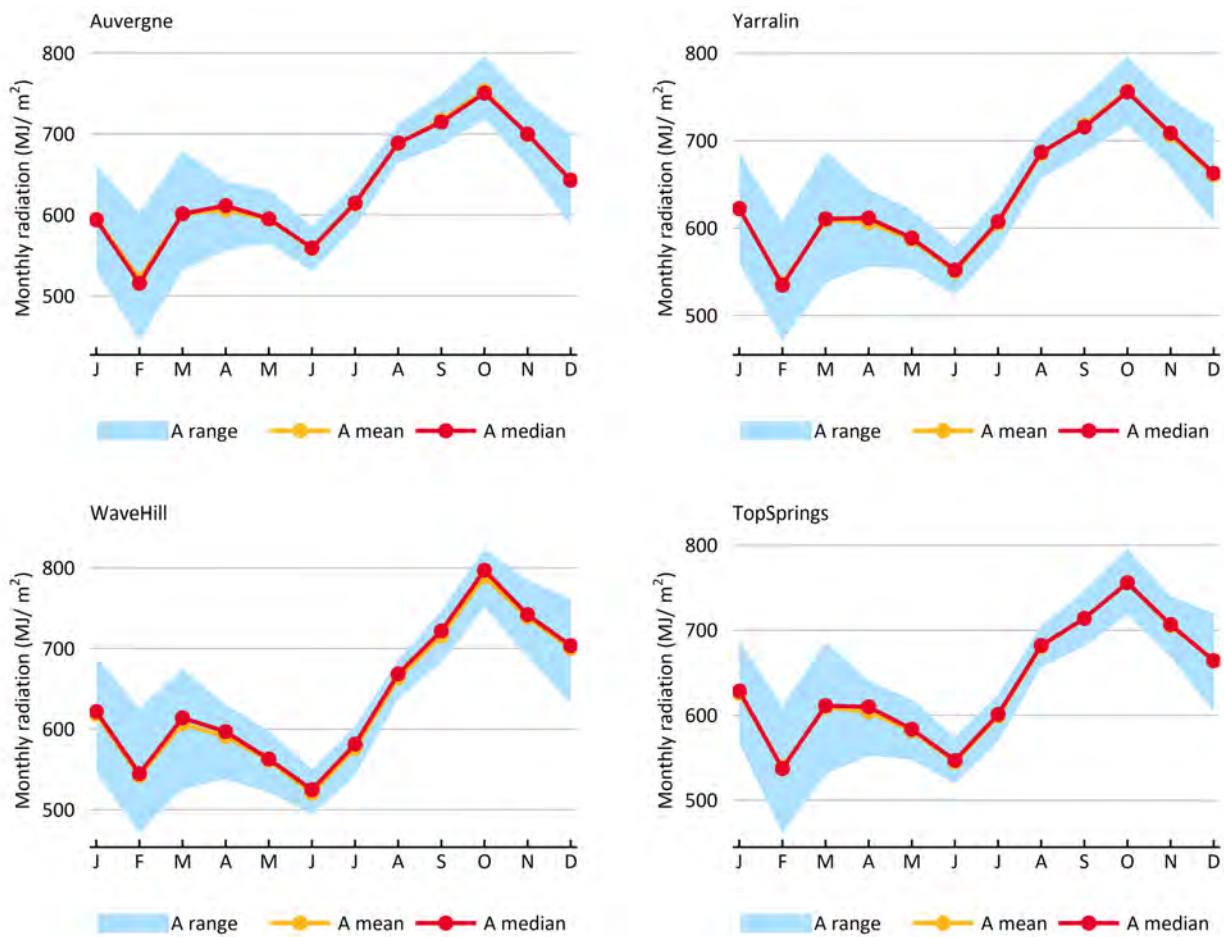


Figure 3-16 Historical monthly radiation in the Victoria catchment at Auvergne, Yarralin, Kalkarindji (Wave Hill) and Top Springs

A range is the 10th to 90th percentile monthly radiation. Note: A mean line is directly under the A median line in these figures.

Relative humidity, fog and dew

Annual relative humidity exceeded in 10, 50 and 90% of years in the Victoria catchment is shown in Figure 3-17. Monthly mean relative humidity at Auvergne, Yarralin, Kalkarindji (Wave Hill) and Top Springs is shown in Figure 3-18. Relative humidity is higher closer to the coast and in the more northerly parts of the catchment. Areas closer to the coast like Timber Creek also experience a larger variation in monthly values than inland locations such as Kalkarindji (Wave Hill) (Figure 3-18).

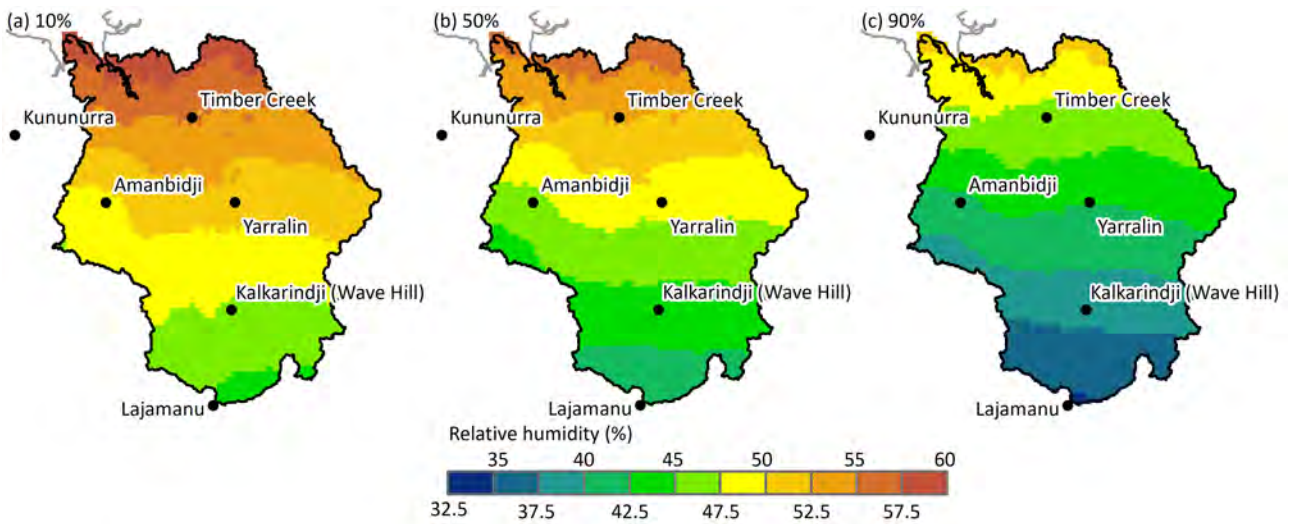


Figure 3-17 Historical annual relative humidity that is exceeded in (a) 10%, (b) 50% and (c) 90% of years in the Victoria catchment

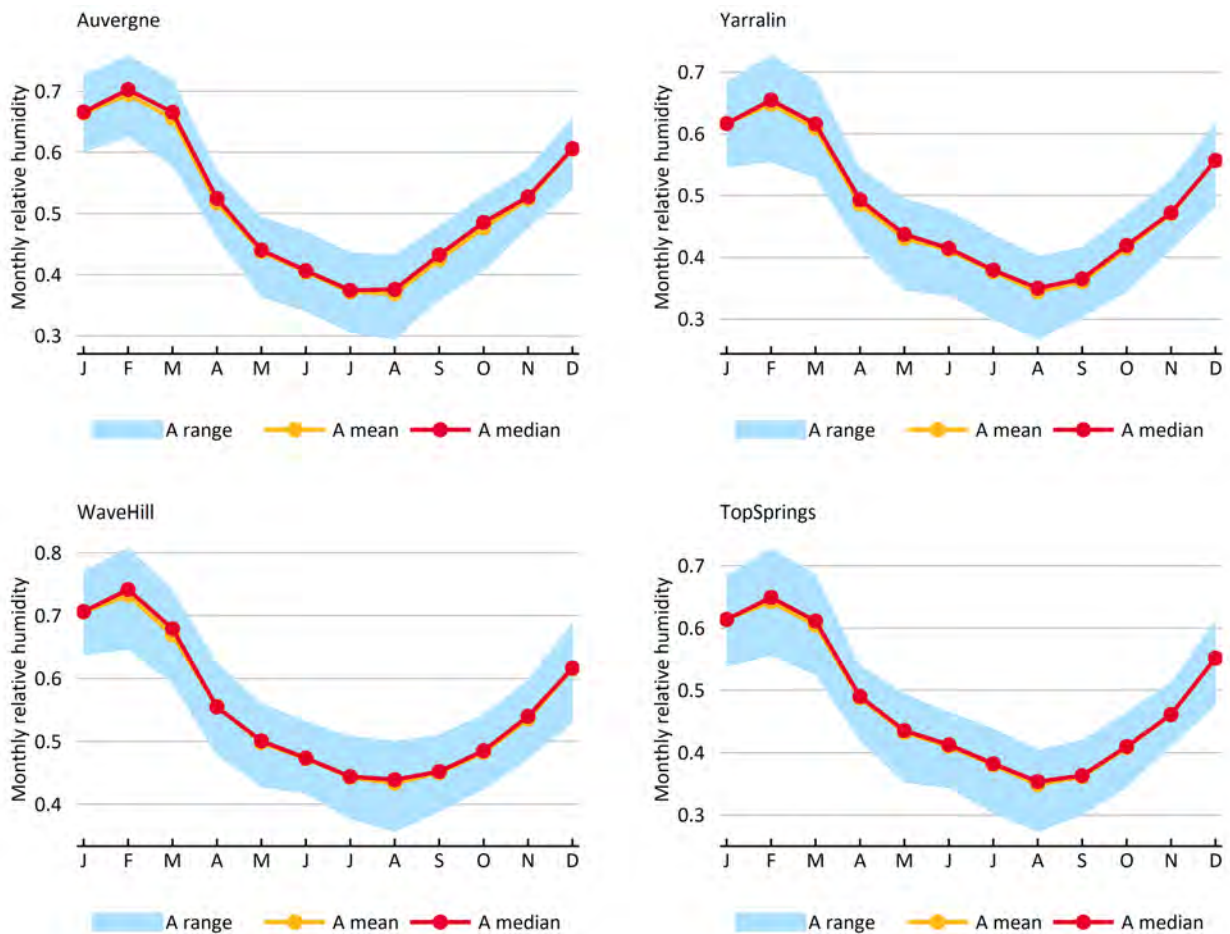


Figure 3-18 Historical monthly relative humidity in the Victoria catchment at Auvergne, Yarralin, Kalkarindji (Wave Hill) and Top Springs

A range is the 10th to 90th percentile monthly relative humidity.

3.2.3 Sea surface temperature

Monthly mean sea surface temperatures (SSTs) for a location off of the Victoria catchment coast (137.1°E, 14.7°S) are shown in Figure 3-19. From December to April the temperature is consistent, close to 30 °C, and then it drops to approximately 27 °C at its lowest point in August.

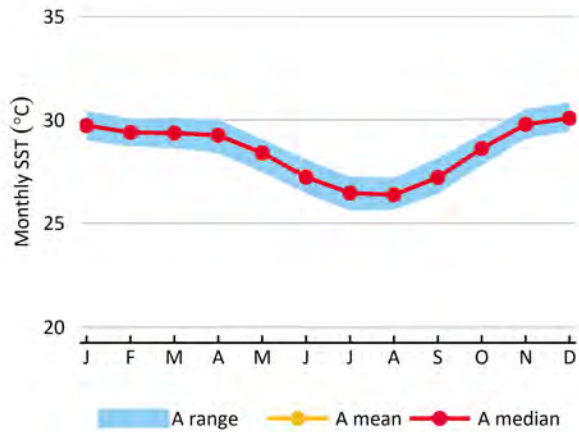


Figure 3-19 Historical monthly SST offshore Victoria catchment

137.1°E, 14.7°S; A range is the 10th to 90th percentile monthly SST for 1970 to 2022 period. Note: A mean line is directly under the A median line in this figure.

Source: <https://psl.noaa.gov/data/gridded/data.noaa.ersst.v5.html>

4 Roper catchment

4.1 Data availability

The Roper catchment's (~77,400 km²) location, major features and relief are shown in Figure 4-1. The distribution of climate stations measuring rainfall and maximum temperature data in the Roper catchment are shown in Figure 4-2 and Figure 4-3. The station density is considerably lower in the Roper catchment, compared to the Murrumbidgee catchment in south-eastern Australia.

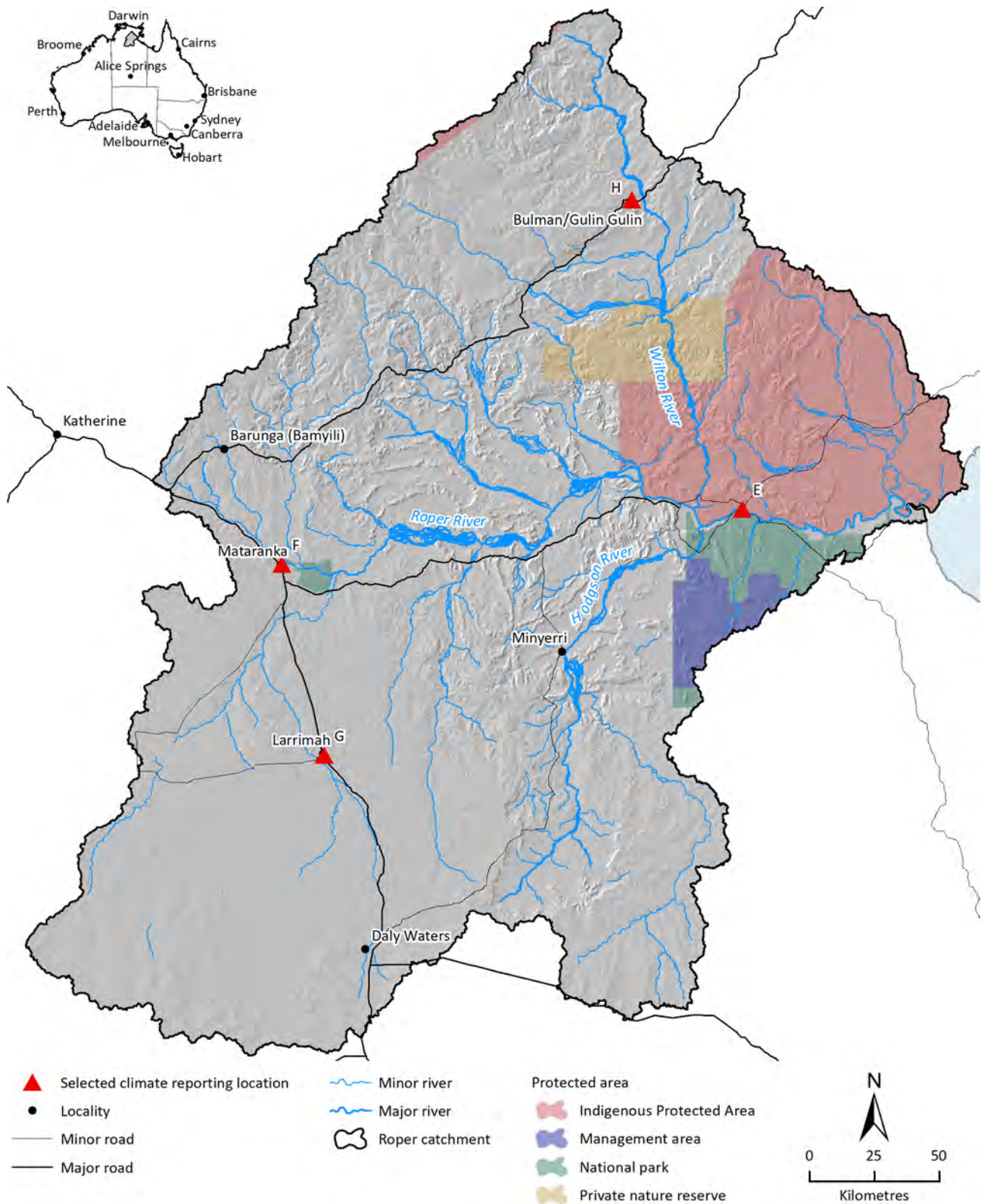


Figure 4-1 A shaded relief map of the Roper catchment

Results are shown later for Ngukurr (E), Mataranka (F), Larrimah (G) and Bulman (H) climate reporting locations.

Source: (Department of Agriculture, Water and the Environment, 2020)

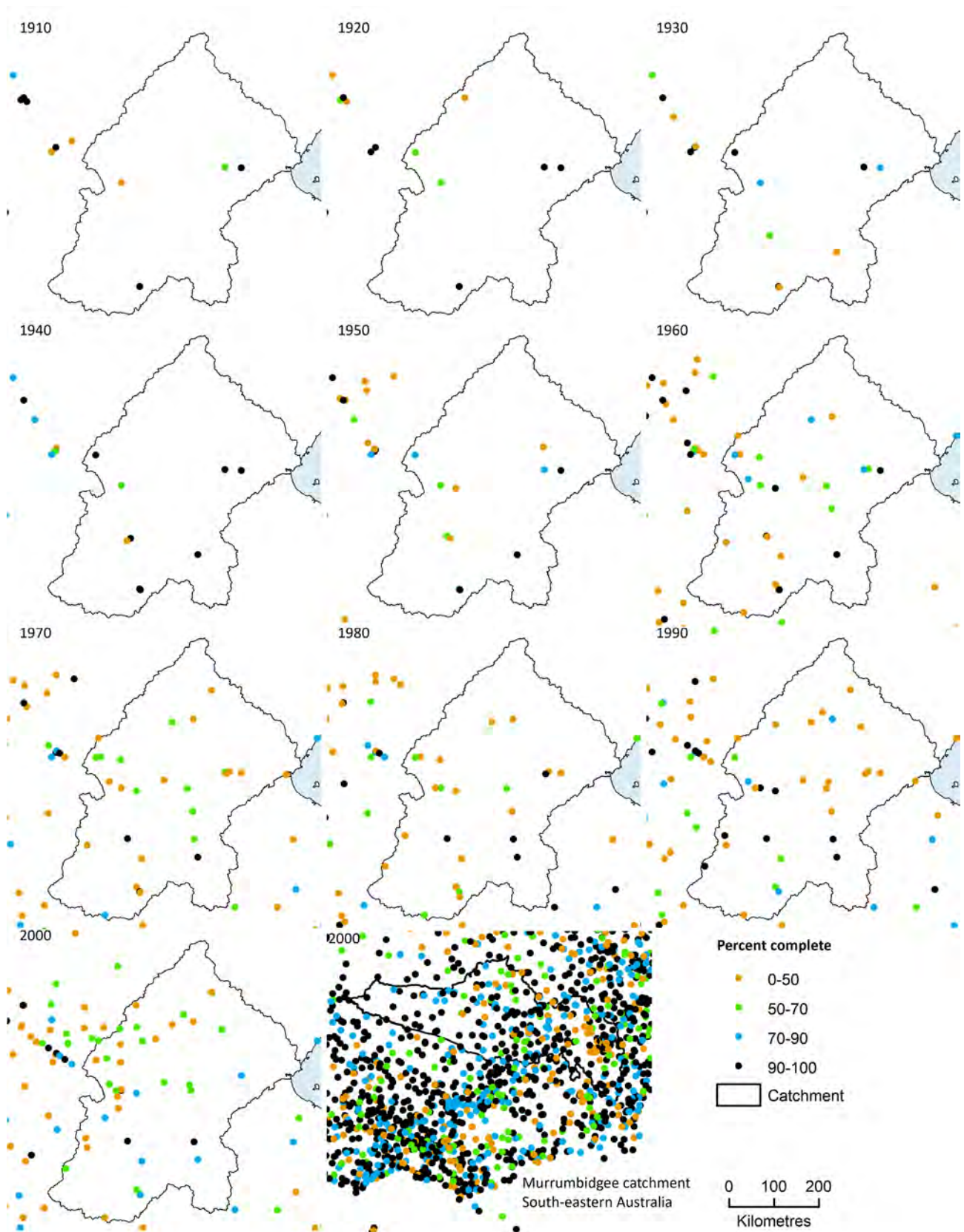


Figure 4-2 Decadal analysis of the location and completeness of Bureau of Meteorology stations measuring daily rainfall used in the SILO database

The decade labelled '1910' is defined from 1 January 1910 to 31 December 1919, and so on. At a station, a decade is 100% complete if there are observations for every day in that decade. The last panel shows the availability of rainfall data in the vicinity of the Murrumbidgee catchment in south-eastern Australia for comparison.

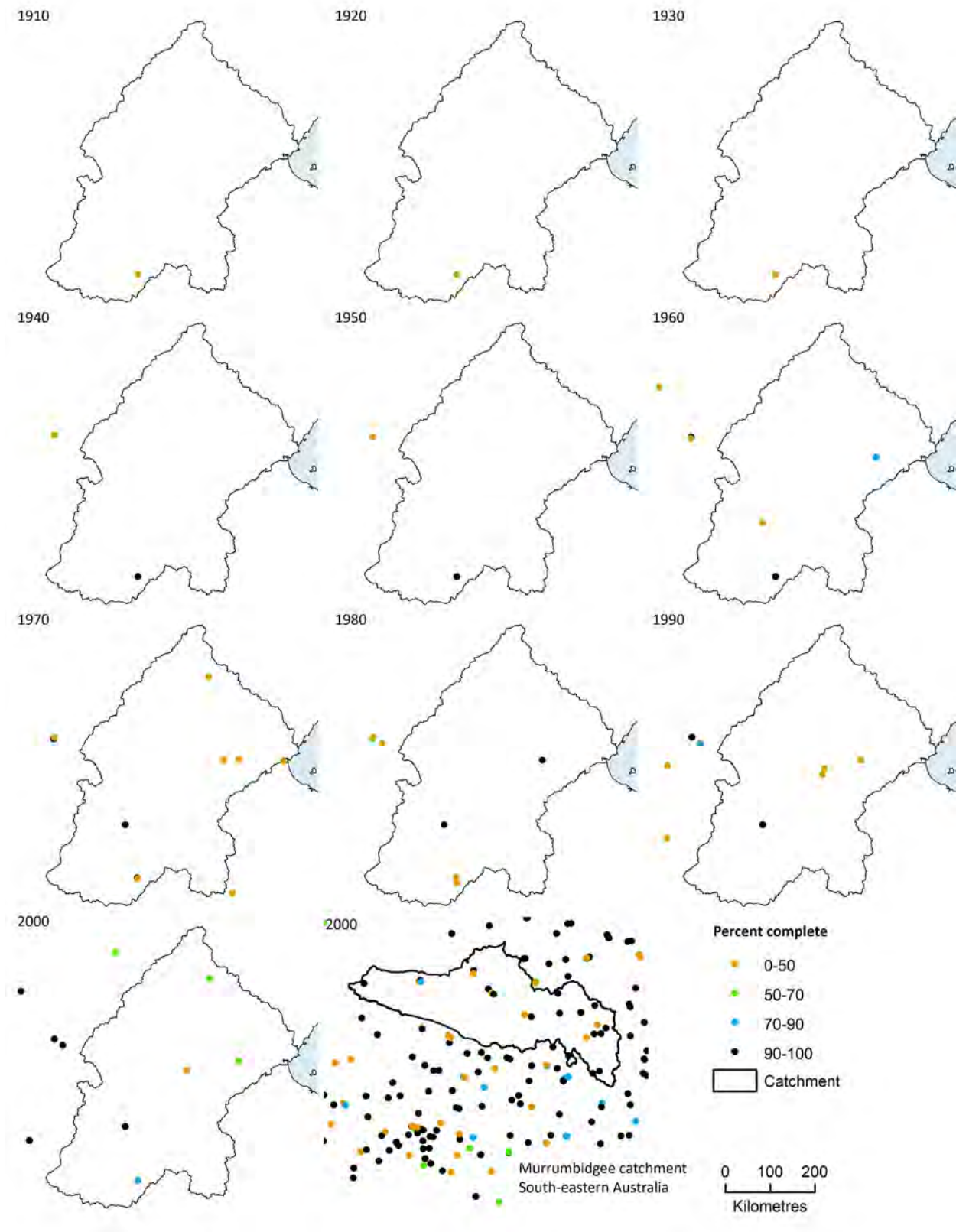


Figure 4-3 Decadal analysis of the location and completeness of Bureau of Meteorology stations in the Roper catchment measuring daily maximum air temperature used in the SILO database

The decade labelled '1910' is defined from 1 January 1910 to 31 December 1919, and so on. At a station, a decade is 100% complete if there are observations for every day in that decade. The last panel shows the availability of maximum temperature data in the vicinity of the Murrumbidgee catchment in south-eastern Australia for comparison.

4.2 Local-scale climate in the Roper catchment

4.2.1 Rainfall

The Roper catchment is characterised by a distinctive wet and dry season due to its location in the Australian summer monsoon belt. The mean annual rainfall, averaged over the Roper catchment for the 109-year historical period (1 September 1910 to 31 August 2019), is 792 mm. Rainfall is highest in the northern part of the catchment and lowest in the southern part (Figure 4-4). This is because the northern zone receives more wet-season rainfall as a result of active monsoon episodes, which are more likely to affect areas closest to the coast. The Roper catchment is flat, and consequently there is no noticeable topographic influence on climate parameters such as rainfall or temperature.

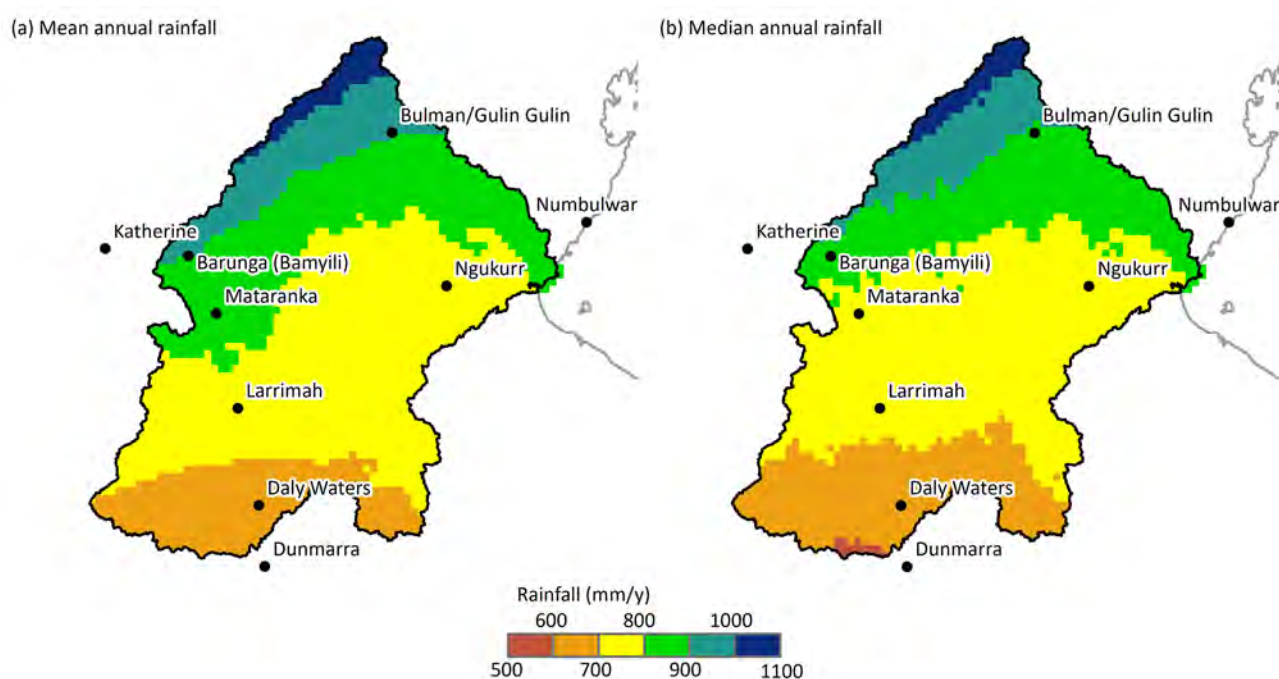
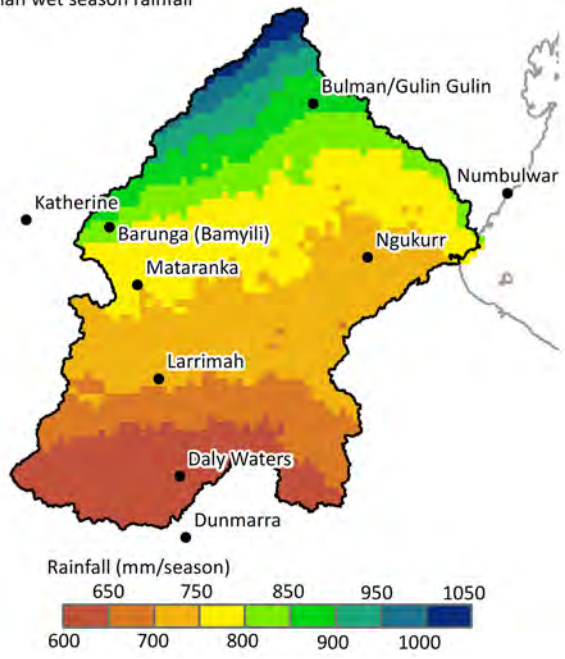


Figure 4-4 Historical (a) mean annual rainfall and (b) median annual rainfall across the Roper catchment

Approximately 96% of rain falls in the Roper catchment during the wet-season months (1 November to 30 April). The spatial distribution of rainfall during the wet and dry seasons is shown in Figure 4-5. Median wet-season rainfall exhibits a very similar spatial pattern to median annual rainfall, while less of a north–south gradient is evident for the dry season. The highest monthly rainfall totals typically occur during January, February and March (Figure 4-6).

The lack of rainfall during the dry season is largely due to the domination of dry continental south-easterlies, and the significant dry air aloft that inhibits shower and thunderstorm formation. During the months where the climate is transitioning to the wet season (i.e. typically mid-September to mid-December) strong sea breezes pump moist air inland, fuelling the steady growth of shower and thunderstorm activity over a period of weeks to months. This can result in highly variable rainfall totals during these months (Figure 4-6).

(a) Median wet season rainfall



(b) Median dry season rainfall

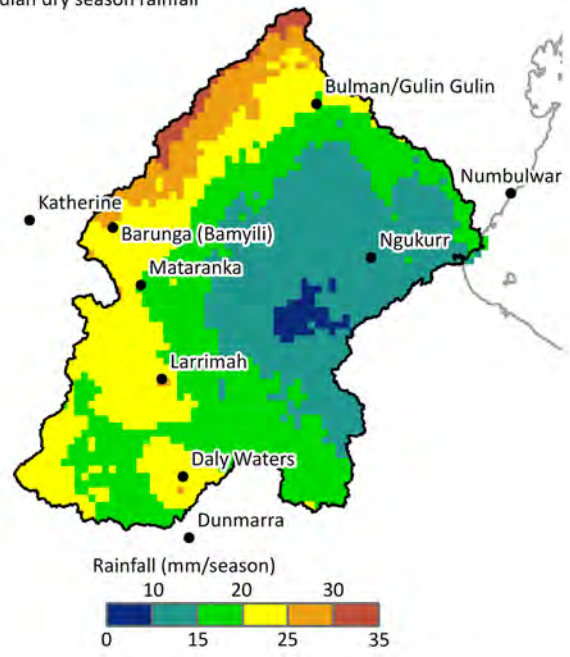


Figure 4-5 Historical median rainfall during the (a) wet and (b) dry season in the Roper catchment

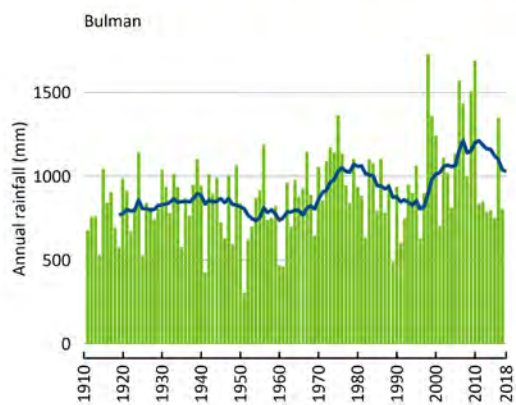
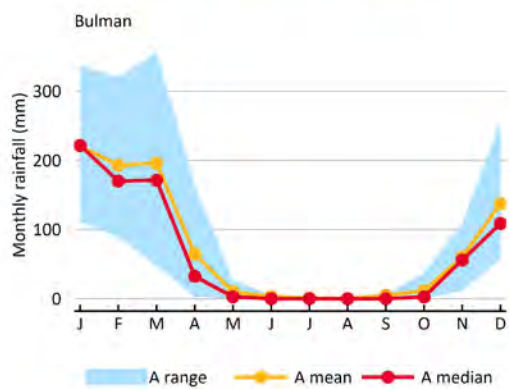
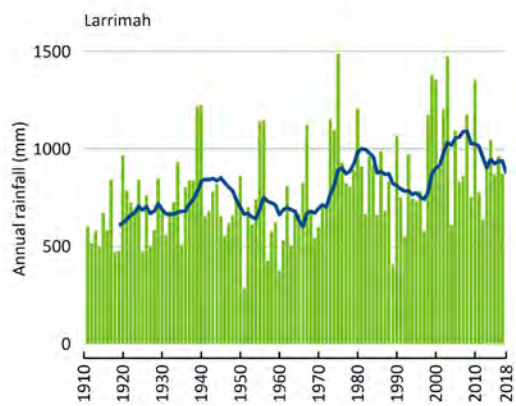
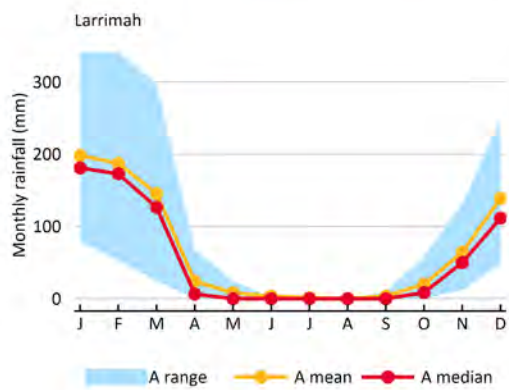
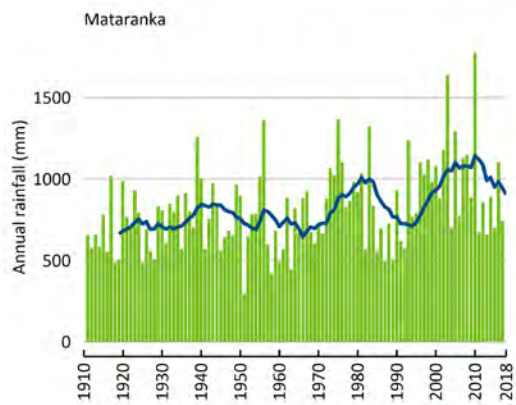
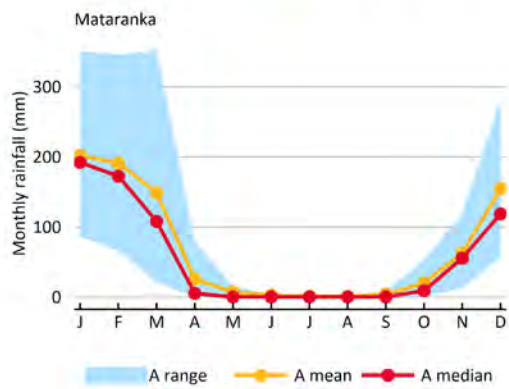
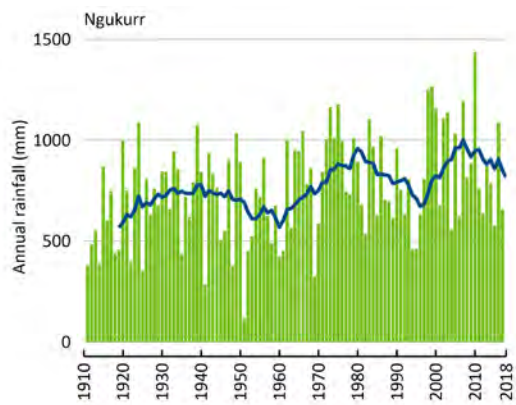
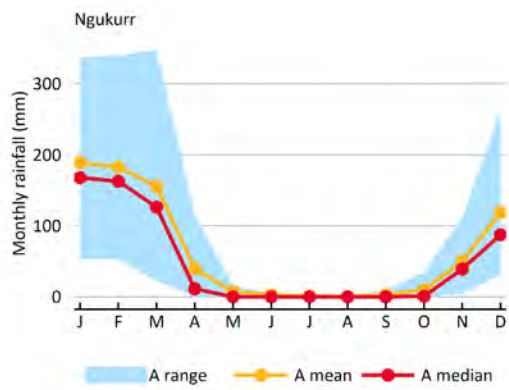


Figure 4-6 Historical monthly rainfall in the Roper catchment at Ngukurr, Mataranka, Larrimah and Bulman
 Left column shows monthly rainfall, right column shows time series of annual rainfall (A range is the 10th to 90th percentile monthly rainfall).

Tropical cyclones

Tropical cyclones (TCs) and tropical lows contribute a considerable proportion of total annual rainfall, but the actual amount is highly variable from one year to the next (Figure 4-7), since TCs do not affect the Roper catchment in more than half of years. For the 53 TC seasons from the 1969–70 to 2021–22 period, 53% of seasons experienced no TCs, 40% one TC, and 8% two. When a TC or low does cross the catchment, typically 200 to 500 mm of rain falls over a 2–5-day period, and daily rainfall totals can exceed 250 mm in coastal areas (Figure 4-8).

Low-level easterly winds

During the build-up to the wet season, continental convection prevails in the Roper catchment and is triggered by sea breeze circulations. It is characterised by light winds and isolated shower and thunderstorm activity, sometimes with gusty squall lines. During this time easterly winds deliver moist air from the Gulf of Carpentaria to the land and the number of convective elements in the region peaks, particularly in the early afternoon. This results in short-lived thunderstorm activity under favourable conditions (Pope et al., 2008). The northern part of the Roper catchment is closer to the Gulf of Carpentaria and is more strongly influenced by this kind of rain.

Low-level westerly winds

In northern Australia, distinct variations in the rainfall distribution pattern are observed and these are modulated by the phase of the monsoon and the location of the MJO. Prevailing winds are usually from the east or southeast for most of the year, but during active monsoon periods (December to March) the winds shift to become north westerly at the surface. Depending on the strength of the monsoon burst, westerly flow can be shallow or deep. Shallow westerly flow is associated with early morning thunderstorms along the coast. During an active monsoon, cloud cover is more widespread, and rain and thunderstorms can be heavy and powerful due to the high moisture content of the atmosphere. Thunderstorms may also persist for longer. During these periods, the lack of surface heating due to increased cloud cover results in suppressed afternoon convection.

Severe thunderstorms and tornadoes

Severe thunderstorms and tornadoes are two other features associated with localised rainfall in the Roper catchment. Severe thunderstorms can occur in the region at any time of year, however they are much more likely during the wet season (October to April). Severe thunderstorms occur most frequently during the build-up months, prior to the onset of the north Australian monsoon, or during break periods of the monsoon. Climatologically, November is the most active month for severe thunderstorms. In the southern parts of the region severe thunderstorms are most likely to occur whenever tropical moisture extends southwards and especially in the presence of vertical wind shear. Tornadoes may form in thunderstorms embedded near intensifying tropical lows or ex-tropical cyclones over land.

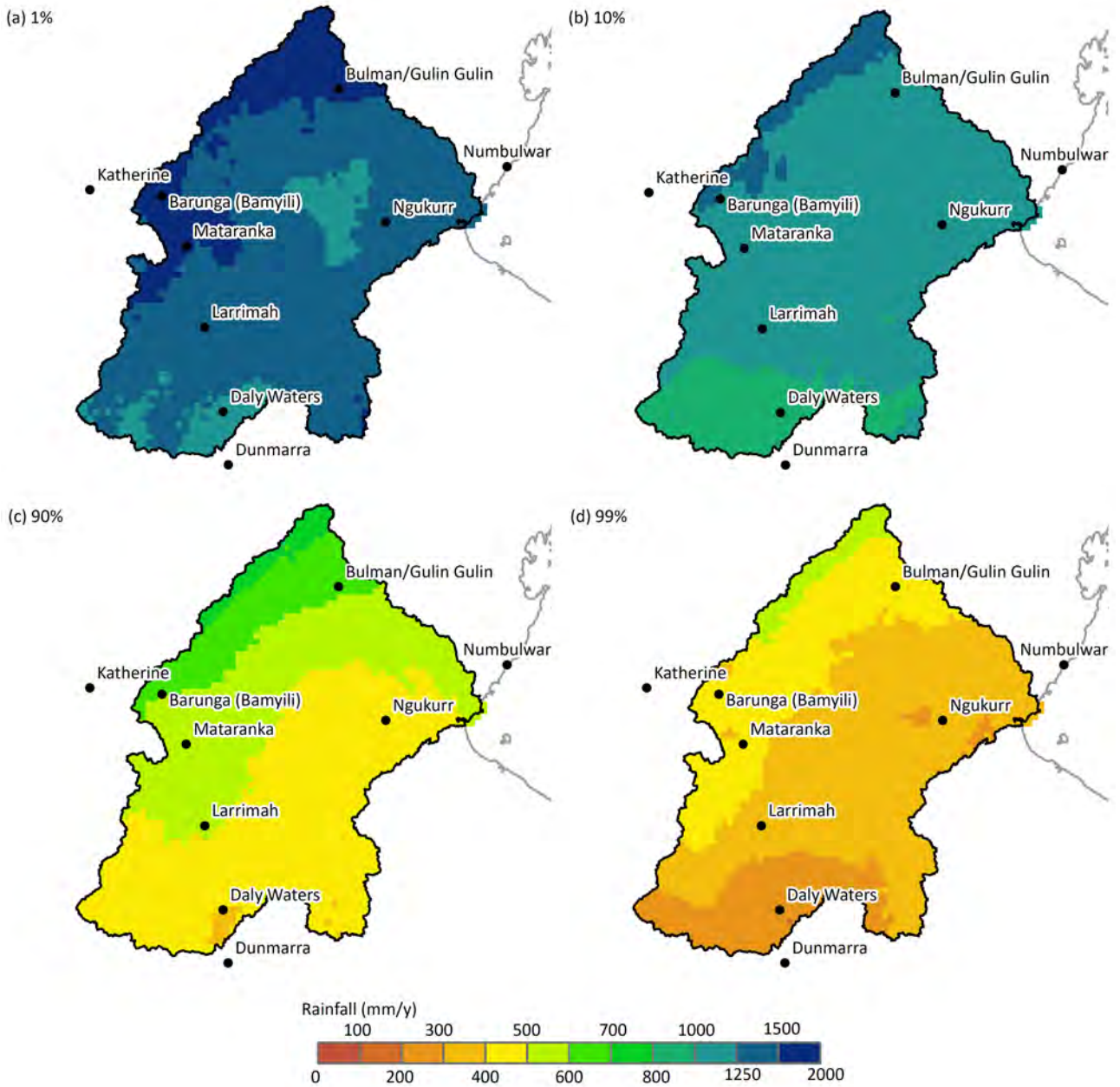


Figure 4-7 Historical annual rainfall that was exceeded in (a) 1%, (b) 10%, (c) 90% and (d) 99% of years in the Roper catchment

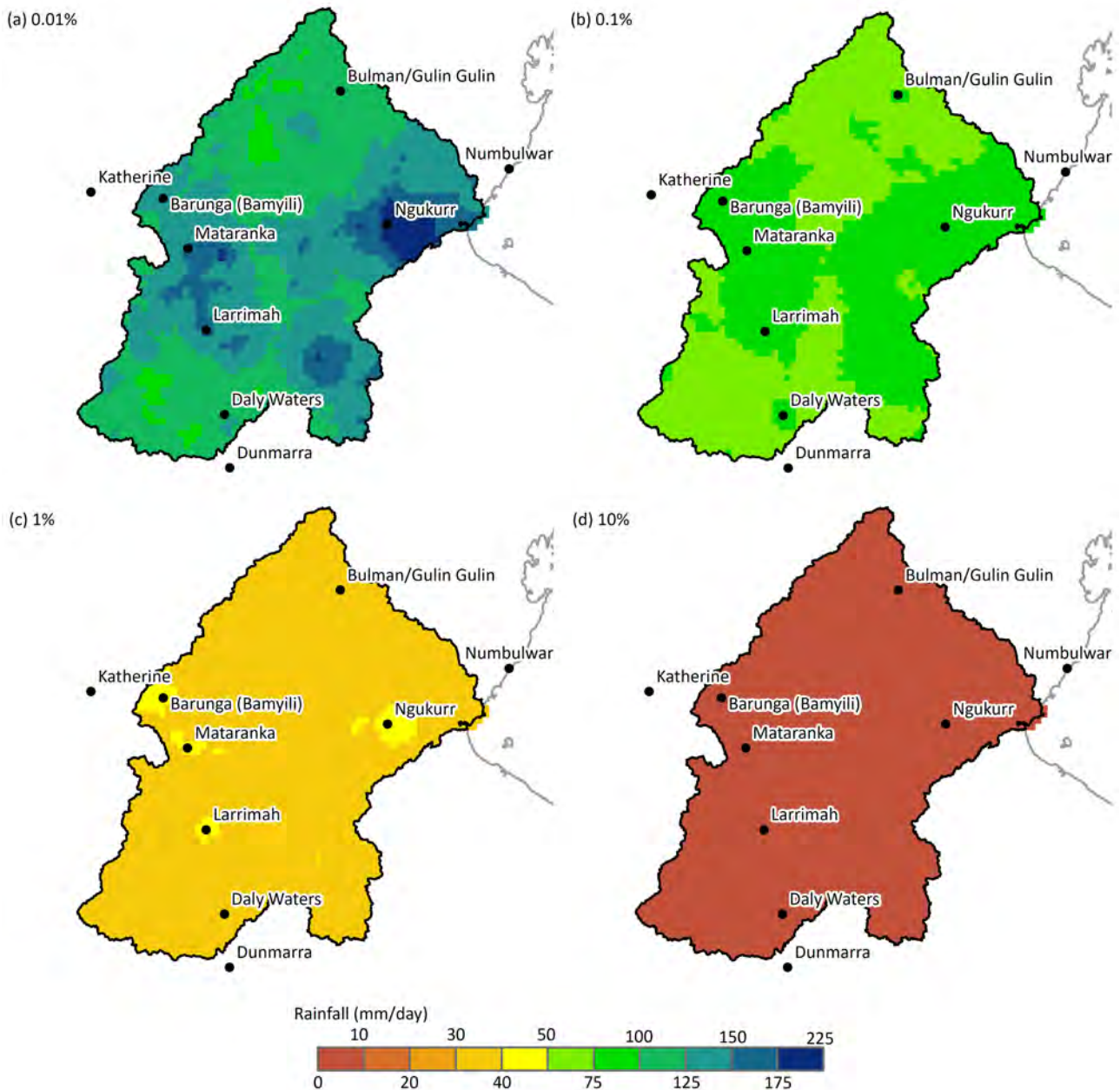


Figure 4-8 Historical daily rainfall that is exceeded in (a) 0.01%, (b) 0.1%, (c) 1% and (d) 10% of days in the Roper catchment

4.2.2 Other climate parameters

Potential evaporation

Areal potential evaporation (APE) (as calculated using Morton's areal wet potential) in the Roper catchment exceeds 1800 mm in most years (Figure 4-9). Evaporation is high all year round, but exhibits a strong seasonal pattern, ranging from about 200 mm per month during the October 'build-up' to about 120 mm per month during the middle of the dry season (June) (Figure 4-9). The high mean annual potential evaporation (PE) and moderate mean annual rainfall result in a large

mean annual rainfall deficit across most of the catchment (Figure 4-10). Consequently, a large proportion of the catchment is semi-arid.

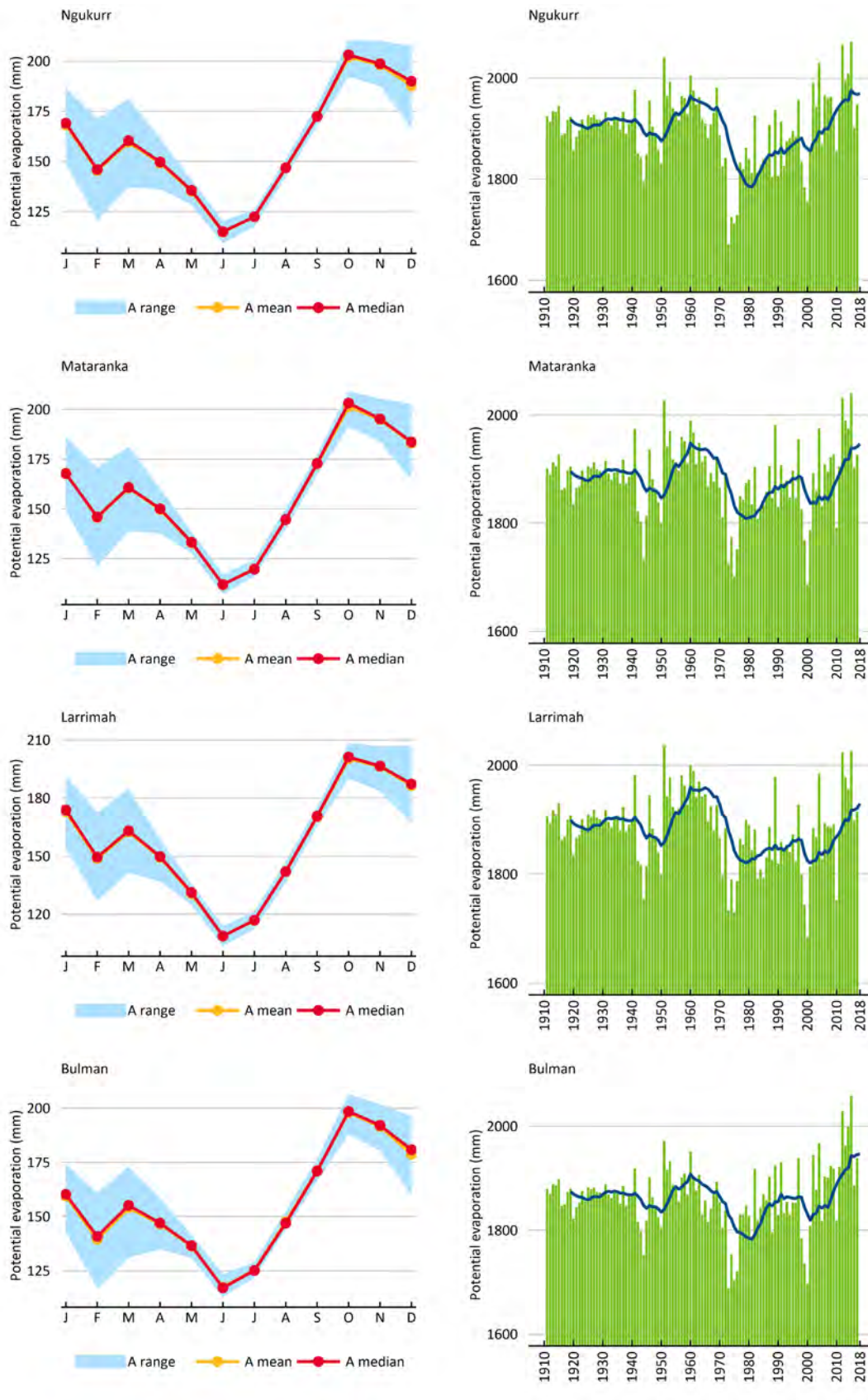


Figure 4-9 Historical potential evaporation in the Roper catchment at Ngukurr, Mataranka, Larrimah and Bulman Left column shows monthly PE, right column shows time series of annual PE (A range is the 10th to 90th percentile monthly rainfall). Note: A mean line is directly under the A median line in these figures.

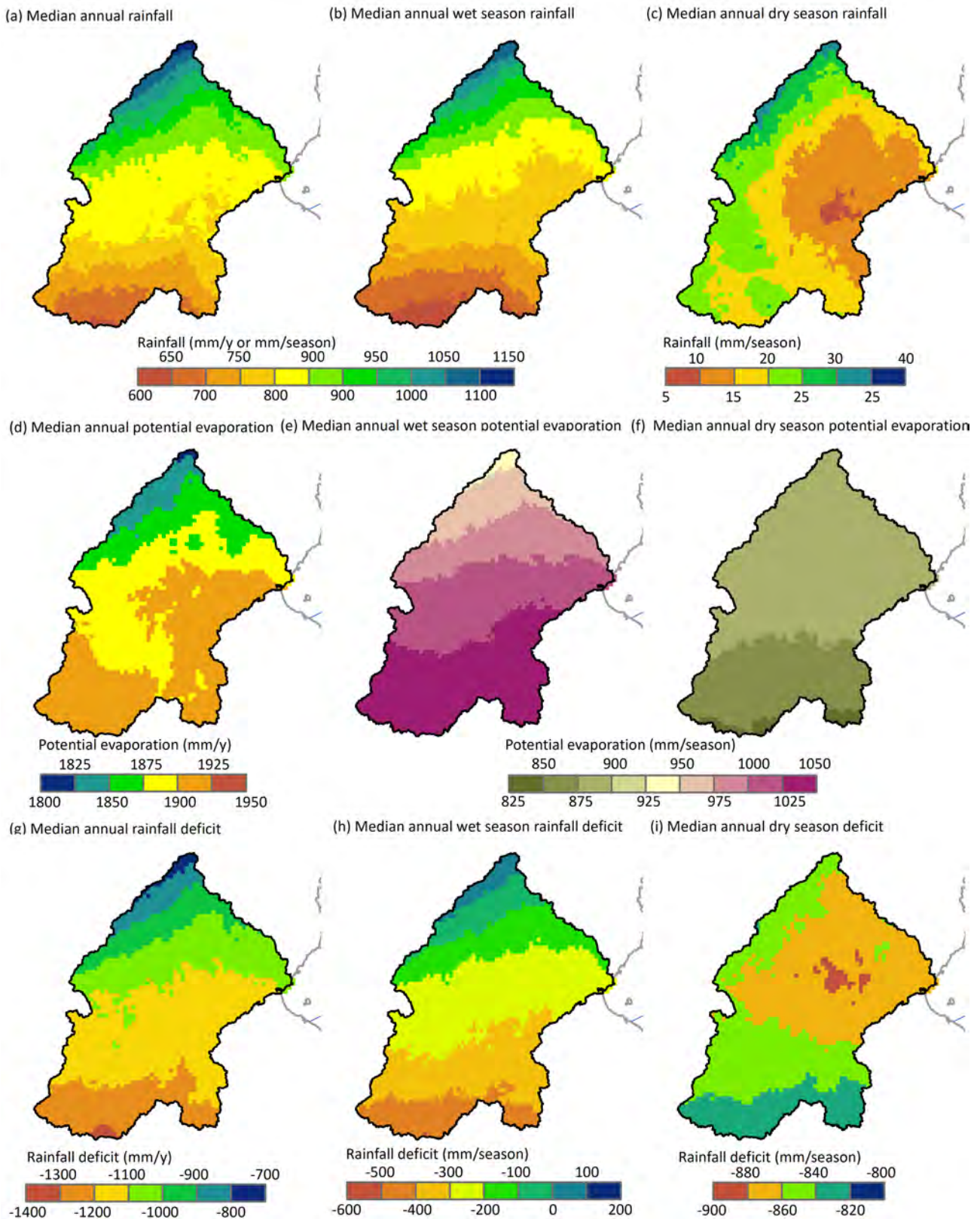


Figure 4-10 Historical median (a) annual, (b) wet-season, (c) dry-season rainfall; (d) annual, (e) wet-season, (f) dry-season potential evaporation; and (g) annual, (h) wet-season and (i) dry-season rainfall deficit in the Roper catchment

Maximum and minimum temperatures

The highest mean monthly maximum temperatures occur in October and November and the lowest mean monthly minimum temperatures occur in July. Diurnal range is largest in winter (June to August, Figure 4-11).

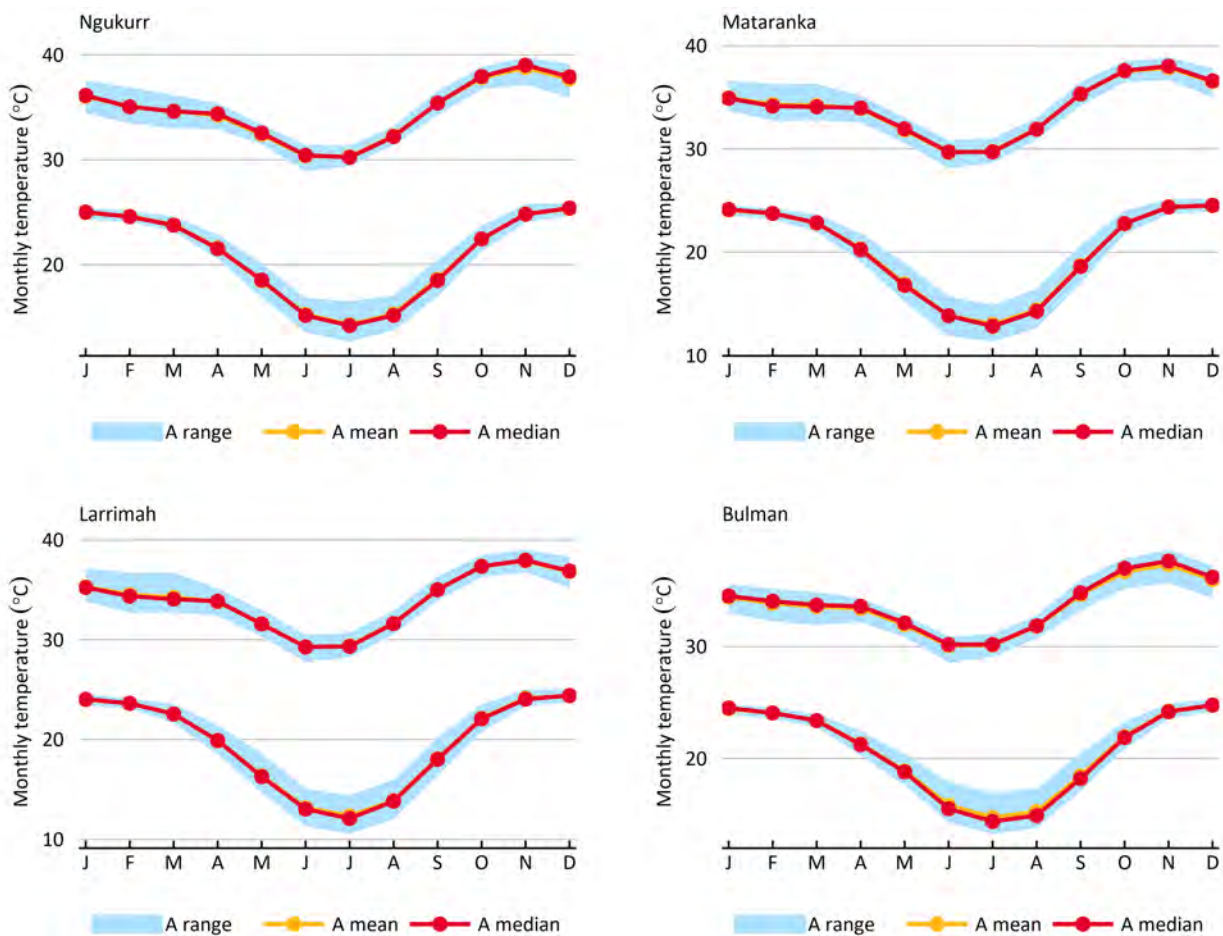


Figure 4-11 Historical maximum and minimum air temperature in the Roper catchment at Ngukurr, Mataranka, Larrimah and Bulman

A range is the 10th to 90th percentile monthly rainfall. Note: A mean line is directly under the A median line in these figures.

Figure 4-12 shows the maximum annual temperature that is exceeded in 10, 50 and 90% of years. Maximum temperatures are particularly important at sensitive stages of crop growth. Figure 4-13 shows the minimum annual temperature that is exceeded in 10, 50 and 90% of years. The highest maximum annual temperatures and the lowest minimum annual temperatures occur in the southern part of the Roper catchment.

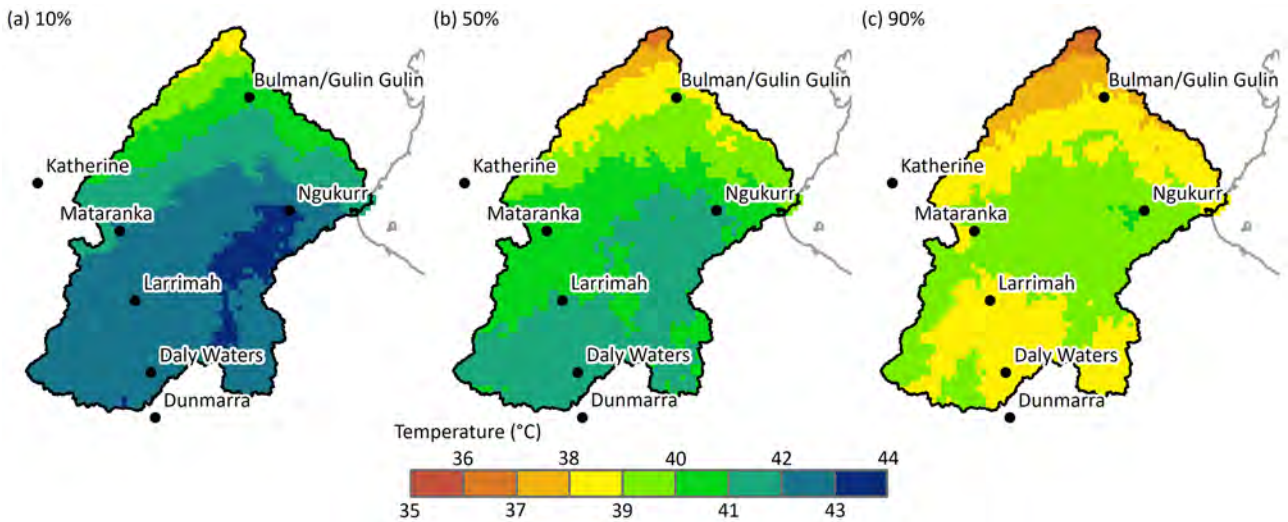


Figure 4-12 Historical maximum air temperature that is exceeded in (a) 10%, (b) 50% and (c) 90% of years in the Roper catchment

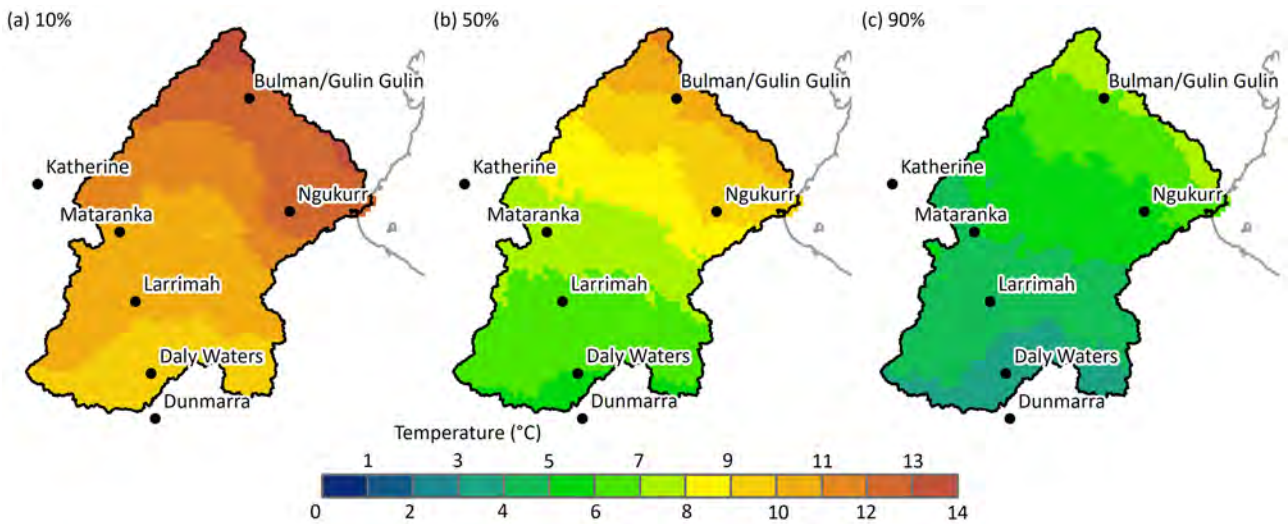


Figure 4-13 Historical minimum air temperature that is exceeded in (a) 10%, (b) 50% and (c) 90% of years in the Roper catchment

Frost hollows are virtually non-existent in the Roper catchment, with minimum temperatures rarely going below 5 °C (Figure 4-14).

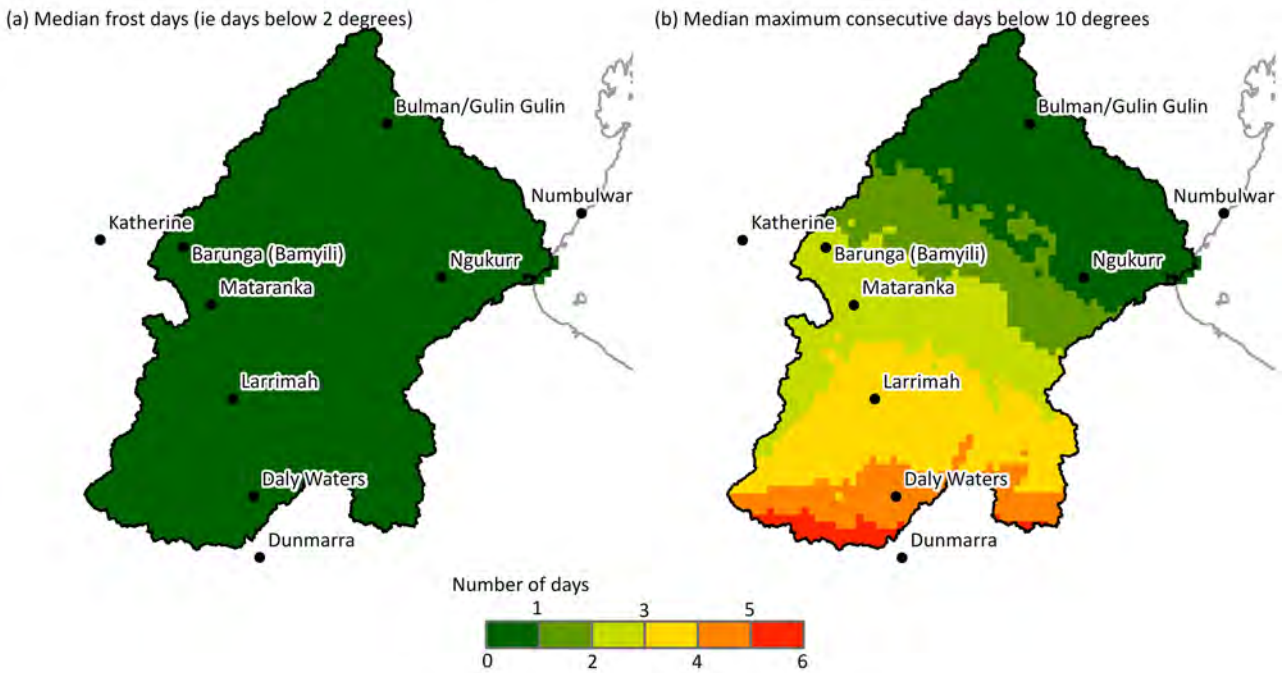


Figure 4-14 Historical minimum temperature thresholds in the Roper catchment
 (a) Median annual frost days (i.e., days below 2 °C); and (b) median annual maximum consecutive days below 10 °C.

Solar radiation

Mean annual radiation exceeded in 10, 50 and 90% of years in the Roper catchment is shown in Figure 4-15, with the lower radiation in the north related to cloud cover. Monthly mean radiation at Ngukurr, Mataranka, Larrimah and Bulman is shown in Figure 4-16, showing a maximum in October during the build-up, wet-season reductions due to cloud cover (November-February, in particular), with annual minimum in February lower than the solar minimum of June.

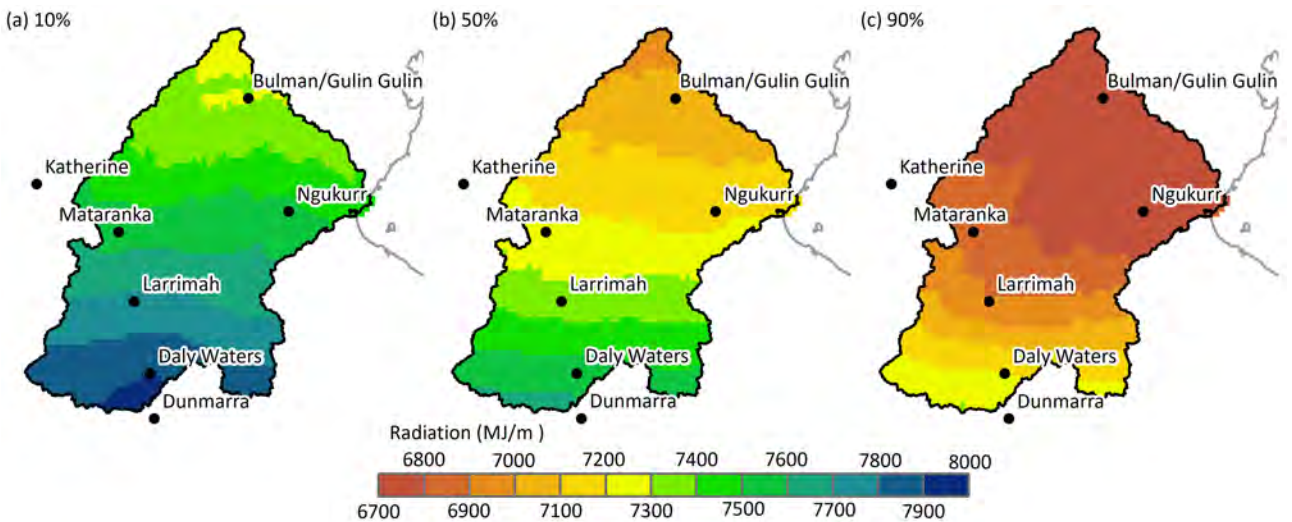


Figure 4-15 Historical annual radiation that is exceeded in (a) 10%, (b) 50% and (c) 90% of years in the Roper catchment

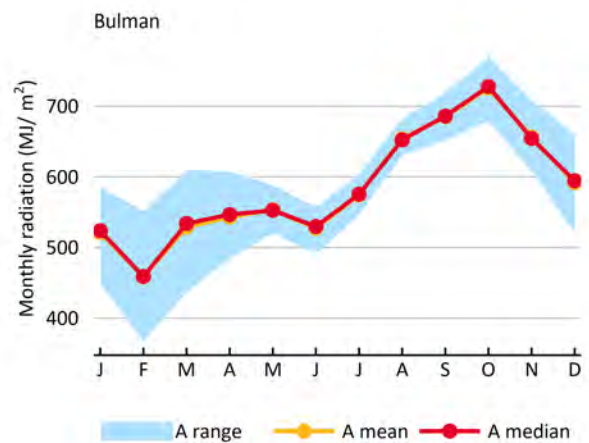
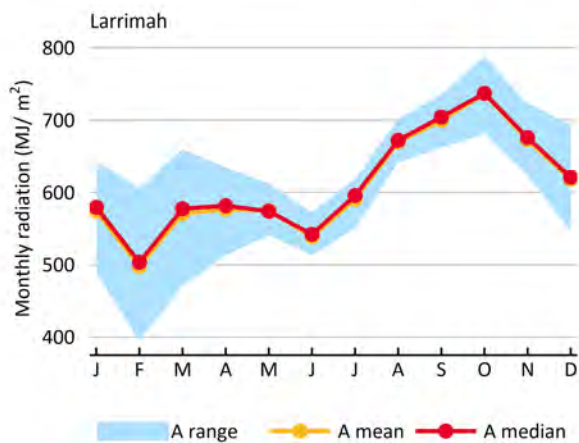
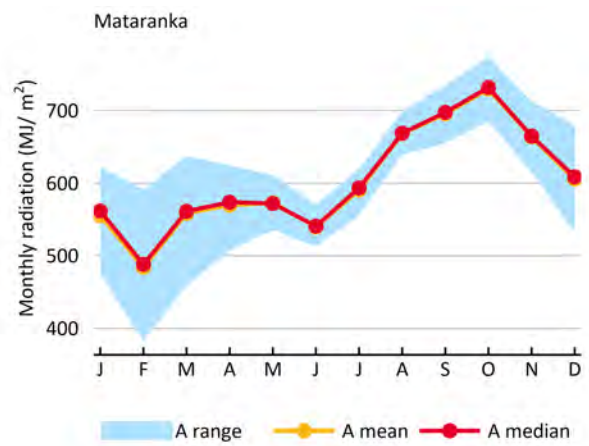
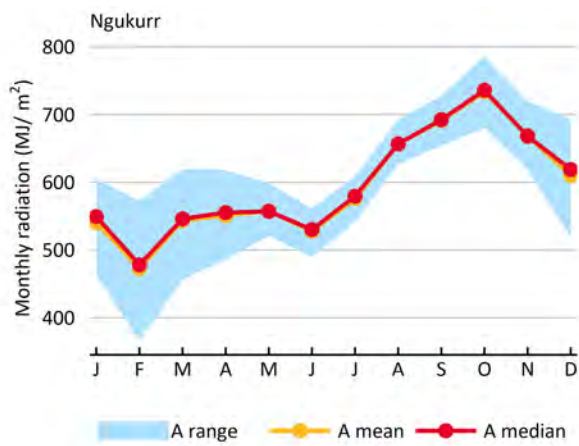


Figure 4-16 Historical monthly radiation in the Roper catchment at Ngukurr, Mataranka, Larrimah and Bulman
 A range is the 10th to 90th percentile monthly rainfall. Note: A mean line is directly under the A median line in these figures.

Relative humidity, fog and dew

Annual relative humidity exceeded in 10, 50 and 90% of years in the Roper catchment is shown in Figure 4-17. Monthly mean relative humidity at Ngukurr, Mataranka, Larrimah and Bulman is shown in Figure 4-18. Relative humidity decreases from the north to the south across the Roper catchment. Northern areas like Bulman experience a larger variation in monthly values in the dry season than inland locations such as Daly Waters (Figure 4-18).

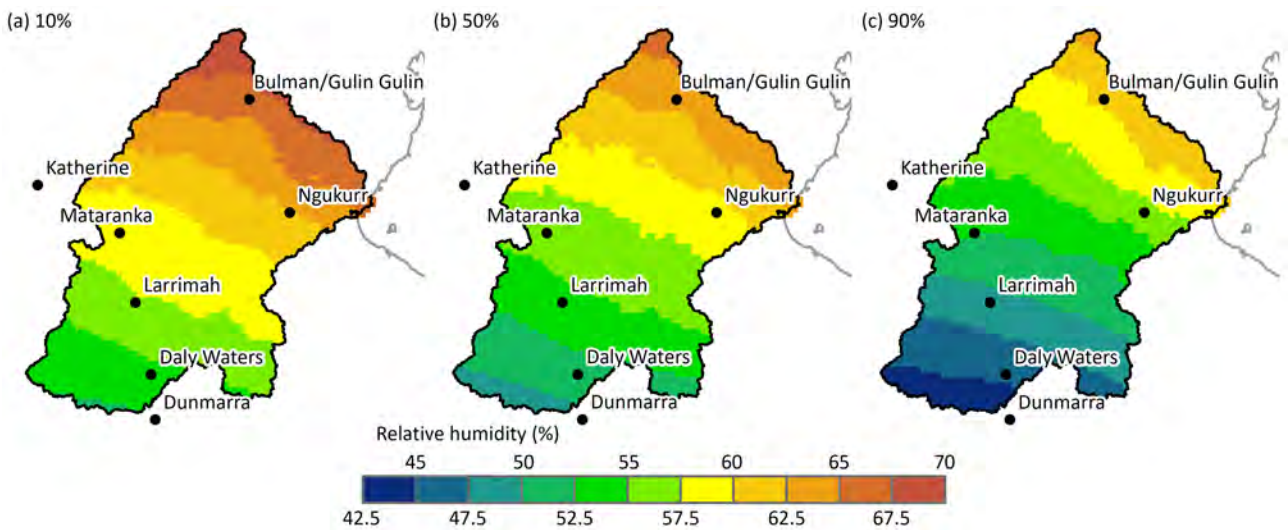


Figure 4-17 Historical annual relative humidity that is exceeded in (a) 10%, (b) 50% and (c) 90% of years in the Roper catchment

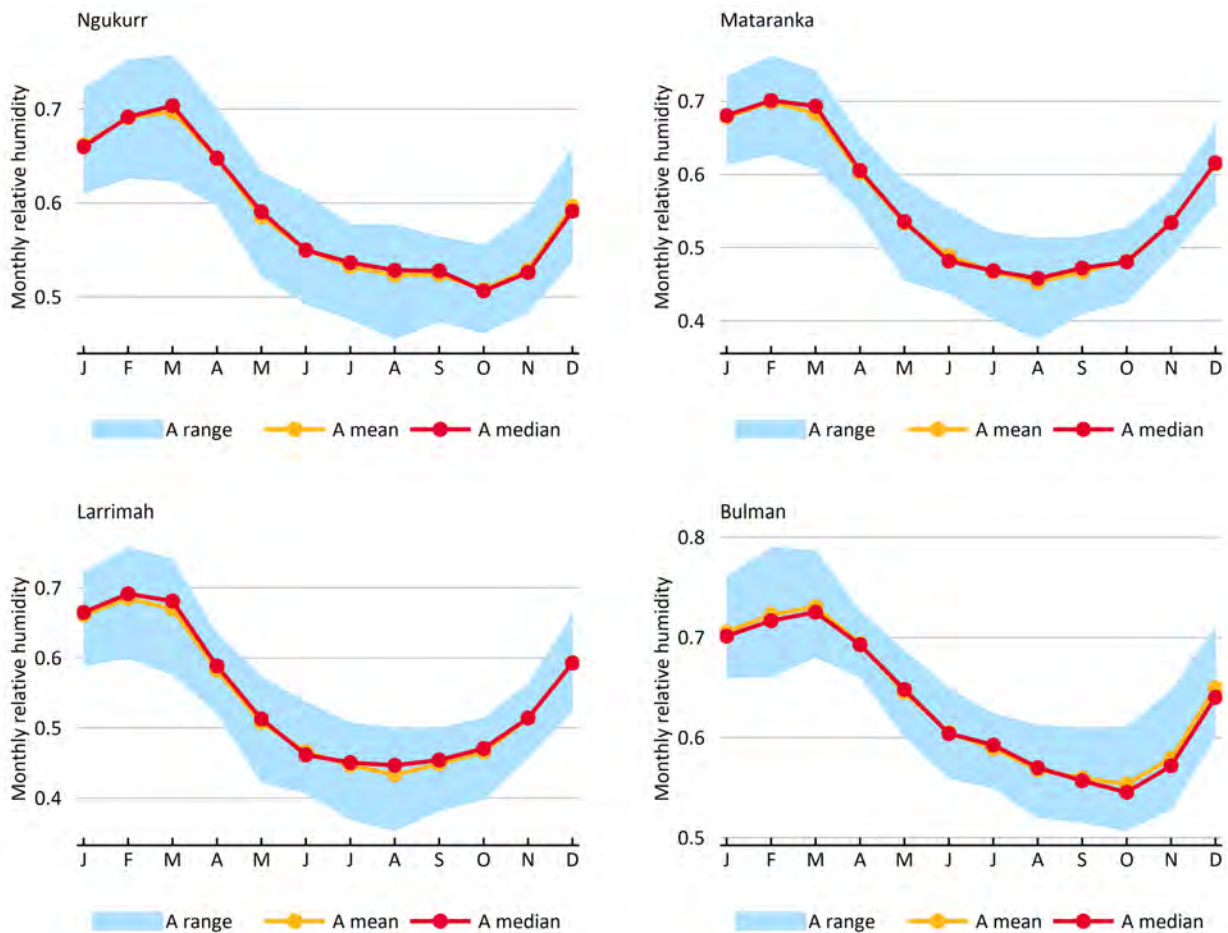


Figure 4-18 Historical monthly relative humidity in the Roper catchment at Ngukurr, Mataranka, Larrimah and Bulman

A range is the 10th to 90th percentile monthly rainfall. Note: A mean line is directly under the A median line in these figures.

4.2.3 Sea surface temperatures

Monthly mean sea surface temperatures (SSTs) for a location off of the Roper catchment coast (137°E, 14.7°S) are shown in Figure 4-19. The strong seasonal cycle is evident, with constant warm seas (29 °C) throughout the wet season (November to April) dropping to around 25 °C in mid-winter (July and August).

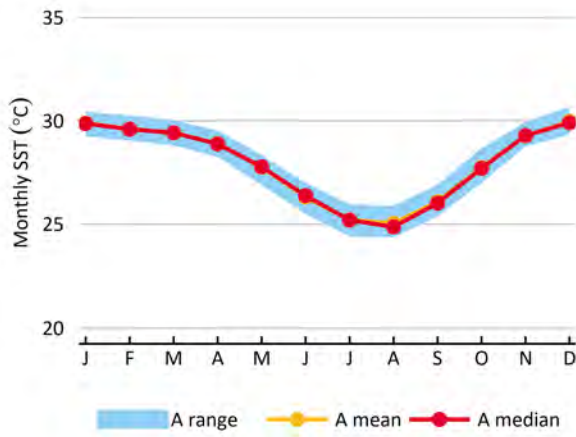


Figure 4-19 Historical monthly SST offshore Roper catchment

137°E, 14.7°S; A range is the 10th to 90th percentile monthly SST for 1970 to 2022 period. Note: A mean line is directly under the A median line in this figure.

Source: <https://psl.noaa.gov/data/gridded/data.noaa.ersst.v5.html>

5 Southern Gulf catchments

5.1 Data availability

The Southern Gulf catchments' (~109,440 km²) location, major features and relief are shown in Figure 5-1. The distributions of rainfall and maximum temperature data are shown in Figure 5-2 and Figure 5-3, respectively. There are considerably fewer stations measuring rainfall and maximum temperature in the Southern Gulf catchments, compared to the comparably sized Murrumbidgee catchment in south-eastern Australia (~84,000 km²).

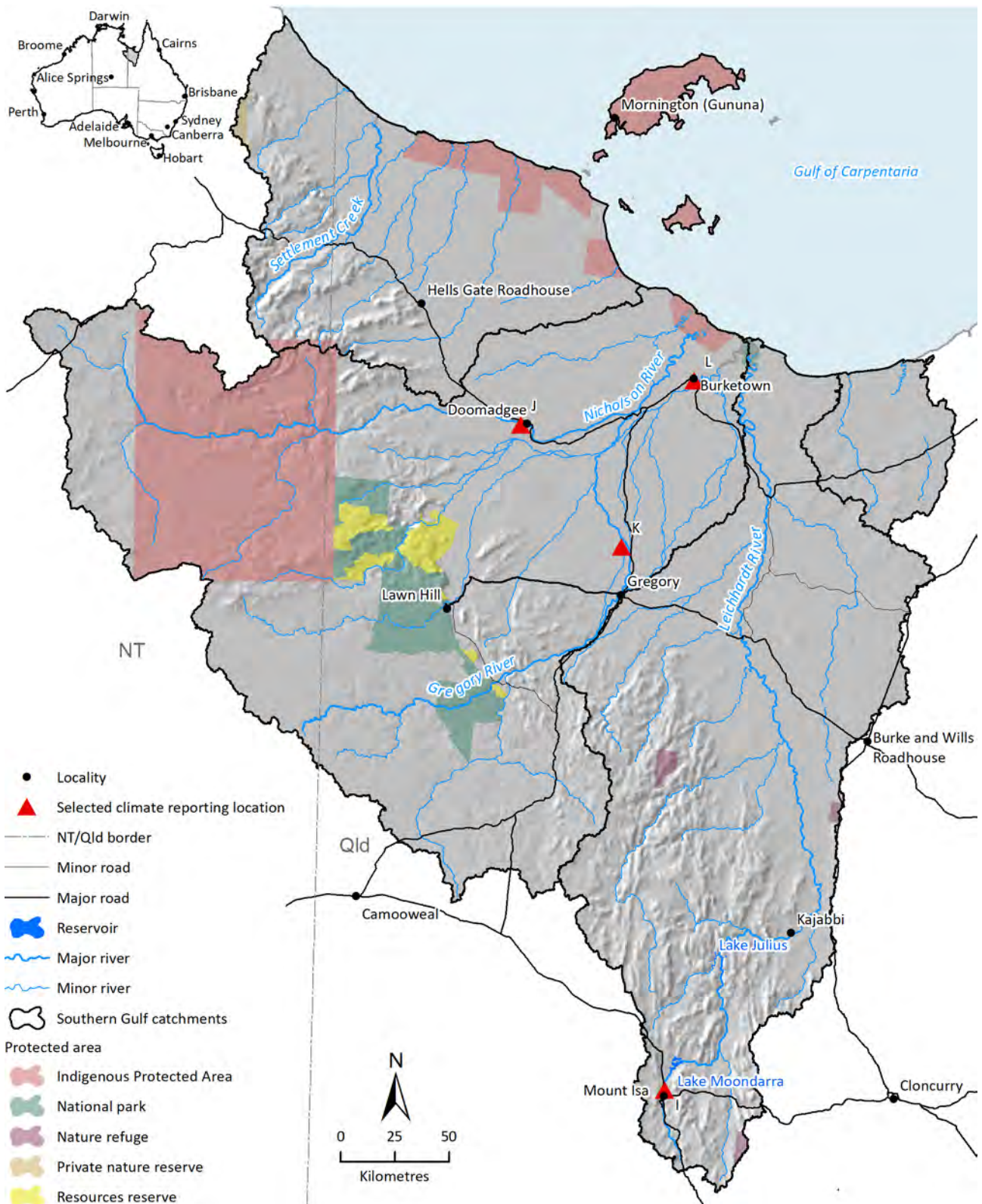


Figure 5-1 A shaded relief map of the Southern Gulf catchments

Results are shown later for Mount Isa (I), Doomadgee (J), Gregory (K) and Burketown (L) climate reporting locations.

Source: (Department of Agriculture, Water and the Environment, 2020)

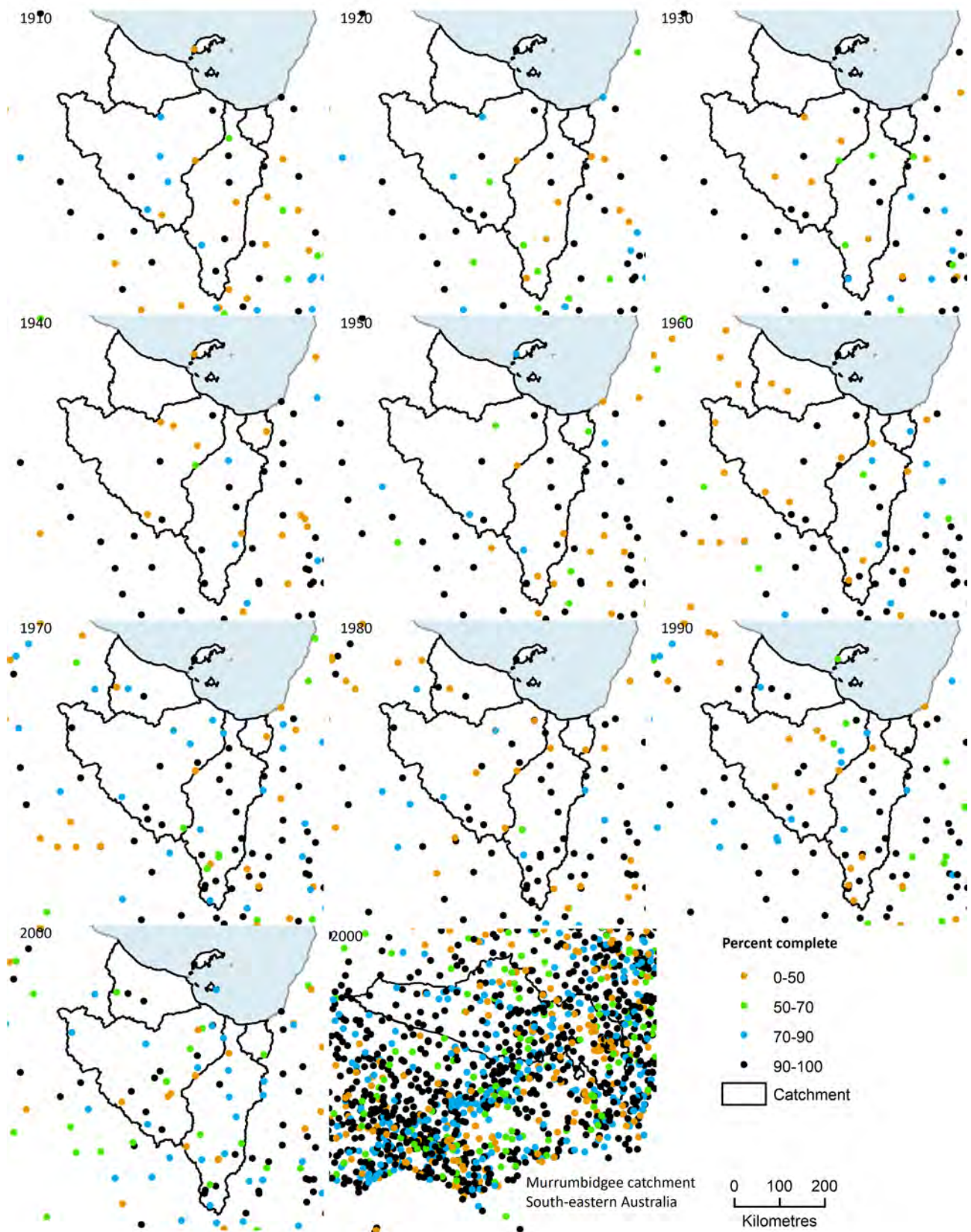


Figure 5-2 Decadal analysis of the location and completeness of Bureau of Meteorology stations in the Southern Gulf catchments measuring daily rainfall used in the SILO database

The decade labelled '1910' is defined from 1 January 1910 to 31 December 1919, and so on. At a station, a decade is 100% complete if there are observations for every day in that decade. The last panel shows the availability of rainfall data in the vicinity of the Murrumbidgee catchment in south-eastern Australia for comparison.

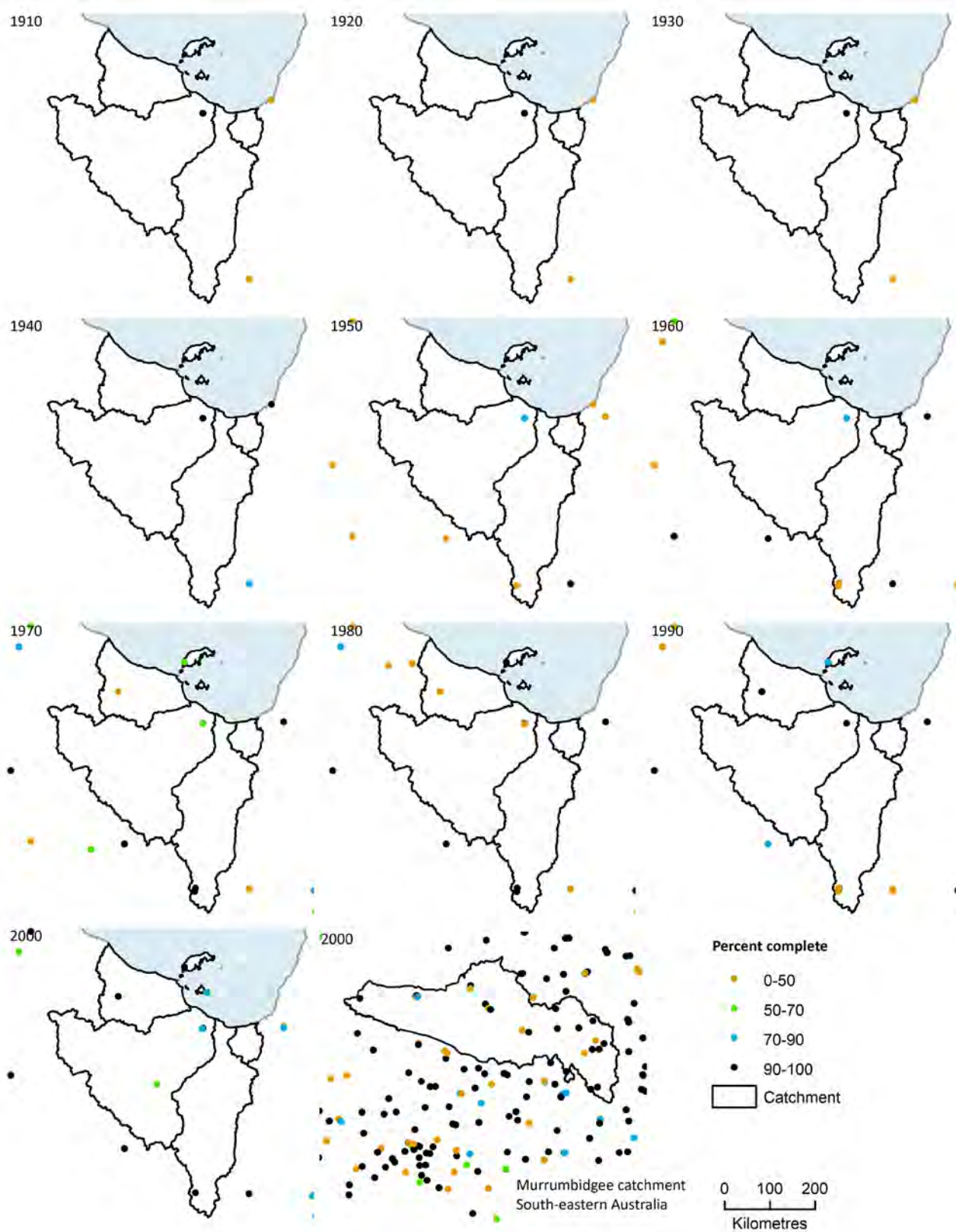


Figure 5-3 Decadal analysis of the location and completeness of Bureau of Meteorology stations in the Southern Gulf catchments measuring daily maximum air temperature used in the SILO database

The decade labelled '1910' is defined from 1 January 1910 to 31 December 1919, and so on. At a station, a decade is 100% complete if there are observations for every day in that decade. The last panel shows the availability of maximum temperature data in the vicinity of the Murrumbidgee catchment in south-eastern Australia for comparison.

5.2 Local-scale climate in the Southern Gulf catchments

5.2.1 Rainfall

The Southern Gulf catchments are characterised by a distinctive wet and dry season due to their location in the northern Australia tropics. The mean annual rainfall, averaged over the Southern Gulf catchments for the 132-year historical period (1 September 1890 to 31 August 2022), is 602 mm. Rainfall totals are highest near the coast and decline in a southerly direction (Figure 5-4).

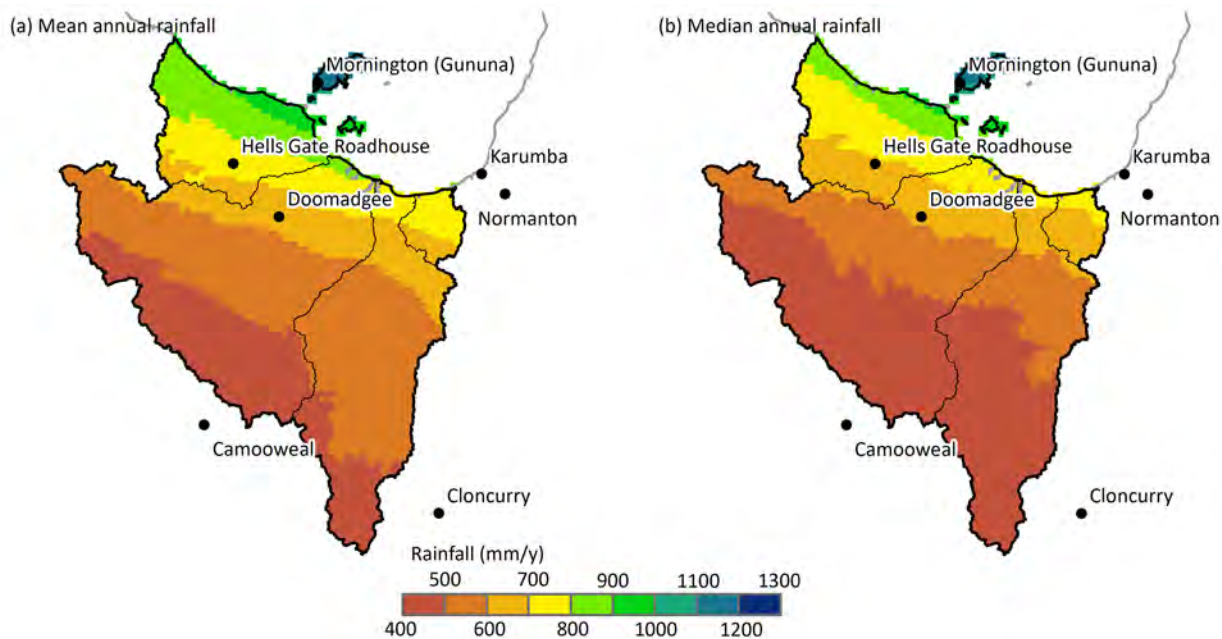


Figure 5-4 Historical (a) mean annual rainfall and (b) median annual rainfall in the Southern Gulf catchments

In the Southern Gulf catchments about 94% of rain falls during the wet-season months (1 November to 30 April). The spatial distribution of rainfall during the wet and dry seasons is shown in Figure 5-5. Median wet-season rainfall exhibits a similar spatial pattern to median annual rainfall. Median dry-season rainfall is highest in the most southern part of the Leichhardt catchment and lowest near the coast (Figure 5-5). Mean and median annual rainfall is highest near the coast primarily due to monsoonal activity, which generates significant rainfall during the wet season. The highest rainfall totals typically occur during January and February (Figure 5-6).

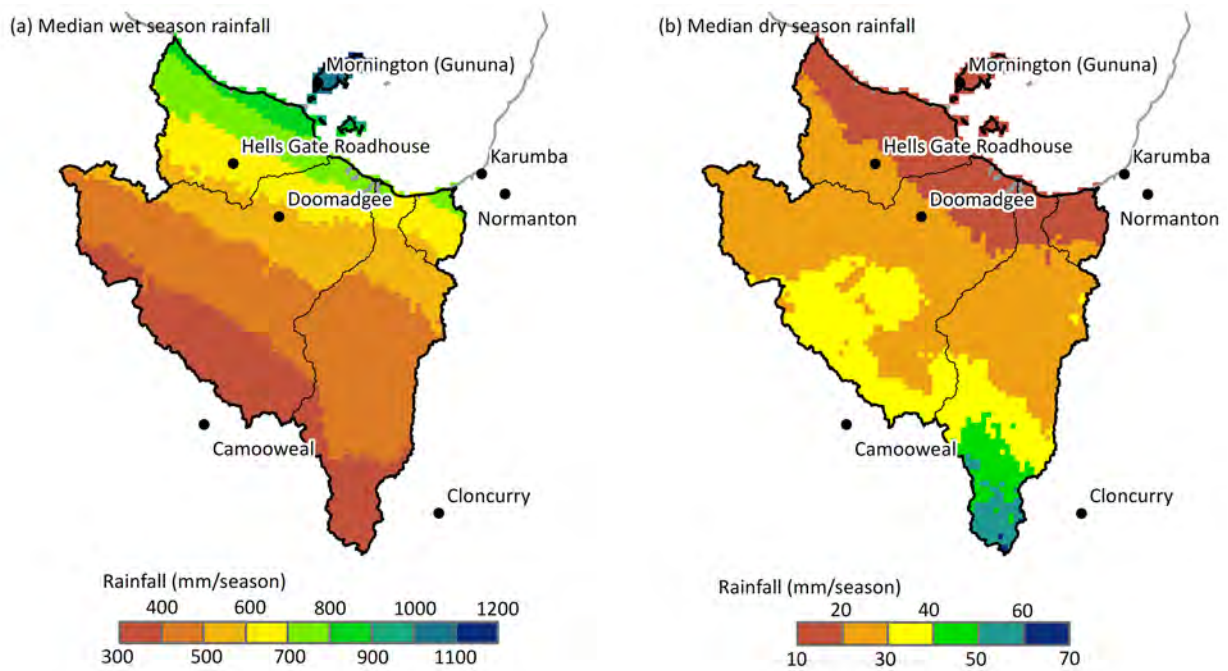


Figure 5-5 Historical median rainfall during the (a) wet and (b) dry season in the Southern Gulf catchments

Tropical cyclones

Tropical cyclones (TCs) and lows contribute large quantities of rainfall over the Southern Gulf catchments in some years (Figure 5-7) and result in high daily rainfall values (Figure 5-8). Increased rainfall as well as storm surge and increased wind speeds are associated with TCs. The cyclone season in the Southern Gulf catchments falls between November and April, and for the 53 TC seasons from the 1969–70 to 2021–22 period, 60% of seasons experienced no TCs, 36% one TC, and 4% two.

Diurnal storm activity

Over inland areas of the Southern Gulf catchment, storms form more frequently during the afternoon because of increased air temperature which enhance instability and leads to convective cloud formation. Therefore, during the build-up months, inland areas have an increased chance of afternoon storms. Storms form more readily near the heat trough that is a semi-permanent feature over inland Queensland (predominantly located south of the catchment) during late spring and summer months. There is also a high incidence of thunderstorms in the Southern Gulf catchments where sea breeze convergence/boundaries act as a trigger. Thunderstorms show a strong diurnal variation, with most occurring during the afternoon and early evening. Dynamic forcing can cause thunderstorms to develop or persist well beyond the normal diurnal cycle, and if the dynamics are strong enough thunderstorms can occur at any time.

Sea breeze convergence

In the Southern Gulf catchments, convection and rain from sea breeze convergence typically occurs just inland from the coast from early afternoon in the warmer months. Rain can continue overnight and into the following morning if conditions are favourable, particularly if there is a moisture feed from a strong easterly nocturnal jet stream. During the day, the air over land warms and rises, resulting in lower pressure at the surface. Air flows from the Gulf of Carpentaria waters

towards the land to fill this area of lower pressure resulting in the sea breeze which can converge with the usually south-easterly synoptic winds. During the wet season, the convergence of persistent easterly winds and broader synoptic north-westerly winds over the Gulf of Carpentaria results in convergence which may trigger storms over the coast after sunset. This phenomenon is most pronounced in the near-coastal areas of the catchment.

Gulf Lines

The Gulf of Carpentaria region experiences frequent formation of long cloud lines, some of which bring significant weather to northern Australia. Cloud lines typically form over Cape York Peninsula in the late afternoon or evening then travel westward. Thunderstorms can form from these cloud lines if the air mass is unstable and these storms are propagated westwards by mid-level easterly winds which are synoptically driven by high pressure systems to the south (Goler et al., 2006). Showers and storms associated with these cloud lines can continue for 24 hours or more, tracking westwards across northern Australia before dissipating over the Timor Sea. Precipitation associated with these cloud lines is most likely to occur over the Southern Gulf catchments during the morning.

Cloud lines are common in the prevailing easterly regime over the north Australian tropics in all months of the year but are absent during periods of strong monsoon westerly flow. There are many forms of these cloud lines, some of which are more likely to trigger rainfall than others, but the most famous is the "Morning Glory". This is the local name for a low-level wind surge, which moves west over the southern Gulf of Carpentaria and adjacent coast during the night and early morning at certain times of the year. The leading edge of the surge is often accompanied by a spectacular roll-cloud, but rainfall from this cloud is rare.

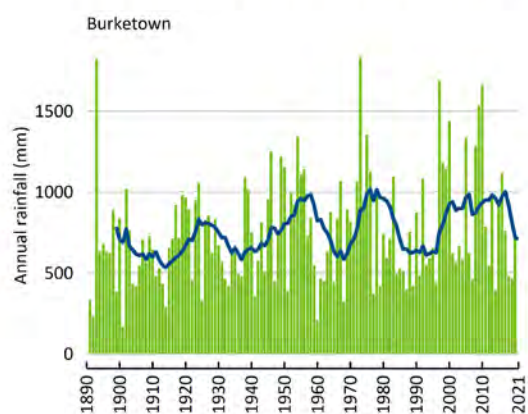
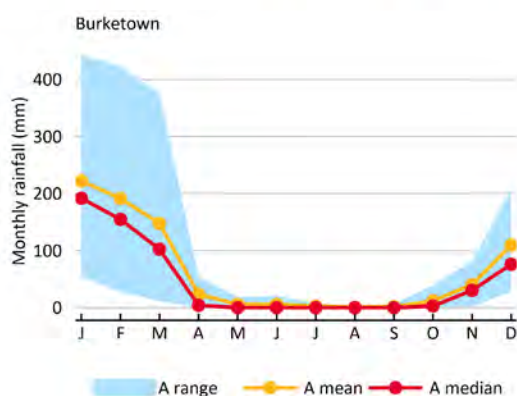
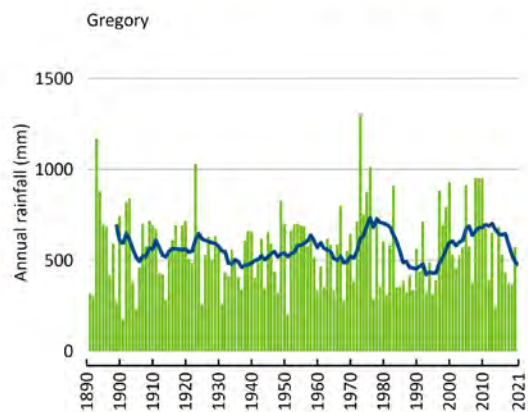
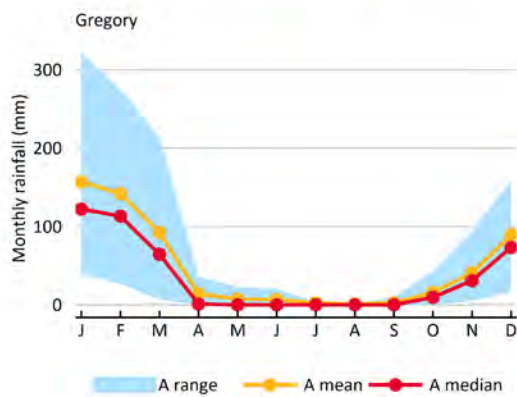
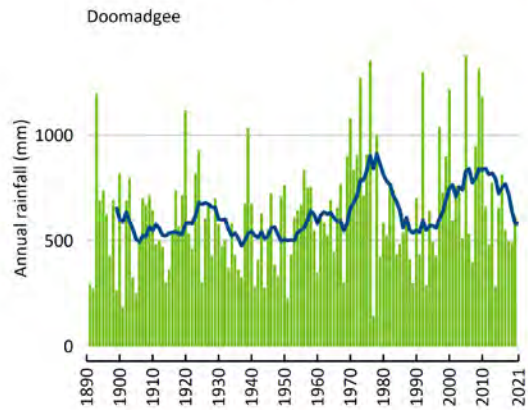
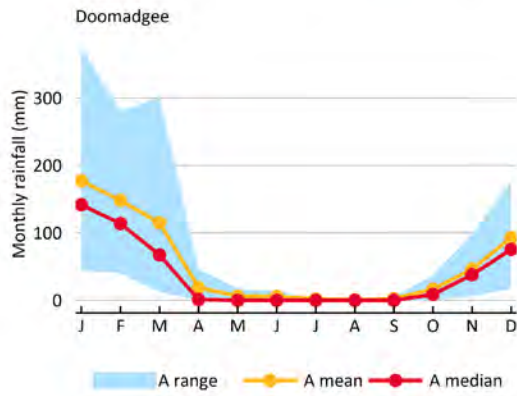
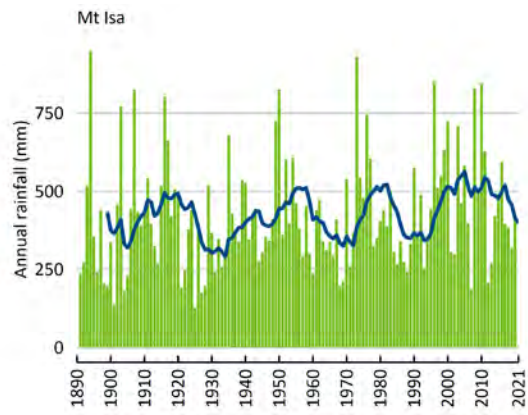
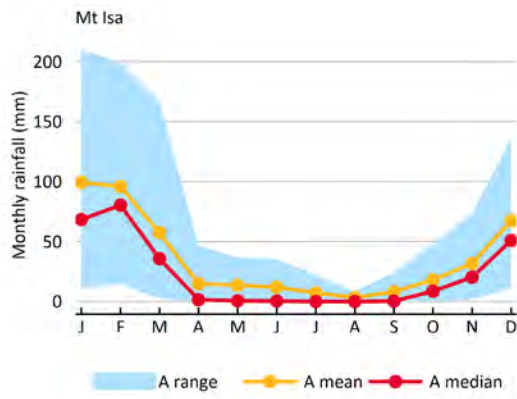


Figure 5-6 Historical rainfall in the Southern Gulf catchments at Mount Isa, Doomadgee, Gregory and Burketown Left column shows monthly rainfall, right column shows time series of annual rainfall (A range is the 10th to 90th percentile monthly rainfall).

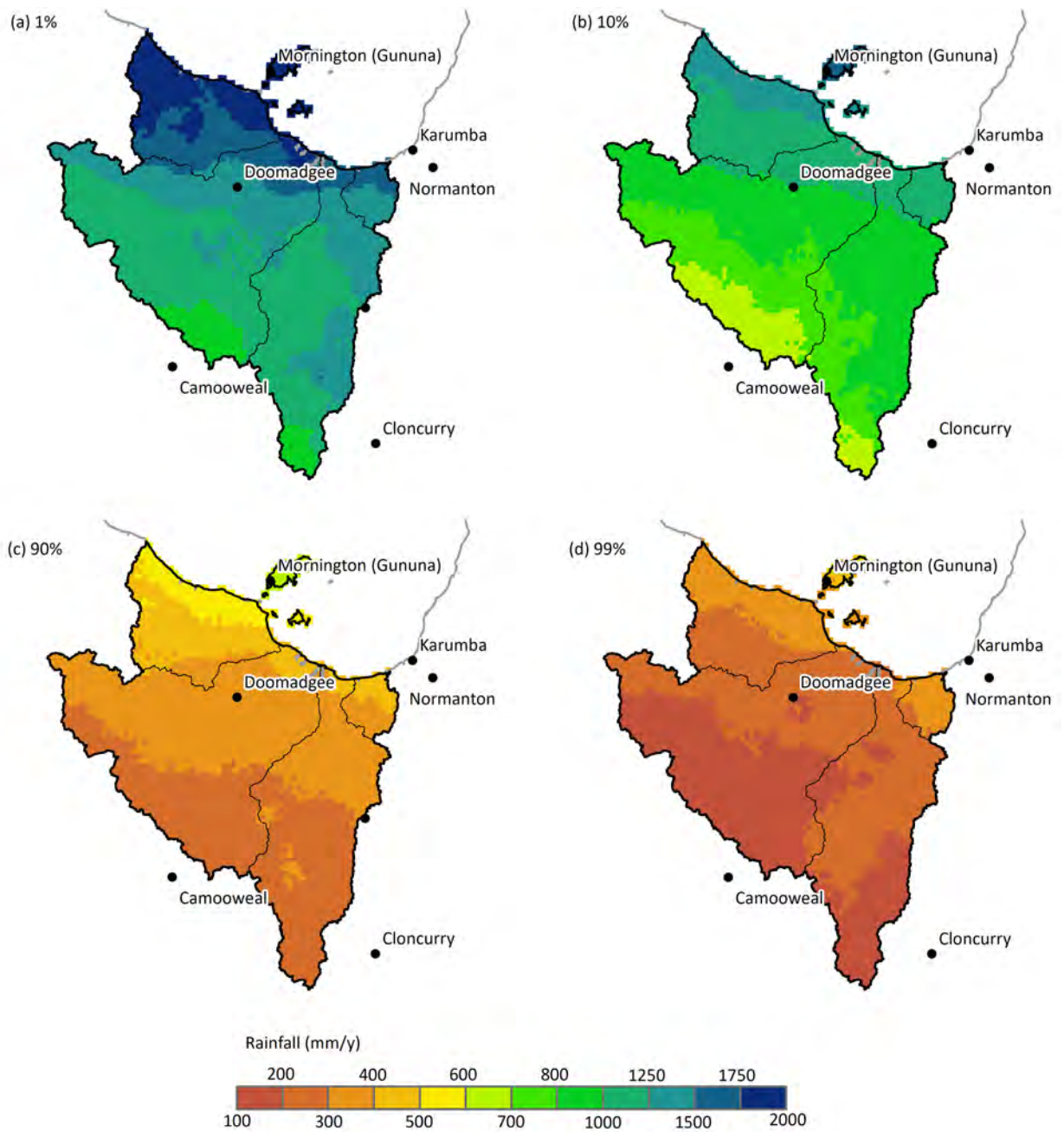


Figure 5-7 Historical annual rainfall that was exceeded in (a) 1%, (b) 10%, (c) 90% and (d) 99% of years in the Southern Gulf catchments

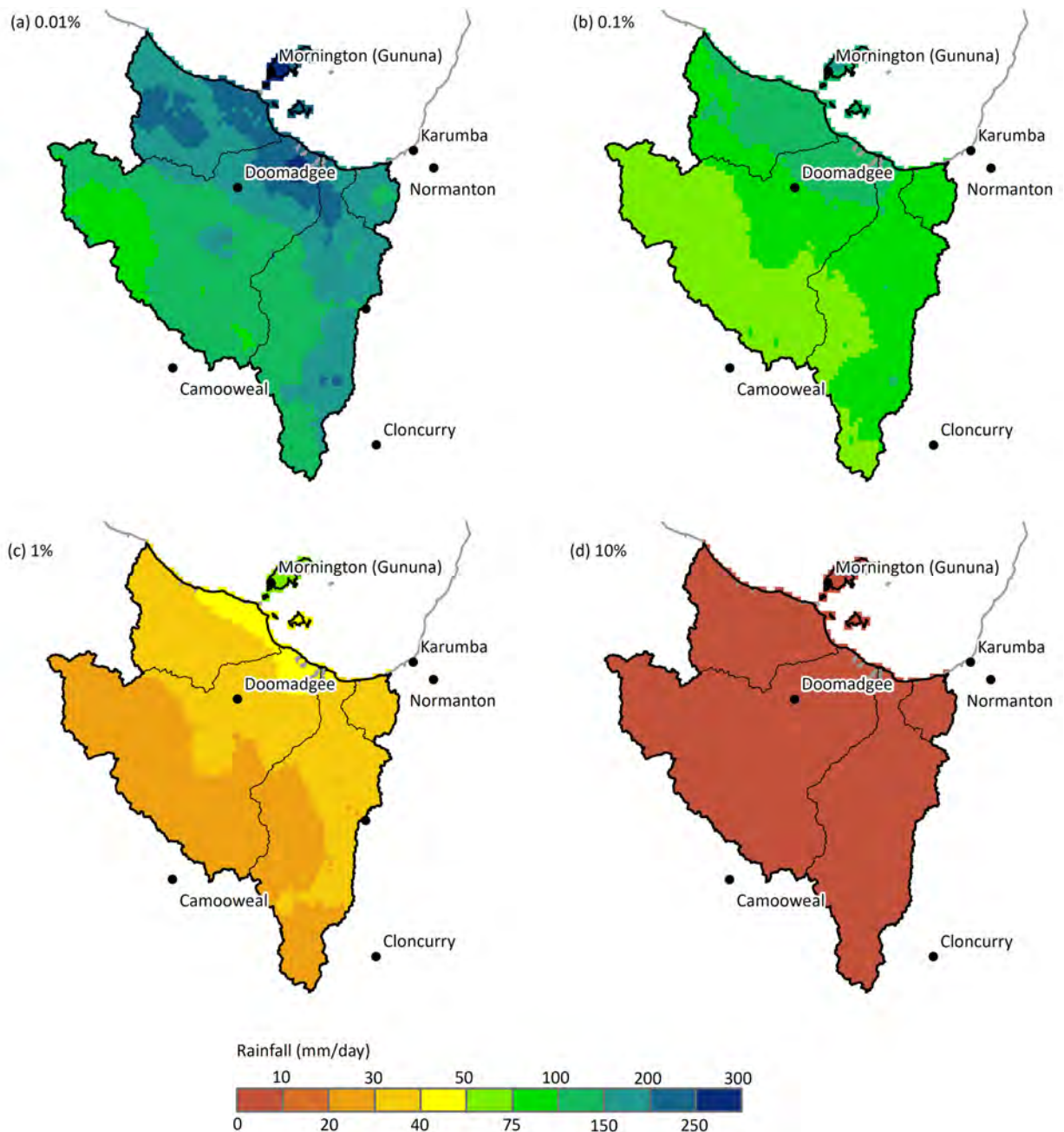


Figure 5-8 Historical daily rainfall that is exceeded in (a) 0.01%, (b) 0.1%, (c) 1% and (d) 10% of days in the Southern Gulf catchments

5.2.2 Other climate parameters

Potential evaporation

Mean areal potential evaporation (APE) (as calculated using Morton's areal wet potential) in the Southern Gulf catchments is about 1900 mm (Figure 5-9). Evaporation is high all year round, but exhibits a strong seasonal pattern, ranging from about 200 mm per month during November and December to about 100 mm per month during the middle of the dry season (June) (Figure 5-9).

The high mean annual potential evaporation (PE) and moderate mean annual rainfall result in a mean annual rainfall deficit across all of the catchment area (Figure 5-10). Consequently, most of the Southern Gulf catchments area is semi-arid (Figure 2-18).

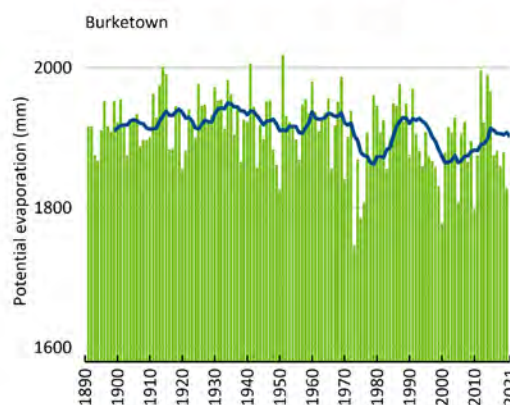
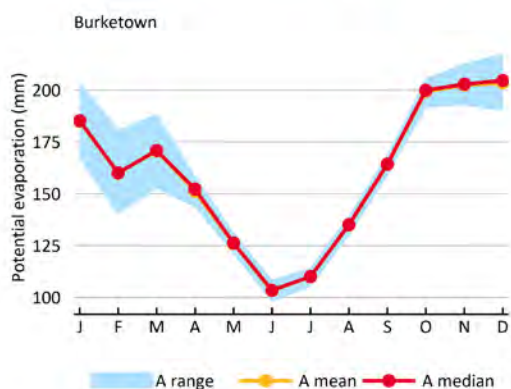
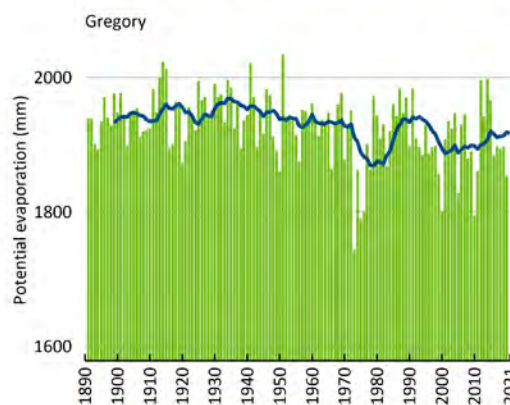
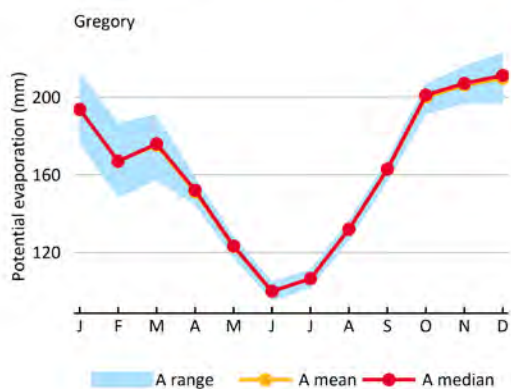
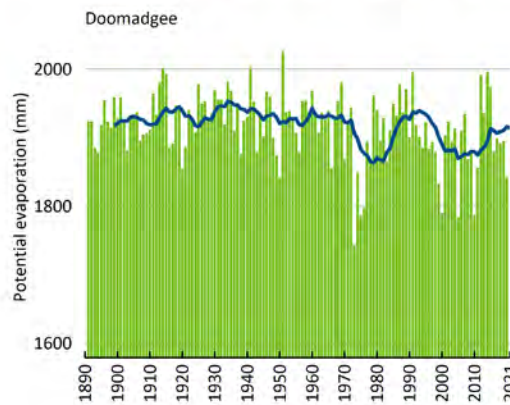
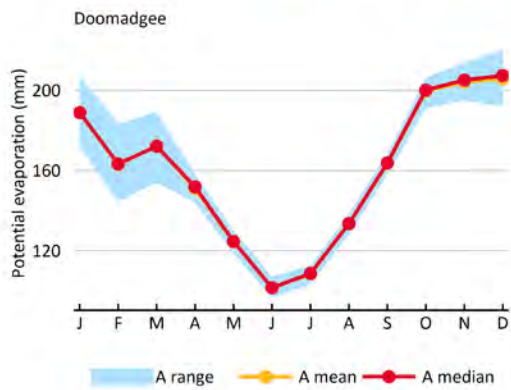
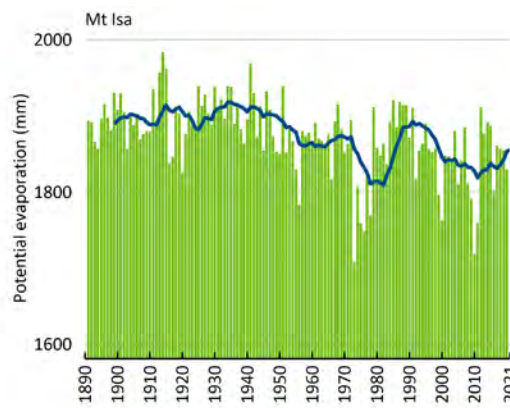
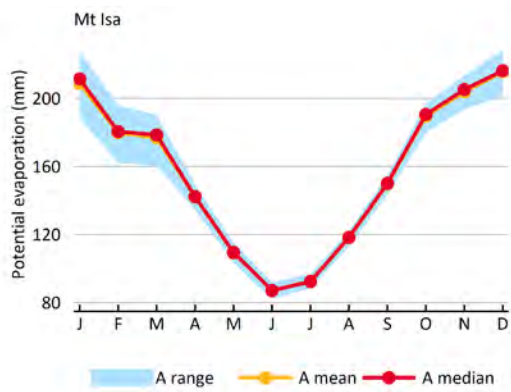


Figure 5-9 Historical potential evaporation in the Southern Gulf catchments at Mount Isa, Doomadgee, Gregory and Burketown

Left column shows monthly PE, right column shows time series of annual PE (A range is the 10th to 90th percentile monthly rainfall). Note: A mean line is directly under the A median line in these figures.

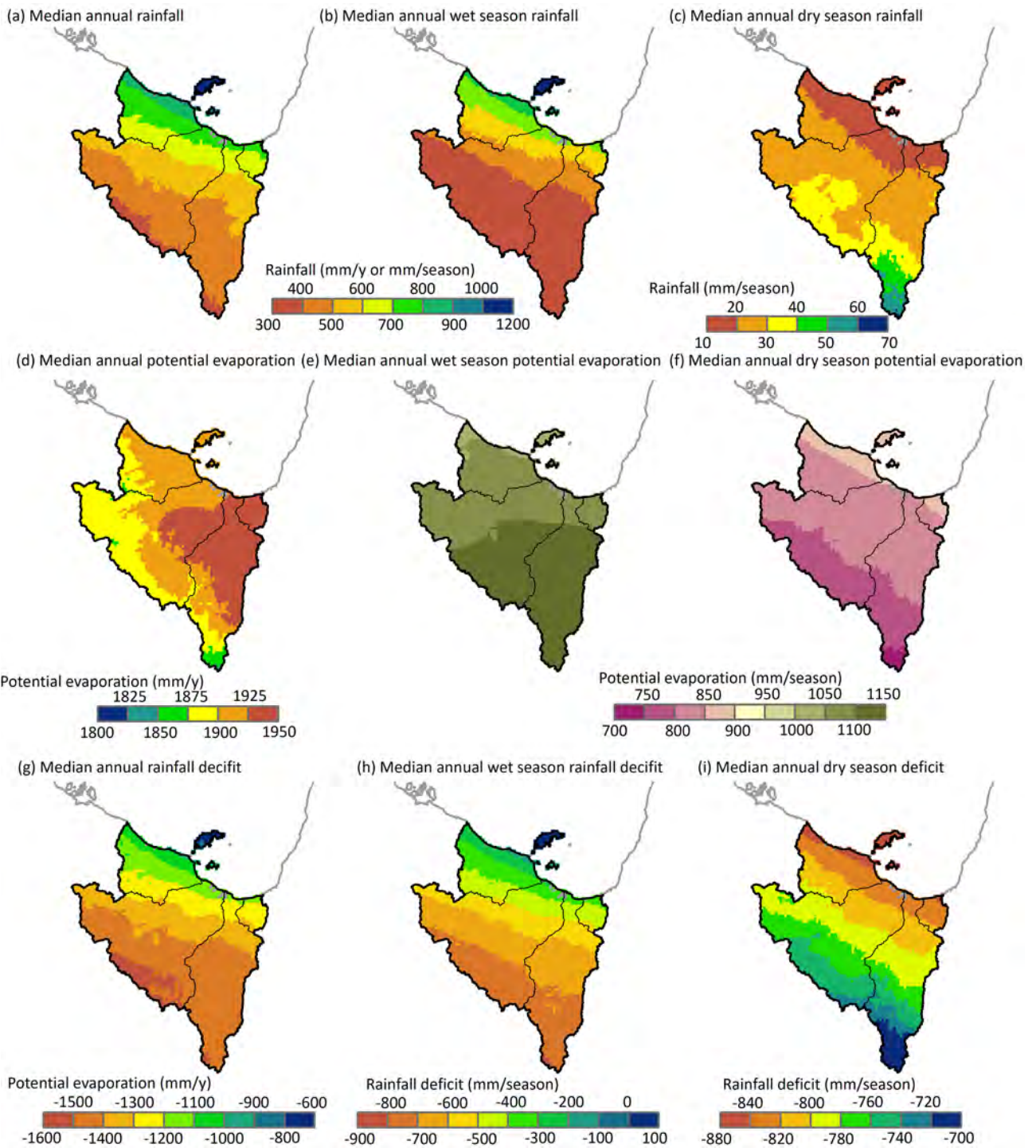


Figure 5-10 Historical median (a) annual, (b) wet-season, (c) dry-season rainfall; (d) annual, (e) wet-season, (f) dry-season potential evaporation; and (g) annual, (h) wet-season and (i) dry-season rainfall deficit in the Southern Gulf catchments

Maximum and minimum temperatures

Monthly mean maximum temperature and monthly mean minimum temperature at Mount Isa, Doomadgee, Gregory and Burketown are shown in Figure 5-11. The highest mean monthly maximum temperatures occur in October to December and the lowest mean monthly minimum temperatures occur in July.

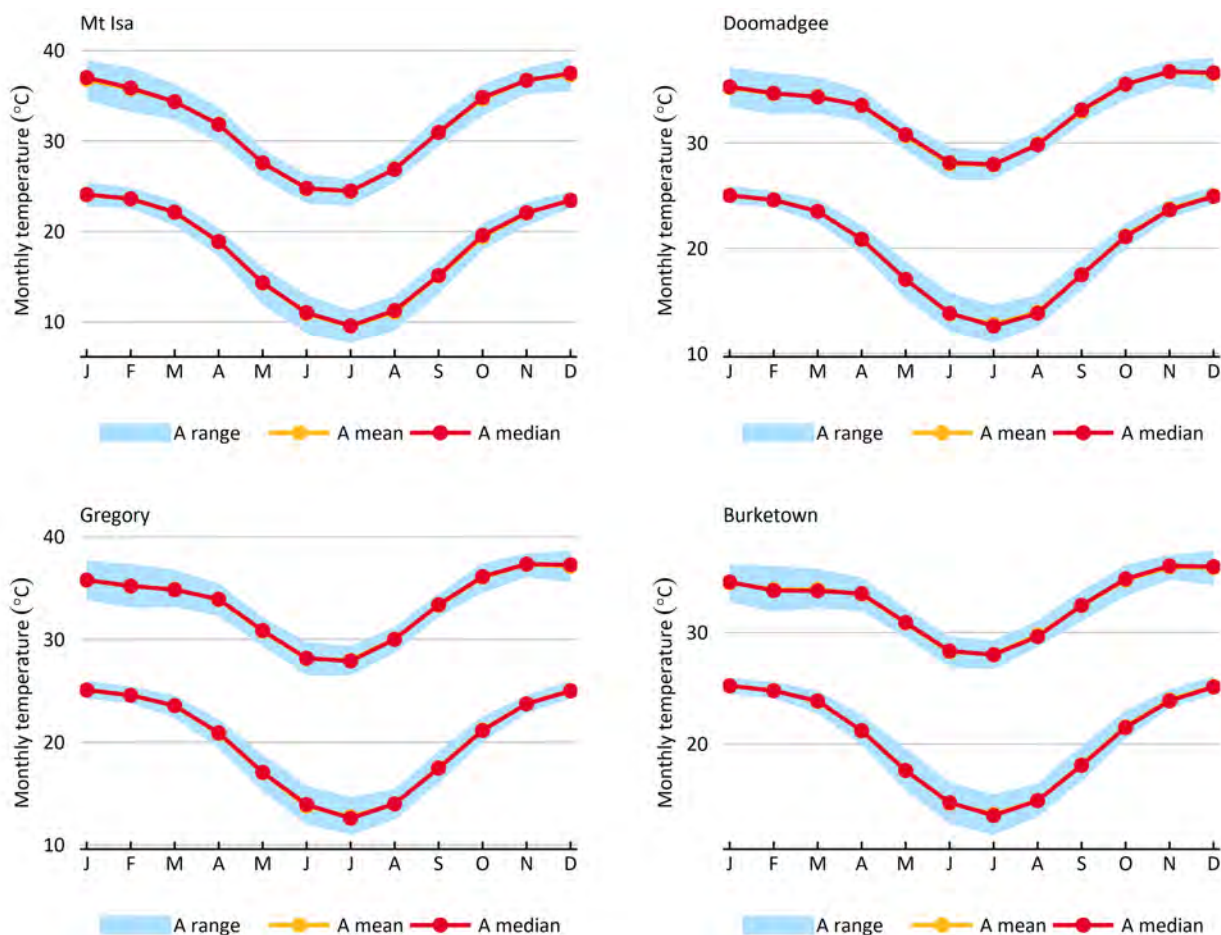


Figure 5-11 Historical maximum and minimum monthly air temperature in the Southern Gulf catchments at Mount Isa, Doomadgee, Gregory and Burketown

A range is the 10th to 90th percentile monthly rainfall. Note: A mean line is directly under the A median line in these figures.

When considering the effect of temperature on crop yield, it is also important to take extreme conditions into account, particularly at sensitive stages of growth. Figure 5-12 shows the maximum annual temperature that is exceeded in 10, 50 and 90% of years, and Figure 5-13 shows the minimum annual temperature that is exceeded in 10, 50 and 90% of years. The highest maximum annual temperatures occur in the southern part of the Southern Gulf catchments and minimum annual temperatures decline in a south-westerly direction (roughly parallel to the coast).

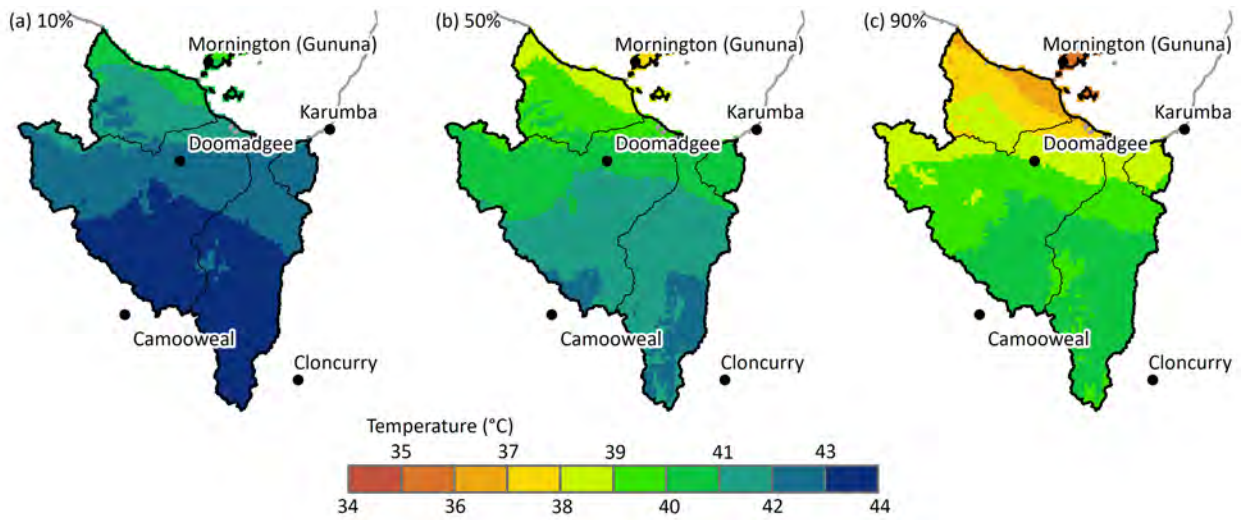


Figure 5-12 Historical maximum air temperature that is exceeded in (a) 10%, (b) 50% and (c) 90% of years in the Southern Gulf catchments

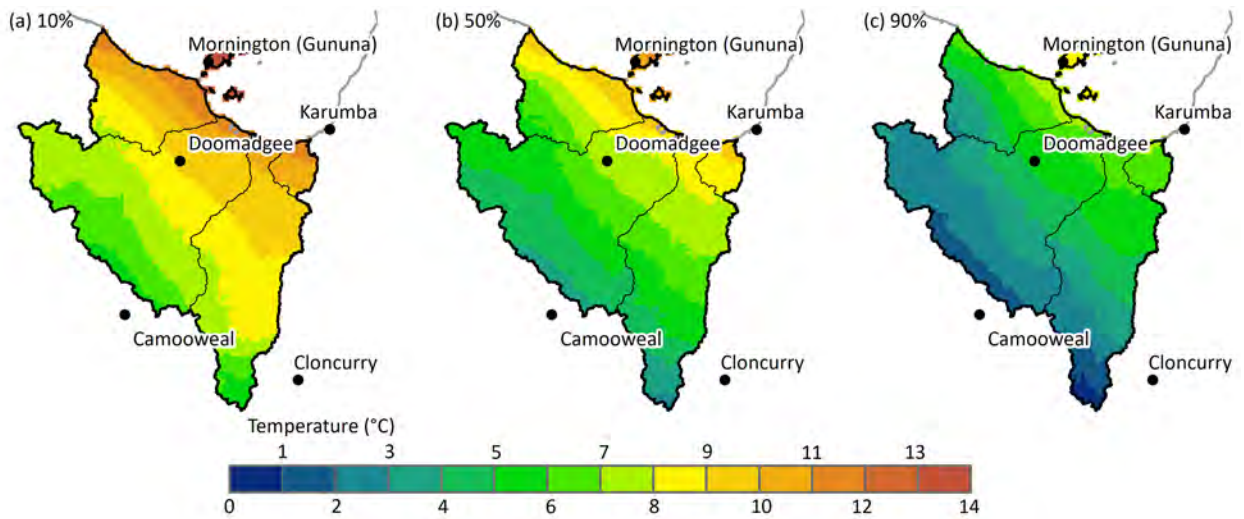


Figure 5-13 Historical minimum air temperature that is exceeded in (a) 10%, (b) 50% and (c) 90% of years in the Southern Gulf catchments

Frost events are uncommon in the Southern Gulf, with minimum temperatures rarely dropping below 5 °C (Figure 5-14). Median maximum consecutive days below 10 °C increases in a south-westerly direction peaking at around 15 days.

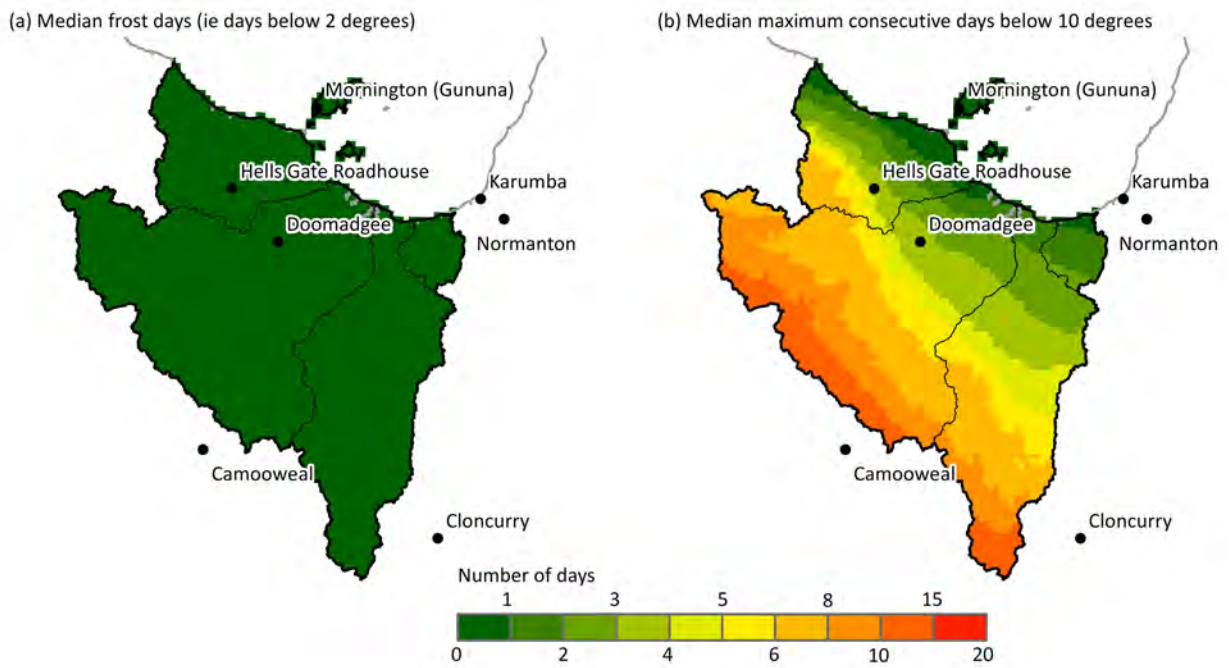


Figure 5-14 Historical minimum temperature thresholds in the Southern Gulf catchments

(a) Median annual frost days (i.e. days below 2 °C); and (b) median annual maximum consecutive days below 10 °C.

Solar radiation

Mean annual radiation exceeded in 10, 50 and 90% of years in the Southern Gulf catchments is shown in Figure 5-15, with a clear north–south gradient. Monthly mean radiation at Mount Isa, Doomadgee, Gregory and Burketown is shown in Figure 5-16, highlighting the reduced radiation of the wet season, resulting in peak radiation in October prior to the break.

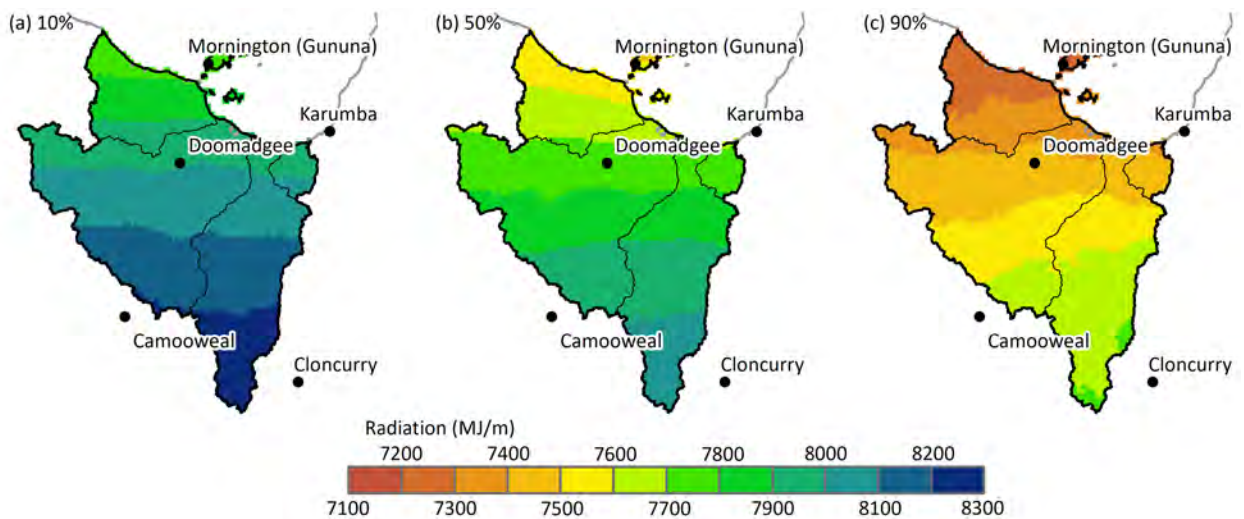


Figure 5-15 Historical annual radiation that is exceeded in (a) 10%, (b) 50% and (c) 90% of years

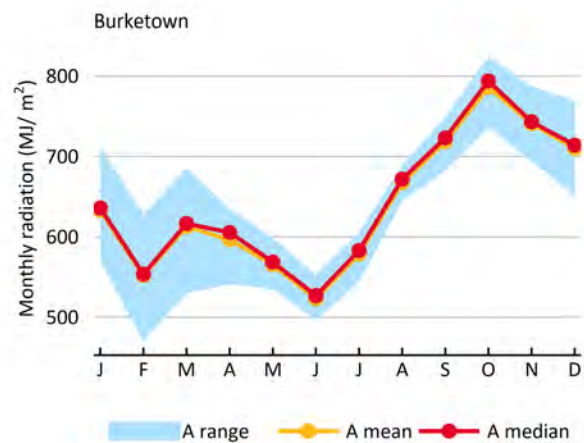
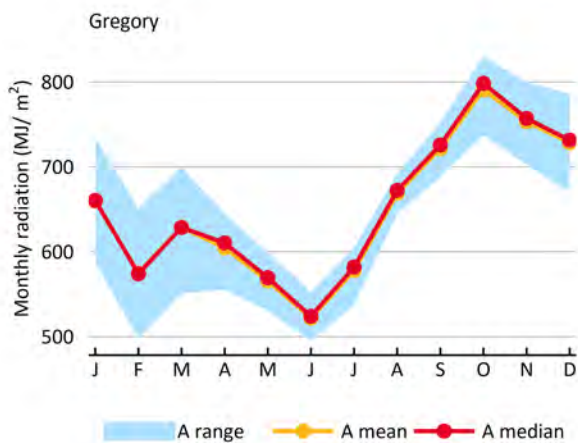
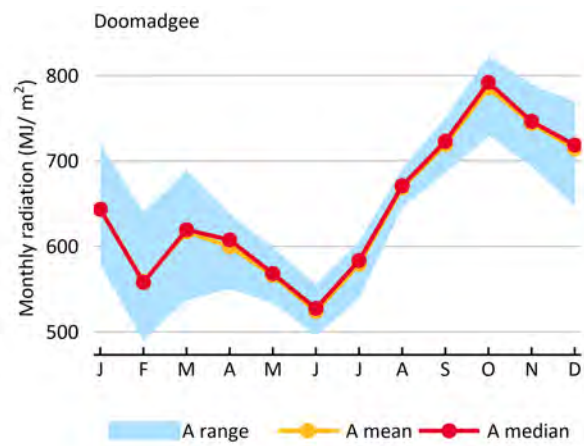
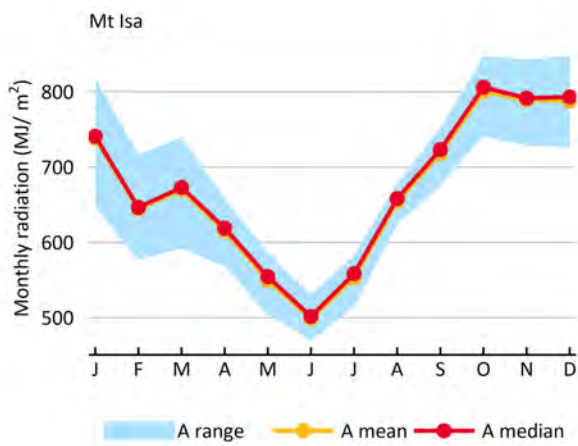


Figure 5-16 Historical monthly radiation in the Southern Gulf catchments at Mount Isa, Doomadgee, Gregory and Burketown

A range is the 10th to 90th percentile monthly rainfall. Note: A mean line is directly under the A median line in these figures.

Relative humidity, fog and dew

Annual relative humidity exceeded in 10, 50 and 90% of years in the Southern Gulf catchments is shown in Figure 5-17. Monthly mean relative humidity at Mount Isa, Doomadgee, Gregory and Burketown is shown in Figure 5-18. Relative humidity is higher closer to the coast and in the more northerly parts of the catchment. Coastal areas like Burketown also experience a larger variation in monthly values than inland locations such as Mount Isa (Figure 5-18).

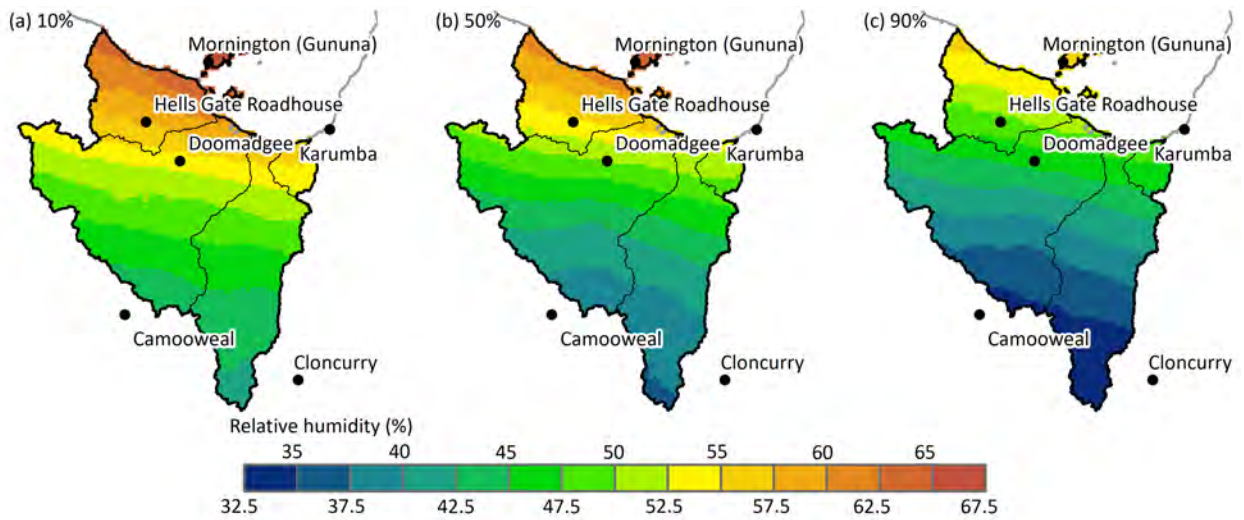


Figure 5-17 Historical annual relative humidity that is exceeded in (a) 10%, (b) 50% and (c) 90% of years in the Southern Gulf catchments

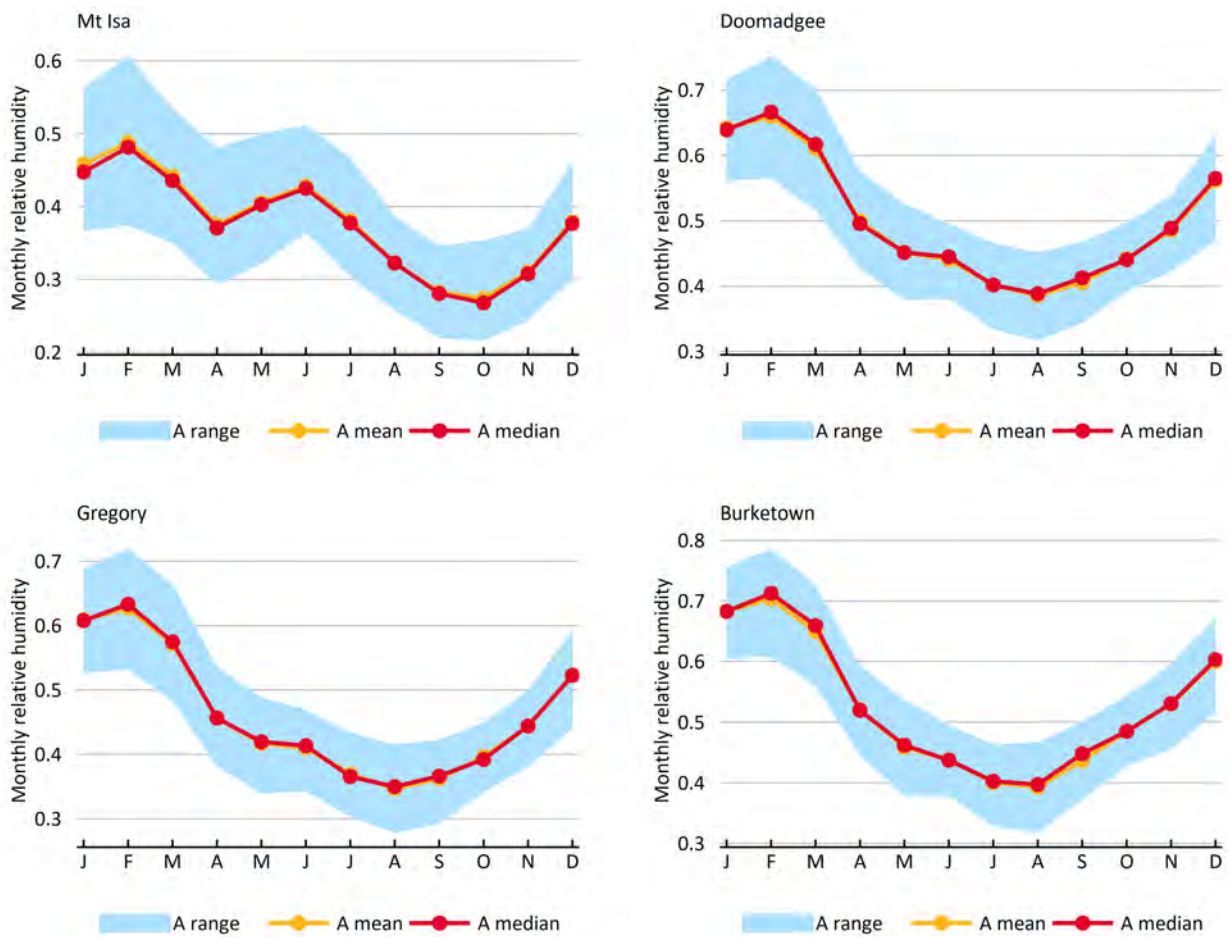


Figure 5-18 Historical monthly relative humidity in the Southern Gulf catchments at Mount Isa, Doomadgee, Gregory and Burketown

A range is the 10th to 90th percentile monthly rainfall.

5.2.3 Sea surface temperatures

Monthly mean sea surface temperatures (SSTs) for a location off the Southern Gulf catchments coast (139.8°E, 15.2°S) are shown in Figure 5-19. There is little variation across the wet season, with temperatures around 30 °C, dropping to 24 °C in July, before increasing from September.

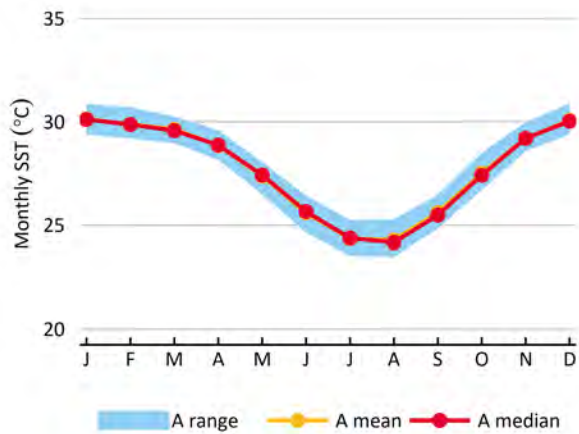


Figure 5-19 Historical monthly SST offshore Southern Gulf catchments

139.8°E, 15.2°S; A range is the 10th to 90th percentile monthly SST for 1970 to 2022 period. Note: A mean line is directly under the A median line in this figure. Source: <https://psl.noaa.gov/data/gridded/data.noaa.ersst.v5.html>

Page deliberately left blank

Part III Future climate projections



6 Future climate projections

6.1 Methods

Global climate models (GCMs) are an important tool for simulating global and regional climate. The climate activity has produced several variants of 109 years of daily climate series, representative of the five different climate scenarios used by the Intergovernmental Panel on Climate Change (IPCC) in its Sixth Assessment Report (IPCC, 2022). These scenarios are called Shared Socioeconomic Pathways, or SSPs, and are defined as follows:

- SSP1-1.9: emissions rapidly decline to net zero by about 2050, and become negative after that
- SSP1-2.6: emissions decline to net zero by about 2075, and become negative after that
- SSP2-4.5: emissions rise slightly, before declining after 2050, but not reaching net zero by 2100
- SSP3-7.0: emissions rise steadily to become double their current amount by 2100
- SSP5-8.5: emissions rise steadily, doubling by 2050 and more than tripling by the end of the century.

Each of these scenarios have associated global temperature changes, which are summarised in Table 6-1. The IPCC does not make statements about which of these scenarios is more likely, however, the Australian Academy of Science recently released a report (Australian Academy of Science, 2021) stating that current emissions trajectories will likely result in Australia experiencing a 3 °C temperature increase by 2100. Hausfather and Peters (2020) provide a qualitative estimate of likelihood for a range of SSPs (Table 6-1). For the approach presented here, SSP2-4.5 will be the main focus.

Table 6-1 Changes in global surface temperature for selected 20-year time periods across the five emissions scenarios presented by the IPCC Sixth Assessment Report

Approximate global temperature differences are expressed relative to the average global surface temperature of a 20-year window centred around 1990 (i.e. not the period 1850 to 1900, which are given in the original table in the IPCC (2022) report). Values are most likely with numbers in parentheses representing the 5 to 95% range. Likelihood based on Hausfather and Peters (2020).

SCENARIO	MID TERM, 2041–2060	LIKELIHOOD
SSP1-1.9	1.0 °C (0.6 to 1.4 °C)	Unlikely
SSP1-2.6	1.2 °C (0.6 to 1.5 °C)	Likely
SSP2-4.5	1.6 °C (1.2 to 1.9 °C)	Likely
SSP3-7.0	1.8 °C (1.4 to 2.3 °C)	Unlikely
SSP5-8.5	2.2 °C (1.7 to 2.8 °C)	Highly unlikely

SSP = Shared Socioeconomic Pathway

GCMs provide information at a resolution that is too coarse to be used directly in catchment-scale hydrological modelling. For example, rainfall occurs too often and at too low intensity (Stephens et al., 2010). This is particularly important in tropical regions, where even high-resolution coupled climate models simulate tropical cyclones as weaker and larger in horizontal extent than those observed (IPCC, 2015). Hence, an intermediate step is generally performed: the broad-scale GCM outputs are transformed to catchment-scale variables.

Two fundamental approaches exist for downscaling broad-scale GCM output to a finer spatial resolution: dynamic downscaling and statistical downscaling (see Fowler et al. (2007), and references therein). Dynamic downscaling is computationally very intensive, while sophisticated statistical downscaling methods (e.g. regression models, weather typing schemes, weather generators) require expertise to optimise. Numerous studies, however, also suggest that no single downscaling method is superior across a range of hydrological metrics (Chiew et al., 2010; Mitchell, 2003; Prudhomme and Davies, 2009; Whetton et al., 2005). In a comparative assessment of scaling methods in an area dominated by large-scale storm events, Salathé (2003) found simple scaling methods to be as effective in simulating hydrological systems. For these reasons, and due to the scale of the catchments being assessed, which makes it resource intensive to undertake dynamic or statistical downscaling, a simple scaling technique – the pattern scaling method (Chiew et al., 2009b) was adopted.

6.1.1 Generation of future climate data

Selection of general circulation models

To simulate and assess the uncertainty of the range of future runoff predictions, future climate projections from a large range of archived GCM simulations were downloaded from the Coupled Model Intercomparison Project (CMIP6) website (<https://pcmdi.llnl.gov/CMIP6/>). Of the 92 available GCMs, 32 included the rainfall, temperature data, solar radiation and humidity data required for the Australian Water Resource Assessment Landscape (AWRA-L) and River (AWRA-R) hydrological modelling, WAVES recharge modelling, agricultural production systems simulator (APSIM) crop modelling and GRASP pasture modelling. Studies evaluating the skill of the CMIP6 GCM at reproducing key features of Australia's circulatory system were not completed at the time of writing, so the full suite of 32 GCM has been adopted for the Assessment.

Scaling method

The seasonal pattern scaling (PS) method employed used output from the 32 GCMs to scale the 109-year historical daily rainfall, temperature, radiation and humidity sequences (i.e. SILO climate data), to construct the 32 by 109-year sequences of future daily rainfall, temperature, radiation and humidity. The method is briefly described below. A more detailed description can be found in Chiew et al. (2009b).

The method comprised two broad steps. The first step involved estimating the seasonal scaling factors for four 3-month blocks (December to February, March to May, June to August and September to November) for the changes between two time slices centred around 1990 (1975 to 2005) and 2060 (2046 to 2075). This is representative of a 1.6 °C temperature rise under an SSP2-4.5 emissions scenario (Table 6-1). For each season and over each time slice, the total rainfall was calculated. Seasonal scaling factors were then calculated as the ratio of the total season's rainfall

over the 2060 time slice divided by the total rainfall over the 1990 time slice. The historical climate sequence was then scaled using these seasonal scaling factors. The second step involved rescaling the entire series so that it matches the annual scaling factors, to maintain consistency with annual projected changes in the GCMs (Chiew et al., 2009b; Petheram et al., 2012).

This process was repeated for each GCM, for each season and for each GCM grid cell. The results were then expressed per degree warming by dividing the projected change in rainfall by the projected representative global temperature rise of 1.6 °C temperature rise (under the SSP2-4.5 emissions scenario). The method was then repeated for each climate parameter, except for temperature where the difference rather than ratio between the two periods was used to scale the historical sequence. The method of using a pattern scaling method to transform broad-scale GCM outputs to catchment-scale variables is denoted herein as 'GCM-PS'.

6.2 Results

6.2.1 Rainfall

The 32 GCM-PS rainfall and potential evaporation (PE) projections per degree global warming were spatially averaged and the GCM-PS ranked in order of increasing mean annual rainfall for each of the Victoria, Roper and Southern Gulf catchments, as shown in Figure 6-1, Figure 6-2 and Figure 6-3 respectively.

Scenario Cwet, Cmid and Cdry for the Victoria, Roper and Southern Gulf catchments were selected as the 10th (3rd), 50th (17th) and 90th (30th) percent exceedance of the 32 GCM-PS shown in Figure 6-1, Figure 6-2 and Figure 6-3 respectively. The percentage change in mean annual rainfall and potential evaporation per degree global warming under scenarios Cwet, Cmid and Cdry were calculated under the SSP5-8.5 emissions scenario (details provided in Appendix A). As shown in Table 6-2, Table 6-3 and Table 6-4 and, for Victoria, Roper and Southern Gulf catchments, respectively, when the SSP5-8.5 emissions scenario is used to calculate percentage change in mean annual rainfall and potential evaporation per degree global, the values for scenario Cwet, Cmid and Cdry are similar to those calculated under the SSP2-4.5 emissions scenario. The similarity in response provides confidence to jointly use the SSP emissions scenario global temperature projections summarised in Table 6-1 and the percentage change rainfall and potential evaporation values per degree warming listed in Table 6-2 to Table 6-4 to approximate the percentage change in rainfall and potential evaporation under a range of SSPs emissions scenarios.

Seasonal comparison of percent change in mean annual rainfall and potential evaporation per degree of global warming under the SSP2-4.5 and SSP5-8.5 emissions scenarios are provided in Appendix B.

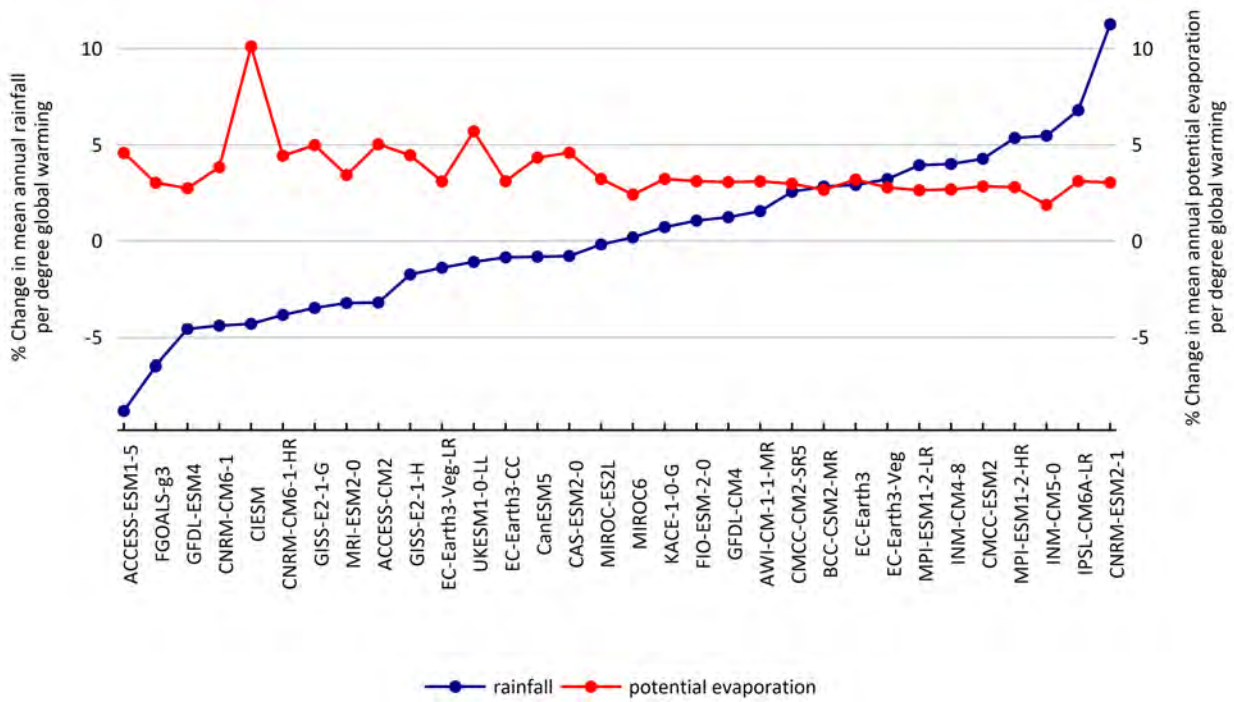


Figure 6-1 Percentage change in rainfall and potential evaporation per degree of global warming for the 32 Scenario C simulations relative to Scenario A values for the Victoria catchment. GCM-PS ranked by increasing rainfall for SSP2-4.5

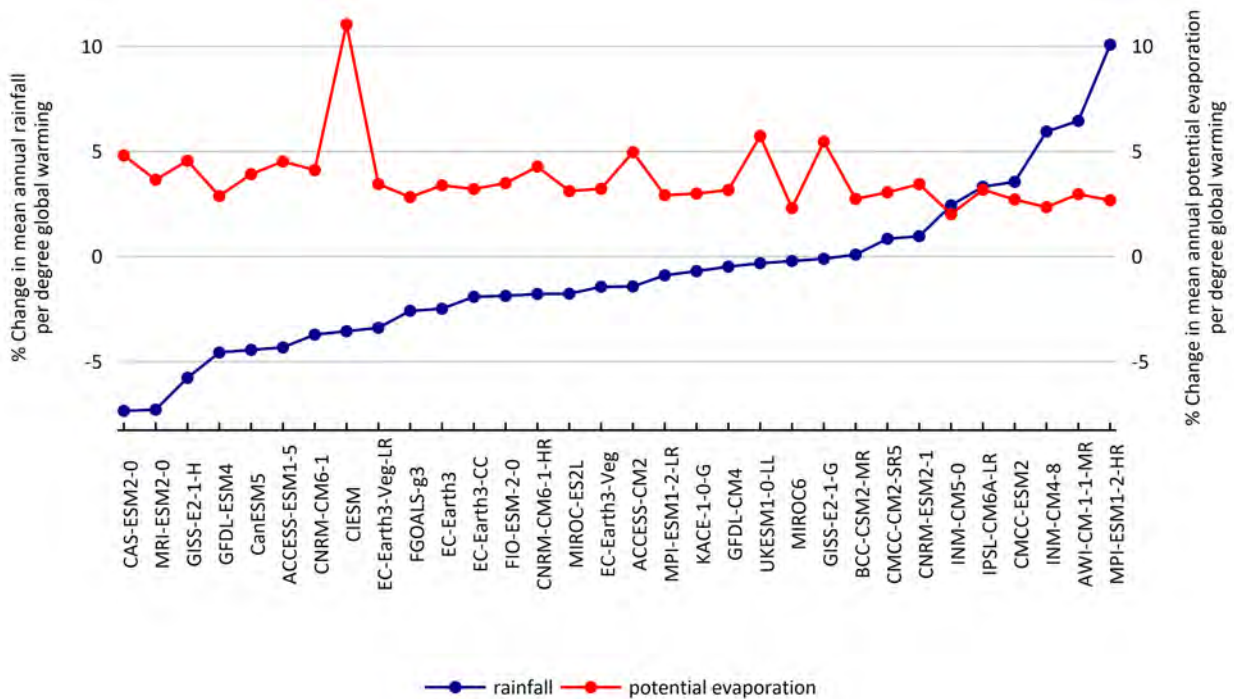


Figure 6-2 Percentage change in rainfall and potential evaporation per degree of global warming for the 32 Scenario C simulations relative to Scenario A values for the Roper catchment. GCM-PS ranked by increasing rainfall for SSP2-4.5

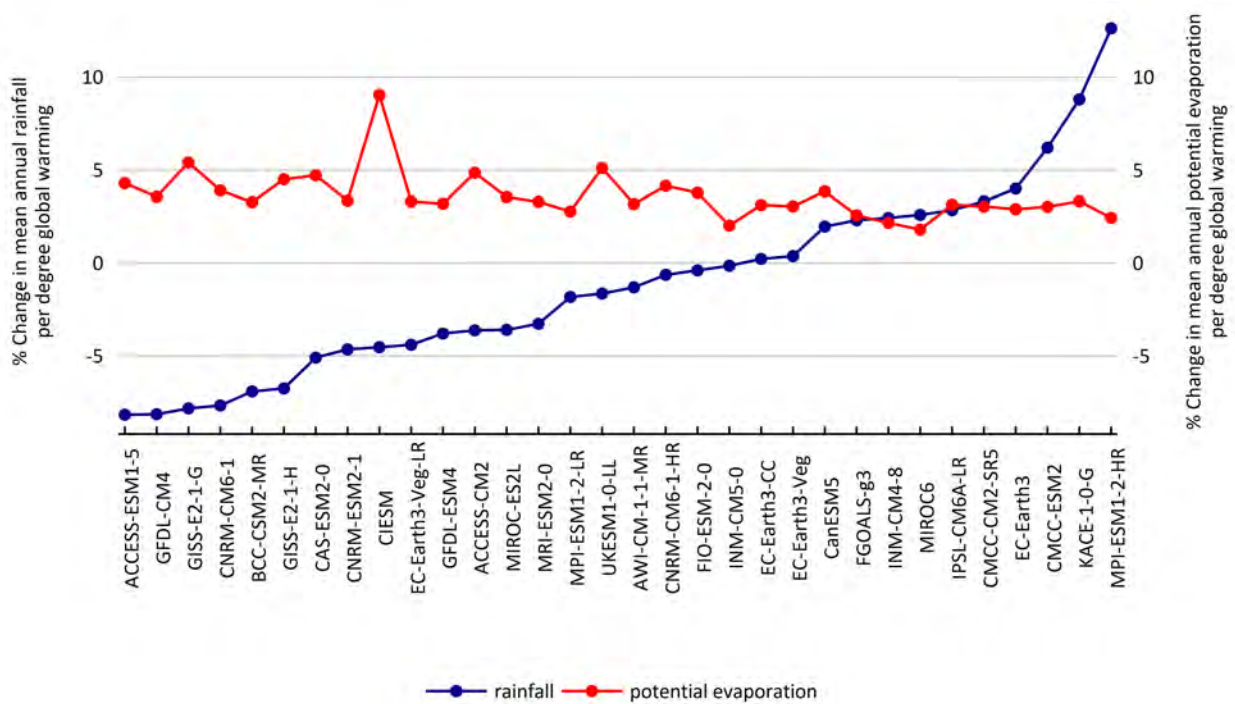


Figure 6-3 Percentage change in rainfall and potential evaporation per degree of global warming for the 32 Scenario C simulations relative to Scenario A values for the Southern Gulf catchments. GCM-PS ranked by increasing rainfall for SSP2-4.5

Table 6-2 Percentage change in mean annual rainfall and potential evaporation per degree warming under scenarios Cwet, Cmid and Cdry for SSP2-4.5 and SSP5-8.5 emissions scenarios for the Victoria catchment

SCENARIO	SSP2-4.5 EMISSIONS SCENARIO (% CHANGE PER DEGREE GLOBAL WARMING)		SSP5-8.5 EMISSIONS SCENARIO (% CHANGE PER DEGREE GLOBAL WARMING)	
	Rainfall	Potential evaporation	Rainfall	Potential evaporation
Cwet	5.5	1.9	5.5	2.5
Cmid	0.2	2.4	1.2	2.9
Cdry	-4.6	2.7	-5	3.1

Table 6-3 Percentage change in mean annual rainfall and potential evaporation per degree warming under scenarios Cwet, Cmid and Cdry for SSP2-4.5 and SSP5-8.5 emissions scenarios for the Roper catchment

SCENARIO	SSP2-4.5 EMISSIONS SCENARIO (% CHANGE PER DEGREE GLOBAL WARMING)		SSP5-8.5 EMISSIONS SCENARIO (% CHANGE PER DEGREE GLOBAL WARMING)	
	Rainfall	Potential evaporation	Rainfall	Potential evaporation
Cwet	5.9	2.4	5.6	2.6
Cmid	-1.4	4.9	0.2	2.7
Cdry	-5.8	4.6	-6.9	4.5

Table 6-4 Percentage change in mean annual rainfall and potential evaporation per degree warming under scenarios Cwet, Cmid and Cdry for SSP2-4.5 and SSP5-8.5 emissions scenarios for the Southern Gulf catchments

SCENARIO	SSP2-4.5 EMISSIONS SCENARIO (% CHANGE PER DEGREE GLOBAL WARMING)		SSP5-8.5 EMISSIONS SCENARIO (% CHANGE PER DEGREE GLOBAL WARMING)	
	Rainfall	Potential evaporation	Rainfall	Potential evaporation
Cwet	6.2	3.0	5.9	2.6
Cmid	-1.3	3.2	-0.7	3.4
Cdry	-7.8	5.4	-6.7	4.4

Over the time slices examined as part of the Assessment, a change within $\pm 5\%$ of the historical mean is not considered large as it is within the bounds of internal variability generated by the GCMs (Cai et al., 2011a). Assuming SSP2-4.5 emissions scenario, which corresponds to $\sim 1.6^\circ\text{C}$ global temperature rise at 2060, for the Victoria catchment, 47% of the 32 GCM-PS fall into this ‘little change’ category, 56% for the Roper catchment and 40% for the Southern Gulf catchments. For the Victoria catchment, 25% GCM-PS indicate a wetter future climate and 28% a drier climate. For the Roper catchment, 28% GCM-PS indicate drier and 16% wetter. For the Southern Gulf catchments, 44% GCM-PS project a drier future and 16% project a wetter future.

Based on the data presented in Figure 6-1, Figure 6-2 and Figure 6-3 there is no clear agreement in the GCM-PS projections for mean annual rainfall. Analysis of the CMIP6 data is on-going. However, based on the CMIP5 data the lack of consensus in future trends over the three study areas and the eastern half of northern Australia in general (Li et al., 2009) is in part because under a warming climate it is not clear how the phase, intensity and amplitude of the ENSO will change (Collins et al., 2010). While ENSO is considered to be the primary source of global climate variability over the 2–6-year time scale, it has its largest influence on weather patterns and climate variability over the tropical Pacific and the continental landmasses on either side (i.e. coastal regions of South America, South-East Asia and north and eastern Australia). In these areas rainfall teleconnections with ENSO are not well simulated in the CMIP5 GCMs and there is a large spread among models (Cai et al., 2011a; Cai et al., 2009b).

The spatial distribution of projected mean annual rainfall under scenarios Cwet, Cmid and Cdry (i.e. the 10th, 50th and 90th percent exceedance mean annual rainfall values from the 32 GCM-PS) are shown for the Victoria (Figure 6-4), Roper (Figure 6-6) and Southern Gulf catchments (Figure 6-8). The corresponding relative changes, under scenarios Cwet, Cmid and Cdry, are shown in Figure 6-5, Figure 6-7 and Figure 6-9 for the Victoria, Roper and Southern Gulf catchments respectively. The linear boundaries evident in the percent change rainfall figures are an artefact of the coarse resolution of the GCM grid cells. In these figures scenario Cwet, Cmid and Cdry values were calculated on a SILO grid cell by SILO grid cell basis (i.e. different SILO grid cells may be assigned different GCM-PS under scenarios Cwet, Cmid and Cdry).

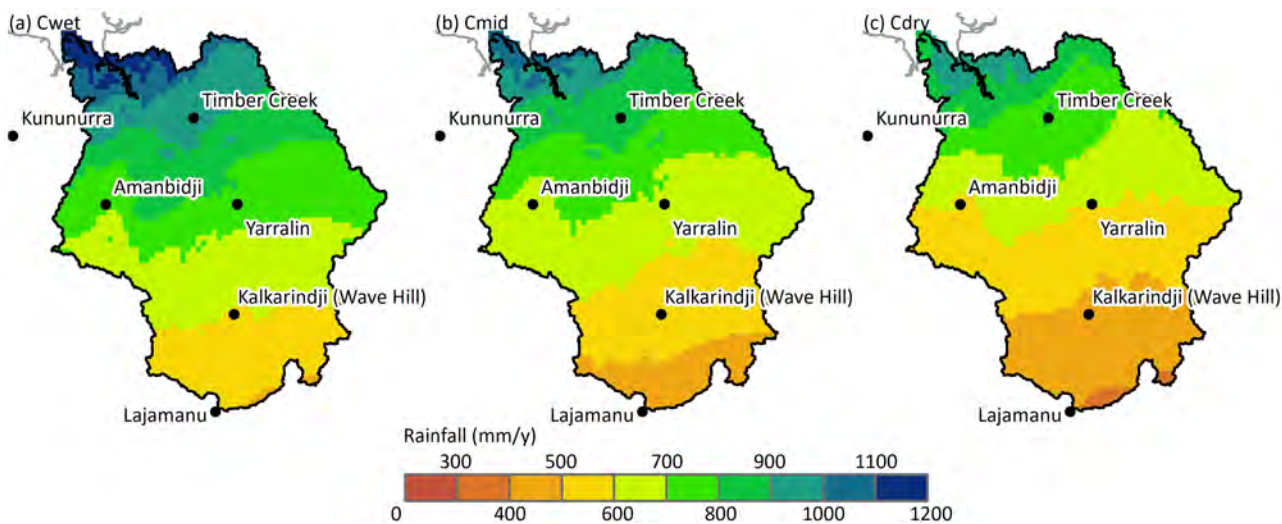


Figure 6-4 Spatial distribution of mean annual rainfall across the Victoria catchment under scenarios Cwet, Cmid and Cdry

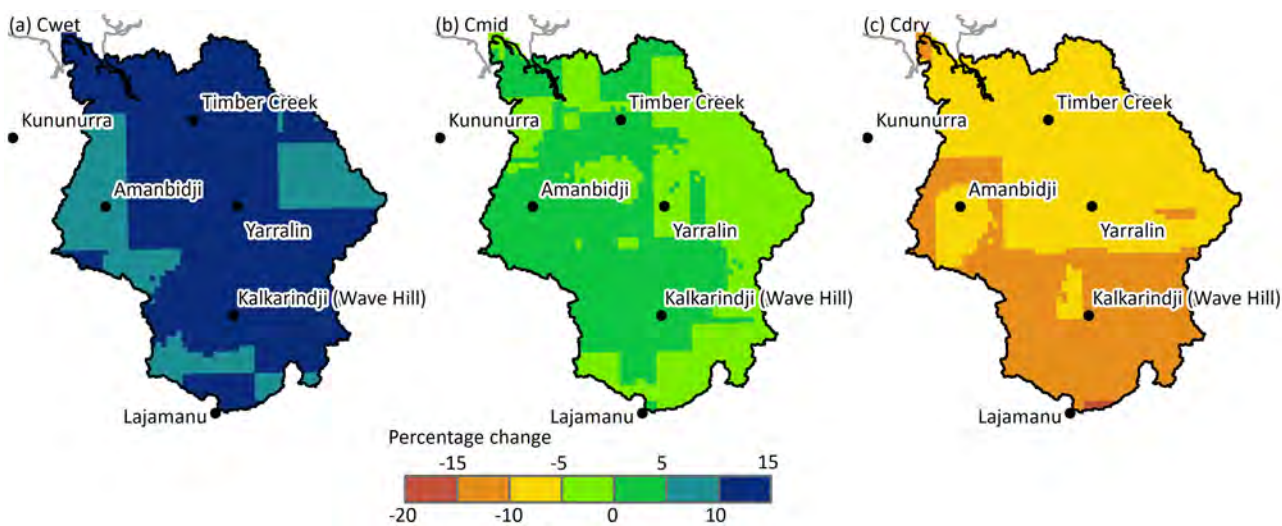


Figure 6-5 Spatial distribution of percentage change in mean annual rainfall relative to Scenario A across the Victoria catchment under scenarios Cwet, Cmid and Cdry

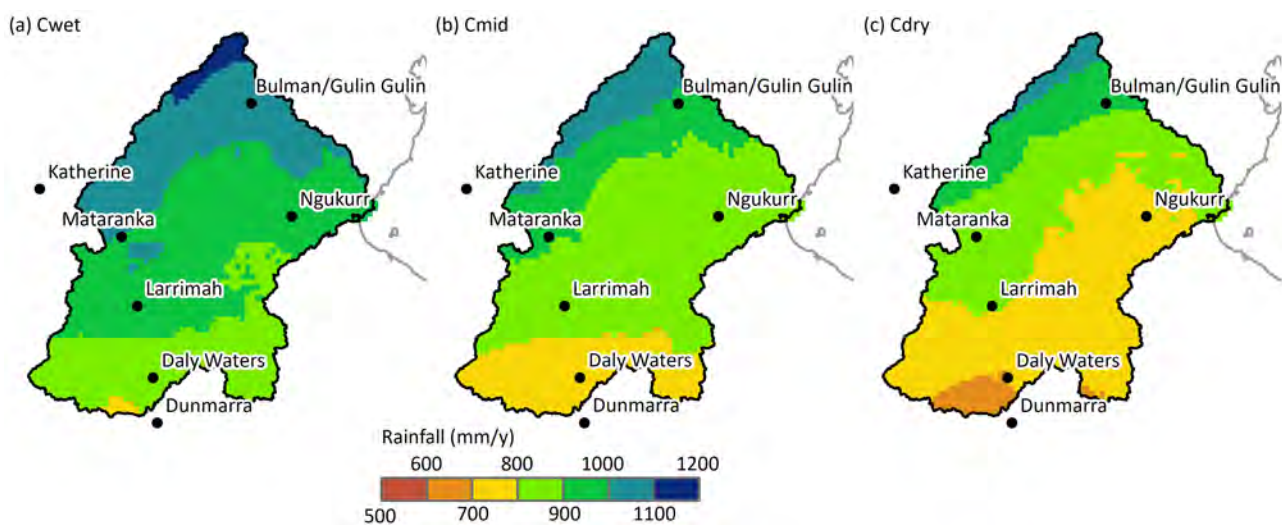


Figure 6-6 Spatial distribution of mean annual rainfall across the Roper catchment under scenarios Cwet, Cmid and Cdry

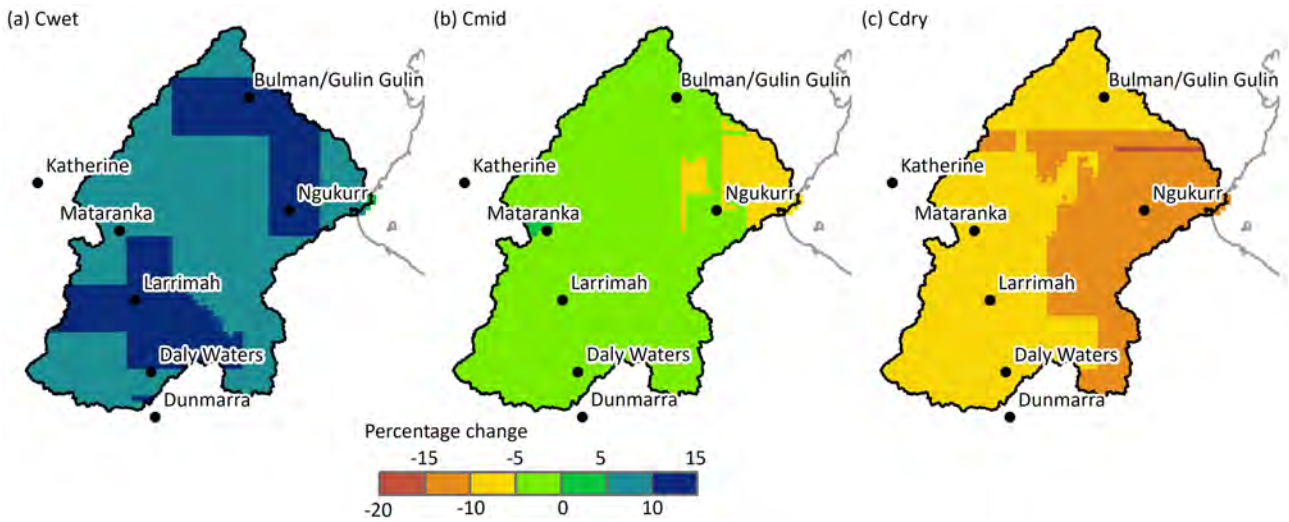


Figure 6-7 Spatial distribution of percentage change in mean annual rainfall relative to Scenario A across the Roper catchment under scenarios Cwet, Cmid and Cdry

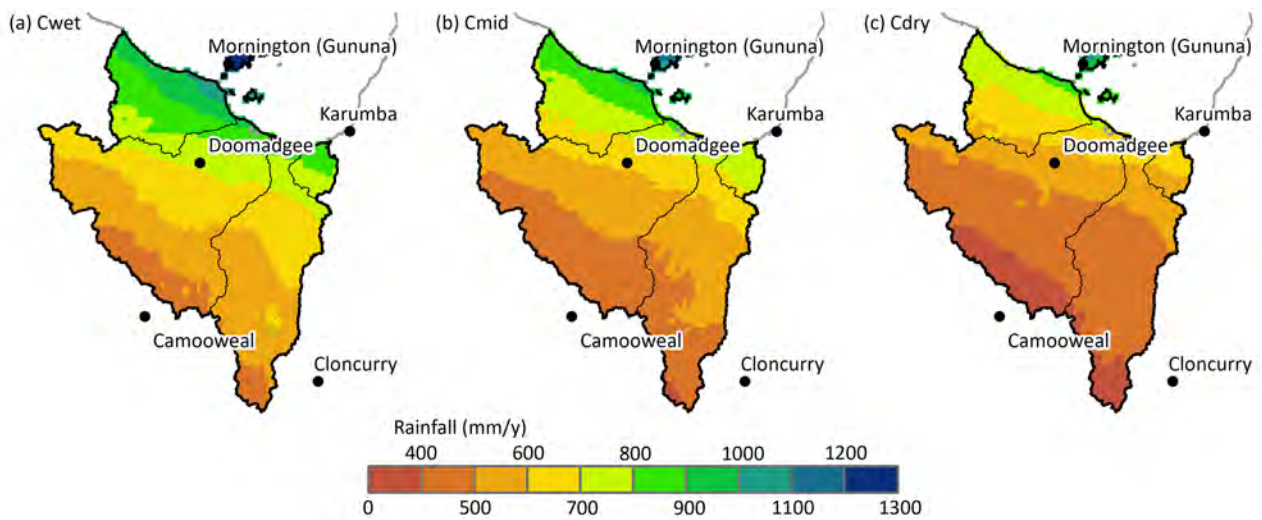


Figure 6-8 Spatial distribution of mean annual rainfall across the Southern Gulf catchments under scenarios Cwet, Cmid and Cdry

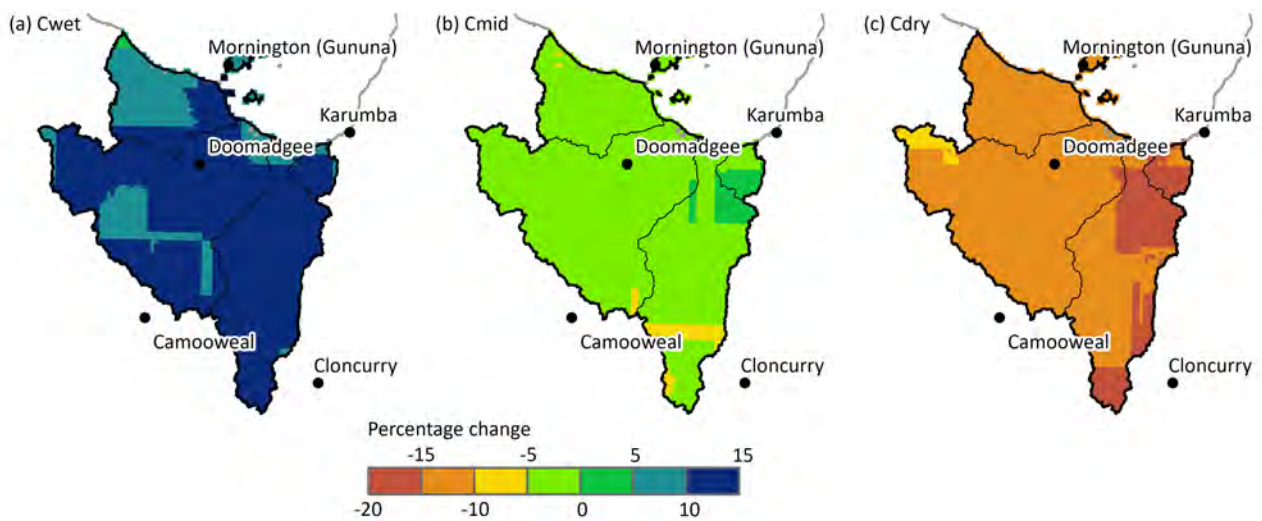


Figure 6-9 Spatial distribution of percentage change in mean annual rainfall relative to Scenario A across the Southern Gulf catchments under scenarios Cwet, Cmid and Cdry

Figure 6-10 illustrates the range in monthly GCM-PS rainfall and potential evaporation projections spatially averaged across each study area. In these plots C range is the difference between the 10th (Cwet) and 90th (Cdry) percent exceedance values of the 32 GCM-PS. GCM-PS were assigned for scenario Cwet, Cmid and Cdry on a month-by-month basis.

6.2.2 Potential evaporation

Projected increases in mean annual areal potential evaporation (APE), using Morton's formulation, vary from 3 to 18% under the SPP2-4.5 emissions scenario. This change has been predominantly driven by the increase in air temperature, which affects Morton's wet area potential both directly via its influence on surface temperature and indirectly via its effect on vapour pressure and on longwave radiation. However, Morton's formulation of APE does not incorporate the effects of wind speed, even though wind speed is a key variable in the aerodynamic component of evaporation.

McVicar et al. (2008) showed that all of northern Australia has experienced declines in wind speed of approximately 0.01 m/second/year over the last 30 years, and this has been shown to be the primary factor driving the observed decreases of pan evaporation across much of Australia, including northern Australia, over the same time period (Roderick et al., 2007). The effect of decreasing wind speed is to moderate the effect of rising temperatures on PE rates. It is uncertain whether wind stilling will continue, however, if decreasing wind speeds were to hold into the future, the projections of APE here (i.e. using Morton's wet area potential formulation) will be higher than they would be if a fully physical potential formation were to be used (that is, one that incorporates net radiation, humidity, wind speed and temperature).

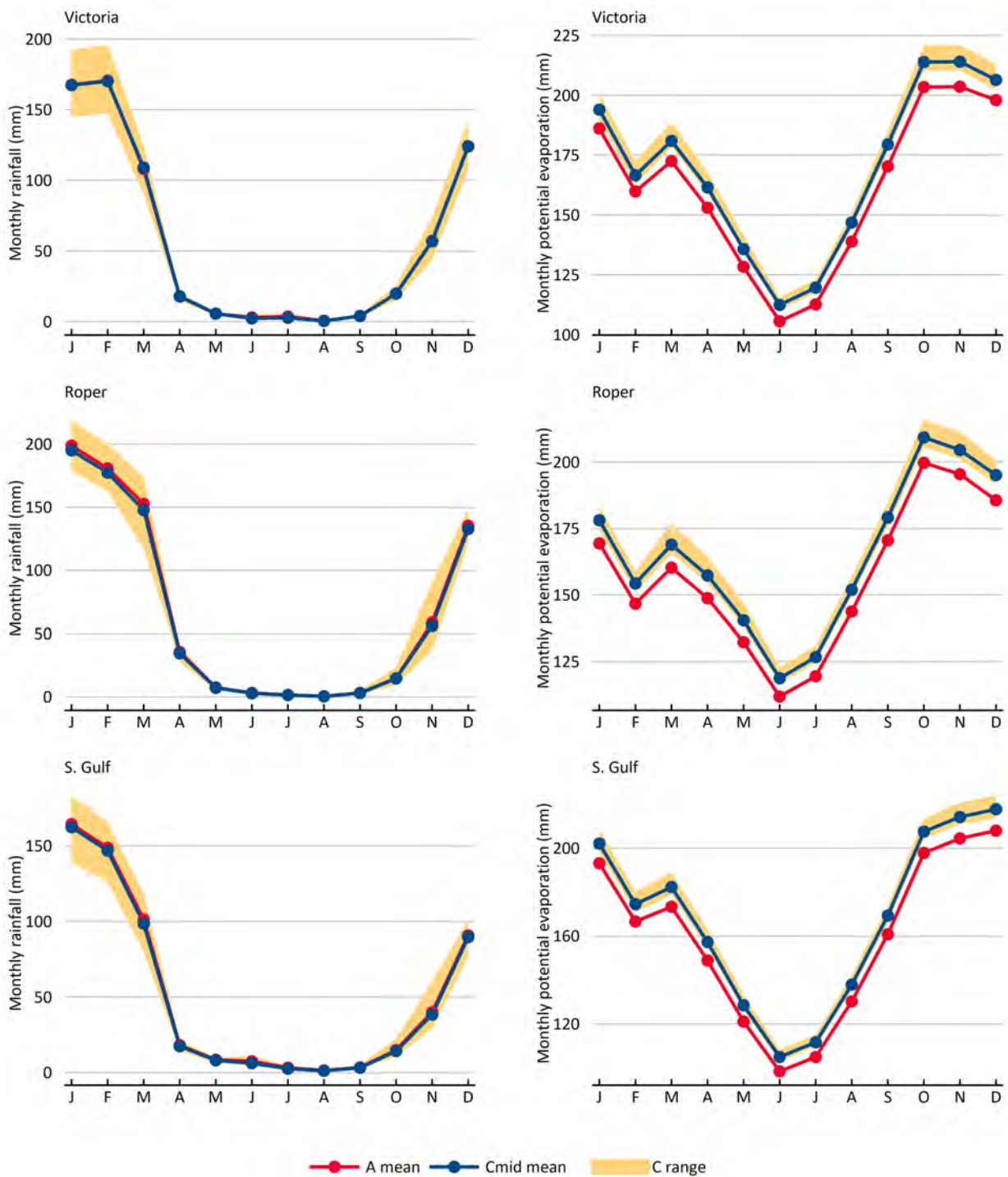


Figure 6-10 Mean monthly rainfall (left column) and potential evaporation (right column) for the Victoria, Roper and Southern Gulf catchments under scenarios A and C

C range is based on the computation of the 10th and 90th percentile rainfall and potential evaporation for each month separately – the lower and upper limits in C range are therefore not the same as scenarios Cdry and Cwet.

6.2.3 Sea-level rise and sea surface temperature projections

Global mean sea levels have risen at a rate of 1.7 ± 0.2 mm/year between 1900 and 2010, a rate on the order of ten times faster than the preceding century. Australian tide gauge trends are similar to the global trends, with a mean of 1.4 ± 0.2 mm/year between 1966 and 2009, ranging from 0.8 mm/year at Fort Denison and Victor Harbour to 2.6 mm/year at Darwin (CSIRO and Bureau of Meteorology, 2015). White et al. (2014) found that past changes in Australian sea level are similar to global mean changes over the last 45 years when influences of ENSO, glacial isostatic adjustment and atmospheric pressure effects are taken into account. They thus conclude that future changes over the 21st century are likely to be consistent with global changes.

The IPCC concludes that there has been significant improvement in understanding and projection of sea-level change over the last few years (improved ability to simulate ocean thermal expansion, glaciers and ice sheets, and thus sea level). Global mean sea-level rise will continue during the 21st century, very likely at a faster rate than observed from 1971 to 2010. There is high confidence that sea-level rise will continue for centuries even if the global mean temperature is stabilised, placing coastal systems and low-lying areas at increased submergence, flooding and erosion risk (IPCC, 2015).

In the only study of its kind in the vicinity of the three study areas, of which the authors are aware, modelling undertaken by Wolanski and Chappell (1996) concluded that a future sea-level rise will generate changes in the dynamics and channel dimensions that mimic post glacial changes. In the macrotidal South Alligator River the floodplain was projected to revert to mangrove, the mouth region widen and sediment move upstream and onto the floodplain. In the mesotidal, diurnal Norman catchment (Gulf region) the channel is projected to widen throughout, and sediment transported seawards.

CSIRO and Bureau of Meteorology (2015), McInnes et al. (2015) and Church et al. (2016) provide an overview of the sea-level projections for Australia. These publications utilise the CMIP5 dataset to provide sea-level change projections for all Australian councils with a coastline, the information is on the web portal <https://coastadapt.com.au/>. An updated product for CMIP6 is yet to be released, however, early analysis by Grose et al. (2020) shows little difference between the CMIP5 and CMIP6 sea-level projections along the northern Australia coastline. For the purposes of this report the readily available CMIP5 results are presented with particular reference to two Representative Concentration Pathways (RCPs); RCP4.5 and RCP8.5, which are most similar to CMIP6 scenarios SSP2-4.5 and SSP5-8.5, respectively. These are summarised for the Victoria catchment in Table 6-5, for the Roper catchment in Table 6-6 and Southern Gulf catchments in Table 6-7.

Sea surface temperature (SST) increases around Australia are projected with very high confidence for all emissions scenarios, with warming of around 0.4 to 1.0 °C in 2030 under RCP4.5 and 2 to 4 °C in 2090 under RCP8.5, relative to a 1986 to 2005 baseline (CSIRO and Bureau of Meteorology, 2015). There will be regional differences in SST warming due to local hydrodynamic responses, however, there is only medium confidence in coastal projections as climate models do not resolve local processes (CSIRO and Bureau of Meteorology, 2015).

Table 6-5 Projected sea-level rise for the coast of the Victoria catchment

Values are median of Coupled Model Intercomparison Project (CMIP) Phase 5 GCMs. Numbers in parentheses are the 5 to 95% range of same. Projected sea-level rise values are relative to a mean calculated between 1986 and 2005.

Source: <https://coastadapt.com.au/sea-level-rise-information-all-australian-coastal-councils> - NT_VICTORIA_DALY

DATE (UNIT)	RCP4.5	RCP8.5
2030 (m)	0.11 (0.07–0.16)	0.12 (0.08–0.16)
2050 (m)	0.21 (0.14–0.29)	0.24 (0.16–0.32)
2070 (m)	0.32 (0.21–0.45)	0.40 (0.27–0.55)
2090 (m)	0.45 (0.27–0.63)	0.60 (0.40–0.83)
Rate of change at 2100 (mm/y)	5.9 (3.1–8.7)	10.9 (6.8–15.7)

RCP = Representative Concentration Pathway

Table 6-6 Projected sea-level rise for the coast of the Roper catchment

Values are median of Coupled Model Intercomparison Project (CMIP) Phase 5 GCMs. Numbers in parentheses are the 5 to 95% range of same. Projected sea-level rise values are relative to a mean calculated between 1986 and 2005.

Source: <https://coastadapt.com.au/sea-level-rise-information-all-australian-coastal-councils> - NT_ROPER_GULF

DATE (UNIT)	RCP4.5	RCP8.5
2030 (m)	0.11 (0.07–0.15)	0.11 (0.07–0.16)
2050 (m)	0.20 (0.13–0.28)	0.23 (0.15–0.31)
2070 (m)	0.31 (0.19–0.43)	0.39 (0.26–0.53)
2090 (m)	0.43 (0.26–0.61)	0.59 (0.38–0.81)
Rate of change at 2100 (mm/y)	5.9 (3.1–8.7)	10.7 (6.7–15.4)

RCP = Representative Concentration Pathway

Table 6-7 Projected sea-level rise for the coast of the Southern Gulf catchments

Values are median of Coupled Model Intercomparison Project (CMIP) Phase 5 GCMs. Numbers in parentheses are the 5 to 95% range of same. Projected sea-level rise values are relative to a mean calculated between 1986 and 2005.

Source: <https://coastadapt.com.au/sea-level-rise-information-all-australian-coastal-councils> - NT_ROPER_GULF

DATE (UNIT)	RCP4.5	RCP8.5
2030 (m)	0.11 (0.07–0.15)	0.11 (0.07–0.16)
2050 (m)	0.20 (0.13–0.28)	0.23 (0.15–0.31)
2070 (m)	0.31 (0.19–0.43)	0.39 (0.26–0.53)
2090 (m)	0.43 (0.26–0.61)	0.59 (0.38–0.81)
Rate of change at 2100 (mm/y)	5.9 (3.1–8.7)	10.7 (6.7–15.4)

RCP = Representative Concentration Pathway

Using the Climate Change in Australia Marine Explorer tool

(<https://www.climatechangeinaustralia.gov.au/en/projections-tools/coastal-marine-projections/marine-explorer/>) for the closest locations to each of the three study areas, under RCP8.5 the SST at Darwin (closest to the Victoria catchment) is projected to increase 0.8 °C (range across climate models 0.6 to 1.1) by 2030 and 3.0 °C (range 2.5 to 3.9) by 2090. For Karumba (closest to the Roper and Southern Gulf catchments), the corresponding projected SST increases are 0.8 (0.6 to 1.1) °C for 2030 and 3.0 (2.5 to 3.9) °C for 2090. These changes are relative to a 1986 to 2005 baseline (CSIRO and Bureau of Meteorology, 2015).

6.2.4 Skill of modelling tropical cyclones under a warmer climate

The IPCC Sixth Assessment Report on extreme events concludes there is low confidence that observed long-term changes in tropical cyclone (TC) activity are robust, and there is low confidence in the attribution of global changes to any particular cause (Seneviratne et al., 2021). Anthropogenic climate change is warming the atmosphere and the oceans and thus is expected to increase the theoretical upper intensity of TCs due to warmer SSTs. A global review by Knutson et al. (2010) summarised the current state of knowledge:

Detection and attribution:

It remains uncertain whether past changes in any tropical cyclone activity (frequency, intensity, rainfall, and so on) exceed the variability expected through natural causes, after accounting for changes over time in observing capabilities.

Tropical cyclone projections:

Frequency: It is likely that the global frequency of tropical cyclones will either decrease or remain essentially unchanged owing to greenhouse warming. We have very low confidence in projected changes in individual basins. Current models project changes ranging from –6 to –34% globally, and up to ±50% or more in individual basins by the late twenty-first century.

Intensity: Some increase in the mean maximum wind speed of tropical cyclones is likely (+2 to +11% globally) with projected twenty-first century warming, although increases may not occur in all tropical regions. The frequency of the most intense (rare/high-impact) storms will more likely than not increase by a substantially larger percentage in some basins.

Rainfall: Rainfall rates are likely to increase. The projected magnitude is on the order 20% within 100 km of the tropical cyclone centre.

Genesis, tracks, duration and surge flooding: We have low confidence in projected changes in tropical cyclone genesis-location, tracks, duration and areas of impact. Existing model projections do not show dramatic large-scale changes in these features. The vulnerability of coastal regions to storm-surge flooding is expected to increase with future sea-level rise and coastal development, although this vulnerability will also depend on future storm characteristics.

Modelling studies of projected changes in TC climatology undertaken for the Australian region by CSIRO (Abbs, 2012; IOCI, 2012) have used multiple levels of dynamical downscaling. Firstly, CSIRO's conformal-cubic atmospheric model (CCAM), a stretched-grid global atmospheric model with a 65 km horizontal resolution over Australia, downscaled from GCM projections and subsequently

the regional atmospheric modelling system (RAMS) down to 5 km resolution was nested in these CCAM runs. The finer spatial scale of dynamic downscaling is required as typical GCM spatial resolutions of 200 to 500 km are larger than TCs, hence GCM-modelled TCs are wider and less intense than observed TCs.

The CCAM simulations account for projected changes in TC occurrence, genesis and decay characteristics but are still too coarse to adequately assess changes to TC intensity as they do not resolve the TC eyewall where the strongest winds and heaviest rainfalls occur. RAMS was applied to one of the CCAM results at a 5 km resolution to resolve such characteristics on an event basis for 120 TC-like vortices in current and future periods. CCAM reproduced the historical patterns of spatial TC occurrence in the Australian region, accounting for the different spatial patterns seen during El Niño and La Niña events. Although the spatial patterns are reproduced, too few TCs are simulated by CCAM so that the frequencies are underestimated by approximately 40%. CCAM downscaling for seven CMIP3 GCMs for the A2 scenario consistently simulate fewer TCs in the north-west region for the period 2051 to 2090 than in 1971 to 2000, on average a 50% decline in the number of TCs. These simulations also show a small decrease in duration (0.6 days) and an approximately 100 km southward shift in genesis and decay regions. Assessment of the projected intensity changes simulated by the RAMS 5 km downscaling for 2051 to 2090, relative to 1961 to 2000, focused on the storm characteristics for the 12 hours centred on the period of maximum TC intensity (i.e. minimum pressure). These show projected increases in the size and intensity of TCs with the proportion of TCs with a maximum wind speed greater than 40 m/second (approximately Category 3 to 5), the integrated kinetic energy (a measure of TC size and wind speed), the radius of maximum winds, and the radius to gale-force winds all increasing. Rainfall intensity in the 12-hour periods simulated increased 33% within 300 km of the TC centre and 23% within 200 km (IOCI, 2012).

While one recent study, downscaling six CMIP5 GCMs, concluded the frequency of TCs could increase throughout the 21st century (Emanuel, 2013), many more CMIP3 and CMIP5 studies concur with CSIRO findings of fewer but more intense TCs in the future (Bell et al., 2013; Gleixner et al., 2014; Murakami et al., 2014; Roberts et al., 2015; Scoccimarro et al., 2014; Tory et al., 2013). Thus, the weight of current understanding supports decreases in the frequency of TCs impacting the Assessment area as more likely than increases. However uncertainties remain, for example research investigating Atlantic TCs suggests atmospheric aerosols from industrial pollution may have suppressed storm development in the 20th century and thus decreasing pollution could lead to an increased frequency of TCs in the future (Dunstone et al., 2013). There are currently no equivalent studies of aerosol impacts on TCs for the Australian region.

Part IV Discussion and Summary



7 Discussion

7.1 Establishment of an appropriate hydroclimate baseline

The allocation of water and the design and planning of water resource infrastructure and systems requires great care and consideration and needs to take a genuine long-term view. A poorly considered design can result in an unsustainable system or preclude the development of a more suitable and possibly larger sustainable system, thus adversely impacting existing and future users, industries and the environment. Once water is overallocated it is economically, financially, socially and political difficult to reduce allocations in the future. Many water resource investments, particularly agricultural investments, require long time frames (e.g. greater than 30 years) as there are often large initial infrastructure costs and a long learning period before full production potential is realised. Consequently, investors require certainty that over their investment time frame (and potentially beyond), their access to water will remain at the level of reliability initially allocated. A key consideration in the development of a water resource plan, or in the assessment of the water resources of a catchment, is the time period over which the water resources will be analysed, also referred to as the hydroclimate 'baseline' (e.g. Chiew et al. (2009a)).

If the hydroclimate baseline is too short it can introduce biases in a water resource assessment, for various reasons. Firstly, the transformation of rainfall to runoff and rainfall to groundwater recharge is non-linear. For example, averaged across the Flinders catchment in northern Australia the mean annual rainfall is only 8% higher than the median annual rainfall, yet the mean annual runoff is 59% higher than the median annual runoff (data sourced (Lerat et al., 2013)). Similarly, between 1895 and 1945 the median annual rainfall was the same as the median annual rainfall between 1948 and 1987 (less than 0.5% difference), yet there was a 21% difference in the median annual runoff between these two time periods (and a 40% difference in the mean annual runoff) (Lerat et al., 2013). Consequently, great care is required if using rainfall data alone to justify the use of short periods over which to analyse the water resources of a catchment.

In developing a water resource plan the amount of water allocated for consumptive purposes is usually constrained by the drier years (referred to as spells where consecutive dry years occur) in the historical record. This is because it is usually during dry spells that water extraction most adversely impacts on existing industries and the environment. All other factors being equal (e.g. market demand, interest rates), consecutive dry years are usually also the most limiting time periods for new water resource developments/investments, such as irrigated agriculture enterprises, particularly if the dry spells coincide with the start of an investment cycle.

Consequently, it is important to ensure a representative range of dry spells (i.e. of different durations, magnitudes and sequencing) are captured over the Assessment time period. For example, it is possible that two time periods may have very similar median annual runoff, but the duration, magnitude and sequencing of the dry spells may be sufficiently different that they pose different risks to investors and result in different modelled ecological outcomes. By way of example, Figure 7-1 shows two consecutive 30-year periods of (water year) annual runoff in the Flinders catchment, 1942 to 1971 (inclusive) and 1972 to 2001 (inclusive). Both time periods have a median annual runoff of 25 mm averaged across the catchment, but they have quite a different

pattern of wet and dry spells. In the first 30-year time period (1942 to 1971) the dry run length, a characteristic measure of the length of dry spells in a time series (Equation 1), is 2.8, while in the second 30-year time period (1972 to 2001) the dry run length is 8.3, considerably higher than the first.

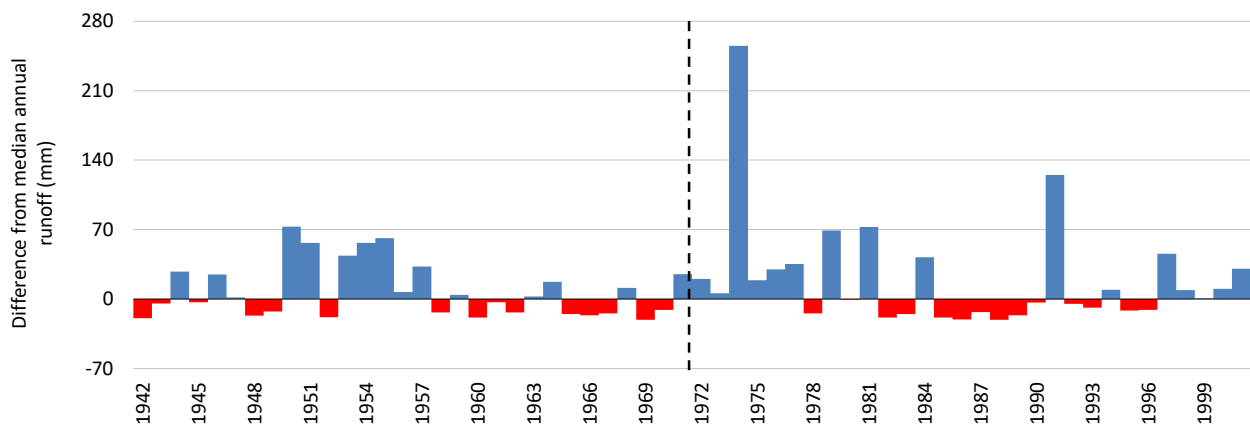


Figure 7-1 Wet and dry spells of catchment average runoff across the Flinders catchment over a 60-year period

Wet spells (blue columns) are single or consecutive years where annual runoff is greater than median annual runoff. Dry spells (red columns) are single or consecutive years where annual runoff is less than median annual runoff. Median annual runoff was calculated over the entire historical record (1890 to 2015). Vertical dashed line (year 1971) indicates the end and start of the two consecutive 30-year periods. Both 30-year periods have a median annual runoff of 25 mm. Data sourced from (Lerat et al., 2013).

Thirdly in those instances where there is the potential for a long memory, such as occurs in intermediate and regional-scale groundwater systems or in river systems with large reservoirs, long periods of record are preferable so as to minimise the influence of initial starting conditions (e.g. assumptions regarding initial reservoir storage volume) and to properly assess the reliability of water supply from large storages and to encapsulate the range of likely conditions (McMahon and Adeloye, 2005).

All of these arguments favour using as long a time period as practically possible. However, there may be some circumstances in which a shorter period may be preferable on the basis that it is a more conservative option. For example, in south-west Western Australia, water resource assessments to support water resource planning are typically assessed from 1975 onwards (Chiew et al., 2012; McFarlane et al., 2012). This is because since the mid-1970s there has been a marked reduction in runoff in south-western Australia, and this declining trend in rainfall is consistent with the majority of global climate model (GCM) projections, which project reductions of rainfall into the future (Charles et al., 2010). Adopting this time period is supported by multiple lines of evidence and is a more conservative option than selecting the entire available period of record, which may result in the overallocation of water if current rainfall patterns continue into the future. Another rationale for using a shorter period of time is where there is little confidence in the early instrument rainfall record. Although there were few rainfall stations in the three study areas at the turn of the 20th century (Section 1.3 and figures therein) relative to current, an exploratory analysis of rainfall statistics of the early period of instrument record do not appear to be anomalous when compared to the longer term instrument record.

In deciding upon an appropriate time period over which to analyse the water resources of the Victoria, Roper and Southern Gulf catchments, consideration was given to the above arguments, as well as palaeoclimate records, observed trends in the historical instrumental rainfall data and

future climate projections. Although the statistically significant increasing trends in some rainfall stations in the Victoria and Roper catchments suggest consideration of using only the more recent instrument record, these trends are only evident since 1990 and it is inappropriate to place too much weight on trends of only short duration (i.e. several decades).

In support, palaeoclimate records indicate multiple wetter and drier periods have occurred in the recent geological past (Section 2.5). Furthermore 28, 28 and 44% of Coupled Model Intercomparison Project (CMIP6) GCM-PS in the Victoria, Roper and Southern Gulf catchments, respectively, project a 'drier' climate than the 1975 to 2005 time period. For these reasons it is recommended that the entire instrument record (i.e. 1890 to 2015) be used for assessing the water resources of these catchments as this is most likely to best capture the full range of potential dry spells, which are critical to assessing the profitability of water resource related developments.

The adoption of an 1890 to 2022 hydroclimate baseline for Victoria and Southern Gulf catchments and 1910 to 2019 hydroclimate baseline for the Roper catchment follows the general principles that hydrological planning should use as long a hydroclimate sequence as possible to encapsulate the range of likely/plausible conditions and variability at different time scales (Chiew et al., 2012; Chiew et al., 2009a). It should be noted, however, that as climate is changing on a variety of time scales, detailed scenario modelling and planning (i.e. the design of major water infrastructure) should be broader than just comparing a single hydroclimate baseline to an alternative future.

8 Summary remarks

Climate variables, water availability and soil data, are generally considered to be the most important environmental information for determining the agricultural suitability of particular locations. Understanding of climate and its variability is especially important for water resource and agricultural assessments in semi-arid and subtropical parts of northern Australia given climate drives hydrology and water availability.

Defining the water year as 1 September to 31 August, climate data for the Assessment were assembled for the Victoria (NT), Roper (NT) and Southern Gulf (Queensland) catchments using daily gridded scientific information for land owners (SILO) data (Jeffrey et al., 2001). Data from 1 September 1890 to 31 August 2022 were used in the Victoria and Southern Gulf catchments and data from 1 September 1910 to 31 August 2019 were used in the Roper catchment. These datasets are referred to herein as the historical period or Scenario A. These data were acquired primarily for preparing a consistent set of input climate data files for the hydrological, agricultural and ecological numerical models being used by other activities in the Assessment (Preface Figure 1).

The Assessment is primarily focused on assessing the opportunity for water resource development, and more specifically irrigation, with currently available environmental resources. However, given the changes in temperature and rainfall projected in the coming decades, and the sensitivity of Australian agriculture (and the natural resource base on which it depends) to that change, the effects of climate change form part of the Assessment. To this end, information from GCM projections were used to produce climate data reflecting the SSP2-4.5 scenario world where the global mean surface air temperatures are 1.6 °C higher (range 1.0 to 1.9 °C) relative to approximately the year 1990 global temperatures. These synthetic future climate data will be used as input to the hydrological, agricultural and ecological numerical models used in the Assessment.

In collating and manipulating these climate data for use by the numerical models, climate statistics and maps were prepared for the Victoria, Roper and Southern Gulf catchments.

Climate data availability

Compared to equivalent-sized catchments in southern Australia the Victoria, Roper and Southern Gulf catchments have about a factor of ten less stations. This reduces the certainty in hydrological modelling, however the density of rainfall stations in the three study areas is considered adequate for water resource planning purposes. Because non-rainfall climate parameters have a higher spatial and temporal auto-correlation than rainfall there is a much lower density of stations recording these variables across northern Australia. This lack of stations measuring non-rainfall climate variables is a limitation for agronomists trying to assess local-scale conditions for growth and yield potential of crops, pastures and trees.

Key rainfall statistics

The mean annual rainfall for the Victoria, Roper and Southern Gulf catchments was 681 mm, 792 mm and 602 mm, respectively. These values are averaged over the 132-year historical period (September 1890 to August 2022) for the Victoria and Southern Gulf catchments and over the

109-year historical period (September 1910 to August 2019) for the Roper catchment. Of this 95, 96 and 94% was calculated as falling during the wet season (1 November to 30 April) in the three catchments respectively. The highest median monthly rainfall in all three study areas occurred during the months of January and February and the months with the lowest median rainfall were July and August.

Primary rainfall-generating mechanisms

The annual northern Australian wet season is due to the Australian summer monsoon, the predominant large-scale circulation process that influences the Australian tropics. The key rainfall-generating mechanisms across northern Australia are monsoonal rainfall, tropical cyclones (TCs) and tropical depressions, and heat lows and thunderstorms. These rainfall mechanisms are interrelated and the proportion of total rainfall produced by each varies between the three study areas.

The southern hemisphere TC season generally runs from November to April. TCs can be a major contributor to large-scale rainfall in many years (i.e. typically producing 200 to 500 mm over the space of 2–5-day period where they cross the coast).

Variability in rainfall

Particularly distinctive characteristics of northern Australia's climate are: (i) the high seasonality of rainfall and temperature driven by the annual solar cycle determining the position of the high pressure belt (subtropical ridge) and associated monsoon processes, and (ii) the high inter-annual variability of rainfall, which is attributed to the strong connection of rainfall to the El Niño–Southern Oscillation (ENSO), whose primary phases El Niño (synonymous with drought in much of Australia) and La Niña have their impact modulated by the Indian Ocean dipole (IOD) and the Interdecadal Pacific Oscillation (IPO). The complex interactions of these phenomena results in highly variable and irregular patterns of rainfall at the inter-annual and inter-decadal scales.

The inter-annual variability of rainfall in the Victoria, Roper and Southern Gulf catchments is moderately high compared to other rainfall stations in northern Australia and high compared to other rainfall stations around Australia with the same mean annual rainfall.

The rainfall-generating systems in northern Australia and their modes of variability combine to produce irregular periods of runs of dry and wet years. The length and magnitude of dry spells, in particular, strongly influences the scale, profitability and risk of water resource related investments. The duration of dry spells (i.e. consecutive years of annual rainfall below the median annual rainfall) in the Victoria, Roper and Southern Gulf catchments is comparable to other areas of eastern Australia and does not appear unusual. The run magnitude of dry years at rainfall stations in the Victoria, Roper and Southern Gulf catchments is slightly larger than that of stations in the Murray–Darling Basin and the east coast of Australia.

Trends in rainfall and temperature

Of 12 long-term rainfall stations analysed as part of the Assessment (four in each catchment), six were found to have an increasing trend in rainfall over the historical period, with the increase usually occurring between 1960 and 1990. These observations are generally consistent with the literature which indicates a statistically significant increasing trend in rainfall over the 'Top End'.

Potential evaporation

Potential evaporation (PE) in the Victoria, Roper and Southern Gulf catchments exceeds 1900, 1800 and 1900 mm respectively in most years. It exhibits a strong seasonal pattern, ranging from 200 mm/month during the build-up (October to December), to about 100 mm/month during the middle of the dry season (June). Mean annual rainfall deficits (i.e. difference between annual rainfall and annual PE) are large (~1250 mm) in the Victoria catchment, moderate in the Roper catchment (~1090 mm) and large in the Southern Gulf catchments (~1300 mm). High rainfall deficits adversely affect surface water storages. This is discussed in more detail in the companion technical report on water storage (Petheram et al., 2022) (see Preface Figure 1).

Palaeoclimate records for northern Australia

Given the instrument record, particularly in northern Australia, is very short in a geological sense, a brief review of palaeoclimate data was provided. The literature indicates that circulation patterns approximating the present climate conditions in northern Australia (e.g. Pacific circulation responsible for ENSO) are thought to have been in place since about 3 to 2.5 million years ago, which would suggest many ecosystems in northern Australia have experienced monsoonal conditions for many millions of years. However, past climates have been both wetter and drier than the instrument record for northern Australia, and that the influence of ENSO has varied considerably over recent geological time. Several authors have found that present low levels of TC activity in northern Australia are possibly unprecedented over the past 550 to 1500 years and that the recurrence frequencies of high intensity TCs (Category 4–5 events) may have been an order of magnitude higher than that inferred from the current short instrumental records.

Future climate and sea-level change projections

Summarising the climate change projections derived in this report, for the:

- Victoria catchment, 25% of global climate model – pattern scaling (GCM-PS) indicated an increase in future mean annual rainfall, 28% indicated a decrease and 47% indicated a change that could be considered to be within internal variability of the models (i.e. $\pm 5\%$ of historical rainfall)
- Roper catchment, 16% of GCM-PS indicated an increase in future mean annual rainfall, 28% indicated a decrease and 56% indicated a change that could be considered to be within internal variability of the models (i.e. $\pm 5\%$ of historical rainfall)
- Southern Gulf catchments, 16% of GCM-PS indicated an increase in future mean annual rainfall, 44% of indicated a decrease and 40% indicated a change that could be considered to be within internal variability of the models (i.e. $\pm 5\%$ of historical rainfall).

Based on the weight of current understanding, the global frequency of TCs will either decrease or remain essentially unchanged owing to greenhouse warming, though there is very low confidence in projected changes in cyclone frequency for individual catchments. Under 21st century warming the current consensus is that some increase in the mean maximum wind speed of TCs is likely (+2 to +11% globally), although increases may not occur in all tropical regions.

There has been significant improvement in understanding and projection of sea-level change in recent years. For the period 2081 to 2100 relative to 1986 to 2005, the Intergovernmental Panel

on Climate Change (IPCC) AR5 reports that global mean sea levels will most likely rise between 0.26 to 0.55 m under RCP2.6, and between 0.45 to 0.82 m under RCP8.5. There is high confidence that sea levels will continue to rise for centuries even if the global mean temperature is stabilised in the short to medium term.

Hydroclimate baseline

Although the statistically significant increasing trends in some rainfall stations in the Victoria and Roper catchments suggest consideration of using only the more recent instrument record, these trends are only evident since 1990. In support, palaeoclimate records indicate multiple wetter and drier periods have occurred in the recent geological past (Section 2.5). Furthermore, 25, 16 and 16% of Coupled Model Intercomparison Project (CMIP6) GCM-PS for SSP2-4.5 in the Victoria, Roper and Southern Gulf catchments respectively project a 'wetter' climate than the 1975 to 2005 time period. For these reasons it is recommended that the entire instrument record be used for assessing the water resources of these three catchments. This follows the general principles that hydrological planning should use as long a hydroclimate sequence as possible to encapsulate the range of likely/plausible conditions and variability at different time scales.

References

- Abbs D (2012) The impact of climate change on the climatology of tropical cyclones in the Australian region. CSIRO Climate Adaptation Flagship Working paper No. 11.
- Allen JT and Karoly DJ (2013) A climatology of Australian severe thunderstorm environments 1979–2011: inter-annual variability and ENSO influence. *International Journal of Climatology*, n/a-n/a. DOI: 10.1002/joc.3667.
- Allen JT, Karoly DJ and Walsh KJ (2014a) Future Australian Severe Thunderstorm Environments. Part I: A Novel Evaluation and Climatology of Convective Parameters from Two Climate Models for the Late Twentieth Century. *Journal of Climate* 27(10), 3827–3847. DOI: 10.1175/JCLI-D-13-00425.1.
- Allen JT, Karoly DJ and Walsh KJ (2014b) Future Australian Severe Thunderstorm Environments. Part II: The Influence of a Strongly Warming Climate on Convective Environments. *Journal of Climate* 27(10), 3848–3868. DOI: 10.1175/JCLI-D-13-00426.1.
- Andréassian V, Perrin C and Michel C (2004) Impact of imperfect potential evapotranspiration knowledge on the efficiency and parameters of watershed models. *Journal of Hydrology* 286(1–4), 19–35. DOI: <http://dx.doi.org/10.1016/j.jhydrol.2003.09.030>.
- Arnup SJ and Reeder MJ (2007) The diurnal and seasonal variation of the northern Australian dryline. *Monthly Weather Review* 135(8), 2995–3008.
- Ashok K, Behera SK, Rao SA, Weng H and Yamagata T (2007) El Niño Modoki and its possible teleconnection. *Journal of Geophysical Research: Oceans* 112(C11), n/a-n/a. DOI: 10.1029/2006JC003798.
- Australian Academy of Science (2021) The risks to Australia of a 3°C warmer world. Australian Academy of Science. Available online: <https://www.science.org.au/files/userfiles/support/reports-and-plans/2021/risks-australia-three-deg-warmer-world-report.pdf>.
- Australian Bureau of Agricultural and Resource Economics (2022) Land use of Australia 2010–11 to 2015–2016, 250 m. Australian Bureau of Agricultural and Resource Economics and Sciences, Canberra, CC BY 4.0. Accessed 9 May 2023. Available online: <https://www.agriculture.gov.au/abares/aclump/land-use/data-download> >.
- Australian Bureau of Statistics (2021) Search census data. Accessed 9 May 2023. Available online: <https://www.abs.gov.au/census/find-census-data/search-by-area>.
- Behera SK and Yamagata T (2003) Influence of the Indian Ocean Dipole on the Southern Oscillation. *Journal of the Meteorological Society of Japan. Ser. II* 81(1), 169–177. DOI: 10.2151/jmsj.81.169.
- Bell R, Strachan J, Vidale PL, Hodges K and Roberts M (2013) Response of Tropical Cyclones to Idealized Climate Change Experiments in a Global High-Resolution Coupled General Circulation Model. *Journal of Climate* 26(20), 7966–7980. DOI: 10.1175/JCLI-D-12-00749.1.

- Berg P, Moseley C and Haerter JO (2013) Strong increase in convective precipitation in response to higher temperatures. *Nature Geosci* 6(3), 181-185. DOI: 10.1038/ngeo1731.
- Bowler JM, Wyrwoll K-H and Lu Y (2001) Variations of the northwest Australian summer monsoon over the last 300,000 years: the palaeohydrological record of the Gregory (Mulan) Lakes System. *Quaternary International* 83–85, 63-80. DOI: [http://dx.doi.org/10.1016/S1040-6182\(01\)00031-3](http://dx.doi.org/10.1016/S1040-6182(01)00031-3).
- Bowman DMJS, Brown GK, Braby MF, Brown JR, Cook LG, Crisp MD, Ford F, Haberle S, Hughes J, Isagi Y, Joseph L, McBride J, Nelson G and Ladiges PY (2010) Biogeography of the Australian monsoon tropics. *Journal of Biogeography* 37(2), 201-216. DOI: 10.1111/j.1365-2699.2009.02210.x.
- Budget Strategy and Outlook (2024) Budget 2024-25. A future made in Australia. Viewed 11 September 2024, <https://budget.gov.au/content/factsheets/download/factsheet-fmia.pdf>.
- Burrows MA, Fenner J and Haberle SG (2014) Humification in northeast Australia: Dating millennial and centennial scale climate variability in the late Holocene. *The Holocene*. DOI: 10.1177/0959683614551216.
- Cai W and Cowan T (2009) La Niña Modoki impacts Australia autumn rainfall variability. *Geophysical Research Letters* 36(12). DOI: 10.1029/2009GL037885.
- Cai W, Cowan T and Sullivan A (2009a) Recent unprecedented skewness towards positive Indian Ocean Dipole occurrences and its impact on Australian rainfall. *Geophysical Research Letters* 36(11). DOI: 10.1029/2009GL037604.
- Cai W, Cowan T, Sullivan A, Ribbe J and Shi G (2011a) Are Anthropogenic Aerosols Responsible for the Northwest Australia Summer Rainfall Increase? A CMIP3 Perspective and Implications. *Journal of Climate* 24(10), 2556-2564. DOI: 10.1175/2010jcli3832.1.
- Cai W, Sullivan A and Cowan T (2009b) Rainfall Teleconnections with Indo-Pacific Variability in the WCRP CMIP3 Models. *Journal of Climate* 22(19), 5046-5071. DOI: 10.1175/2009JCLI2694.1.
- Cai W, van Rensch P, Cowan T and Hendon HH (2011b) Teleconnection Pathways of ENSO and the IOD and the Mechanisms for Impacts on Australian Rainfall. *Journal of Climate* 24(15), 3910-3923. DOI: 10.1175/2011JCLI4129.1.
- Cai W, van Rensch P, Cowan T and Sullivan A (2010) Asymmetry in ENSO Teleconnection with Regional Rainfall, Its Multidecadal Variability, and Impact. *Journal of Climate* 23(18), 4944-4955. DOI: 10.1175/2010JCLI3501.1.
- Cai W, Whetton HP and Pittock BA (2001) Fluctuations of the relationship between ENSO and northeast Australian rainfall. *Climate Dynamics* 17(5), 421-432. DOI: 10.1007/pl00013738.
- Chand SS, Tory KJ, McBride JL, Wheeler MC, Dare RA and Walsh KJE (2013) The Different Impact of Positive-Neutral and Negative-Neutral ENSO Regimes on Australian Tropical Cyclones. *Journal of Climate* 26(20), 8008-8016. DOI: 10.1175/JCLI-D-12-00769.1.
- Charles S, Silberstein R, Teng J, Fu G, Hodgson G, Gabrovsek C, Crute J, Chiew F, Smith I, Kirono D, Bathols J, Li L, Yang A, Donohue R, Marvanek S, McVicar T, Van Niel T and Cai W (2010) Climate analyses for south-west Western Australia. A report to the Australian Government from the CSIRO South-West Western Australia Sustainable Yields Project. CSIRO, Australia.

- Charles SP, Fu G, Silberstein RP, Mpelasoka F, McFarlane D, Hodgson G, Teng J, Gabrovsek C, Ali R, Barron O, Aryal SK and Dawes W (2015) Hydroclimate of the Pilbara: past, present and future. A technical report to the Government of Western Australian and industry partners from the CSIRO Pilbara Water Resource Assessment. CSIRO Land and Water Flagship, Australia.
- Chiew F, Post D and Moran R (2012) Hydroclimate baseline and future water availability projections for water resources planning. 34th Hydrology and Water Resources Symposium 2012, Sydney, NSW, 19-22 November 2012. Barton, ACT: Engineers Australia. 461-468.
- Chiew FHS, Cai W and Smith IN (2009a) Advice on defining climate scenarios for use in Murray-Darling Basin Authority Basin Plan modelling, CSIRO report for the Murray-Darling Basin Authority.
- Chiew FHS, Kirono DGC, Kent DM, Frost AJ, Charles SP, Timbal B, Nguyen KC and Fu G (2010) Comparison of runoff modelled using rainfall from different downscaling methods for historical and future climates. *Journal of Hydrology* 387(1–2), 10-23. DOI: <http://dx.doi.org/10.1016/j.jhydrol.2010.03.025>.
- Chiew FHS, Teng J, Vaze J, Post DA, Perraud JM, Kirono DGC and Viney NR (2009b) Estimating climate change impact on runoff across southeast Australia: Method, results, and implications of the modeling method. *Water Resources Research* 45(10), W10414. DOI: 10.1029/2008WR007338.
- Church JA, McInnes KL, Monselesan D and O'Grady J (2016) Sea-Level Rise and Allowances for Coastal Councils around Australia – Guidance Material. CSIRO Report 64 pp.
- Cleugh HA, Miller JM and Böhm M (1998) Direct mechanical effects of wind on crops. *Agroforestry Systems* 41(1), 85-112. DOI: 10.1023/a:1006067721039.
- Collins M, An S-I, Cai W, Ganachaud A, Guilyardi E, Jin F-F, Jochum M, Lengaigne M, Power S, Timmermann A, Vecchi G and Wittenberg A (2010) The impact of global warming on the tropical Pacific Ocean and El Nino. *Nature Geosci* 3(6), 391-397.
- Cook GD and Heerdegen RG (2001) Spatial variation in the duration of the rainy season in monsoonal Australia. *International Journal of Climatology* 21(14), 1723-1732. DOI: 10.1002/joc.704.
- Crosbie RS, Pollock DW, Mpelasoka FS, Barron OV, Charles SP and Donn MJ (2012) Changes in Köppen-Geiger climate types under a future climate for Australia: hydrological implications. *Hydrol. Earth Syst. Sci.* 16(9), 3341-3349. DOI: 10.5194/hess-16-3341-2012.
- CSIRO (2009a) Water in the Fitzroy region, pp 61-128 in CSIRO (2009) Water in the Timor Sea Drainage Division. A report to the Australian Government from the CSIRO Northern Australia Sustainable Yields Project. CSIRO Water for a Healthy Country Flagship, Australia. xl + 508pp.
- CSIRO (2009b) Water in the Mitchell region, pp 347-416 in CSIRO (2009) Water in the Gulf of Carpentaria Drainage Division. A report to the Australian Government from the CSIRO Northern Australia Sustainable Yields Project. CSIRO Water for a Healthy Country Flagship, Australia. xl + 479pp.

- CSIRO (2009c) Water in the Van Diemen region, pp 363-452 in CSIRO (2009) Water in the Timor Sea Drainage Division. A report to the Australian Government from the CSIRO Northern Australia Sustainable Yields Project. CSIRO Water for a Healthy Country Flagship, Australia. xl + 508pp.
- CSIRO and Bureau of Meteorology (2015) Climate Change in Australia Information for Australia's Natural Resource Management Regions: Technical Report. CSIRO and Bureau of Meteorology, Australia.
- Dare RA (2013) Seasonal Tropical Cyclone Rain Volumes over Australia. *Journal of Climate* 26(16), 5958-5964. DOI: 10.1175/JCLI-D-12-00778.1.
- Dare RA, Davidson NE and McBride JL (2012) Tropical Cyclone Contribution to Rainfall over Australia. *Monthly Weather Review* 140(11), 3606-3619. DOI: 10.1175/MWR-D-11-00340.1.
- De Deckker P, Barrows TT and Rogers J (2014) Land–sea correlations in the Australian region: post-glacial onset of the monsoon in northwestern Western Australia. *Quaternary Science Reviews* 105, 181-194. DOI: <http://dx.doi.org/10.1016/j.quascirev.2014.09.030>.
- Denniston RF, Villarini G, Gonzales AN, Wyrwoll K-H, Polyak VJ, Ummenhofer CC, Lachniet MS, Wanamaker AD, Humphreys WF, Woods D and Cugley J (2015) Extreme rainfall activity in the Australian tropics reflects changes in the El Niño/Southern Oscillation over the last two millennia. *Proceedings of the National Academy of Sciences* 112(15), 4576-4581. DOI: 10.1073/pnas.1422270112.
- Denniston RF, Wyrwoll K-H, Polyak VJ, Brown JR, Asmerom Y, Wanamaker Jr AD, LaPointe Z, Ellerbroek R, Barthelmes M, Cleary D, Cugley J, Woods D and Humphreys WF (2013) A Stalagmite record of Holocene Indonesian–Australian summer monsoon variability from the Australian tropics. *Quaternary Science Reviews* 78, 155-168. DOI: <http://dx.doi.org/10.1016/j.quascirev.2013.08.004>.
- Department of Agriculture, Water and the Environment (2020) CAPAD2020 Terrestrial. Creative Commons Attribution 3.0 Australian License. Viewed 17/04/2023. (<http://www.environment.gov.au/fed/catalog/search/resource/downloadData.page?uuid=%7B4448CACD-9DA8-43D1-A48F-48149FD5FCFD%7D>).
- Department of State Development, Manufacturing, Infrastructure and Planning (2019) North west Queensland economic diversification strategy 2019. Viewed 12 September 2024, <https://www.statedevelopment.qld.gov.au/regions/regional-priorities/a-strong-and-prosperous-north-west-queensland/north-west-queensland-economic-diversification-strategy>.
- Dowdy A and Kuleshov Y (2012) An analysis of tropical cyclone occurrence in the Southern Hemisphere derived from a new satellite-era data set. *International Journal of Remote Sensing* 33(23), 7382-7397. DOI: 10.1080/01431161.2012.685986.
- Dowdy AJ (2014) Long-term changes in Australian tropical cyclone numbers. *Atmospheric Science Letters* 15(4), 292-298. DOI: 10.1002/asl2.502.
- Dowdy AJ (2016) Seasonal forecasting of lightning and thunderstorm activity in tropical and temperate regions of the world. *Scientific Reports* 6, 20874. DOI: 10.1038/srep20874 <http://www.nature.com/articles/srep20874#supplementary-information>.

- Dowdy AJ and Kuleshov Y (2014) Climatology of lightning activity in Australia: spatial and seasonal variability. *Australian Meteorological and Oceanographic Journal* 64, 103-108.
- Dracup JA, Lee KS and Paulson EG (1980) On the definition of droughts. *Water Resources Research* 16(2), 297-302. DOI: 10.1029/WR016i002p00297.
- Drosowsky W and Wheeler MC (2014) Predicting the Onset of the North Australian Wet Season with the POAMA Dynamical Prediction System. *Weather and Forecasting* 29(1), 150-161. DOI: 10.1175/WAF-D-13-00091.1.
- Dunstone NJ, Smith DM, Booth BBB, Hermanson L and Eade R (2013) Anthropogenic aerosol forcing of Atlantic tropical storms. *Nature Geosci* 6(7), 534-539. DOI: 10.1038/ngeo1854.
- Emanuel KA (2013) Downscaling CMIP5 climate models shows increased tropical cyclone activity over the 21st century. *Proceedings of the National Academy of Sciences*. DOI: 10.1073/pnas.1301293110.
- Evans S, Marchand R and Ackerman T (2014) Variability of the Australian Monsoon and Precipitation Trends at Darwin. *Journal of Climate* 27(22), 8487-8500. DOI: 10.1175/JCLI-D-13-00422.1.
- Forsyth AJ, Nott J and Bateman MD (2010) Beach ridge plain evidence of a variable late-Holocene tropical cyclone climate, North Queensland, Australia. *Palaeogeography, Palaeoclimatology, Palaeoecology* 297(3-4), 707-716. DOI: <http://dx.doi.org/10.1016/j.palaeo.2010.09.024>.
- Fowler HJ, Ekström M, Blenkinsop S and Smith AP (2007) Estimating change in extreme European precipitation using a multimodel ensemble. *Journal of Geophysical Research: Atmospheres* 112(D18), n/a-n/a. DOI: 10.1029/2007JD008619.
- Gagan MK, Hendy EJ, Haberle SG and Hantoro WS (2004) Post-glacial evolution of the Indo-Pacific Warm Pool and El Niño-Southern oscillation. *Quaternary International* 118-119, 127-143. DOI: [http://dx.doi.org/10.1016/S1040-6182\(03\)00134-4](http://dx.doi.org/10.1016/S1040-6182(03)00134-4).
- Gallant AJE, Phipps SJ, Karoly DJ, Mullan AB and Lorrey AM (2013a) Nonstationary Australasian Teleconnections and Implications for Paleoclimate Reconstructions. *Journal of Climate* 26(22), 8827-8849. DOI: 10.1175/JCLI-D-12-00338.1.
- Gallant AJE, Reeder MJ, Risbey JS and Hennessy KJ (2013b) The characteristics of seasonal-scale droughts in Australia, 1911-2009. *International Journal of Climatology* 33(7), 1658-1672. DOI: 10.1002/joc.3540.
- Garnett ST and Williamson G (2010) Spatial and temporal variation in precipitation at the start of the rainy season in tropical Australia. *The Rangeland Journal* 32(2), 215-226. DOI: <http://dx.doi.org/10.1071/RJ09083>.
- Gleixner S, Keenlyside N, Hodges K, Tseng W-L and Bengtsson L (2014) An inter-hemispheric comparison of the tropical storm response to global warming. *Climate Dynamics* 42(7-8), 2147-2157. DOI: 10.1007/s00382-013-1914-6.
- Goler R, Reeder MJ, Smith RK, Richter H, Arnup S, Keenan T, May P and Hacker J (2006) Low-Level Convergence Lines over Northeastern Australia. Part I: The North Australian Cloud Line. *Monthly Weather Review* 134(11), 3092-3108. DOI: 10.1175/MWR3239.1.

- Grant AP and Walsh KJE (2001) Interdecadal variability in north-east Australian tropical cyclone formation. *Atmospheric Science Letters* 2(1), 9-17. DOI: <http://dx.doi.org/10.1006/asle.2001.0029>.
- Griffiths ML, Drysdale RN, Gagan MK, Zhao JX, Ayliffe LK, Hellstrom JC, Hantoro WS, Frisia S, Feng YX, Cartwright I, Pierre ES, Fischer MJ and Suwargadi BW (2009) Increasing Australian-Indonesian monsoon rainfall linked to early Holocene sea-level rise. *Nature Geosci* 2(9), 636-639. DOI: http://www.nature.com/ngeo/journal/v2/n9/supinfo/ngeo605_S1.html.
- Grose MR, Narsey S, Delage FP, Dowdy AJ, Bador M, Boschat G, Chung C, Kajtar JB, Rauniyar S, Freund MB, Lyu K, Rashid H, Zhang X, Wales S, Trenham C, Holbrook NJ, Cowan T, Alexander L, Arblaster JM and Power S (2020) Insights From CMIP6 for Australia's Future Climate. *Earth's Future* 8(5), e2019EF001469. DOI: <https://doi.org/10.1029/2019EF001469>.
- Haig J, Nott J and Reichert G-J (2014) Australian tropical cyclone activity lower than at any time over the past 550-1,500 years. *Nature* 505(7485), 667-671. DOI: 10.1038/nature12882 <http://www.nature.com/nature/journal/v505/n7485/abs/nature12882.html#supplementary-information>.
- Hall JD, Matthews AJ and Karoly DJ (2001) The modulation of tropical cyclone activity in the Australian region by the Madden-Julian oscillation. *Monthly Weather Review* 129(12), 2970-2982. DOI: 10.1175/1520-0493(2001)129<2970:tmtoca>2.0.co;2.
- Harper BA, Stroud SA, McCormack M and West S (2008) A review of historical tropical cyclone intensity in Northwestern Australia and implications for climate change trend analysis. *Australian Meteorological Magazine* 57(2), 121-141.
- Hashimoto T, Stedinger JR and Loucks DP (1982) Reliability, resiliency, and vulnerability criteria for water resource system performance evaluation. *Water Resources Research* 18(1), 14-20. DOI: 10.1029/WR018i001p00014.
- Hausfather Z and Peters GP (2020) Emissions—the ‘business as usual’ story is misleading. *Nature* 577(7792), 618-620.
- Hobbs J (1998) Present climates of Australia and New Zealand. In: Hobbs J, Lindesay JA and Bridgman HA (eds), *Climates of the Southern Continents: Present, Past and Future*, Wiley.
- Hughes J, Yang A, Marvanek S, Wang B, Petheram C and Philip S (2023) River model calibration and scenario analysis for the Roper catchment. A technical report from the CSIRO Roper River Water Resource Assessment for the National Water Grid. CSIRO, Australia.
- Hughes L (2003) Climate change and Australia: Trends, projections and impacts. *Austral Ecology* 28(4), 423-443. DOI: 10.1046/j.1442-9993.2003.01300.x.
- IOCI (2012) Western Australia's Weather and Climate: A Synthesis of Indian Ocean Climate Initiative Stage 3 Research. Australia. Available online: <http://www.ioci.org.au/publications/io-ci-stage-3/cat_view/17-io-ci-stage-3/23-reports.html>.
- IPCC (2015) *Climate Change 2014: Synthesis Report. Contribution of Working Groups I, II and III to the Fifth Assessment Report of the Intergovernmental Panel on Climate Change* [Core Writing Team, R.K. Pachauri and L.A. Meyer (eds.)]. IPCC, Geneva, Switzerland, 151 pp.

- IPCC (2022) *Climate Change 2022: Impacts, Adaptation, and Vulnerability. Contribution of Working Group II to the Sixth Assessment Report of the Intergovernmental Panel on Climate Change*. Cambridge University Press. Cambridge University Press, Cambridge, UK and New York, NY, USA.
- Jeffrey SJ, Carter JO, Moodie KB and Beswick AR (2001) Using spatial interpolation to construct a comprehensive archive of Australian climate data. *Environmental Modelling and Software* 16, 309-330.
- Kiem AS and Franks SW (2004) Multi-decadal variability of drought risk, eastern Australia. *Hydrological Processes* 18(11), 2039-2050. DOI: 10.1002/hyp.1460.
- Kiladis GN, Wheeler MC, Haertel PT, Straub KH and Roundy PE (2009) Convectively coupled equatorial waves. *Reviews of Geophysics* 47(2), n/a-n/a. DOI: 10.1029/2008RG000266.
- Klingaman NP, Woolnough SJ and Syktus J (2013) On the drivers of inter-annual and decadal rainfall variability in Queensland, Australia. *International Journal of Climatology* 33(10), 2413-2430. DOI: 10.1002/joc.3593.
- Knapton A, Taylor AR, Petheram C and Crosbie RS (2023) An investigation into the effects of climate change and groundwater development scenarios on the water resources of the Roper catchment using two finite element groundwater flow models. A technical report from the CSIRO Roper River Water Resource Assessment for the National Water Grid. CSIRO, Australia.
- Knutson TR, McBride JL, Chan J, Emanuel K, Holland G, Landsea C, Held I, Kossin JP, Srivastava AK and Sugi M (2010) Tropical cyclones and climate change. *Nature Geosci* 3(3), 157-163. DOI: 10.1038/ngeo779.
- Köppen W (1936) Das geographische System der Klimate. In: Köppen W and Geiger G (eds), *Handbuch der Klimatologie*, 1. C. Gebr, Borntraeger, 1-44, 1936.
- Kuleshov Y (2012) Southern Hemisphere Tropical Cyclone Climatology. In: Wang S-Y (ed.), *Modern Climatology*. InTech, Croatia.
- Kuleshov Y, Fawcett R, Qi L, Trewin B, Jones D, McBride J and Ramsay H (2010) Trends in tropical cyclones in the South Indian Ocean and the South Pacific Ocean. *Journal of Geophysical Research: Atmospheres* 115(D1), D01101. DOI: 10.1029/2009JD012372.
- Kullgren K and Kim K-Y (2006) Physical mechanisms of the Australian summer monsoon: 1. Seasonal cycle. *Journal of Geophysical Research: Atmospheres* 111(D20), n/a-n/a. DOI: 10.1029/2005JD006807.
- Lavender SL (2016) A climatology of Australian heat low events. *International Journal of Climatology*, n/a-n/a. DOI: 10.1002/joc.4692.
- Lavender SL and Abbs DJ (2013) Trends in Australian rainfall: contribution of tropical cyclones and closed lows. *Climate Dynamics* 40(1-2), 317-326. DOI: 10.1007/s00382-012-1566-y.

- Lerat J, Egan C, Kim S, Gooda M, Loy A, Shao Q and Petheram C (2013) Calibration of river models for the Flinders and Gilbert catchments. A technical report to the Australian Government from the CSIRO Flinders and Gilbert Agricultural Resource Assessment, part of the North Queensland Irrigated Agriculture Strategy., CSIRO Water for a Healthy Country and Sustainable Agriculture flagships, Australia.
- Lewis SC and LeGrande AN (2015) Stability of ENSO and its tropical Pacific teleconnections over the Last Millennium. *Clim. Past* 11(10), 1347-1360. DOI: 10.5194/cp-11-1347-2015.
- Li J, Feng J and Li Y (2012) A possible cause of decreasing summer rainfall in northeast Australia. *International Journal of Climatology* 32(7), 995-1005. DOI: 10.1002/joc.2328.
- Li L, Donohue R, McVicar T, Van Niel T, Teng J, Potter N, Smith I, Kirono D, Bathols J, Cai W, Marvanek S, Gallant S, Chiew F and Frost A (2009) Climate data and their characterisation for hydrological scenario modelling across northern Australia. A report to the Australian Government from the CSIRO Northern Australia Sustainable Yields Project. CSIRO Water for a Healthy Country Flagship, Australia.
- Liu KS and Chan JCL (2012) Interannual variation of Southern Hemisphere tropical cyclone activity and seasonal forecast of tropical cyclone number in the Australian region. *International Journal of Climatology* 32(2), 190-202. DOI: 10.1002/joc.2259.
- Lo F, Wheeler MC, Meinke H and Donald A (2007) Probabilistic Forecasts of the Onset of the North Australian Wet Season. *Monthly Weather Review* 135(10), 3506-3520. DOI: 10.1175/MWR3473.1.
- Lough JM, Llewellyn LE, Lewis SE, Turney CSM, Palmer JG, Cook CG and Hogg AG (2014) Evidence for suppressed mid-Holocene northeastern Australian monsoon variability from coral luminescence. *Paleoceanography* 29(6), 581-594. DOI: 10.1002/2014PA002630.
- Madden RA and Julian PR (1972) Description of Global-Scale Circulation Cells in the Tropics with a 40–50 Day Period. *Journal of the Atmospheric Sciences* 29(6), 1109-1123. DOI: 10.1175/1520-0469(1972)029<1109:DOGSCC>2.0.CO;2.
- McBride J (1998) Indonesia, Papua New Guinea, and Tropical Australia: The Southern Hemisphere Monsoon. In: Karoly DJ and Vincent DG (eds), *Meteorology of the Southern Hemisphere*. American Meteorological Society, Boston, Mass.
- McBride JL and Nicholls N (1983) Seasonal Relationships between Australian Rainfall and the Southern Oscillation. *Monthly Weather Review* 111(10), 1998-2004. DOI: 10.1175/1520-0493(1983)111<1998:SRBARA>2.0.CO;2.
- McFarlane D, Stone R, Martens S, Thomas J, Silberstein R, Ali R and Hodgson G (2012) Climate change impacts on water yields and demands in south-western Australia. *Journal of Hydrology* 475, 488-498. DOI: <http://dx.doi.org/10.1016/j.jhydrol.2012.05.038>.
- McGowan H, Marx S, Moss P and Hammond A (2012) Evidence of ENSO mega-drought triggered collapse of prehistory Aboriginal society in northwest Australia. *Geophysical Research Letters* 39(22), n/a-n/a. DOI: 10.1029/2012GL053916.

- McGregor S, Timmermann A, England MH, Elison Timm O and Wittenberg AT (2013) Inferred changes in El Niño–Southern Oscillation variance over the past six centuries. *Clim. Past* 9(5), 2269-2284. DOI: 10.5194/cp-9-2269-2013.
- McInnes KL, Church J, Monselesan D, Hunter JR, O'Grady JG, Haigh ID and Zhang XB (2015) Information for Australian Impact and Adaptation Planning in response to Sea-level Rise. *Australian Meteorological and Oceanographic Journal* 65(1), 127-149.
- McMahon TA and Adeloje AJ (2005) *Water Resources Yield*. Water Resources Publications LLC, Colorado USA.
- McVicar TR, Van Niel TG, Li LT, Roderick ML, Rayner DP, Ricciardulli L and Donohue RJ (2008) Wind speed climatology and trends for Australia, 1975–2006: Capturing the stilling phenomenon and comparison with near-surface reanalysis output. *Geophysical Research Letters* 35(20), n/a-n/a. DOI: 10.1029/2008GL035627.
- Meynecke J-O and Lee SY (2011) Climate-coastal fisheries relationships and their spatial variation in Queensland, Australia. *Fisheries Research* 110(2), 365-376. DOI: <http://dx.doi.org/10.1016/j.fishres.2011.05.004>.
- Micevski T, Franks SW and Kuczera G (2006) Multidecadal variability in coastal eastern Australian flood data. *Journal of Hydrology* 327(1–2), 219-225. DOI: <http://dx.doi.org/10.1016/j.jhydrol.2005.11.017>.
- Mitchell TD (2003) Pattern Scaling: An Examination of the Accuracy of the Technique for Describing Future Climates. *Climatic Change* 60(3), 217-242. DOI: 10.1023/a:1026035305597.
- Morton FI (1983) Operational estimates of areal evapotranspiration and their significance to the science and practice of hydrology. *Journal of Hydrology* 66(1–4), 1-76. DOI: [http://dx.doi.org/10.1016/0022-1694\(83\)90177-4](http://dx.doi.org/10.1016/0022-1694(83)90177-4).
- Murakami H, Hsu P-C, Arakawa O and Li T (2014) Influence of Model Biases on Projected Future Changes in Tropical Cyclone Frequency of Occurrence*. *Journal of Climate* 27(5), 2159-2181. DOI: 10.1175/JCLI-D-13-00436.1.
- Negrón-Juárez R, Chambers J, Hurtt G, Annane B, Cocke S, Powell M, Stott M, Goosem S, Metcalfe D and Saatchi S (2014) Remote Sensing Assessment of Forest Disturbance across Complex Mountainous Terrain: The Pattern and Severity of Impacts of Tropical Cyclone Yasi on Australian Rainforests. *Remote Sensing* 6(6), 5633.
- Ng B, Walsh K and Lavender S (2015) The contribution of tropical cyclones to rainfall in northwest Australia. *International Journal of Climatology* 35(10), 2689-2697. DOI: 10.1002/joc.4148.
- Nicholls N, Drosowsky W and Lavery B (1997) Australian rainfall variability and change. *Weather* 52, 66-72.
- Noonan JA and Smith RK (1986) Sea-breeze circulations over Cape York Peninsula and the generation of Gulf of Carpentaria cloud line disturbances. *Journal of the Atmospheric Sciences* 43(16), 1679-1693.

- Nott J, Haig J, Neil H and Gillieson D (2007) Greater frequency variability of landfalling tropical cyclones at centennial compared to seasonal and decadal scales. *Earth and Planetary Science Letters* 255(3–4), 367-372. DOI: <http://dx.doi.org/10.1016/j.epsl.2006.12.023>.
- Nott JF and Jagger TH (2013) Deriving robust return periods for tropical cyclone inundations from sediments. *Geophysical Research Letters* 40(2), 370-373. DOI: 10.1029/2012GL054455.
- NT Government (2023) Territory Water Plan. A plan to deliver water security for all Territorians, now and into the future. Viewed 6 September 2024, https://watersecurity.nt.gov.au/__data/assets/pdf_file/0003/1247520/territory-water-plan.pdf.
- Paul PA and Munkvold GP (2005) Influence of Temperature and Relative Humidity on Sporulation of *Cercospora zeaе-maydis* and Expansion of Gray Leaf Spot Lesions on Maize Leaves. *Plant Disease* 89(6), 624-630. DOI: 10.1094/PD-89-0624.
- Peel MC, Finlayson BL and McMahon TA (2007) Updated world map of the Köppen-Geiger climate classification. *Hydrol. Earth Syst. Sci.* 11(5), 1633-1644. DOI: 10.5194/hess-11-1633-2007.
- Peel MC, McMahon TA and Pegram GGS (2005) Global analysis of runs of annual precipitation and runoff equal to or below the median: run magnitude and severity. *International Journal of Climatology* 25(5), 549-568. DOI: 10.1002/joc.1147.
- Peel MC, Pegram GGS and McMahon TA (2004) Global analysis of runs of annual precipitation and runoff equal to or below the median: run length. *International Journal of Climatology* 24(7), 807-822. DOI: 10.1002/joc.1041.
- Petheram C and Bristow KL (2008) Towards an understanding of the hydrological factors, constraints and opportunities for irrigation in northern Australia: A review. CRC for Irrigation Futures Technical Report No. 06/08, CSIRO Land and Water Science Report No. 13/08.
- Petheram C, McMahon TA and Peel MC (2008) Flow characteristics of rivers in northern Australia: Implications for development. *Journal of Hydrology* 357(1–2), 93-111. DOI: <http://dx.doi.org/10.1016/j.jhydrol.2008.05.008>.
- Petheram C, Rustomji P, McVicar TR, Cai W, Chiew FHS, Vleeshouwer J, Van Niel TG, Li L, Cresswell RG, Donohue RJ, Teng J and Perraud J-M (2012) Estimating the Impact of Projected Climate Change on Runoff across the Tropical Savannas and Semiarid Rangelands of Northern Australia. *Journal of Hydrometeorology* 13(2), 483-503. DOI: 10.1175/jhm-d-11-062.1.
- Petheram C and Yang A (2013) Climate data and their characterisation for hydrological and agricultural scenario modelling across the Flinders and Gilbert catchments. A technical report to the Australian Government from the CSIRO Flinders and Gilbert Agricultural Resource Assessment, part of the North Queensland Irrigated Agriculture Strategy. CSIRO Water for a Healthy Country and Sustainable Agriculture flagships, Australia. Available online: <<https://publications.csiro.au/rpr/pub?pid=csiro:EP13826>>.
- Petheram C, Yang A, Seo L, Rogers L, Baynes F, Devlin K, Marvanek S, Hughes J, Ponce Reyes R, Wilson P, Stratford D, Philip S (2022) Assessment of surface water storage options and reticulation infrastructure in the Roper catchment. A technical report from the CSIRO Roper River Water Resource Assessment for the National Water Grid. CSIRO, Australia.

- Pope M, Jakob C and Reeder MJ (2008) Convective Systems of the North Australian Monsoon. *Journal of Climate* 21(19), 5091-5112. DOI: 10.1175/2008JCLI2304.1.
- Power S, Casey T, Folland C, Colman A and Mehta V (1999) Inter-decadal modulation of the impact of ENSO on Australia. *Climate Dynamics* 15(5), 319-324. DOI: 10.1007/s003820050284.
- Power S, Haylock M, Colman R and Wang X (2006) The Predictability of Interdecadal Changes in ENSO Activity and ENSO Teleconnections. *Journal of Climate* 19(19), 4755-4771. DOI: 10.1175/JCLI3868.1.
- Prudhomme C and Davies H (2009) Assessing uncertainties in climate change impact analyses on the river flow regimes in the UK. Part 2: future climate. *Climatic Change* 93(1), 197-222. DOI: 10.1007/s10584-008-9461-6.
- Queensland Government (2023) Queensland Water Strategy. Water. Our life resource. Viewed 11 September 2024, <https://www.rdmw.qld.gov.au/qld-water-strategy/strategic-direction>.
- Ramsay HA, Leslie LM, Lamb PJ, Richman MB and Leplastrier M (2008) Interannual variability of tropical cyclones in the Australian region: role of large-scale environment. *Journal of Climate* 21(5), 1083-1103. DOI: 10.1175/2007JCLI1970.1.
- Rashid HA, Hendon HH, Wheeler MC and Alves O (2011) Prediction of the Madden–Julian oscillation with the POAMA dynamical prediction system. *Climate Dynamics* 36(3), 649-661. DOI: 10.1007/s00382-010-0754-x.
- Reisinger A, Kitching R, Chiew F, Hughes L, Newton P, Schuster S, Tait A and Whetton P (2014) Australasia. In: Field C and Barros V (eds), *Climate Change 2014: Impacts, Adaptation, and Vulnerability. Part B: Regional Aspects. Contribution of Working Group II to the Fifth Assessment Report of the Intergovernmental Panel on Climate Change*. Cambridge University Press, Cambridge, United Kingdom and New York, NY, USA.
- Reynolds RW, Rayner NA, Smith TM, Stokes DC and Wang W (2002) An Improved In Situ and Satellite SST Analysis for Climate. *Journal of Climate* 15(13), 1609-1625. DOI: 10.1175/1520-0442(2002)015<1609:AIISAS>2.0.CO;2.
- Risbey JS, Pook MJ, McIntosh PC, Wheeler MC and Hendon HH (2009) On the Remote Drivers of Rainfall Variability in Australia. *Monthly Weather Review* 137(10), 3233-3253. DOI: 10.1175/2009MWR2861.1.
- Roberts MJ, Vidale PL, Mizielinski MS, Demory M-E, Schiemann R, Strachan J, Hodges K, Bell R and Camp J (2015) Tropical Cyclones in the UPSCALE Ensemble of High-Resolution Global Climate Models. *Journal of Climate* 28(2), 574-596. DOI: 10.1175/JCLI-D-14-00131.1.
- Roderick ML, Rotstayn LD, Farquhar GD and Hobbins MT (2007) On the attribution of changing pan evaporation. *Geophysical Research Letters* 34(17), n/a-n/a. DOI: 10.1029/2007GL031166.
- Rouillard A, Skrzypek G, Dogramaci S, Turney C and Grierson PF (2015) Impacts of high inter-annual variability of rainfall on a century of extreme hydrologic regime of northwest Australia. *Hydrol. Earth Syst. Sci.* 19(4), 2057-2078. DOI: 10.5194/hess-19-2057-2015.
- Saji NH, Goswami BN, Vinayachandran PN and Yamagata T (1999) A dipole mode in the tropical Indian Ocean. *Nature* 401(6751), 360-363.

- Salathé EP (2003) Comparison of various precipitation downscaling methods for the simulation of streamflow in a rainshadow river basin. *International Journal of Climatology* 23(8), 887-901. DOI: 10.1002/joc.922.
- Scoccimarro E, Gualdi S, Villarini G, Vecchi GA, Zhao M, Walsh K and Navarra A (2014) Intense Precipitation Events Associated with Landfalling Tropical Cyclones in Response to a Warmer Climate and Increased CO₂. *Journal of Climate* 27(12), 4642-4654. DOI: 10.1175/JCLI-D-14-00065.1.
- Seneviratne SI, X. Zhang MA, W. Badi, C. Dereczynski, A. Di Luca, S. Ghosh, I. Iskandar, J. Kossin, S. Lewis, F. Otto, I. Pinto, M. Satoh, S.M. Vicente-Serrano, M. Wehner and B. Zhou (2021) 2021: Weather and Climate Extreme Events in a Changing Climate. In *Climate Change 2021: The Physical Science Basis. Contribution of Working Group I to the Sixth Assessment Report of the Intergovernmental Panel on Climate Change*. In: Masson-Delmotte V et al. (eds). Cambridge University Press, Cambridge, United Kingdom and New York, NY, USA.
- Shulmeister J and Lees BG (1995) Pollen evidence from tropical Australia for the onset of an ENSO-dominated climate at c. 4000 BP. *The Holocene* 5(1), 10-18. DOI: 10.1177/095968369500500102.
- Shuttleworth WJ (1993) Evaporation. In: Maidment DR (ed.), *Handbook of hydrology*, McGraw-Hill, New York.
- Smith IN, Wilson L and Suppiah R (2008a) Characteristics of the Northern Australian Rainy Season. *Journal of Climate* 21(17), 4298-4311.
- Smith TM, Reynolds RW, Peterson TC and Lawrimore J (2008b) Improvements to NOAA's Historical Merged Land–Ocean Surface Temperature Analysis (1880–2006). *Journal of Climate* 21(10), 2283-2296. DOI: 10.1175/2007JCLI2100.1.
- Stephens GL, L'Ecuyer T, Forbes R, Gettleman A, Golaz J-C, Bodas-Salcedo A, Suzuki K, Gabriel P and Haynes J (2010) Dreary state of precipitation in global models. *J. Geophys. Res.* 115(D24), D24211. DOI: 10.1029/2010jd014532.
- Stokes C, Jarvis D, Webster A, Watson I, Jalilov S, Oliver Y, Peake A, Peachey A, Yeates S, Bruce C, Philip S, Prestwidge D, Liedloff A, Poulton P, Price B and McFallan S (2023) Financial and socio-economic viability of irrigated agricultural development in the Roper catchment. A technical report from the CSIRO Roper River Water Resource Assessment for the National Water Grid. CSIRO, Australia.
- Suppiah R (2004) Trends in the southern oscillation phenomenon and Australian rainfall and changes in their relationship. *International Journal of Climatology* 24(3), 269-290. DOI: 10.1002/joc.1001.
- Taschetto AS and England MH (2009a) An analysis of late twentieth century trends in Australian rainfall. *International Journal of Climatology* 29(6), 791-807. DOI: 10.1002/joc.1736.
- Taschetto AS and England MH (2009b) El Niño Modoki Impacts on Australian Rainfall. *Journal of Climate* 22(11), 3167-3174. DOI: 10.1175/2008JCLI2589.1.

- Taschetto AS, Ummenhofer CC, Sen Gupta A and England MH (2009) Effect of anomalous warming in the central Pacific on the Australian monsoon. *Geophysical Research Letters* 36(12), n/a-n/a. DOI: 10.1029/2009GL038416.
- Tory KJ, Chand SS, McBride JL, Ye H and Dare RA (2013) Projected Changes in Late-Twenty-First-Century Tropical Cyclone Frequency in 13 Coupled Climate Models from Phase 5 of the Coupled Model Intercomparison Project. *Journal of Climate* 26(24), 9946-9959. DOI: 10.1175/JCLI-D-13-00010.1.
- Trapasso LM (2005) Heat Low. In: Oliver JE (ed.), *Encyclopedia of World Climatology*. Springer Netherlands, Dordrecht.
- Trenberth KE (1997) The Definition of El Niño. *Bulletin of the American Meteorological Society* 78(12), 2771-2777. DOI: 10.1175/1520-0477(1997)078<2771:TDOENO>2.0.CO;2.
- Warner RF (1986) Hydrology. In: Jeans DN (ed.), *Australia - A Geography*, vol. 1: The Natural Environment, Sydney University Press, Sydney.
- Webster T, Poulton P, Yeates S, Hornbuckle J, Brennan McKellar L, Cocks B, Gentle J, Mayberry D, Jones D and Wixon A (2013) Agricultural productivity in the Flinders and Gilbert catchment. A technical report to the Australian Government from the CSIRO Flinders and Gilbert Agricultural Resource Assessment, part of the North Queensland Irrigated Agriculture Strategy. . CSIRO Water for a Healthy Country and Sustainable Agriculture flagships, Australia.
- Wheeler M and Weickmann KM (2001) Real-Time Monitoring and Prediction of Modes of Coherent Synoptic to Intraseasonal Tropical Variability. *Monthly Weather Review* 129(11), 2677-2694. DOI: 10.1175/1520-0493(2001)129<2677:RTMAPO>2.0.CO;2.
- Wheeler MC and Hendon HH (2004) An All-Season Real-Time Multivariate MJO Index: Development of an Index for Monitoring and Prediction. *Monthly Weather Review* 132(8), 1917-1932. DOI: 10.1175/1520-0493(2004)132<1917:AARMMI>2.0.CO;2.
- Wheeler MC, Hendon HH, Cleland S, Meinke H and Donald A (2009) Impacts of the Madden-Julian Oscillation on Australian Rainfall and Circulation. *Journal of Climate* 22(6), 1482-1498. DOI: 10.1175/2008jcli2595.1.
- Wheeler MC and McBride JL (2005) Australian-Indonesian monsoon. In: Lau WKM and Waliser DE (eds), *Intraseasonal Variability in the Atmosphere-Ocean Climate System* Springer.
- Wheeler MC and McBride JL (2012) Australasian monsoon. In: Lau WKM and Waliser DE (eds), *Intraseasonal Variability in the Atmosphere-Ocean Climate System* (2nd edition). Springer Berlin Heidelberg, Berlin, Heidelberg.
- Whetton PH, McInnes KL, Jones RN, J. HK, Suppiah R, Page CM, Bathols J and Durack PJ (2005) Australian climate change projections for impact assessment and policy application: A review CSIRO Marine and Atmospheric Research Paper [Online] No. 1. Available online: <<https://publications.csiro.au/rpr/download?pid=procite:2918eca0-62c0-420e-b197-793267401560&dsid=DS1>>.

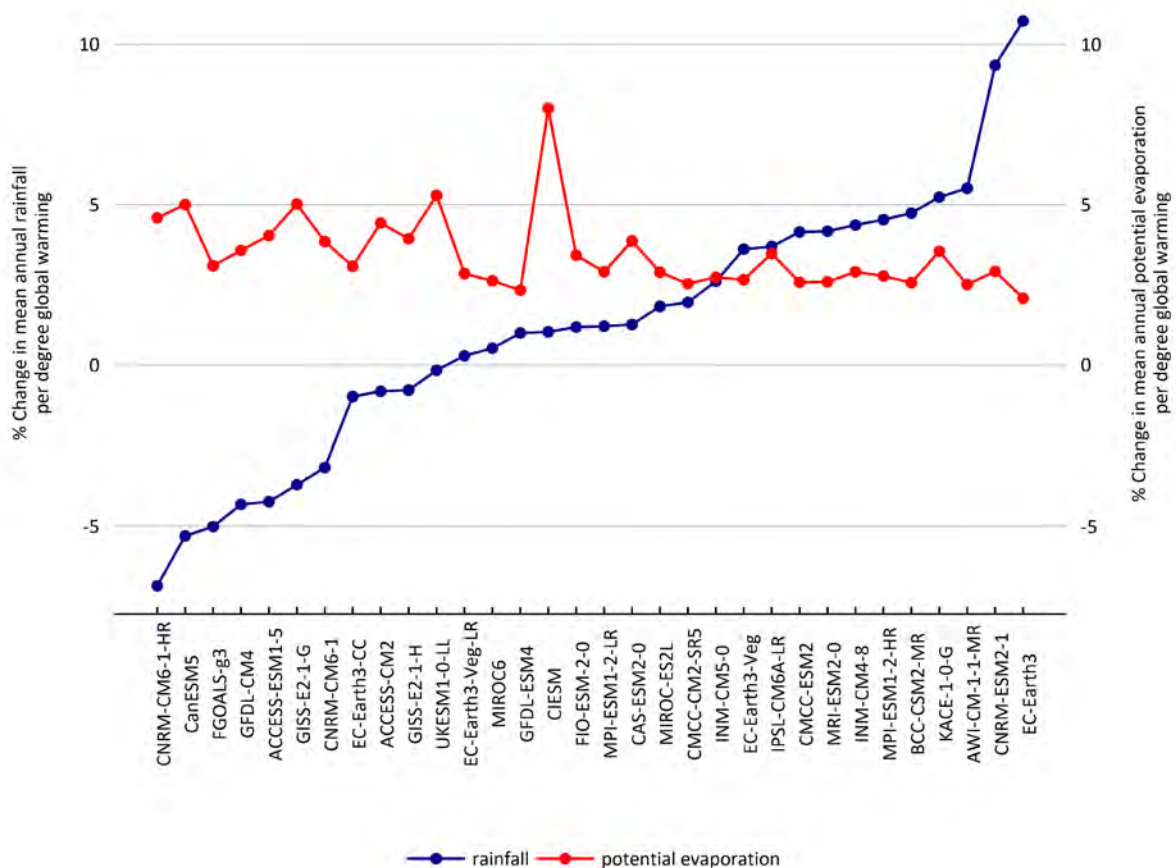
- White NJ, Haigh ID, Church JA, Koen T, Watson CS, Pritchard TR, Watson PJ, Burgette RJ, McInnes KL, You Z-J, Zhang X and Tregoning P (2014) Australian sea levels—Trends, regional variability and influencing factors. *Earth-Science Reviews* 136, 155-174. DOI: <http://dx.doi.org/10.1016/j.earscirev.2014.05.011>.
- Wohl EE, Fuertsch SJ and Baker VR (1994) Sedimentary records of late Holocene floods along the Fitzroy and Margaret Rivers, Western Australia. *Australian Journal of Earth Sciences* 41(3), 273-280. DOI: 10.1080/08120099408728136.
- Wolanski E and Chappell J (1996) The response of tropical Australian estuaries to a sea level rise. *Journal of Marine Systems* 7(2), 267-279. DOI: [http://dx.doi.org/10.1016/0924-7963\(95\)00002-X](http://dx.doi.org/10.1016/0924-7963(95)00002-X).
- Woodward E, Jackson S, Finn M and McTaggart PM (2012) Utilising Indigenous seasonal knowledge to understand aquatic resource use and inform water resource management in northern Australia. *Ecological Management & Restoration* 13(1), 58-64. DOI: 10.1111/j.1442-8903.2011.00622.x.
- Yevjevich VM (1967) An objective approach to definitions and investigations of continental hydrologic droughts. Colorado State University, Hydrology Paper No. 23.
- Zhang CD (2005) Madden-Julian oscillation. *Reviews of Geophysics* 43(2). DOI: 10.1029/2004rg000158.

Part V Appendices

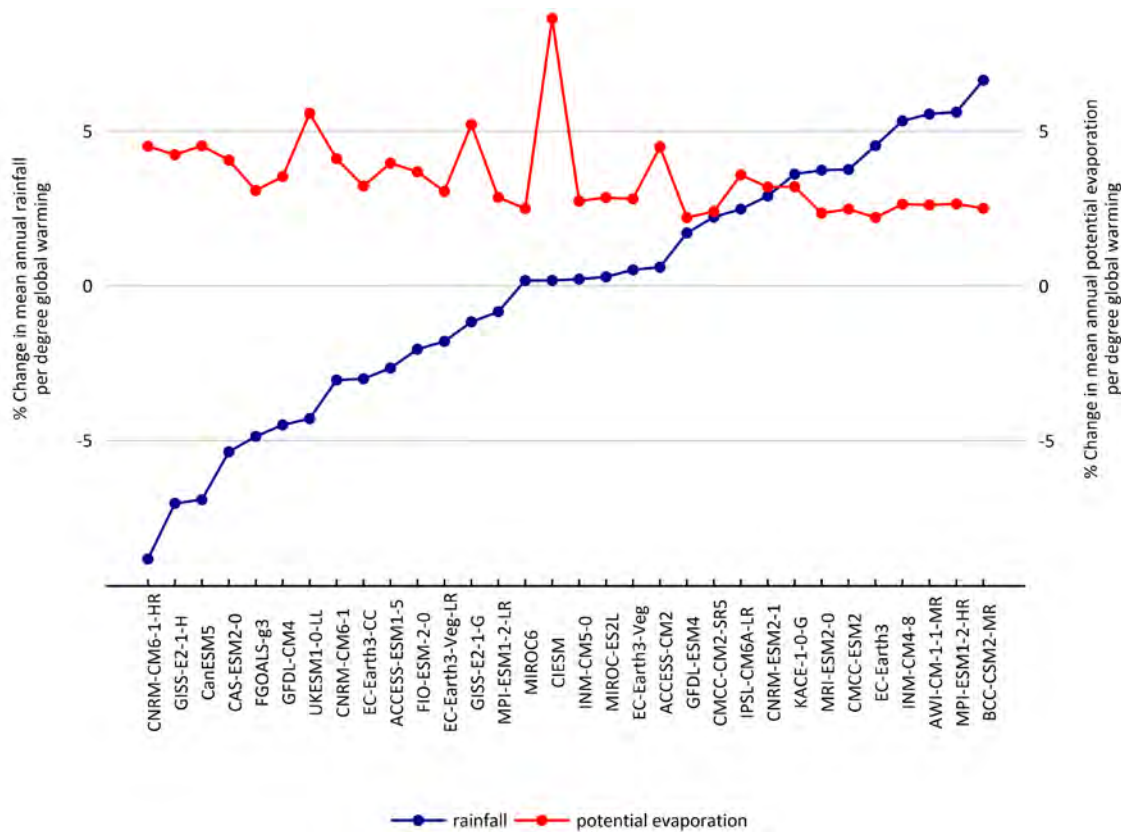


Appendix A Annual future climate variations under global warming scenario SSP5-8.5

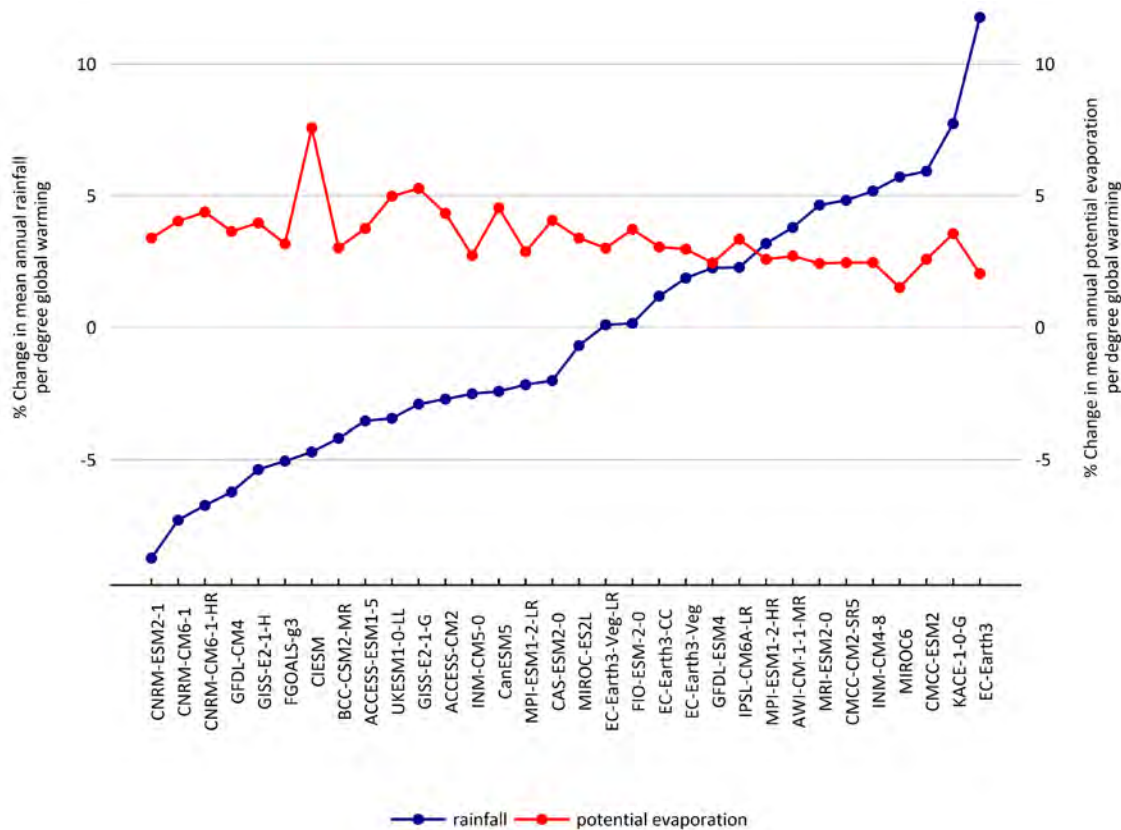
Apx Figure A-1 , Apx Figure A-2 and Apx Figure A-3 show spatially averaged rainfall and potential evaporation (PE) projections for each of the study catchments with the 32 global climate models – pattern scaling (GCM-PS) ranked in order of increasing mean annual rainfall. In these figures, the percent changes in rainfall and PE are expressed on a per degree of global warming for the SSP5-8.5 scenario.



Apx Figure A-1 Percentage change in rainfall and potential evaporation per degree of global warming for the 32 Scenario C simulations relative to Scenario A values for the Victoria catchment. GCM-PS ranked by increasing rainfall for SSP5-8.5



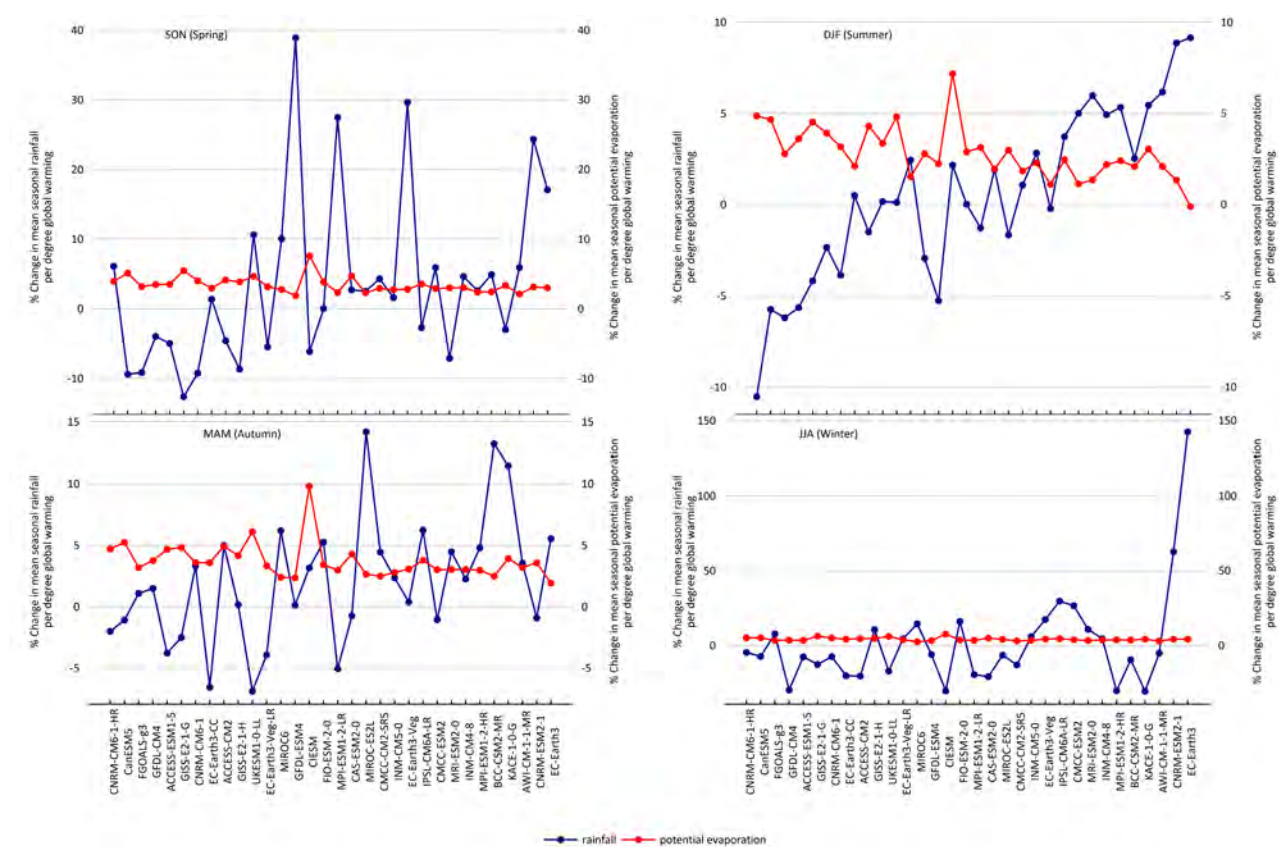
ApX Figure A-2 Percentage change in rainfall and potential evaporation per degree of global warming for the 32 Scenario C simulations relative to Scenario A values for the Roper catchment. GCM-PS ranked by increasing rainfall for SSP5-8.5



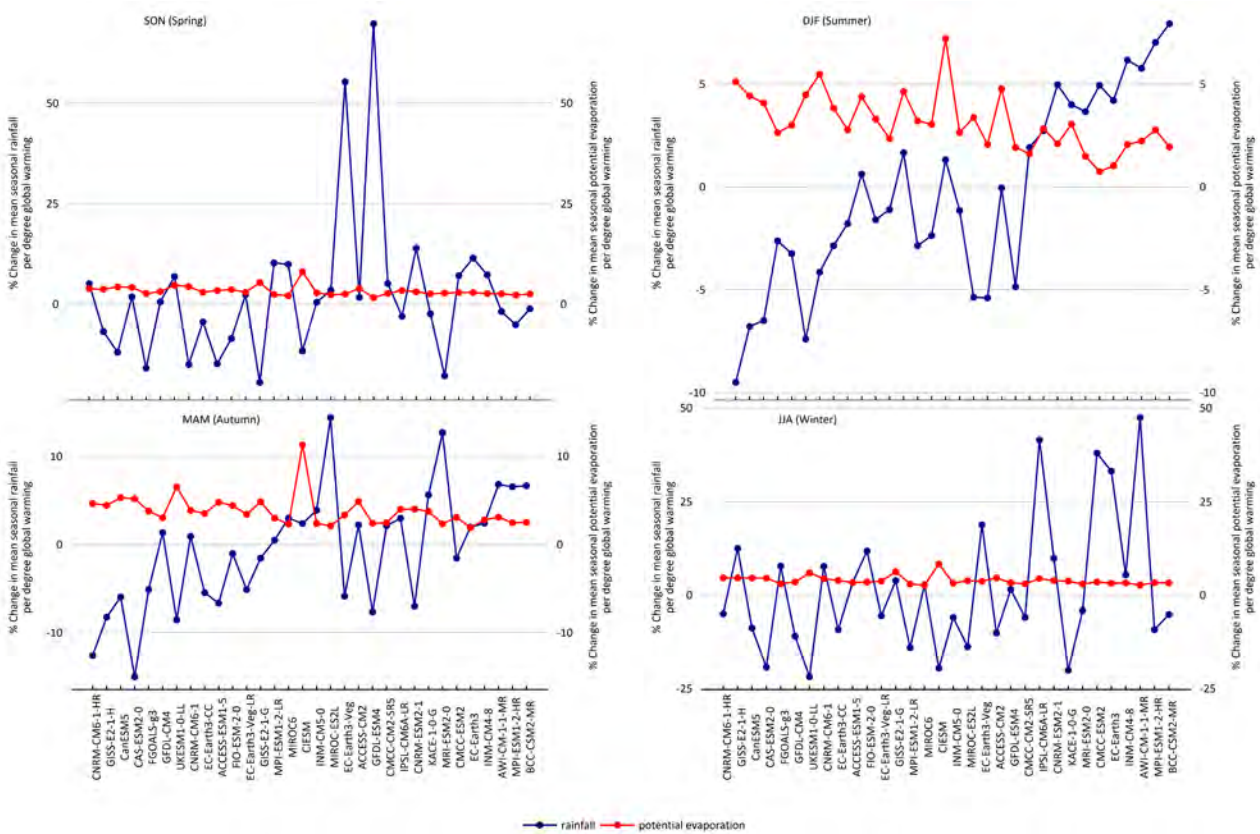
ApX Figure A-3 Percentage change in rainfall and potential evaporation per degree of global warming for the 32 Scenario C simulations relative to Scenario A values for the Southern Gulf catchments. GCM-PS ranked by increasing rainfall for SSP5-8.5

Appendix B Seasonal future climate variations under global warming scenario SSP5-8.5

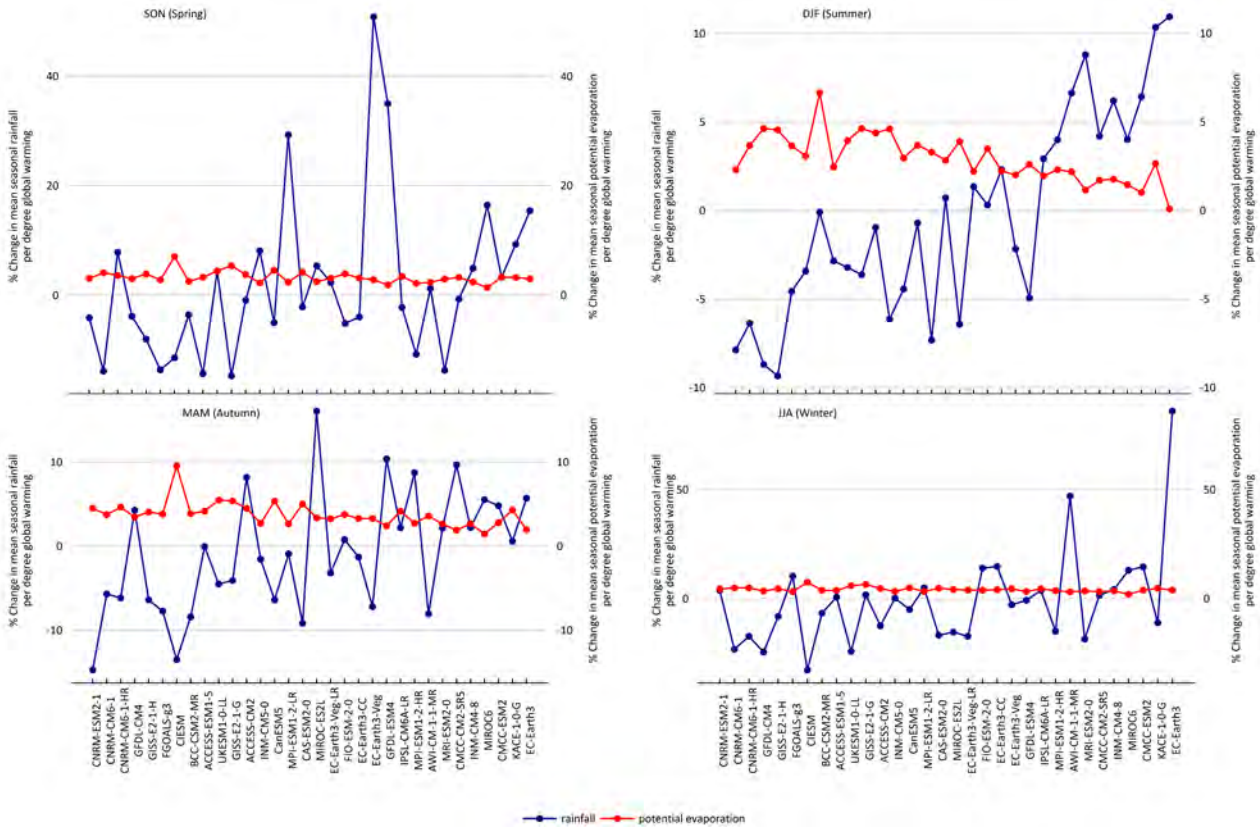
Apx Figure B-1, Apx Figure B-2 and Apx Figure B-3 show range in monthly GCM-PS rainfall and PE for the Victoria, Roper and Southern Gulf catchments respectively under the SSP5-8.5 scenario. In these plots the C range is the difference between the 10th and 90th percentile spatially averaged GCM-PS mean monthly value computed for each month.



Apx Figure B-1 Seasonal comparison of percent change in mean annual rainfall and mean potential evaporation per degree of global warming under SSP5-8.5 and SSP2-4.5 scenarios for the Victoria catchment



Apx Figure B-2 Seasonal comparison of percent change in mean annual rainfall and mean potential evaporation per degree of global warming under SSP5-8.5 and SSP2-4.5 scenarios for the Roper catchment



Apx Figure B-3 Seasonal comparison of percent change in mean annual rainfall and mean potential evaporation per degree of global warming under SSP5-8.5 and SSP2-4.5 scenarios for the Southern Gulf catchments

As Australia's national science agency and innovation catalyst, CSIRO is solving the greatest challenges through innovative science and technology.

CSIRO. Unlocking a better future for everyone.

Contact us

1300 363 400
+61 3 9545 2176
csiroenquiries@csiro.au
csiro.au

For further information

Environment

Dr Chris Chilcott
+61 8 8944 8422
chris.chilcott@csiro.au

Environment

Dr Cuan Petheram
+61 467 816 558
cuan.petheram@csiro.au

Agriculture and Food

Dr Ian Watson
+61 7 4753 8606
ian.watson@csiro.au